Imperial College London

British Heart Foundation

Regulation of human cardiomyocyte excitation-contraction coupling by human cardiac fibroblasts

by

Brian Xiangzhi Wang

National Heart and Lung Institute

Imperial College London

August 2019

Submitted in partial fulfilment of the requirements for the degree of Doctor of Philosophy of Imperial College London

I. Declaration

Declaration of originality

I, Brian X. Wang, certify that this thesis, and the research to which it refers, are the product of my own work and ideas, unless specifically referenced and acknowledged.

Copyright declaration

Brian Wang

August 2019

II. Abstract

Physiologically, cardiomyocytes develop features that enable them to meet the contractile demands of the healthy, adult heart. Among the structural and functional changes during development, there is an engagement of the sarcoplasmic reticulum as the main regulator of cytoplasmic Ca^{2+} cycling. In human cardiac disease and in ageing, there is progressive disengagement of the sarcoplasmic reticulum, reducing the efficiency of excitation-contraction coupling. In this project, we used human induced pluripotent stem cell-derived cardiomyocytes (hiPSC-CMs) to investigate the role of human cardiac fibroblasts in regulating cardiomyocyte Ca^{2+} cycling.

In chapter 3, we use hiPSC-CMs with a genetically encoded Ca^{2+} indicator to perform optical recording of changes in hiPSC-CM intracellular Ca^{2+} in various co-culture setups with human cardiac fibroblasts. Co-culture setups that only allowed paracrine interactions between the two cell types led to prolongation of the hiPSC-CM Ca^{2+} transients. There was an abbreviation in Ca^{2+} transient duration when the two cell types were in direct physical contact, indicating an increase in Ca^{2+} cycling efficiency.

In chapter 4, we investigated the role of the extracellular matrix in regulating hiPSC-CM Ca^{2+} cycling. As matrix proteins are known to form interactions with cardiomyocytes via integrin ligand-receptor interactions, we utilised synthetic peptides with the integrin-binding tripeptide motif, Arginine-Glycine-Aspartic Acid, to show that fibril-forming integrin ligands abbreviated hiPSC-CM Ca^{2+} transients by recruiting the sarcoplasmic reticulum to Ca^{2+} cycling.

In chapter 5, we focus on the role of extracellular vesicles, which have emerged over the last decade as a major secretory vehicle for non-soluble paracrine interactions. A major limitation in the investigation of extracellular vesicles is that isolation techniques, and thus sample purity, varies considerably between studies. In chapter 5, we validated an ultrafiltration- and chromatography-based technique for the isolation of extracellular vesicles from cardiac fibroblast-conditioned culture media and showed that cardiac fibroblast extracellular vesicles significantly abbreviate the hiPSC-CM Ca^{2+} transient time to peak, indicating an increase in the efficiency of Ca^{2+}-induced Ca^{2+}-release.

The findings of this project indicate that cardiac fibroblasts have differential effects on hiPSC-CM Ca^{2+} cycling depending on the modality of interaction. The findings also indicate that fibroblast-mediated modulation of hiPSC-CM Ca^{2+} cycling can be mediated by fibroblast-

regulated turnover of the extracellular matrix. This project demonstrates the importance of the extracellular interactions in utilising hiPSC-CMs and understanding the modulators of cardiomyocyte structure and function.

III. Acknowledgements

I would like to acknowledge a number of people who have helped me along the way to completion of this thesis.

Firstly, I thank Prof. Cesare Terracciano. His continuous support and advice throughout the project were indispensable and he has been a constant source of motivation. For the countless times he has gone above and beyond the role of just being an academic supervisor, I will be eternally grateful. He will continue to inspire me for the rest of my lifetime.

I thank my secondary supervisor Prof. Ken MacLeod for his support throughout the project.

I am truly grateful for the amazing atmosphere created by my colleagues in the ICTEM. I have always felt comfortable, encouraged and supported by everyone around me. I thank my close colleagues for their support and contributions to the thesis; Dr. Sam Kit-Anan, Dr. Liam Couch, Mr. Oisín King, Mr. Jerome Fourre, Ms. Laura Nicastro and Mr. Barrett Downing. These fantastic scientists have contributed greatly to the project and without their input this PhD would not have been achieved successfully. To all of the other researchers on the 4th floor at the ICTEM, thank you for making the last three years an absolute joy.

Finally, I thank my parents and sister for their unwavering love, support and encouragement. Without them I wouldn't be who and where I am today. This accomplishment is as much mine as theirs.

IV. Publications and Presentations

Publications

Wang, B., Kit-Anan, W. & Terracciano, C., 2018. Many Cells Make Life Work—Multicellularity in Stem Cell-Based Cardiac Disease Modelling. International Journal of Molecular Sciences, 19(11), p.3361. doi: 10.3390/ijms19113361.

Zwi-Dantsis, L., **Wang, B**., Marijon, C., Zonetti, S., Ferrini, A., Massi, L., Stuckey, D., Terracciano, C. & Stevens, M., 2019. Remote Magnetic Nanoparticle Manipulation Enables the Dynamic Patterning of Cardiac Tissues. Advanced Materials, 1904598, pp. 1-6. doi: 10.1002/adma.201904598**.**

Wang, B., Kane, C., King, O., Kit-Anan, W., Nicastro, L., Downing, B., Deidda, G., Arulampalam, N., Couch, L., Pinali, C., Mitraki, A., MacLeod, K. and Terracciano, C., Integrin Binding Recruits the Sarcoplasmic Reticulum to Excitation-Contraction Coupling in Human Induced Pluripotent Stem Cell-Derived Cardiomyocytes. Manuscript in submission.

Perbellini, F., King, O., Kit-Anan, W., Jabbour, R., Watson, S., Saskia, M., **Wang, B**., Pitoulis, F., Broyles, C., Daniels, M., Thum, T., Harding, S., Terraciano, C., Human-induced pluripotent stem cell-derived cardiomyocytes integration and maturation studied at a cellular/sub-cellular level using living myocardial slices. Manuscript in submission.

Couch, L., Fiedler, J., Chick, G., Clayton, R., Dries, E., Wienecke, L., Fourre, J., Derda, A., **Wang, B**., Jabbour, R., Shanmuganathan, M., Lyon, A., Wright, P., Terracciano, C., Thum, T. & Harding, S., Circulating MicroRNAs Predispose to Takotsubo Syndrome Following High Dose Adrenaline Exposure. Manuscript in submission.

Kit-Anan, W., Mazo, M., **Wang, B**., Leonardo, V., Pence, I., Gopal, S., Gelmi, A., Nagelkerke, M., Becce, M., Chiappini, C., Harding, S., Terracciano, C. & Stevens, M.

CardioArrays: A Novel Platform for the Multidimensional in Vitro Manipulation of the Myocyte Niche. Manuscript in submission.

Jabbour, R., Owen, T., Pandey, P., Reinsch, M., Pantou, D., **Wang, B**., Watson, S., Couch, L., Kodagoda, T., Handa, B., Perbellini, F., Pitcher, D., King, O., Siong Ng, F., Terracciano, C., Peters, N., Eschenhagen, T., Weinberger, F. & Harding, S. Preclinical Testing of Upscaled Engineered Heart Muscle. Manuscript in preparation.

Oral Presentations

‘Self-assembling integrin Ligands Increase Sarcoplasmic Reticulum Contribution to Human Cardiomyocyte Excitation-Contraction Coupling’ - UK Cell Adhesion Society Meeting – UCL, London; September 2018.

‘Regulation of Cardiac Excitation-Contraction Coupling by Fibroblasts in Health and Disease’ - National Heart and Lung Institute Post-Graduate Research Day – Hammersmith Hospital, London; July 2018.

‘Extracellular Vesicles Secreted from Human Fibroblasts Modulate Human Induced Pluripotent Stem Cell-Cardiomyocyte Calcium Cycling’ - UK Extracellular Vesicles Forum – University of Sheffield, Sheffield; December 2018.

Poster Presentations

‘Regulation of Cardiac Excitation-Contraction Coupling by Fibroblasts in Health and Disease’ - European Society of Cardiology Basic Science Summer School - Sophia Antipolis, France; June 2017.

‘Regulation of Cardiac Excitation-Contraction Coupling by Fibroblasts in Health and Disease’ - iForum London Meeting – South Kensington Campus, London; September 2017.

‘Extracellular Vesicles Secreted from Human Fibroblasts Modulate Human Induced Pluripotent Stem Cell-Cardiomyocyte Calcium Cycling’ - American Heart Association Congress - Anaheim, CL; November 2017.

‘Arginine-Glycine-Aspartic Acid-Motif Containing Peptides and Integrin Binding Modulate Human Induced Pluripotent Stem-Cell Derived Cardiomyocyte Calcium Cycling’ - American Heart Association Congress - Anaheim, CL; November 2017.

‘Self-Assembling Integrin Ligands Increase Sarcoplasmic Reticulum Contribution to Human Cardiomyocyte Excitation-Contraction Coupling’ – European Society of Cardiology Congress - Munich, Germany; August 2018.

‘Human Cardiac Fibroblast-Secreted Exosomes Improve the Efficiency of Human Cardiomyocyte Calcium Cycling’ – British Society for Cardiovascular Research meeting - University of Sheffield, Sheffield; September 2018.

‘Extracellular Vesicles Secreted from Human Fibroblasts Increase Sarcoplasmic Reticulum-Dependency of Human Induced Cardiomyocyte Calcium Handling’ - American Heart Association Congress – Chicago, IL; November 2018.

‘Regulation of Cardiac Excitation-Contraction Coupling by Fibroblasts in Health and Disease’ - Pharmacology Society Conference – Westminster, London; December 2018.

‘Integrin Ligands Improve Human Stem Cell–Derived Cardiomyocyte Excitation-Contraction Coupling Efficiency’ – International Society of Heart Research World Congress – Beijing, China; June 2019.

V. Funding and Awards

MB/PhD Studentship - FS/16/76/32409 – 'Regulation of cardiac myocyte excitation-contraction coupling by cardiac fibroblasts in health and in disease' – British Heart Foundation; September 2016.

Travel Award – Physiological Society; November 2017.

Travel Award – Imperial College Trust; November 2017.

Best Poster Award – 'Integrin ligands and receptor inhibition abbreviate human cardiomyocyte calcium transients' – London Stem Cell Network Symposium; February 2018.

President's Awards for Excellence in Research for Outstanding Research Team – Human Tissue Team; May 2018.

Travel Award – Physiological Society; November 2018.

Travel Award – UK Extracellular Vesicles Society; December 2018.

Travel Award – National Heart and Lung Institute; June 2019.

TABLE OF CONTENTS

VI. List of tables

VII. List of Figures

VIII. List of abbreviations

α-SMA	Alpha-Smooth Muscle Actinin
BCA	Bicinchoninic Acid
BSA	Bovine Serum Albumin
CDI	Cellular Dynamic International
CICR	Ca^{2+}-Induced Ca^{2+}-Release
CM	Cardiomyocyte
CHO	Chinese Hamster Ovary
Cryo-TEM	Cryogenic Transmission Electron Microscopy
DDR2	Discoidin Domain Receptor 2
DHPR	Dihydropyridine Receptor
DMEM	Dulbecco's Modified Eagle Medium
EC	Excitation-Contraction
ECM	Extracellular Matrix
EDTA	Ethylene-Diamine-Tetraacetic Acid
EM	Electron Microscopy
EMT	Epithelial-Mesenchymal Transition
EndMT	Endothelial-Mesenchymal Transition
EPDC	Epicardium-Derived Cell
ESCRT	Endosomal Sorting Complexes Required for Transport
ET-1	Endothelin 1
EV	Extracellular Vesicle
FAC	Focal Adhesion Complex
FBS	Foetal Bovine Serum
FDA	Food and Drug Administration
FFR	Force-Frequency Relationship
FGF	Fibroblast Growth Factor
FGF2	Fibroblast Growth Factor-2
FSP-1	Fibroblast-Specific Protein 1
GFP	Green Fluorescent Protein
HCN	Hyperpolarisation-Activated Cyclic Nucleotide-gated K^+
HDL	High-Density Lipoprotein

HEK	Human Embryonic Kidney
HEPES	4-(2-Hydroxyethyl)-1- Piperazineethanesulfonic Acid
hERG	Human Ether-a-go-go-Related Gene
hESC	Human Embryonic Stem Cell
hiPSC	Human Induced Pluripotent Stem Cell
hiPSC-CM	Human Induced Pluripotent Stem Cell-Derived Cardiomyocyte
I_{Ca}	Ca^{2+} Current
$I_{Ca,L}$	L-type Ca^{2+} Current
$I_{Ca,T}$	T-type Ca^{2+} Current
I_f	Funny Current
I_{k1}	Inward Rectifying K^+ Current
I_{kr}	Rapid Delayed Rectifier K^+ Channel
I_{ks}	Slow Delayed Rectifier K^+ Current
IL-6	Interleukin-6
I_{NCX}	Na^+/Ca^{2+} Current
I_{TO}	Transient Outward K^+ Current
jSR	Junctional Sarcoplasmic Reticulum
KO	Knock Out
LQTS	Long-QT Syndrome
mESC	Mouse Embryonic Stem Cell
MMP	Matrix Metalloproteinase
MVB	Multivesicular Body
NCX	Na^+/Ca^{2+}-Exchanger
NCX1	Gene Encoding the Cardiac Isoform of Na^+/Ca^{2+}-Exchanger
NRVM	Neonatal Rat Ventricular Myocyte
NTA	Nanosight Tracking Analysis
PA	Peptide Amphiphile
PBS	Phosphate-Buffered Saline
PDGF	Platelet-Derived Growth Factor
PDMS	Polydimethylsiloxane
Po	Opening Probability
RB – INS	Roswell Park Memorial Institute media with B27 Minus Insulin
RB + INS	Roswell Park Memorial Institute media with B27 Plus Insulin

RGD	Arginine-Glycine-Aspartate
ROCK	Rho-associated Protein Kinase
RPMI	Roswell Park Memorial Institute
RyR	Ryanodine Receptor
RyR2	Gene Encoding the Cardiac Isoform of Ryanodine Receptor
SEC	Size-Exclusion Chromatography
SERCA	Sarco-Endoplasmic Reticulum Ca^{2+}-ATPase
SR	Sarcoplasmic Reticulum
T-tubule	Transverse Tubule
TBS	Tris-Buffered Saline
TBS-T	Tris-Buffered Saline with Tween
TGF	Transforming Growth Factor
TIMP	Tissue Inhibitor of Matrix Metalloproteinase
VSMC	Vascular Smooth Muscle Cell
WTC	Wild Type C

1 Introduction

1.1 Heart failure

Heart failure is a global pandemic affecting over 26 million people worldwide and is becoming increasingly prevalent with an ageing global population (British Heart Foundation, 2015). Despite recent advances in disease therapies and prevention, the rates of mortality and morbidity are still very high and quality of life in patients diagnosed with heart failure is poor (Savarese and Lund, 2017). The cardiomyocytes are the contractile cells of the heart so loss of cardiomyocyte function as a result of loss of cardiomyocyte number or reduced contractility causes progressive reduction in heart function. The subsequently increased burden in contractile requirements on the remaining cardiomyocytes causes further cardiomyocyte dysfunction (Bergmann *et al.*, 2009).

The progressive loss of cardiomyocyte viability is exacerbated by the poor regenerative potential of cardiomyocytes in the adult mammalian heart. Human adult cardiomyocytes have been reported to turnover 1% per year, but this progressively decreases to 0.45% by the age of 75 (Bergmann *et al.*, 2009). Current treatments are able to delay the progression of cardiac disease but we still have no treatment to effectively reverse the maladaptive changes that occur (Inamdar and Inamdar, 2016). In order to develop earlier prevention strategies and more effective treatments for disease, we need to be able to develop methods to identify patients with a predisposition to cardiac disease or develop a greater understanding of key therapeutic targets and strategies to combat disease progression.

1.2 Cardiac Development

The human heart is one of the first organs to develop during embryogenesis. Its formation is crucial for the establishment of a circulatory system that supports subsequent foetal development. Three weeks after fertilisation, the three layers of the heart (epicardium, myocardium and endocardium) are formed as cardiac development commences. The mesodermal cells are separated into the splanchnic and somatic mesoderm. The splanchnic mesoderm differentiates into the myocardium, which provides the early contractile

properties of the primitive heart. The cells in the somatic mesoderm develop into the body wall lining as well as the dermis. The mesodermal lining gives rise to the epicardium (Rana, Christoffels and Moorman, 2013). The major changes that occur in cardiac development are outlined in **Figure 1.1**.

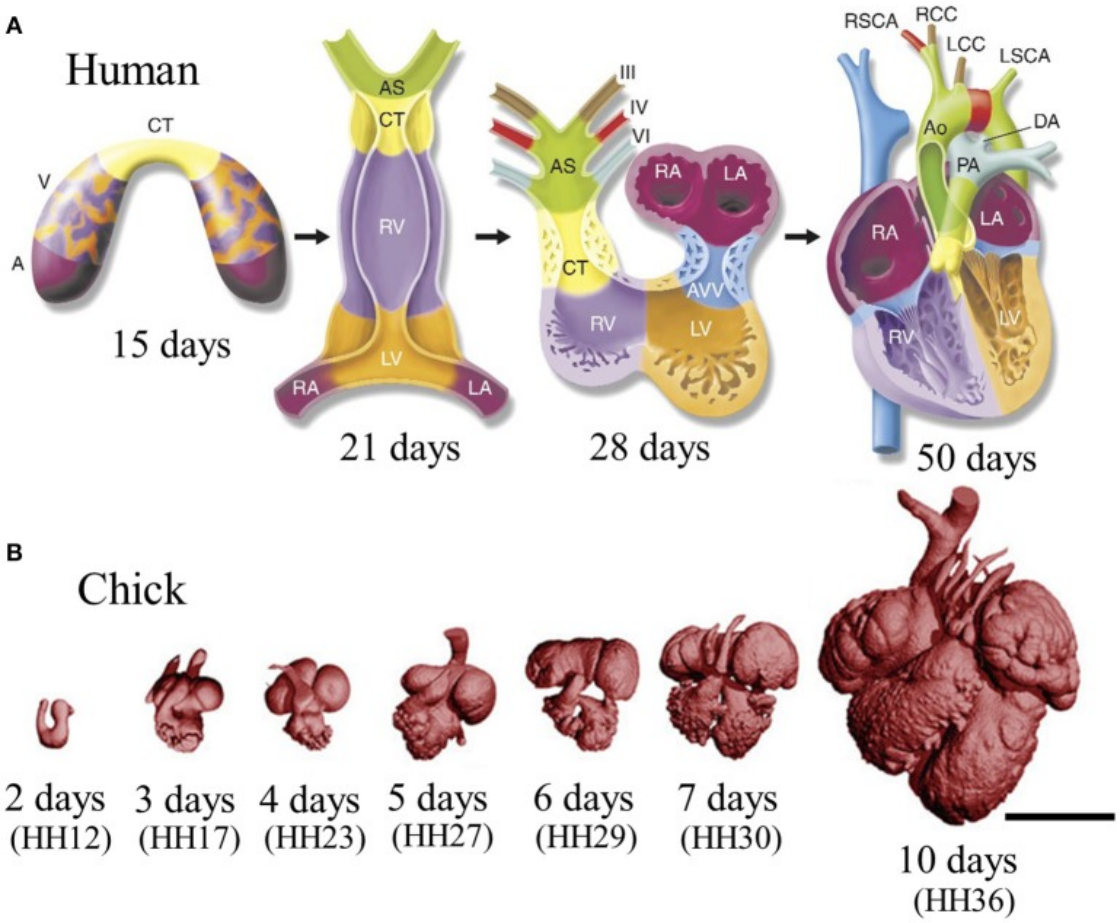

Figure 1.1 Schematic overview of heart development*. (A) Schematic of cardiac morphogenesis in human. Colour coding of morphologically related regions, seen from a ventral view. At day 15, cardiogenic precursors for a crescent of segments that form the linear heart tube. Cardiac chambers balloon out from the outer curvature of the lopped heart tube. Neural crest cells populate the aortic arch arteries (III, IV and VI) and aortic sac (AS) that form the mature aortic arch. Mesenchymal cells form the cardiac valves from the contruncal (CT) and the atrioventricular valve (AVV) segments. Corresponding days of human embryonic development indicated under each panel. A, atrium; V, ventricle; R/L A, right/left atrium; R/L V, right/left ventricle; PA, pulmonary artery; Ao, aorta; DA, ductus arteriosus; R/L SCA, right/left subclavian artery; R/L CC, right/left common carotid. (B) Scaled micro-computerised tomography images of chicken embryonic hearts at representative days. Corresponding Hamburger-Hamilton (HH) stages shown in parenthesis* (Lindsey, Butcher and Yalcin, 2014).

During human cardiac development, mesodermal cardiac progenitor cells (CPCs) give rise to many cell types, including cardiomyocytes, endothelial cells, fibroblasts and smooth muscle cells. The differentiation of CPCs is driven by biochemical, physical and electrical stimuli (Michela *et al.*, 2011). Bone morphogenetic proteins, insulin-like growth factor and WNT are all known to be significant signalling pathways for cardiac development (van Wijk, Moorman and van den Hoff, 2007; R. N. Wang *et al.*, 2014). Early in cardiac development, these pathways cause formation of the endocardial tube. From this point, the intrinsic rhythmic electrical activity in the cardiomyocytes is initiated, starting in close proximity to the pacemaker cells. As distance extends from these pacemaker cells, the depolarisation time is also lengthened (Rana, Christoffels and Moorman, 2013).

As the heart continues to develop, the expression of transcription factors causes localised proliferation and differentiation in areas that become the atria and ventricles, which are separated by the atrioventricular canal; an area that retains the primary myocardial properties (Rana, Christoffels and Moorman, 2013). The foetal circulation drives blood from the venous poles into the atria, through the atrioventricular canal and into the embryonic ventricle before it leaves through the outflow tract (Rana, Christoffels and Moorman, 2013). As the human heart continues to develop, there are important changes in cardiomyocyte function – notably, an increase in conduction, contractility and automaticity in the cardiomyocytes that form the atria and ventricles (Rana, Christoffels and Moorman, 2013).

As well as the working, contractile cardiomyocytes, there is development of the cardiac conduction system formed from non-migrating CPCs found at specific locations in the developing myocardium (Evans *et al.*, 2010). Molecular genetic studies have shown that the formation of the sinus and atrioventricular nodes, which determine the rate of contractility in the myocardium, and the rapidly conducting ventricular pathways critical for the spread of synchronous, electrical current across the ventricles, is dependent on the expression of key transcription factors (Christoffels and Moorman, 2009). Notably, transcription repressors have been shown to be critical in the formation of the cardiac conduction system. Analysis of mice deficient of Id2, a member of the Id gene family of transcription repressors, show both structural and functional conduction system abnormalities, including left bundle branch block. It has been demonstrated that these transcription repressors are crucial for maintaining the conduction system phenotype, and insufficient expression within the

embryonic myocardium causes these cells to differentiate into the contractile cells of the working myocardium (Christoffels and Moorman, 2009).

1.3 Heart structure

The myocardium is composed of numerous cell types, but the contractile activity of the cardiomyocytes that form the muscle fibres is central to myocardial function (**Figure 1.2**). For optimal functioning of the myocardium, healthy adult cardiomyocytes are highly specialised. Sarcomeres, the contractile units within cardiomyocytes, regulate Ca^{2+}-dependent contraction via the movement of sliding filaments. Individual cardiomyocytes are cross-linked by intercalated discs that also allow mechanical and electrical coupling. Adherens junctions within the intercalated discs anchor the myofibrils and aid synchronous contraction within compartments of the myocardium. The intercalated discs allow action potential propagation, and this trigger for contractile activity gives rise to the phenomena of excitation-contraction coupling. Insufficient contractile function of the cardiac muscle fibres underlies the primary deficit of heart failure.

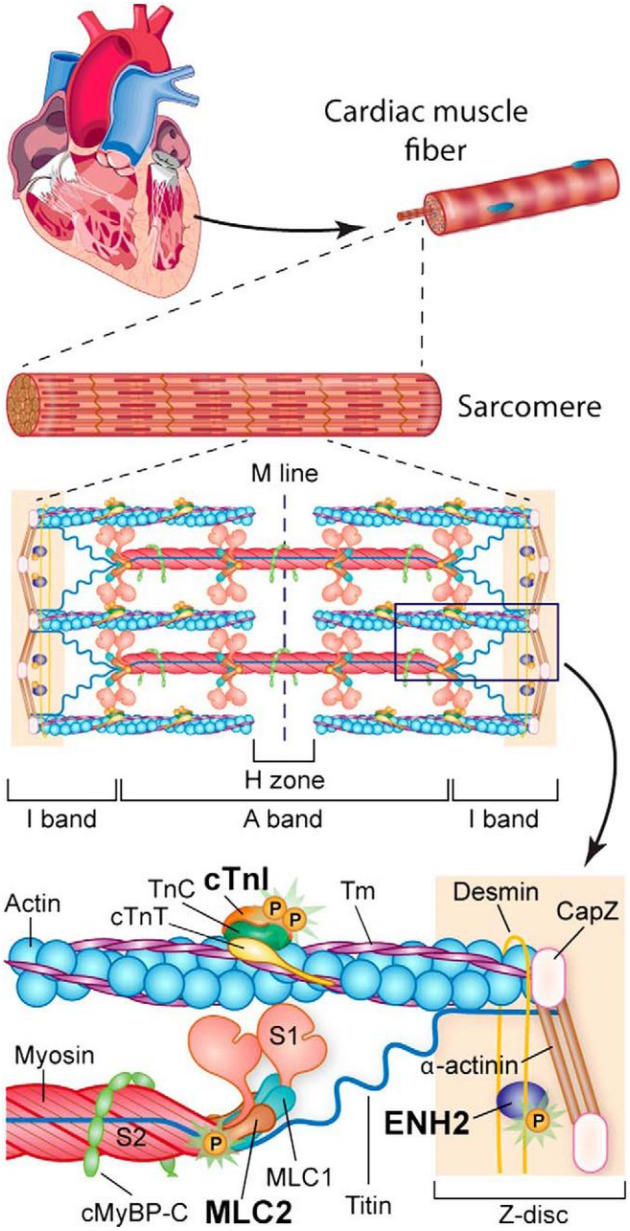

Figure 1.2. Contractile apparatus of the myocardium*. The cardiac muscle fibres are organised into sarcomeres. The synchronous sliding of actin and myosin filaments is responsible for physiological contraction activity at a macroscopic level. Phosphorylation of cTnI, MLC2 and ENH2 are highlighted. Dysfunction in this apparatus underlies the phenotype of many cardiac diseases* (Peng *et al.*, 2014).

1.4 Multicellularity in the myocardium

This section has been partly published in Wang, B., Kit-Anan, W. & Terracciano, C. Many Cells Make Life Work—Multicellularity in Stem Cell-Based Cardiac Disease Modelling. Int. J. Mol. Sci. 19, 3361 (2018).

To determine how the myocardium functions, we must understand it as a multicellular organ, rather than considering the contractile cardiomyocytes in isolation. Within the myocardium, there is a wide range of non-myocyte cell types and the extracellular matrix (ECM) scaffold that support the contractile function of cardiomyocytes. The most abundant non-myocyte cell types are thought to be fibroblasts, endothelial cells and perivascular cells, although many others are also present (Perbellini *et al.*, 2018). The cardiomyocytes are currently considered to occupy most of the healthy, adult human myocardium in terms of volume; between 70-80% in the adult, but they are thought to constitute to only 30-40% of the cells by number (Zhou and Pu, 2016; Perbellini *et al.*, 2018).

Although estimates for the density of the non-myocytes vary substantially, it is widely agreed that these cell types play a vital role in the development of the normal homeostasis in health and the pathophysiological changes that occur in chronic cardiac disease (**Table 1.1**).The non-myocyte components of the myocardium provide the chemical, electrical and mechanical stimulation for cardiomyocytes during myocardial maturation and form the structures essential for the vascular supply and extracellular scaffold required for contractile function and long-term survival (Perbellini *et al.*, 2018). The importance of the non-myocyte cell types and the ECM have been shown in numerous studies in which the isolation of human cardiomyocytes from the native myocardium leads to a rapid loss of contractile function and prominent changes in the structure (Dispersyn *et al.*, 2001; Zhang *et al.*, 2010; Pinz *et al.*, 2011). It is thought that the loss of the extracellular modulation from these non-myocyte components of the myocardium drive the remodelling that occurs following the isolation of human cardiomyocytes.

Cell type	Activity in Health	Activity in Disease	Reference
Endothelial cells	Structural support Vasculature homeostasis Biochemical factors such as nitric oxide, endothelin-1, IL-6 Progenitor of cardiac pericytes and vascular smooth muscle cells	Inflammation (hypertrophy, inotropy, apoptosis, mitosis) Neovascularization increase the density of peri-infarct vessels Paracrine	(Rajendran *et al.*, 2013; Chen *et al.*, 2016; He *et al.*, 2017)
VSMCs	Mechanical support of vasculature: contractile or synthetic (proliferative) mode	Loss of elasticity Reduced contractile Increased proliferation	(Cheung *et al.*, 2012; White *et al.*, 2016)
Leucocytes	Few residents Mast cells act as inflammatory mediator storage and activating the local renin-angiotensin system Macrophage performs a janitorial homeostasis and facilitates electrical conduction	Macrophage has a role in ECM turnover/cell death, scar formation, neutrophil recruitment, and vascularization support	(Hofmann and Frantz, 2015; Marino *et al.*, 2016; Tejada *et al.*, 2016; Hulsmans *et al.*, 2017)
Neurons	Conduction fibre and pacemaker (AV, SA, Purkinje) Control of rhythmic beating	Block, slow down conduction Essential component for embryo development	(Gilbert *et al.*, 2006; Akar *et al.*, 2007; Margariti, 2014; Ardell *et al.*, 2016)
Fibroblasts	ECM turnover, maintaining a balance between the synthesis and degradation of the matrix	Scar formation (fibrosis) Increase ECM protein Phagocytose apoptotic cells Crosstalk to EC and macrophage for angiogenesis and matrix synthesis	(Fan *et al.*, 2012; Cartledge *et al.*, 2015; Doppler *et al.*, 2017; Nakaya *et al.*, 2017)
ECM	Periostin, laminin, vimentin, fibronectin, and collagen types I (90%), III, V, and VI Alignment Mechanical support	Increase in collagen I, III, IV, V, and VI laminin, fibronectin, thrombospondin, and tenascin	(Snider *et al.*, 2009; Jourdan-LeSaux, Zhang and Lindsey, 2010; Fan *et al.*, 2012; Howard and Baudino, 2014; Kong, Christia and Frangogiannis, 2014)

Table 1.1: The role of key non-myocyte components of the heart in health and changes in activity during disease. EC = endothelial cell, ECM = Extracellular Matrix, VSMCs = Vascular smooth muscle cells (Wang, Kit-Anan and Terracciano, 2018).

1.4.1 Endothelial cells

Endothelial cells are essential for the formation of myocardial vasculature required for cardiomyocyte function and are considered to be the most abundant cell type in the heart (Pinto *et al.*, 2016). Functional endothelial cells are critical in the delivery of oxygen and nutrients to cardiomyocytes and, thus, momentum has gathered in the modelling of vascularised microenvironments (Endemann and Schiffrin, 2004; Hsieh *et al.*, 2006). The importance of endothelial cells in vessel formation has been shown in fibril gel co-culture constructs, where endothelial cells and patient-derived pericytes that surround capillaries increase the stability of perfusable micro-vessels (Ryan *et al.*, 2016). In the context of disease progression, the vascular endothelium is critical in the initiation of the inflammatory response, regulation of vasomotor tone and the control of the vascular permeability (Rajendran *et al.*, 2013). Therefore, accurate models of the myocardium must consider the role of endothelial cells in the function of the cardiomyocytes, and in the wider context, the myocardium.

1.4.2 Vascular smooth muscle cells (VSMCs)

VSMCs are stroma-derived cells crucial for the construction of the vascular wall of both large and small vessels (Perbellini *et al.*, 2018). Large arteries receive the highest pressure of blood flow and are more elastic to accommodate the high pressure. Smaller arteries, such as arterioles, have more smooth muscle which contract or relax to regulate blood flow to specific portions of the organs. VSMCs have been shown to display functional plasticity in switching expression between contractile and proliferative (synthetic) phenotypes involved in the regulation of vessel tone and blood pressure (Myasoedova *et al.*, 2018; Kyotani, Takasawa and Yoshizumi, 2019). Changes in the stimuli in the microenvironment causes a reduction in contractility and elasticity, altering their phenotype (Cheung *et al.*, 2012; Chen *et al.*, 2016). The ability of VSMCs to regulate the lumen diameter of blood vessels means that improving our understanding the role of VSMCs in health and in disease would aid our understanding about the functioning of the human myocardium.

1.4.3 Leucocytes

Heart failure is a state of chronic inflammation, with stimuli in the diseased myocardium contributing to the activation and recruitment of aspects of both the innate and adaptive immune response (Shirazi *et al.*, 2017). The cellular components of the innate immunity are myeloid cells, including monocytes, macrophages, dendritic cells, natural killer cells, as well as neutrophilic, basophilic and eosinophilic granulocytes (Kopf *et al.*, 1994; Janeway and Medzhitov, 2002; Frangogiannis, 2008; Paulson *et al.*, 2010). The central cellular components of the adaptive immune response are T- and B-cells that arise from lymphoid progenitor cells in the bone marrow (Mallat *et al.*, 2009; Epelman, Liu and Mann, 2015). During heart failure, there is a characteristic increase in circulating and myocardial pro-inflammatory cytokines that have been shown to promote pathological left ventricular remodelling (Ikeuchi *et al.*, 2004; Nian *et al.*, 2004). Pre-clinical and early human studies have indicated that cytokine antagonism could have a therapeutic role in heart failure (Rehsia and Dhalla, 2010; Kahlenberg, 2016). Poor characterisation of the cascade of events that occur as a result of inflammation during heart failure may play a key role in the failure of many immunomodulation trials.

1.4.4 Neurons

Modulation of myocardial function by the autonomic nervous system is mediated through the activity of sympathetic neurons. The peripheral neural networks mediate reflex control of the heart (Ardell *et al.*, 2016), such that the nervous system has tonic control over cardiac function in the quiescent environment and can effectively respond to stressors by altering the work done by the myocardium (Normand *et al.*, 2019). The finding that intercellular crosstalk between neurons and cardiomyocytes *in vitro* improves the function of both these cell types indicates that bidirectional interactions are vital for efficient myocardial function (Oh *et al.*, 2016).

The intercellular dependence between cardiomyocytes and neurons is also well documented in cardiac disease progression. In hyperglycaemia-related neuropathy secondary to diabetes, the risk of developing cardiac disease is higher than in non-diabetic patients (Gilbert *et al.*, 2006; Margariti, 2014). Conversely, neuronal dysfunction has also been shown to follow cardiac injury, which is a term that is given to any insult that triggers a molecular

cascade that culminates in cell death. In the healthy, adult myocardium, sympathetic control via norepinephrine activity enables the organ to respond to changes in cardiac demand and maintain homeostasis. However, remodelling in response to injury increases the heterogeneity of norepinephrine release. This heterogeneity is thought to increase the risk of arrhythmias, which are described as changes in rate or regularity of myocardial contractions due to abnormalities in the electrical impulses of the myocardium. The mechanisms of cardiac arrhythmias are typically divided into either (1) enhanced or abnormal impulse formation (i.e. focal activity) and (2) conduction disturbances (i.e. re-entry). The activity of neurons can either mask or accentuate the effects of either one of these mechanisms. As arrhythmias are a leading cause of mortality in patients with cardiac disease (Gardner *et al.,* 2016), greater understanding of the role neurons play in physiology and disease is crucial in developing our knowledge of the native myocardium.

1.5 Cardiac fibroblasts

1.5.1 Cardiac fibroblast origin in development and health

This project focuses on investigating the role of cardiac fibroblasts in the myocardium. Fibroblasts are characterised as being flat, spindle-shaped cells of mesenchymal origin, with multiple processes originating from their cell body (Camelliti, Borg and Kohl, 2005; Krenning, Zeisberg and Kalluri, 2010). Within fibroblasts is a highly granular cytoplasm and extensive rough endoplasmic reticulum (Camelliti, Borg and Kohl, 2005).

The principal origin of the cardiac fibroblasts in the cardiac interstitium and annulus fibrosis has been reported to be from the mesenchymal cells of the embryonic pro-epicardium (Christoffels, Burch and Moorman, 2004; Norris *et al.*, 2008). These mesenchymal cells migrate over the surface of the embryonic heart, eventually giving rise to the epicardium, and formation of epicardium-derived cells (EPDCs) (Lie-Venema *et al.*, 2007). The EPDCs in the primitive cardiac wall then undergo epithelial-mesenchymal transition (EMT) (Munoz-Chapuli *et al.*, 2001). This transition is thought to be driven by the influence of growth factors including platelet-derived growth factor (PDGF), fibroblast growth factor (FGF) and transforming growth factor (TGF) (Olivey *et al.*, 2006). This transition causes the cells to differentiate into the characteristic fibroblast phenotype (Gittenberger-de Groot *et al.*, 1998; Zhou *et al.*, 2010).

As well as the development of cardiac interstitial fibroblasts following EMT, studies have also identified fibroblasts present in the interventricular septum and right ventricle that are of endothelial origin (de Lange *et al.*, 2004). These endothelial-derived fibroblasts are thought to constitute 20% of the resident cardiac fibroblasts (Ali *et al.*, 2014; Moore-Morris *et al.*, 2014). Separate studies reported that endothelial cells in the region of the forming cardiac cushion delaminate and undergo endothelial-mesenchymal transition (EndMT) driven by cytokines TGF-β, PDGF, and Wnt (Armstrong and Bischoff, 2004; de Lange *et al.*, 2004). Following transformation, these cells invade the cardiac jelly and mature into the characteristic fibroblastic phenotype.

Markers currently used to determine the presence of fibroblasts target different populations of fibroblast-like cells, as summarised in **Table 1.2**. The lack of a robust cardiac fibroblast-specific marker indicates that there may be multiple spatio-temporal sources of

cardiac fibroblasts, hinting at considerable fibroblast heterogeneity in the native myocardium.

Protein	Function	Expressed by other cell types	Reference
α-Smooth muscle actin	Intermediate-filament associated protein	Smooth muscle cells, pericytes, myoepithelial cells	(Akpolat *et al.*, 2005; Azuma *et al.*, 2009)
Cadherin-9	Ca^{2+}-dependent adhesion molecule	Neurons; tumor vasculature	(Hirano, Suzuki and Redies, 2003; Thedieck *et al.*, 2007)
CD40	TNFα receptor family	Antigen presenting cells	(Smith, 2004)
CD248 (TEM1)	Collagen receptor	Pericytes, endothelial cells	(MacFadyen *et al.*, 2005; Bagley *et al.*, 2008)
Discoidin domain receptor 2 (DDR2)	Collagen-binding tyrosine kinase receptor	Smooth muscle, hepatic stellate cells, endothelial cells	(Mohan, Mohan and Wilson, 2001; Olaso *et al.*, 2001; Vogel, Abdulhussein and Ford, 2006)
Fibroblast activation protein-1 (FAP1)	Serine protease (gelatinase)	Activated melanocytes	(Rettig *et al.*, 1993; Ramirez-Montagut *et al.*, 2004)
Fibroblast-specific protein-1	Intermediate-filament associated Ca^{2+}-binding protein	Smooth muscle cells, invasive carcinoma cells	(Strutz *et al.*, 1995; Sugimoto *et al.*, 2006)
Fibroblast surface antigen (FSA)	Fibronectin-binding molecule	Monocytes/macrophages	(Wartiovaara *et al.*, 1974)
Heat shock protein-47 (HSP47)	Collagen-binding serpin chaperone	Monocytes/macrophages, various collagen-producing cells	(Shioshita *et al.*, 2000; Sauk, Nikitakis and Siavash, 2005)
Platelet-derived growth factor receptor- β	Receptor tyrosine kinase	Smooth muscle cells, pericytes	(Lindahl *et al.*, 1997; Kaur *et al.*, 2009)
Prolyl-4-hydroxylase	Collagen biosynthesis	Endothelial cells, epithelial cells	(Mussini, Hutton and Udenfriend, 1967; Langness and Udenfriend, 1974)
Thymus cell antigen-1	Cell adhesion molecule	Leukocytes, endothelial cells, various progenitor cells	(Wetzel *et al.*, 2006; Dezso *et al.*, 2007)
Vimentin	Intermediate-filament associated protein	Endothelial cells, smooth muscle cells, pericytes, myoepithelial cells	(Franke *et al.*, 1979; Mork, van Deurs and Petersen, 1990)

Table 1.2 Fibroblast markers and co-expression in non-fibroblast cell types *(adapted from Krenning, Zeisberg and Kalluri, 2010).*

Despite there being no consensus on markers that exclusively distinguish fibroblasts, discriminative markers have been identified for organ-specific subsets of cells that display the fibroblastic phenotype. For example, in both human and mouse cardiac tissue, the collagen-activated receptor tyrosine kinase discoidin domain receptor 2 (DDR2) and the intermediate-filament associated Ca^{2+}-binding protein S100A4 (also known as fibroblast-specific protein 1 (FSP-1)) are thought to be expressed primarily by cardiac fibroblasts (Camelliti, Borg and Kohl, 2005; Banerjee *et al.*, 2007). Gene single cell analysis and genetic lineage tracing, together with the finding of organ-specific markers of fibroblastic cells, indicate that the cardiac fibroblast population may not be as diverse as previously thought (Kanisicak *et al.*, 2016; Moore-Morris *et al.*, 2018).

1.5.2 Cardiac fibroblasts in pathology

A major hallmark of the onset of cardiac disease is an increase in the activity of cardiac fibroblasts (Porter and Turner, 2009). The activation of fibroblasts substantially increases the expression of intracellular myofilament bundle, and these cells are often called myofibroblasts because of the identification of these bundles by alpha-smooth muscle actinin (α-SMA) antibody (Camelliti, Borg and Kohl, 2005). This is often used as a marker of myofibroblast phenotype. But, as alluded to by the name, this is also expressed by smooth muscle cells so is used together with the absence of markers against other cell types to identify fibroblasts (**Table 1.2**).

The consensus for many years was that the cardiac fibroblasts in disease originate from the native resident pool of fibroblastic cells in the myocardium (Krenning, Zeisberg and Kalluri, 2010). More recent studies have indicated that fibroblasts from beyond the myocardium are also involved in disease remodelling. Haematopoietic bone marrow-derived cells have been shown to be a substantial source of fibroblasts recruited in disease. Mice received a transplant with green fluorescent protein (GFP)-expressing bone marrow before myocardial infarction (van Amerongen *et al.*, 2008; Kania *et al.*, 2009) or injury by aortic banding (Zeisberg *et al.*, 2007). Fibroblasts expressing GFP were subsequently found in the fibrotic cardiac tissue of these mice. These bone-marrow derived fibroblasts have been reported to represent 25-60% of all fibroblasts at the site of cardiac injury, but numbers are seen to be highly reduced 2 weeks post-myocardial infarction (van Amerongen *et al.*, 2008).

Greater understanding of these fibroblastic cells will enable us to determine if these are truly fibroblasts or display a phenotype of inflammatory cells.

As well as haematopoietic bone marrow-derived cells being a prominent source of fibroblastic cells in disease, monocyte-to-fibroblast transition has also been reported in studies that investigate non-acute forms of cardiac disease. Haudek and colleagues reported that these cells of fibroblastic morphology express markers of both monocytes (CD45;CD11b) and active fibroblasts (S100A4, αSMA) and account for 3% of all non-myocytes components of the myocardium in ischaemic cardiomyopathy (Haudek *et al.*, 2008). Other studies have reported the presence of monocyte-derived fibroblasts in myocardial infarction and pressure overload animal models (Endo *et al.*, 2007; Fujita *et al.*, 2007). In studies that inhibited the recruitment of monocytes, both the cardiac fibroblast population and myocardial remodelling that occurs following myocardial infarction were diminished (van Amerongen *et al.*, 2007). The distinct potential origins that have been reported for cardiac fibroblasts make it difficult to attribute the effects of fibroblastic cells in development, health and in disease. It indicates that we must consider cardiac fibroblasts as a heterogeneous population of cells. In our study, we utilise human cardiac fibroblasts *in vitro*, and we must consider the changes that occur to these cells in culture.

1.5.3 Cardiac fibroblasts *in vitro*

Studies that utilise human cardiac fibroblasts *in vitro* isolate primary cells from myocardial tissue and rely on the proliferative and adhesive properties of fibroblasts to isolate these from other cell types. However, the dynamic nature of the fibroblast phenotype leads to changes in phenotype, including cell activity, in culture. A major driver of increase in fibroblast activity is the change in mechanical force induced by the rigidity of culture substrates such as plastic and glass substrates. Goffin and colleagues identified that substrates with a stiffness <15 kPa reduces expression of α-SMA (Goffin *et al.*, 2006). Glass, by comparison, has an elastic modulus in the 10-20 GPa range. Further evidence for this phenotype dependency on substrate stiffness has been shown in studies that suspend fibroblasts in softer, three-dimensional culture conditions. Fibroblasts in this environment show reduced α-SMA expression and have a cell morphology closer to the quiescent state reported for cardiac fibroblasts *in vivo* (Vozenin *et al.*, 1998; Perrone *et al.*, 2003).

1.5.4 Cardiac fibroblast paracrine signalling

Cardiac fibroblasts secrete a vast array of bioactive substances. Paracrine mechanisms from cardiac fibroblasts have been implicated in cardiomyocyte hypertrophy, contributing to impaired cardiac function (Gray *et al.*, 1998; Jiang *et al.*, 2007). Factors including TGF- β, Interleukin-6 (IL-6) and endothelin 1 (ET-1) have been identified as playing a major role in regulating cardiomyocyte function (Cartledge *et al.*, 2015).

Secretion of TGF-β, typically induced by changes in mechanical loading (Bujak and Frangogiannis, 2007), results in cardiomyocyte hypertrophy (Gray *et al.*, 1998) and profound electrophysiological changes (Cartledge *et al.*, 2015). IL-6 is also associated with cardiomyocyte hypertrophy, alongside diastolic dysfunction and reduced expression of SERCA2a (Wu *et al.*, 2011). ET-1 induces a potent hypertrophy in cardiomyocytes and its expression directly correlates with ventricular remodelling (Inada *et al.*, 1999; Tsutamoto *et al.*, 2000). At the whole heart level, the changes mediated by paracrine signalling are initially protective, but ultimately result in maladaptive remodelling (Ikeuchi *et al.*, 2004).

This complexity of cardiac fibroblast-cardiomyocyte intercellular interactions was further demonstrated by our group in a study that identified that cardiomyocyte Ca^{2+} transient amplitude, a measure of Ca^{2+} availability for contractile function, is reduced by co-culture with myofibroblasts, but increased when in culture with freshly isolated fibroblasts (Cartledge *et al.*, 2015). We must continue in our efforts to delineate these complex pathways if we are to utilise cardiac fibroblasts in the modulation of cardiomyocytes in therapies.

1.5.5 Cardiac fibroblast function through electronic coupling

Cardiac fibroblasts are considered to be a non-excitable cell type, but are thought to contribute to cardiac electrophysiology. Cardiac fibroblasts have been shown to have a high cell membrane resistance, making them good conductors for electrical signals (Kohl, 2003). Cardiac fibroblasts and cardiomyocytes have been shown to be coupled through connexins, hemichannels that form gap junctions between the two cell populations. Connexin-43 and connexin-45 have been identified between cardiac fibroblasts and cardiomyocytes (Kohl, 2003; Chilton, Giles and Smith, 2007). Studies have shown that there is measurable electronic coupling between the two cell types, mediated by connexins (Gaudesius *et al.*, 2003; Miragoli, Gaudesius and Rohr, 2006). This allows for cardiomyocytes that would otherwise be

separated by the insulating extracellular scaffold to be bridged electrically, aiding synchronicity of electrical activity in the native myocardium (Rohr, 2004).

1.6 Non-soluble intercellular signalling

There is growing evidence that paracrine interactions in the myocardium can be achieved via non-soluble mediators. Extracellular vesicles (EVs) were first reported in 1981, by Trams and colleagues who identified that cell culture supernatant in rat glioma and mouse neuroblastoma cells displayed plasma membrane ATPases and 5'-nucleotidease enzyme activity (Trams *et al.*, 1981). To this day, every mammalian cell type has been demonstrated to produce EVs in culture (Yáñez-Mó *et al.*, 2015).

EVs have been implicated in physiology and in disease. Much work has investigated the role of EVs in carcinogenesis, and these have been implicated in the processes of proliferation, angiogenesis, immunosuppression and preparation of pre-metastatic niches in secondary organs (Ruivo *et al.*, 2017). It has been widely reported that EVs mediate both local and systemic intercellular communication through the horizontal transfer of information via microRNAs, long non-coding RNAs, proteins, mRNAs, metabolites and other substances (**Figure 1.3**) (de Jong *et al.*, 2012; Sung *et al.*, 2015; Purushothaman *et al.*, 2016; Li *et al.*, 2017; Paolillo and Schinelli, 2017). Fibroblast-secreted EVs have also been implicated as an important modulator of cardiomyocyte function in disease. Rat fibroblast secretion of miR-21 in EVs has been shown to induce mice cardiomyocyte hypertrophy (Bang *et al.*, 2014). However, the role of human cardiac fibroblasts in regulating human cardiomyocyte function has yet to be explored.

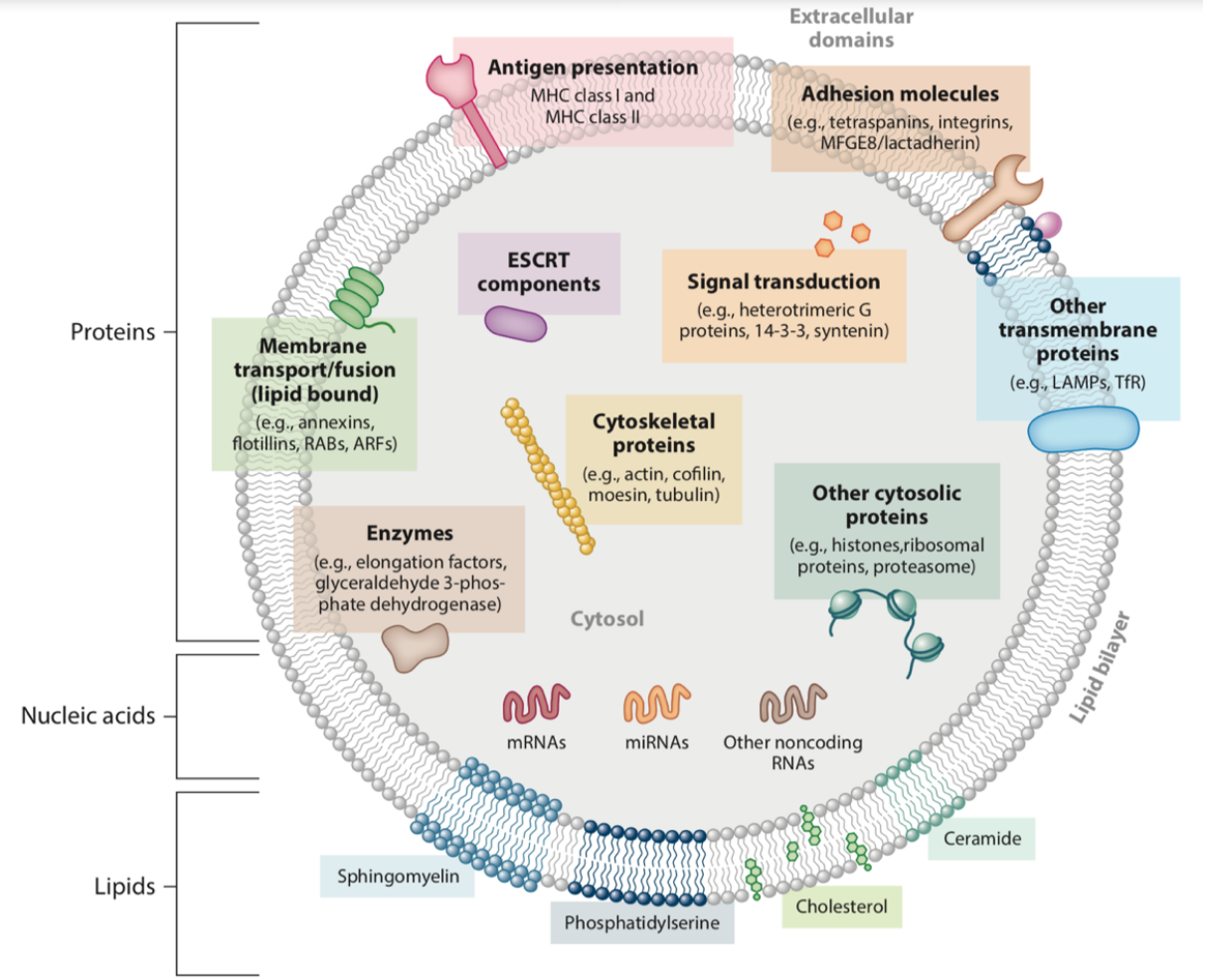

***Figure 1.3 Extracellular vesicle (EV) composition**. Schematic representation of the composition of EVs. ARF = ADP robosylation factor; ESCRT = endosomal sorting complex required for transport; LAMP = lysosome-associated membrane protein; MHC = major histocompatibility complex; MFGE8 = milk fat globule-epidermal growth factor-factor VIII; RAB = Ras-related protein in brain; TfR = Transferrin receptor. (Colombo, Raposo and Théry, 2014).*

1.6.1 EV classification

There are two major classes of EVs produced from non-apoptotic cells – exosomes and microvesicles (**Figure 1.4**). These are distinct in their biological origins, size distributions and expression of marker proteins. However, current methods for isolating and purifying EVs are unable to separate these populations from a mixed biological sample (Aalberts *et al.*, 2012; Bobrie *et al.*, 2012; Willms *et al.*, 2016).

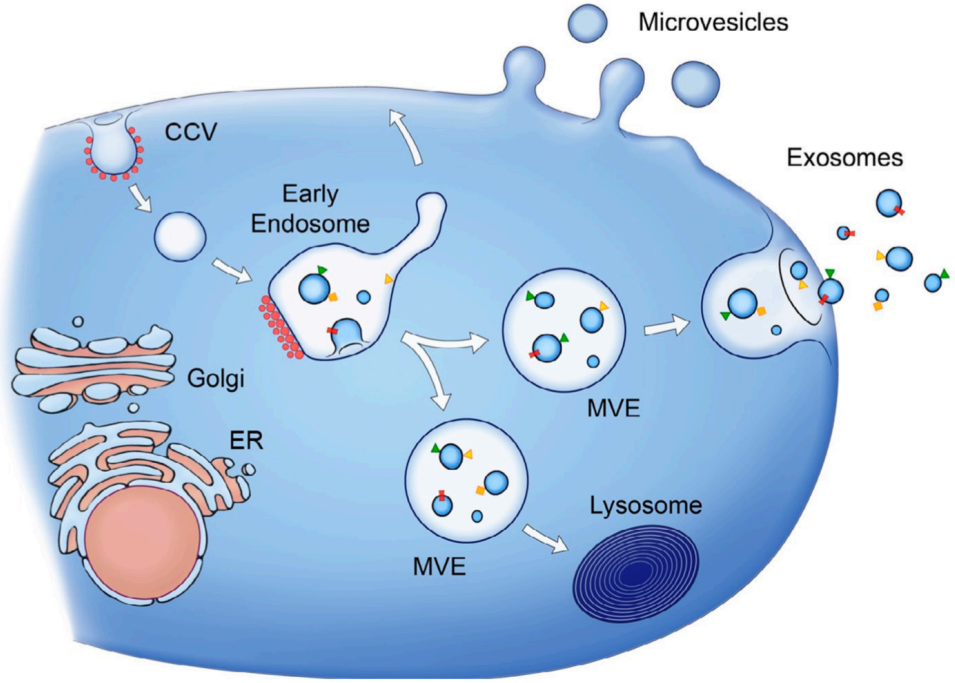

***Figure 1.4 Release of microvesicles and exosomes**. Microvesicles are formed by direct budding from the plasma membrane. Exosomes are smaller vesicles formed as intraluminal vesicles by budding into early endosomes and multivesicular endosomes. The multivesicular endosomes fuse with the plasma membrane to release exosomes. CCV = Clathrin coated vesicle, ER = endoplasmic reticulum, MVE = multivesicular endosome. (Raposo and Stoorvogel, 2013).*

1.6.1.1 Exosome synthesis and release

Exosomes are formed by a multistep process, producing vesicles 40-100 nm in diameter. In this process, late endosomal vesicles invaginate, allowing cytosolic material to be encapsulated in internal vesicles (multivesicular bodies (MVBs)) (Subra *et al.*, 2007; Colombo, Raposo and Théry, 2014). Although the mechanism for MVB formation is yet to be fully delineated, it is likely that there are multiple pathways. To the best of the authors knowledge, there are at least three mechanisms – ceramide-dependent, tetraspanin-dependent and ESCRT (endosomal sorting complexes required for transport) dependent (Colombo, Raposo and Théry, 2014). It is not known why cells are dependent on different pathways and whether the pathways act simultaneously. It has been shown that the exosome synthesis mechanism affects the cargo content in vesicles, and blocking of one pathway changes EV content produced by others (Nazarenko *et al.*, 2010; Colombo, Raposo and Théry, 2014). Therefore, while some studies use chemical inhibition of EV production, such as

GW4869-mediated inhibition of ceramide-dependent exosome production (Trajkovic *et al.*, 2008), there are currently no stringent mechanisms for blocked exosome synthesis and release. Studies that utilise any techniques that target EV biogenesis pathways must be interpreted with caution.

In contrast to exosomes, microvesicles are 80-200nm in diameter and formed by direct budding from the plasma membrane (Raposo and Stoorvogel, 2013). The mechanism for microvesicle formation and release is even less well known than that of exosomes. However, early reports demonstrated that it was highly dependent on cytoskeletal activity (Liepins, 1983). Colchicine, vinblastine and cold temperatures, all of which disrupt the microtubule cytoskeleton, have been shown to induce microvesicle formation and shedding (Muralidharan-Chari *et al.*, 2010). Delineating the mechanism for formation and release of exosomes and microvesicles will help us to determine their role in physiology and therapeutic potential.

1.6.2 EV interactions with recipient cells

The evidence to support the role of EVs in intercellular interactions include studies that demonstrate that the luminal content of EVs are delivered to and internalised by target cells. The use of fluorescent dye labelling (Feng *et al.*, 2010) and luciferase-based (Montecalvo *et al.*, 2012) approaches has allowed real time observations of functional transfer of macromolecules. Although it would be plausible that there is direct membrane fusion of the liposome-like EVs and the recipient cells, this can only occur if the membranes are of similar fluidity. As EVs and their parent cells are distinct in their membrane composition, this passive membrane fusion can only occur with certain cell types so cannot account for all intercellular EV transfer observed. Studies have demonstrated that the internalisation of EV content is cytoskeleton-dependent, requiring endocytosis or phagocytosis (Mulcahy, Pink and Carter, 2014). Beyond this, the mechanism for EV selectivity for recipient cells is unknown but understanding how EVs can recognise their target would help unlock their potential in drug therapeutics as a mechanism for delivery of therapies to specific recipient cell types.

As the topology of EVs is similar to cells, with extracellular ligands and receptors positioned on the outside, ligand-receptor interactions between the EV membrane and the recipient cell are likely to play a key role in the targeting of EVs to cells. This interaction has

been shown in some cell types to be the mechanism by which EVs can modulate cellular activity. For example, natural killer (NK) cell-derived EVs have been shown to display both markers of NK cells as well as Fas ligands on the surface, the latter a key inducer of programmed cell death. It was shown that the crosslink with recipient cell surface death receptors induced apoptosis in various cell types. In this way, EV interaction with the recipient cell without the transfer of vesicular content can mediate the intercellular interactions.

1.6.3 EV isolation

Part of the reason why there are limited studies into EV activity is that the isolation and detection of EVs is often a complicated process with many steps. When starting from cell culture media or biofluids, EVs are often present in relatively low quantities, yet potential contaminants (typically soluble proteins in cell culture media, but also large protein and lipoprotein complexes in biofluids and plasma) are present in relatively high quantities (Li *et al.*, 2017). These contaminants may potentially themselves be bioactive and able to influence biological activity, leading to false or exaggerated identification of EVs as signalling molecules. There is an increasing concern in the field of EV research that some commonly used isolation techniques are prone to contamination or excess loss of EVs (Gámez-Valero *et al.*, 2016; Benedikter *et al.*, 2017; Monguió-Tortajada *et al.*, 2019).

Isolation of EVs is further hampered by the presence of lipoprotein particles in conditioned media. These particles often have a density and diameter similar to EVs. Consequently, isolation of vesicles from serum-containing media by density-gradient ultracentrifugation results in co-isolation of high-density lipoprotein (HDL) and isolation of HDL results in co-isolation of vesicles (Vickers *et al.*, 2011; Wagner *et al.*, 2013). A fast and simple alternative to ultracentrifugation for the separation of vesicles from serum-rich samples involves the replacement of the serum by buffer in a process called size-exclusion chromatography (SEC), also known as 'gel filtration' (Grubisic, Rempp and Benoit, 2011; Boing *et al.*, 2014). In this process, isolated fractions with the highest concentrations of particles within the diameter range for exosomes also contain less than 5% of HDL and less than 1% of proteins. As chromatography produces a purer population of EVs than ultracentrifugation, it will be employed in this project in investigations of EV function in cardiac fibroblast-cardiomyocyte crosstalk.

1.7 Cardiac ECM

Cardiac fibroblasts are widely known for role they play in the synthesis and degradation of the cardiac ECM, which form the crucial mechanical scaffold for cardiomyocytes. The complex tissue and organ architecture of the heart is maintained by extensive ECM networks. These networks are composed of fibrous proteins (e.g., collagen, elastin), adhesive glycoproteins (e.g., fibronectin, laminin), and proteoglycans. The ECM serves multiple purposes; (1) it forms an organizational network that surrounds and interconnects cells and provides scaffold for cardiac cell types, (2) it distributes mechanical forces throughout the cardiac tissue and conveys mechanical signals to individual cells, contributing to the stress-strain relationships of the heart and (3) electrically separates the atria and the ventricles to facilitate proper cardiac contraction (Zhou *et al.*, 2010).

Cardiac fibroblasts mediate 5% turnover of the ECM every day (Bonnin, Sparrow and Taylor, 1981; McAnulty and Laurent, 1987). In response to several growth factors (e.g., TGFβ, PDGF), cytokines (e.g., TNFα, IL1β, IL6) or mechanical stimulation (e.g., stretch), cardiac fibroblasts produce the fibrillar collagens type I and type III that together comprise approximately 90% of all collagen in the heart, as well as the less abundant ECM molecules collagen types IV, V, VI, elastin, and laminin (Bosman and Stamenkovic, 2003). Alternatively, activated cardiac fibroblasts modulate the turnover of ECM components by modulating the expression of the matrix metalloproteinases (MMPs) and their natural inhibitors that mediate ECM remodelling (tissue inhibitor of MMP; TIMP) (Tsuruda, Costello-Boerrigter and Burnett, 2004). Following an MI, the myofibroblasts are often found within the area of infarct. Following the onset of more diffuse disease, such as in ischaemic cardiomyopathy, myofibroblasts are found more interstitially. In either case, they alter the balance of ECM turnover such that there is increased laying down of ECM components, driving the changes that occur in myocardial remodelling (Porter and Turner, 2009).

1.7.1 ECM in disease

In general, net deposition of collagen in the adult human myocardium is limited. However, an increase in expression of growth factor following cardiac injury and the subsequent changes in enzyme activity leads to an increase in the laying down of cross-linked ECM proteins, which form scar tissue (Gurtner *et al.*, 2008). The active fibroblasts then

undergo apoptosis, causing cessation of ECM protein production. In the case of cardiac injury, cardiac fibroblasts overcome this negative feedback regulation such that the laying down of ECM components persists, which causes further cardiac dysfunction and progression to heart failure. The mechanism by which cardiac fibroblasts avoid the regulatory mechanisms are unclear, but understanding the stimuli that cause cardiac fibroblast activation could enable us to manipulate cardiac fibroblast function.

The increased deposition of ECM proteins in the myocardium is a hallmark of heart disease. This is associated with cardiac fibrosis that is either termed "reactive interstitial fibrosis" when there is expansion of the cardiac interstitium without significant cardiomyocyte loss, or "reparative fibrosis" when there is formation of a scar in response to ischaemic injury such as following a myocardial infarction (Anderson, Sutton and Lie, 1979; Weber, 1989). The laying down of collagen within (endomysial) and around (perimysial) the bundles of contractile cardiomyocytes causes interstitial fibrosis. In contrast, the laying down of collagen deposits in the adventitia of coronary arterioles is termed perivascular fibrosis. In animal models of left ventricular pressure overload, there is initial reactive interstitial fibrosis as well as perivascular fibrosis. The interstitial fibrosis without significant loss of cardiomyocytes is coupled with cardiomyocyte hypertrophy as an adaptive response to the overload and an attempt to maintain cardiac output while normalising stress. However, the increase in ECM proteins in the myocardium causes an increase in mechanical stiffness, leading to dysfunction in the contractility of the heart (Chaturvedi *et al.*, 2010). The formation of a fibrotic scar following cardiac injury also becomes a barrier at that interferes with physiological propagation of electrical signals between cardiomyocytes, increasing the risk of arrhythmias (Spach and Boineau, 1997). As cardiomyocytes eventually undergo necrosis and apoptosis, reparative fibrosis starts to take place during chronic adaption to haemodynamic overload (Isoyama and Nitta-Komatsubara, 2002). The thickening of the ECM around hypertrophied cardiomyocytes as well as the perivascular fibrosis is thought to contribute to a mismatch in the supply and demand of nutrients, leading to cell death (Kai *et al.*, 2006).

1.7.2 ECM-cardiomyocyte interactions via integrins

Beyond its role as a scaffold for three-dimensional formation of the myocardium, the ECM has also been shown to modulate intracellular signalling in myocytes and non-myocytes. The ability of ECM proteins to bind to cardiomyocytes is mediated by integrins; non-covalently associated, heterodimeric, transmembrane receptors formed from a family of alpha or beta subunits (Ruoslahti and Pierschbacher, 1987). Their positioning and signalling is shown in **Figure 1.5**. Integrins were first identified in studies that suggested physical interactions between fibronectin in the ECM and intracellular cytoskeleton. Studies then identified glycoproteins with characteristics of membrane proteins and antibodies against these proteins prevented cellular adhesion. The importance of these in maintaining the integrity of interactions between extra- and intra-cellular environments led to their classification as 'integrins'. Integrins function by mechanically binding the ECM to cell cytoskeleton and sense when adhesion of cells to the ECM has occurred (Harston and Kuppuswamy, 2011).

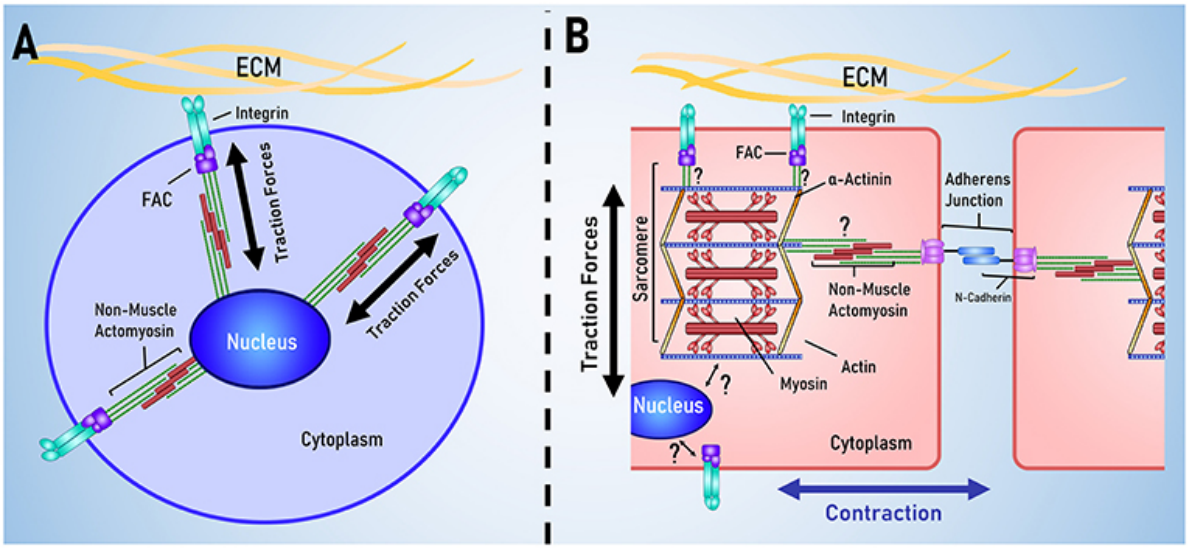

Figure 1.5 Integrin positioning and signalling in stem cells and cardiomyocytes. *In both stem cell and cardiomyocytes, integrins in the cell membrane bridge communications between the extracellular matrix (ECM) and intracellular structures. (A) in stem cell models of mechanotransduction, mechanical signals received by integrins result in traction force generation by non-muscle actinomysin. (B) in cardiomyocytes, integrins in the sarcolemmal membrane bridge communication between the ECM and aligned muscle actinomysin. Cardiomyocytes also have intercalated disks; intercellular links for mechanical and electrical coordination of contraction between neighbouring cardiomyocytes. FAC, focal adhesion complex* (Chin, Hool and Choi, 2019)

1.7.2.1 Integrins in health

The importance of integrin-mediated interactions with the ECM in cardiac morphogenesis and maintaining the adult phenotype has been shown in animal studies. Ablation of α5 integrin, which forms major interactions with fibronectin in the ECM, disrupts cardiac chamber specification in mouse embryos in a manner that is similar to studies in which fibronectin is knocked down (Pulina *et al.*, 2011; Mittal *et al.*, 2013). β1 integrins knockdown has been shown to be critical in embryonic development, as knockdown causes embryonic lethality in mice (Stephens *et al.*, 1995). Inducible knockout of β1 integrin later in mouse myocardium development prevented proper compaction of ventricles, causing progressive fibrosis in the myocardium and ultimately led to dilated cardiomyopathy in subjects (Shai *et al.*, 2002; Ieda *et al.*, 2009).

The principal integrin-binding domain of integrin ligands is a tripeptide sequence of Arginine-Glycine-Aspartic acid (RGD) (Ruoslahti and Pierschbacher, 1987). Soluble peptides with this RGD-tripeptide sequence have been used to assess the effect of integrin activation in an *in vitro* setting (Yu *et al.*, 2011). Studies investigating the mechanisms mediating integrin function have identified integrin localisation to cardiomyocyte costameres, serving as an anchor to strengthen the Z-disc of cardiomyocytes and the connection to the sarcolemma membrane (Israeli-Rosenberg *et al.*, 2014). Integrins have also been found at the intercalated discs, forming intercellular connections between cardiomyocytes (Zhang *et al.*, 2001). Integrins have been shown to play a vital role in the assembly of costamere. Costameres are sensitive to mechanical force, such that force-dependent changes in the load-bearing molecules present at the ECM attachment sites alters the biochemical activities of these molecules, causing stress-dependent remodelling of the costameric site and signal transduction. The external mechanical forces elicited by ECM proteins regulate costamere assembly, such that arresting contraction has been shown to cause integrin loss from costameres and conversely, stretch has been shown to increase integrin expression in cardiomyocytes (Sharp *et al.*, 1997). These studies all show that integrins are key determinants of the cardiomyocyte response to extracellular stimuli in physiology.

1.7.2.2 Integrins in pathology

Due to their integral role in maintenance of the myocardium in physiology, cardiomyocyte integrin-ECM interactions are also fundamental in bringing about the hypertrophic response to changes in mechanical load (Harston and Kuppuswamy, 2011). Genetic ablation of either β1 or β3 integrins in mice inhibit compensatory hypertrophic growth in response to pressure overload, causing a reduction in cardiac output and an increase in the rate of progression to heart failure (Li *et al.*, 2012). Mechanical stress has been shown to signal via integrins to initiate formation of focal adhesion complexes (FACs) (Kuppuswamy *et al.*, 1997; Laser *et al.*, 2000). Complex formation has been shown to mediate downstream pro-survival signalling through PI3K/AKT and caspase inhibition (Menon *et al.*, 2007; Johnston *et al.*, 2009). In addition, induction of mTOR via cardiomyocyte integrin-ECM interactions also enhance protein synthesis and cell growth (Balasubramanian and Kuppuswamy, 2003).

A less well studied manner in which integrins mediate the response to cardiac disease is via direct mechanotransduction. Changes in the extracellular mechanical environment of cardiomyocytes can be translated directly to the nucleus via the cytoskeletal network, potentially altering nuclear shape, chromatin organisation, DNA replication, gene transcription and RNA translation (Ross and Borg, 2001; Wang, Tytell and Ingber, 2009). In this way, integrin-mediated signalling pathways underlie the sensitivity of cardiomyocytes to mechanical stresses induced by the ECM (Brancaccio *et al.*, 1999; McCain and Parker, 2011). The study by Brancaccio and colleagues identified that melusin, a muscle-specific protein that interacts with the cytoplasmic domain of integrin β1, is essential for the hypertrophic response to mechanical overload (Brancaccio *et al.*, 2003). Melusin-null mice had normal myocardial structure and function in physiological conditions, but when these mice were subject to pressure overload, they did not demonstrate the hypertrophic response identified in wild-type control. Instead, the melusin-null mice demonstrated abnormal remodelling characterised that culminated in dilated cardiomyopathy and cardiac dysfunction (Brancaccio *et al.*, 2003). This indicates that integrins play critical role in disease. However, the complexity of interplay between cardiomyocyte subtypes makes delineation of key pathways difficult.

1.7.2.3 Integrins in EC-coupling

Early *in vitro* animal studies identified crucial roles for integrins in cardiomyocyte contractile function. Cardiac fibroblast-derived ECM expressing integrin ligands have been used as a culture substrate for neonatal rat ventricular myocytes (NRVMs), increasing spontaneous activity, metabolic activity and expression of key proteins involved in cardiomyocyte contractile function (Guo *et al.*, 2013; Zeng *et al.*, 2013). The α7β1 integrins in rats have been shown to have a protective role in ischaemia-reperfusion injury, protecting cardiomyocyte mitochondria from Ca^{2+} overload and preventing cell death (Okada *et al.*, 2013). This same study also identified that β1D integrin splice variants co-localise with RyRs in transverse (T)-tubules of adult cardiomyocytes. The direct physical interactions between the cytoplasmic tail of integrins and the cytoplasmic aspect of RyRs were found to decrease the opening probability (P_o) of RyRs in a manner dependent on ECM interactions (Okada *et al.*, 2013).

Nitric oxide (NO) has been shown to be a common transducer of ECM integrin signalling. Stretch of the myocardium is associated with an increase in nitric oxide synthesis (Pinsky *et al.*, 1997; Prendergast, Sagach and Shah, 1997; Petroff *et al.*, 2001) as well as increasing the force-frequency response (Khan *et al.*, 2003). The role of NO in the modulation of $I_{Ca,L}$ has been demonstrated by studies that utilise SNAP, a S-nitrosothiol, which augments beta-adrenergic stimulation of $I_{Ca,L}$ (Abi-Gerges *et al.*, 2002).

NO has also been proposed to directly activate Ca^{2+} release from the SR via activation of RyR2. Van der Wees and colleagues have investigated the role of integrin stimulation on Ca^{2+} cycling in NRVMs and identified that soluble pentapeptides with the integrin-binding Arginine-Glycine-Aspartic acid (RGD) domain increase Ca^{2+} release from the SR and proposed that this is due to S-nitrosylation of RyR2 and/or L-type Ca^{2+} channels (Van Der Wees *et al.*, 2006). In their study, the effects of RGD peptides and NO donors are additive, and thus they propose that there are at least two independent pathways that contribute to the modulation of SR Ca^{2+} release from RyRs (Van Der Wees *et al.*, 2006).

Integrins have also been shown to modulate adrenergic regulation of cardiomyocyte Ca^{2+} cycling. Overexpression of β1A in NRVMs causes a reduced response of cardiomyocytes to beta-adrenergic receptor agonist isoproterenol (Cheng, Ross and Walsh, 2004), but induced cardiomyocyte-specific excision of the β1 integrin gene in adult mouse

cardiomyocytes blunted the hypertrophic response of these cardiomyocytes and also caused defective hypertrophic-stress signalling in the intact mouse heart (Li *et al.*, 2012). It is clear that integrins have a critical role in modulation of EC-coupling in physiology and disease, and multiple pathways finely tune the contractile function of the cardiomyocyte.

1.8 *In vitro* models of heart disease

Virtually all models used for drug screening and disease modelling heavily rely on the use of cardiomyocytes from animal models or isolated human adult cardiomyocytes (Parameswaran *et al.*, 2013; Li *et al.*, 2014). Among the challenges of current human and animal models are high costs, difficulties in manipulation and ethical issues (Wang, Kit-Anan and Terracciano, 2018). These *in vitro* models also lack much of the biological and mechanical properties of the complex myocardium, so they are thought to poorly predict the mechanisms regulating the structure and function of the native myocardium. The limitations to current models must be overcome if we are to accurately model human cardiac disease.

1.8.1 Adult human cardiomyocytes

Isolated adult human cardiomyocytes have been used to investigate cardiomyocyte function as well as how the contractile capabilities can be modulated *in vitro* (Bird *et al.*, 2003). Isolated adult human cells are able to mirror aspects of the progressive of disease (Nguyen *et al.*, 2017; Wang *et al.*, 2017). However, these tissues are of limited availability, and even following isolation from consenting adults, there is rapid loss of key cardiomyocyte ultrastructural features required for efficient production of contractile force (Dispersyn *et al.*, 2001; Zhang *et al.*, 2010). Therefore, adult human cardiomyocytes are thought to only provide a snapshot of cardiac disease progression.

1.8.2 Animal cardiomyocytes

The limitations of adult human cardiomyocytes has led to much research utilising animals as a source of cardiomyocytes in cardiac research. Historically, animal models were developed either from defined genetic backgrounds that mimic some human conditions or by imposing acute interventions such as coronary obstruction to mimic the initial type of insult

such that we can investigate single, discrete time points in disease progression (Ericsson, Crim and Franklin, 2008; Henrique Franco, 2013). Studies using small animals have aided advancement in understanding molecular pathways in heart failure and models with large animals have provided preclinical proof of concept of novel therapies before clinical trials with human subjects (Erickson, 1988; Smithies, 1993; Whitelaw *et al.*, 2016). Animal cardiomyocytes therefore still provide some use in cardiac research.

However, animal cardiomyocytes are still intrinsically limited in their ability to model adult human cardiomyocyte function (Klocke *et al.*, 2007; Bracken, 2009; Shanks, Greek and Greek, 2009). Gene expression silencing and drug- or surgically-induced pathogenesis often employed in animal studies do not recapitulate the native, complex initiation of cardiac disease in humans (Wang, Kit-Anan and Terracciano, 2018). As a result, compensatory mechanisms may mask the pathways for disease progression in humans. In addition, the specificity of many human cardiac diseases to the human species also prevents animal studies from fully recapitulating cardiomyocyte function in disease models and drug discovery. Rodent models are thought to only correctly predict human toxicity in 43% of cases (Olson *et al.*, 2000). Despite these limitations in the use of animal cells, they do overcome the availability issue of adult human cardiomyocytes.

1.8.3 Human specific expression in animal cells

Species mismatch in animal cardiomyocytes and limited availability of human cardiomyocytes led to the development of models that use human-specific ion channel expression in animal cells. A source of cells widely used are Chinese Hamster Ovary (CHO) cells (Johns, Nuss and Marban, 1997). While much of the burden of disease is acquired due to environmental factors, a substantial proportion of it is inherited so can be modelled by expression human genes in animal cells (Dumont *et al.*, 2016). The expression of human ion channels in animal cells goes some way to mitigate the species mismatch in animal studies. However, investigation of the activity of a single ion channel often does not recapitulate the complex progression of human disease (Braam, Passier and Mummery, 2009).

1.8.4 Stem cells and derivatives

A major asset in our search for models that accurately represent the human myocardium has been the development of human stem cell-derived cell types. Stem cells are undifferentiated cells that have indefinite renewal potential through mitotic cell division and have the capacity to differentiate into specialised cell types. Pluripotent stem cells have the ability to differentiate into any type of somatic cell, and include embryonic stem cells (ESCs) and induced pluripotent stem cells (iPSCs).

The first human stem cell-derived cell types were derived from human embryonic stem cells (hESCs) over 20 years ago (Thomson *et al.*, 1998; Takahashi *et al.*, 2007; Shelton *et al.*, 2016). The genes encoding transcription factors implicated as being pivotal in the maintenance of pluripotency were *Oct4, Sox2* and *Nanog* (Boyer *et al.*, 2005; Loh *et al.*, 2006). The unique ability for unlimited self-renewal and differentiation into all adult cell types made these cells an attractive tool for research (Smith, 2001). However, unless the embryo for the hESCs carried a specific, highly-penetrant disease mutation, hESC-derived cell types had poor predictive value. Importantly, the sourcing and use of these cells involved major ethical issues which limit their use (Deb and Sarda, 2008).

1.8.4.1 Generation of iPSCs

A more recent approach for producing stem cell-derived cell types, including cardiomyocytes, came following the production of iPSCs (Takahashi and Yamanaka, 2006). There are many approaches to achieve pluripotency from differentiated cell types and are extensively described elsewhere. These include somatic cell nuclear transfer (Campbell *et al.*, 1996; Hochedlinger and Jaenisch, 2003), cell fusion (Taranger *et al.*, 2005), transduction of transcription factors (Singh *et al.*, 2015) and reprogramming with small molecules (Singh *et al.*, 2015). The most common reprogramming technique involves the direct reprogramming of somatic adult murine cells using transcription factors encoded by four genes – *Oct4, Sox2, Klf4,* and *c-Myc* - enabled production of these iPSCs, which had the capability of differentiation into any of the primary germ layers (Okita, Ichisaka and Yamanaka, 2007). This was followed by the generation of human iPSCs (hiPSCs), using the gene set of *Oct4, Sox2, Nanog* and *Lin28* (Yu *et al.*, 2007), and led to the production of human induced pluripotent stem cell-derived cardiomyocytes (hiPSC-CMs) (Takahashi *et al.*, 2007; Zwi *et al.*, 2009; Lian

et al., 2012). Importantly, producing hiPSC-CMs could be done without the ethical issues surrounding the use of embryos as the cell source. Therefore, hiPSC-derived cell types have gained traction as a suitable alternative for hESC-derived cell types (Takahashi and Yamanaka, 2006; Takahashi *et al.*, 2007).

As well as bypassing the ethical issues surrounding the production and use of human embryos for hESCs, hiPSC-derived cell types exhibit properties that render them appropriate as model systems for studying human diseases. They are of human origin, so they carry human genomes; they are pluripotent, so they can be differentiated into any of the human body's somatic cell types; and as stem cells, they can be an autologous source of cells for medical applications (Medvedev, Shevchenko and Zakian, 2010). The retention of a person's unique genotype means that hiPSC-CMs provides the opportunity to study cells genetically matched to individual patients. Together with genome-editing tools, hiPSC-CMs allow us to introduce or correct genetic variants (Musunuru *et al.*, 2018).

1.8.4.2 Differentiation of pluripotent stem cells into cardiomyocytes

There are numerous techniques for differentiation pluripotent stem cells into cardiomyocytes. Initial studies used the embryoid body (EB) technique. By recapitulating the early stages of embryogenesis, both ESCs and iPSCs can be induced to differentiate into cardiomyocyte-like cells. Initially, the stem cells are aggregated by suspension as a hanging drop or via centrifugation, leading to formation of the three primary germ layers. After several days in culture, these EBs form outgrowings seen to spontaneously contract like cardiomyocytes (Kehat *et al.*, 2001; Mummery *et al.*, 2012). However, this technique is very inefficient and there is significant heterogeneity in the cardiomyocytes formed (Vidarsson, Hyllner and Sartipy, 2010).

A more efficient technique for stem cell differentiation into cardiomyocytes, and the one used for this study, is based on inducing differentiation of monolayers of pluripotent stem cells using small molecules. We use a biphasic protocol manipulating the Wnt signalling pathway. In early differentiation, activation of Wnt signalling enhances cardiogenesis. Signalling late in the differentiation process inhibits cardiogenesis. Thus, inhibition of Wnt signalling is then required to maintain the presence of spontaneously beating cardiomyocytes (Ueno *et al.*, 2007). This biphasic differentiation process has been shown produce 80-98%

purity of cardiomyocytes before cell sorting (Lian *et al.*, 2013). Despite the many different techniques for the production of hiPSC-CMs, comparisons of the electrophysiological properties of hiPSC-CMs generated from multiple iPSC lines using monolayer-based methods identifies that they exhibit comparable and functional Ca^{2+} cycling, the major determinant of cardiomyocyte contractile function (Hwang *et al.*, 2015).

1.9 Cardiomyocyte structure

There is huge potential for the use of hiPSC-CMs in research and in therapy, but it is critical that we consider the immaturity in hiPSC-CM structure (Karakikes *et al.*, 2015). hiPSC-CMs are considered to have structural features more akin to neonatal or embryonic cardiomyocytes than adult cardiomyocytes (Table 1.2). hiPSC-CMs have a morphology that is generally large, flat and round with a single nucleus, although studies have shown that they are largely adaptive to the culture environment (Gherghiceanu *et al.*, 2011; Du *et al.*, 2015) and highly heterogenous, demonstrating very different cell morphologies and electrophysiological properties (**Figure 1.6** and **Table 1.3**).

The general characteristics of hiPSC-CMs are considered to recapitulate the phenotype of human cardiomyocytes during the early cardiogenesis phase. During this phase of development, the transition from hyperplastic to physiological hypertrophic growth of the myocardium has not yet occurred. During physiological hypertrophic growth, there is anisotropic alignment of elongated, rod-like cardiomyocytes connected electrically by unidirectional gap junctions (Bernardo *et al.*, 2010). This movement allows efficient contraction of the syncytium of cardiomyocytes in the developing heart, but the directional propagation of cardiomyocyte excitation does not occur in hiPSC-CMs spontaneously beating *in vitro*. This lack of development in cardiomyocyte phenotype is thought to be, at least in part, due to a lack of extracellular stimuli present in the developing heart (Wang, Kit-Anan and Terracciano, 2018).

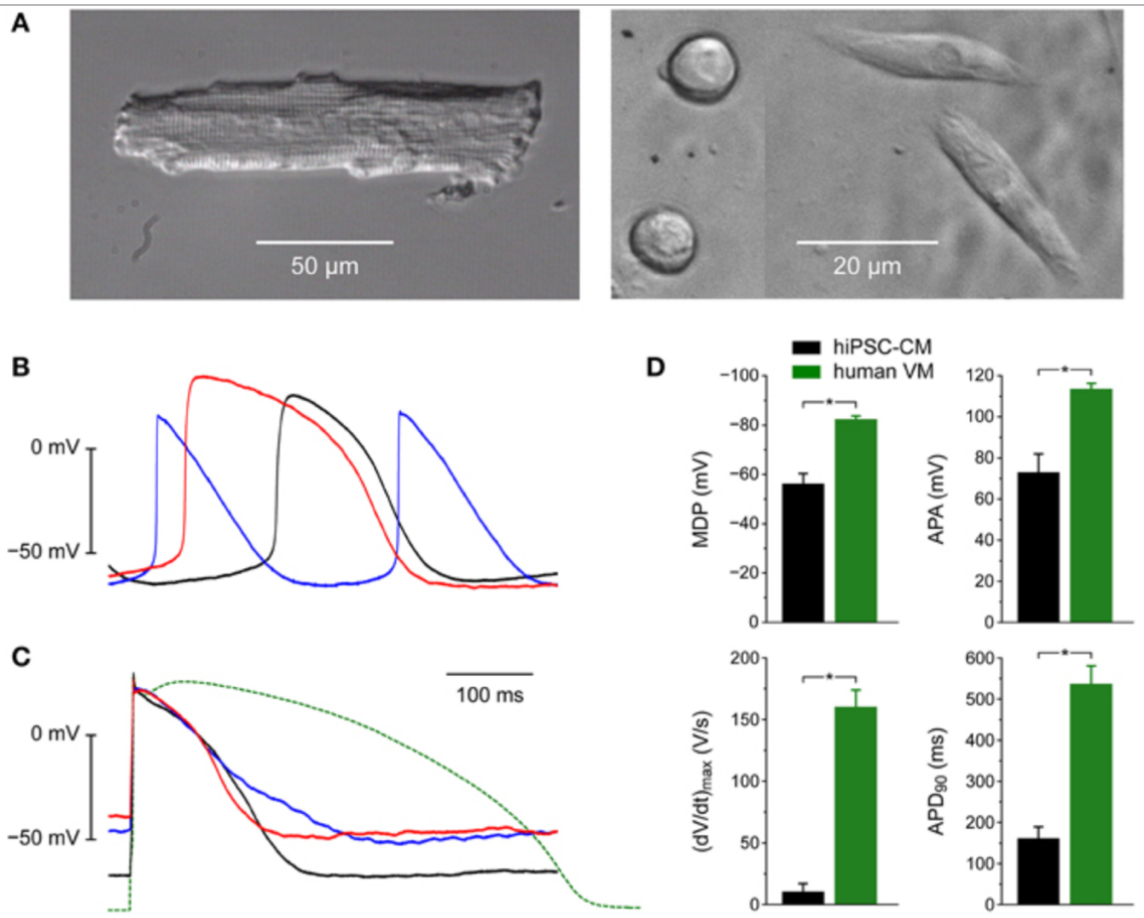

Figure 1.6 Comparing the morphology and electrophysiology of human induced pluripotent stem cell derived cardiomyocytes (hiPSC-CMs) and native human ventricular myocytes. *(A) Phase-contrast micrographs of a typical human ventricular myocytes (left) and four hiPSC-CMs (right). Differently shaped hiPSC-CMs were present at close distance in the same microscope field. (B) Action potentials of three different spontaneously active hiPSC-CMs. (C) Action potentials of three different hiPSC-CMs upon 1 Hz stimulation (solid lines) and a typical action potential of a single human ventricular myocyte isolated from a failing heart upon 1 Hz stimulation (dashed line) (D) Maximum diastolic potential (MDP), maximum upstroke velocity [$(dV/dt)_{max}$], action potential amplitude (APA) and action potential duration at 90% repolarisation (APD_{90}) of 9 hiPSC-CMs (left bars) and 9 human ventricular myocytes (right bars), all stimulated at 1 Hz. Human ventricular myocytes were isolated from explanted hearts of male patients in end-stage heart failure, * $P < 0.05$. Reproduced from (Van Putten et al., 2015).*

Structure				
		hiPSC-CM	Atrial	Ventricular
Shape		Any, not defined	Cylindrical	Cylindrical and bifurcated
Volume		Small	Large	Very large
Sarcomere Organization		Random	Orderly and aligned	Orderly and aligned
Mitochondria population		Few	Abundant	Abundant
Transverse-tubule organization		Absent	Scarce	Abundant
Glucose Metabolism		High	Low	Low
Nucleus morphology		Mono	Mono, bi, multi	Mono, bi, multi
Electrophysiology				
Spontaneous activity		Very frequent	Absent	Absent
Maximum diastolic potential		−60 mV	−70 mV	−80 mV
Maximum upstroke velocity		44–187 V/s	200 V/s	200 V/s
Action potential amplitude		94–113 mV	80–130 mV	100 mV
*Action potential duration at 50%		60–130 ms	200 ms	200–300 ms
*Action potential duration at 90%		80–160 ms	200–400 ms	250–400 ms
Force Generation		100–150 Pa for a single cell	Myocardium tensile force ≈ 56 kPa	Myocardium tensile force ≈ 56 kPa
Elastic modulus		466 Pa	22–55 kPa	22–55 kPa
Molecular Marker				
Gap junction	Cx40	-	+	-
	Cx43	+	+	+
	Cx45	+	-	-
Ion channel	KCNA5	+	+	-
	NCX1	+	+	+
	SERCA2a	+	+	+
	RYR2	+	+	+
	Ca_v 1.2	+	+	+
	K_{ir} 2.1	+	+	+
	K_v 4.3	+	+	+
	KChip 2	+	+	+
	KCNH2 (HERG)	+	+	+
Structural protein	TNNT2	+	+	+
	ACTN2	+	+	+
	MLC2A	+	+	+
	MLC2V	+	-	+
	MYL2	+	+	+
	MYH6	+	+	+
Master gene	NKX2.5	+	±	±

Table 1.3 Comparing human induced pluripotent stem cell-derived and adult cardiomyocytes. ** Action potential duration for hiPSC-CMs is dependent on cell seeding conditions (Du et al., 2015). (reproduced from Wang et al., 2018)*

An important aspect of hiPSC-CMs that limits their use is their restricted contractility due to immaturity in sarcomere structure (Zhang *et al.*, 2009; Zwi *et al.*, 2009). A sarcomere is determined as being the distance between two Z-lines and is directly linked to the production of force. The optimum length for the highest contractile force in adult cardiomyocytes is 2.2 µm under loaded situations, and 1.8 µm under unloaded situations (Hanft and McDonald, 2010). hiPSC-CMs have short (1.6 µm) and disorganised sarcomeres, similar to foetal cardiomyocytes (Wheelwright *et al.*, 2018). Many studies have also identified that only Z-disk and I-bands are present in hiPSC-CMs, but it has also been shown that these features are highly dependent on seeding conditions, and thus extracellular interactions (Kamakura *et al.*, 2013). Despite the differences in hiPSC-CM phenotypes between studies, there is a consensus that these cardiomyocytes display substantially lower force production than healthy, adult cardiomyocytes (Schick *et al.*, 2017).

In addition, hiPSC-CMs have been reported to display suboptimal mitochondria maturation. In the development of the adult phenotype, mitochondrial biogenesis greatly increases the mitochondrial content in response to increased energetic demands (Dorn, Vega and Kelly, 2015). The number of mitochondria in hiPSC-CMs is significantly lower than the adult cardiomyocytes – mitochondria account for 30% of the total cell volume in the adult ventricular myocyte (Schaper, Meiser and Stammler, 1985) vs 2% in hiPSC-CMs (Dai *et al.*, 2017). Mitochondria in hiPSC-CMs have reduced activity compared to the mitochondria in the adult human CMs, as they have immature cristae on their inner membrane (Dai *et al.*, 2017). Notably, the source of energy production in hiPSC-CMs, like the foetal heart, is glycolysis, but in the healthy adult cardiomyocyte this switches to predominantly fatty acid oxidation (Lopaschuk, Spafford and Marsh, 1991).

Many of the ultrastructural features of hiPSC-CM maturation have been shown to develop over prolonged culture. An increase in nucleation, myofibril density and expression of contractile proteins (e.g. β-myosin heavy chain) have been reported in cultures 120-360 days post-differentiation (Kamakura *et al.*, 2013; Lundy *et al.*, 2013). However, it is yet to be determined if the development of these ultrastructural features is truly a result of maturation over time or a result of senescence due to culture conditions.

1.10 Excitation-Contraction (EC)-Coupling

EC-coupling, the production of mechanical force following electrophysiological stimulation, is a key feature of healthy, adult cardiomyocytes. This process is mediated by the tight regulation of Ca^{2+} availability, such that cycling of cytosolic Ca^{2+} underlies cardiac performance and all mechanical function of the heart (Bers, 2002). The feature distinguishing cardiomyocytes from other muscle cell types is Ca^{2+}-induced Ca^{2+}-release (CICR), the key link between the electrophysiological stimulation by the action potential and the production of mechanical force (Kane *et al.*, 2015). The process of Ca^{2+} cycling and its role in EC-coupling is outlined in **Figure 1.7**.

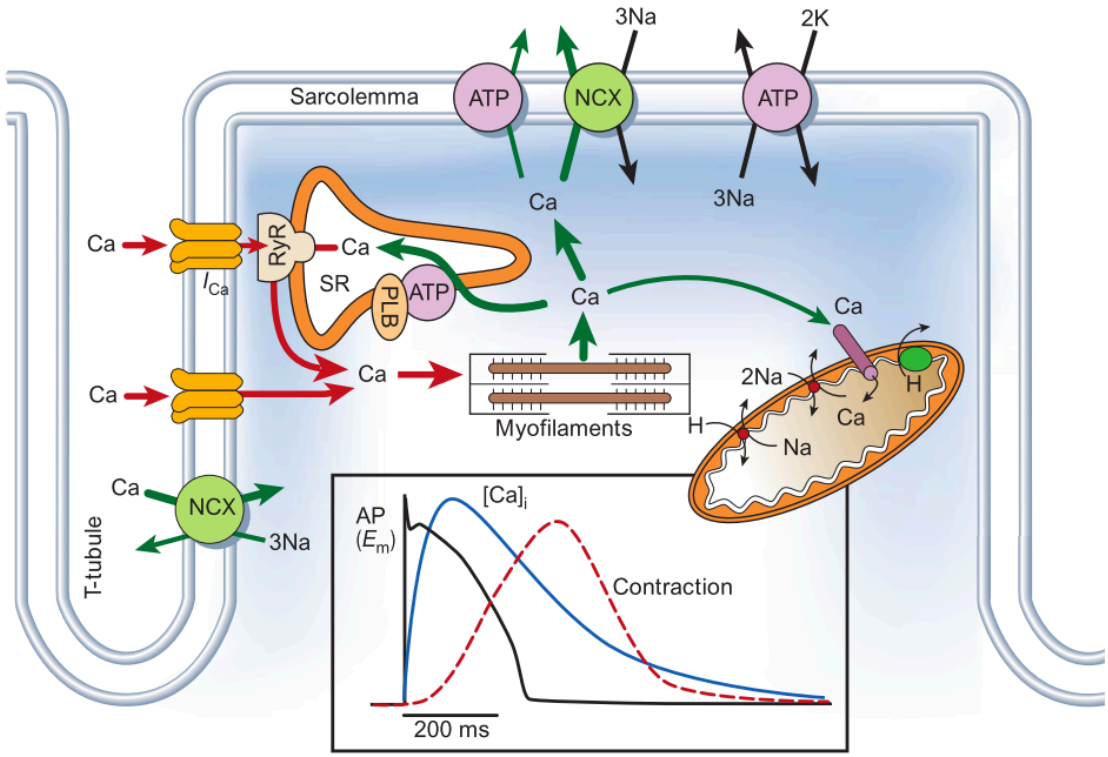

***Figure 1.7: Ca^{2+} cycling in adult ventricular myocytes**. The action potential (AP) triggers opening of the L-type Ca^{2+} channels during the plateau phase of the AP, causing an influx of Ca^{2+} into the cardiomyocyte cytosol. Increase in Ca^{2+} is sensed by the ryanodine receptors (RyRs) on the sarcoplasmic reticulum (SR) Ca^{2+} stores, increasing the open probability of these channels. Ca^{2+} released by the SR greatly increases the cytoplasmic Ca^{2+} availability for binding to Troponin C. This binding allows the myosin head to bind to actin filament, facilitating cross-bridge cycling and cell shortening. Following contraction, relaxation is achieved by removing the Ca^{2+} from the cytosol. Ca^{2+} is resequestered back into the SR through sarco-endoplasmic reticulum Ca^{2+}-ATPase (SERCA), or extruding through the sarcolemma by Na^+/Ca^{2+}Exchanger (NCX). In this way, cardiomyocyte contraction is mediated by Ca^{2+}-induced Ca^{2+} release (CICR) (Bers, 2002).*

1.10.1 Action Potential

The action potential is unique for the subtypes of cardiomyocytes (atrial, ventricular, pacemaker and Purkinje), governed by the differences in membrane permeability and ion channel expression (Spater *et al.*, 2014). In the adult cardiomyocyte, the resting membrane potential is considered to be -70 to -80 mV. In hiPSC-CMs, resting membrane potential is significantly less negative (-60mV) with action potentials that demonstrate automaticity (**Figure 1.8**), Differences in the ion channels and currents between hiPSC-CMs and adult cardiomyocytes contribute to inaccurate predictive capacity of drug screening and toxicity studies.

1.10.1.1 Depolarising currents – Funny current (I_f)

The rate of depolarisation in spontaneously beating hiPSC-CMs is slower than in electrically-paced conditions, contributed to by presence of a prominent $I_{f.}$ In the myocardium, I_f is present in the sinus node, flowing through hyperpolarisation-activated cyclic nucleotide-gated potassium (HCN) channels. During maturation, expression of HCN4 is maintained at high levels in the adult pacemaker cardiomyocytes but significantly reduced in the adult atrial and ventricular cardiomyocytes. This reduction in HCN4 expression does not occur in hiPSC-CMs, such that I_f remains high (X. Liang *et al.*, 2013; Saito *et al.*, 2015; Verkerk and Wilders, 2015). In both adult cardiomyocytes and hiPSC-CMs, once the depolarising membrane potential reaches the Na^+ current (I_{Na}) activation threshold, there is an influx of Na^+ into the cytoplasm, producing the rapid depolarisation upstroke of the action potential.

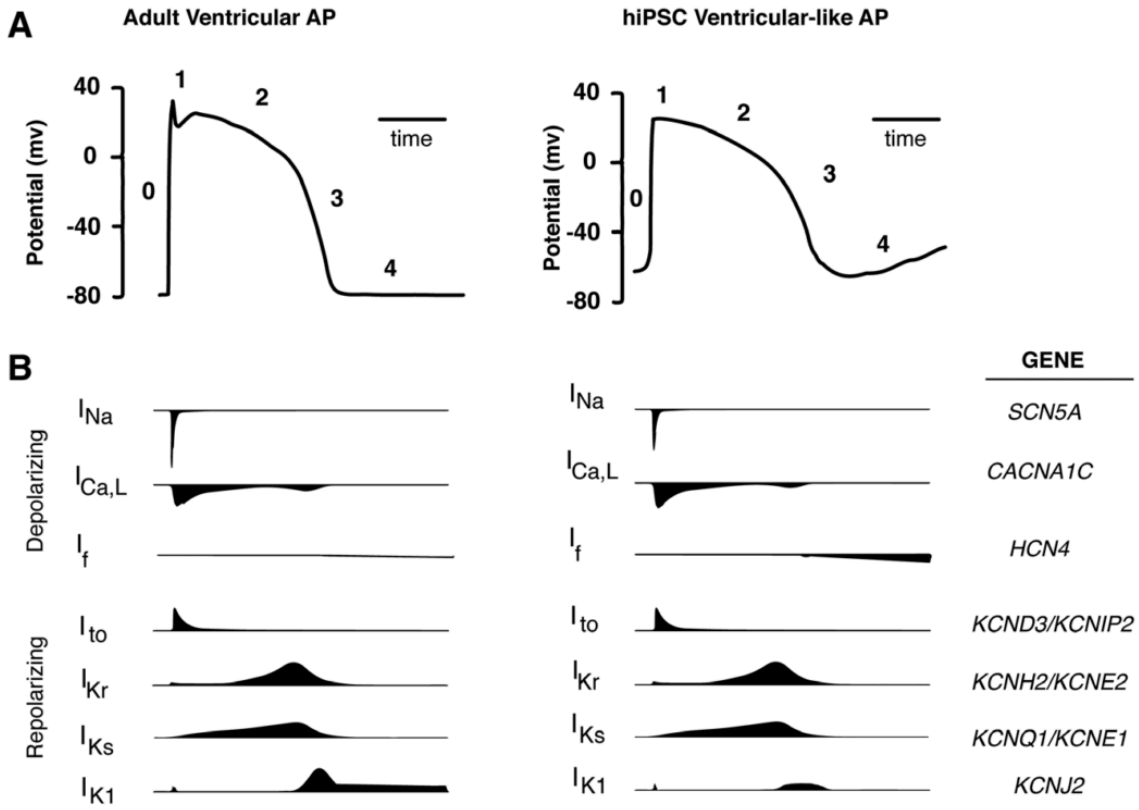

Figure 1.8: Comparison of action potentials (APs) of ventricular-like human induced pluripotent stem cell-derived (hiPSC)-cardiomyocytes and adult ventricular cardiomyocytes. *(A) Schematic of cardiomyocyte APs denoted as Phases 0-4. Phase 0 = rapid upstroke, 1 = early repolarisation, 2 = plateau, 3 = late repolarisation, and 4 = diastole. (B) The ionic currents and the genes that generate the currents with schematics of the current trajectories are shown. Significant differences are a reduced or absent inward rectifier K^+ current (I_{k1}) and presence of a prominent pacemaker current, contributing to hiPSC ventricular-like cardiomyocyte automaticity (Karakikes et al., 2015).*

1.10.1.2 Repolarising transient outward (I_{TO}) and inward rectifying (I_{k1}) K^+ currents

The rapid depolarisation of the membrane potential ends due to the time-dependent inactivation of Na^+ channels and the activation of $I_{TO.}$ I_{TO1} is a current found in the repolarisation phase of both early and late stage foetal cardiomyocytes, producing an efflux of K^+ from cells and a subsequent net loss of charge (Nerbonne and Kass, 2005). The expression of this current is higher in atrial cardiomyocytes compared to ventricular cardiomyocytes, contributing to the faster repolarisation and shorter action potentials in the atrial cells (Amos *et al.*, 1996; Gaborit *et al.*, 2007). In comparison, I_{TO1} has considerably

slower kinetics in hiPSC-CMs. It is often reduced or absent in hiPSC-CMs, leading to more positive resting membrane potentials and slower rates of repolarisation, prolonging the action potential duration compared to adult cardiomyocytes (Cordeiro *et al.*, 2013). However, gene regulation in hiPSC-CMs is highly dependent on seeding conditions (Du *et al.*, 2015)

hiPSC-CMs have very low levels of I_{k1} in comparison to adult human cardiomyocytes, contributing to a longer action potential duration (**Figure 1.8**). This current has strong inward conductance at membrane potentials below its reversal potential and therefore participates in the repolarisation of the action potential and is a key determinant of the resting membrane potential (Dhamoon and Jalife, 2005). This current is produced by channels from the Kir2.x family, particularly Kir2.1 (KCNJ2). The density of the I_{k1} current varies throughout the heart – up to 10 times greater in the ventricular cardiomyocytes than in atrial cardiomyocytes, resulting in a more negative resting membrane potential and faster phase 3 repolarisation in ventricular cardiomyocytes (Dhamoon and Jalife, 2005). The reduced expression in hiPSC-CMs leads to a less negative resting membrane potential in hiPSC-CMs (-50 to -60 mV) (Magyar *et al.*, 2000; Sartiani *et al.*, 2007; Zhang *et al.*, 2009; Ma *et al.*, 2011). Variation mutations in KCNJ2 have been shown to alter the cellular trafficking of these channels, leading to failure in forming a functional channel and subsequent long QT-syndrome (Gelinas *et al.*, 2017).

1.10.1.3 Delayed rectifier K^+ channel (I_{kr})

The delayed rectifier current, mediated by the Kv11.1 ion channels, conducts K^+ ions out of the cardiomyocyte and is critical in correctly timing the repolarisation of the cell membrane. A common cause of cardiotoxicity is inhibition of Kv11.1 ion channels, encoded by the hERG gene (Yu, IJzerman and Heitman, 2015). This channel exists in three conformational states: closed, open and inactivated (de la Peña, Domínguez and Barros, 2018). The slow transition between closed and open states of the channel is crucial for maintaining the cardiac action potential plateau phase (Perry *et al.*, 2015) contributed to by entry of Ca^{2+} from the cardiomyocyte extracellular environment, which subsequently triggers Ca^{2+} release from intracellular Ca^{2+} stores. Structural differences between hERG channels and other K^+ channels have allowed synthesis of compounds from several therapeutic drug classes that are able to bind to hERG channels, blocking the channels and subsequently reducing

conduction of K^+ ions through the channel (Vandenberg *et al.*, 2012). Inhibition of channel activity causes prolongation of the QT interval shown in electrocardiograms and is associated with ventricular arrhythmias (Sanguinetti and Tristani-Firouzi, 2006; Perry *et al.*, 2015). The risk this poses has prompted the US FDA (Food and Drug Administration) and pharmaceutical companies to introduce mandatory pre-clinical drug screening studies to detect potential cardiotoxicity prior to market release (P. Liang *et al.*, 2013).

The action potential morphology is widely used to classify the hiPSC-CMs into cardiomyocyte subpopulations found in the myocardium. The repolarising currents (1) rapid delayed rectifier K^+ channels (I_{kr}) and (2) slow delayed rectifier K^+ currents (I_{ks}) are present in hiPSC-CMs at similar levels to adult cardiomyocytes. However, categorisation of hiPSC-CMs into subtypes of adult cardiomyocytes due to similarities with cardiomyocytes in different chambers must be done with caution. The Terracciano group have identified that action potential morphology is modulated by the cellular density and cells exhibit a spectrum of characteristics with considerable overlap between the characteristics of the adult cardiomyocyte chamber subtypes (Du *et al.*, 2015). The extensive heterogeneity of hiPSC-CMs is considered by some to prevent these from being categorised into adult cardiomyocyte chamber subtypes. Instead, we must consider multiple variables of the hiPSC-CM phenotype when characterising these cells (Kane and Terracciano, 2017).

1.10.2 Ca^{2+} regulation

The indicator for successful differentiation of hiPSC-CMs is the observation of a rhythmic contraction of the hiPSC-CM population and these cells demonstrate robust Ca^{2+} transients in studies utilising fluorescent Ca^{2+}-sensitive indicators (Kane and Terracciano, 2018). The kinetics of the Ca^{2+} transients are considerably slower than the healthy, adult cardiomyocyte. An assessment of the Ca^{2+} kinetics of numerous hiPSC-CM cell lines shows significantly prolonged time to peak, indicating inefficient CICR. There are also reports of significant prolongation in the time to decay in hiPSC-CMs, with rates of decay reported at 0.84-1.15 s^{-1} vs 2.41 s^{-1}-and 5.75 s^{-1} in the adult rabbit and mouse cardiomyocyte, respectively (Hwang et al., 2015). These measurements indicate that despite hiPSC-CMs displaying robust Ca^{2+} transients; they have slower kinetics than mammalian adult cardiomyocytes, closer to that of neonatal or diseased cardiomyocytes. Studies have demonstarted key differences in

the ultrastructural domains that regulate intracellular Ca^{2+}cycling in hiPSC-CMs and adult cardiomyocytes (**Figure 1.9**)

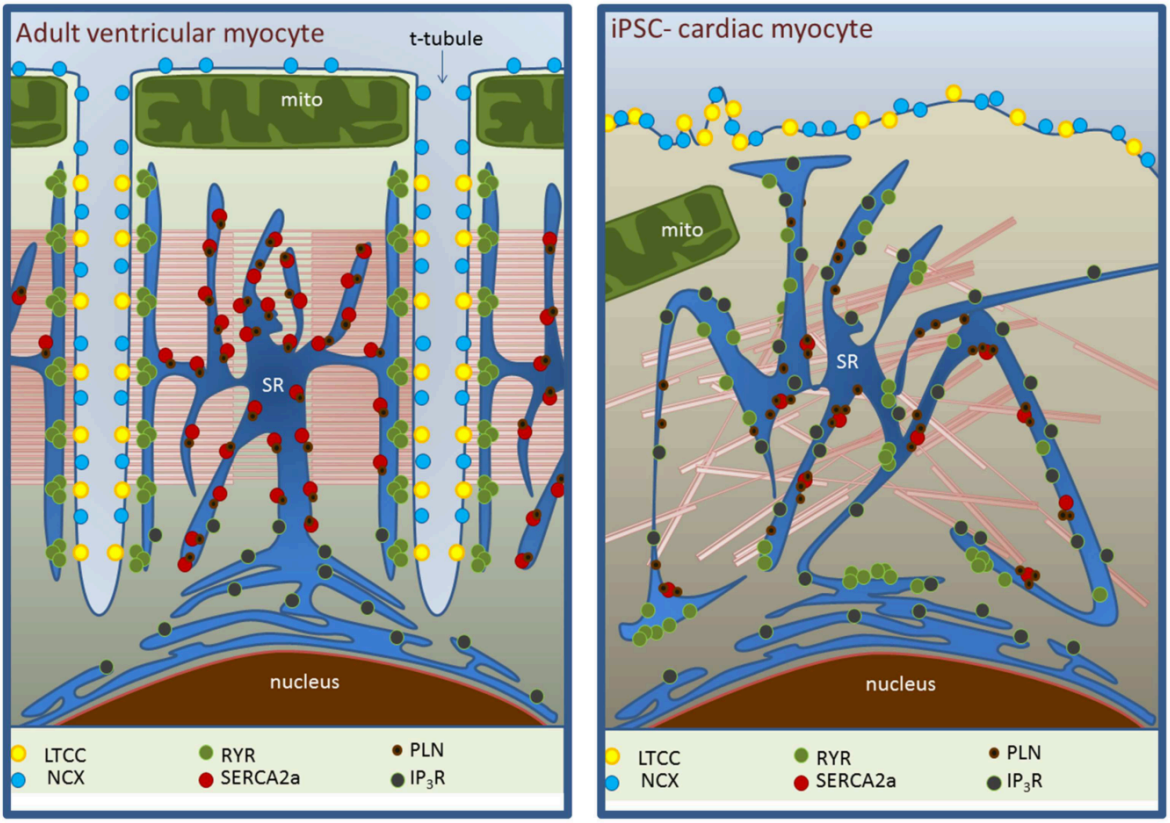

Figure 1.9 Ultrastructural differences between adult cardiomyocytes and hiPSC-CMs in excitation-contraction coupling domains*. Schematics shown for Ca^{2+} cycling ultrastructural domain of an adult ventricular myocytes (left) and iPSC-cardiac myocyte (right). The absence of T-tubules in hiPSC-CMs (right) is associated with a lack of regular L-type Ca^{2+} channel (LTCC)-Ryanodine receptor (RyR) complexes and less homogenous distribution of RyRs. SERCA expression in iPSC-CMs is reduced with a maintained expression of phospholamban (PLN). NCX expression may be maintained in iPSC-cardiac myocytes but its ability to extrude Ca^{2+} in diastole is reduced. Activity of inositol-triphosphate receptor (IP_3R) is substantially higher in iPSC-cardiac myocytes (Kane et al., 2015).*

1.10.2.1 T-tubules

Notably, these hiPSC-CMs lack T-tubule structures in both two-dimensional and three-dimensional cultures, contributing to inefficient CICR (Gherghiceanu *et al.*, 2011). T-tubules are regularly organised invaginations along the Z-lines in the adult cardiomyocytes, enabling rapid excitation, initiation and synchronous triggering of intracellular Ca^{2+} release from the SR Ca^{2+} stores (Peachey and Huxley, 1962; Orchard, Pasek and Brette, 2009). In hiPSC-CMs, the inefficient CICR causes a high number of Ca^{2+} sparks, which causes non-uniform Ca^{2+} release from the SR stores (Poindexter *et al.*, 2001; Pioner *et al.*, 2016; Ronaldson *et al.*, 2018). Although this is a limitation when comparing hiPSC-CMs to healthy, adult cardiomyocytes, the phenotype is very similar to developing cardiomyocytes until the late embryogenesis stage. Also, hiPSC-CM morphology does reduce the need for T-tubule structures. hiPSC-CMs are flat and much thinner (5µm diameter) than the comparably thicker, adult cardiomyocyte (15 µm diameter). Instead of T-tubules, hiPSC-CM plasma membranes express caveolae and coated pits (Cyganek *et al.*, 2018). Caveolae in both hiPSC-CMs and neonatal cardiomyocytes host adrenergic receptors and L-type Ca^{2+} channels, and this localisation is required for the physiological signalling during development (Xiang *et al.*, 2002). In this way, hiPSC-CMs reflect the phenotype of the developing cardiomyocyte.

While cardiomyocytes in the healthy, adult myocardium demonstrate efficient CICR, contributed to by the presence of T-tubule invaginations in ventricular myocytes, the CICR in hiPSC-CMs is considered to be very inefficient (Kane *et al.*, 2015). The initial rise in cytosolic Ca^{2+} has been widely observed to occur at the sarcolemma before spreading inwards, with more internal, non-coupled RyRs being activated by the rise in Ca^{2+} at the periphery as opposed to direct activation by Ca^{2+} channels (Lee *et al.*, 2011; Zhang *et al.*, 2013). This is a similar observation to that of other neonatal cardiomyocytes as well as adult cardiomyocytes that lack T-tubules. Detailed electron microscopy studies have identified that hiPSC-CMs demonstrate some apposition of the SR with the sarcolemma, but there is poor co-localisation between Cav1.2 and RyR2 indicating inefficient CICR in hiPSC-CMs (Gherghiceanu *et al.*, 2011; Rao *et al.*, 2012).

1.10.2.2 Sarcolemma Ca^{2+} channels

The two types of Ca^{2+} channels in the adult human heart that mediate Ca^{2+} current (I_{Ca}) are L-type ($I_{Ca,L}$) found in the adult cardiomyocyte, and T-type ($I_{Ca,T}$), typically found in foetal cardiomyocytes and the conductive system. Both of these Ca^{2+} channels are detected in hiPSC-CMs but the expression and function of both are lower than in the adult cardiomyocytes (Otsuji *et al.*, 2010; Itzhaki *et al.*, 2011; Kim *et al.*, 2017).

Cav1.2, the α-1C subunit of L-type Ca^{2+} channels, is the predominant subunit for $I_{Ca,L}$ conductance in mammalian cardiomyocytes. Expression of Cav1.2 in hiPSC-CMs has been shown to be comparable to adult human cardiomyocytes (Rao et al., 2013). However, I_{Ca} amplitude has been shown to vary greatly in hiPSC-CMs, ranging from -80 pA/pF to -17 pA/pF (Zhang *et al.*, 2009; Ma *et al.*, 2011). Despite this wide variability, the I_{CaL} has also been shown to have an important role in hiPSC-CMs. Nifedipine, an L-type Ca^{2+} channel blocker, causes complete suppression of whole cell Ca^{2+} transients in hiPSC-CMs at 1 µM and is observed to still cause a stepwise reduction in Ca^{2+} transient amplitude at very low concentrations (Itzhaki *et al.*, 2011). This demonstrates the importance that L-type Ca^{2+} channel transmembrane flux plays in the generation of the hiPSC-CM whole cell Ca^{2+} transients.

1.10.2.3 Ryanodine receptors (RyRs)

RyRs are Ca^{2+}-sensitive channels that mediate Ca^{2+} release from the SR Ca^{2+} stores in cardiomyocytes, and play a pivotal role in the release of Ca^{2+} from the intracellular stores. In healthy adult human cardiomyocytes, there is close apposition of the SR to the sarcolemma. This enables Ca^{2+} to be efficiently released from the SR via the RyRs at the junction between the SR domains closest to the sarcolemma (junctional SR (jSR)) in response to Ca^{2+} entry through the dihydropyridine receptors (DHPRs) or L-type Ca^{2+} channels expressed on the sarcolemma. The microdomain between the jSR and the sarcolemma forms discrete Ca^{2+} release units (CRUs), such that the localised increase in Ca^{2+} in this region triggers opening of the Ca^{2+}-sensitive RyRs. The release from these channels then triggers opening of neighbouring RyRs. The T-tubule invaginations contribute to rapid global Ca^{2+} rise following SR Ca^{2+} release (Bers, 2002). This coupling between sarcolemma Ca^{2+} entry and SR Ca^{2+} release is stabilised by the formation of macromolecular complexes containing RyRs and DHPRs in the CRU between the SR and sarcolemma (Olivetti *et al.*, 1996). The main cardiac isoform (RyR2)

is expressed diffusely throughout the hiPSC-CM cytosol, but there is intense, punctate perinuclear (Itzhaki *et al.*, 2011) and subsarcolemmal (Zhang *et al.*, 2013) staining, suggesting some localisation within the cell. The expression of RyR2, as well as regulatory proteins calsequestrin and triadin, is substantially reduced in hiPSC-CMs compared to adult human cardiomyocytes, all contributing to inefficient Ca^{2+} cycling (Wu *et al.*, 2011; Rao *et al.*, 2012).

Despite the reduced expression of RyR2, hiPSC-CMs exhibit a rapid release of SR Ca^{2+} in response to the RyR agonist caffeine (Itzhaki *et al.*, 2011; Wu *et al.*, 2011; Hwang *et al.*, 2015). This response enables assessment of SR Ca^{2+} content using caffeine application, which has shown that SR Ca^{2+} content is similar to that found in adult rabbit cardiomyocytes (Hwang *et al.*, 2015). However, as described by our group in response to the report conducted by Hwang and colleagues, the presence of a functional SR responsive to caffeine does not prove that this compartment is utilised in Ca^{2+} cycling to the same extent, and there may be crucial differences despite the apparent comparable SR contents (Hwang *et al.*, 2015; Kane and Terracciano, 2015a). Firstly, inhibition of SR Ca^{2+} uptake, and thus SR Ca^{2+} content, has been shown to only moderately reduce the Ca^{2+} transient amplitude in rabbits (Elliott *et al.*, 2012). Secondly, we must consider not only the overall changes in the contribution of mechanisms for Ca^{2+} release and reuptake, but also the absolute changes in activity, as changes such as a reduction in the activity of multiple mechanisms could still be seen as no change in relative contributions (Piacentino *et al.*, 2003). Feedback mechanisms that regulate Ca^{2+} storage, release and reuptake may compensate or mask the underlying differences. Attributing findings from hiPSC-CMs to adult human cardiomyocytes or other animal cardiomyocytes must therefore be done with caution.

1.10.2.4 Sarco-endoplasmic reticulum Ca^{2+}-ATPase (SERCA) and Phospholamban (PLN)

Following contraction, relaxation is then achieved by removing the Ca^{2+} from the cytosol (Bers, 2002). One mechanism is uptake into the SR via SERCA. The cardiac isoform of SERCA, SERCA2a, is expressed in hiPSC-CMs at significantly lower levels compared to the adult human heart (Rao *et al.*, 2013). Functionally, the rate of SR Ca^{2+} uptake mediated by SERCA is reported to be substantially slower in hiPSC-CMs compared to both rabbit and mouse cardiomyocytes (0.49-0.72 s^{-1} vs 1.52 s^{-1} and 5.12 s^{-1}, respectively) (Hwang *et al.*, 2015).

SR Ca^{2+} uptake is controlled by the SERCA negative regulator, PLN, which inhibits SERCA activity when it is in its unphosphorylated form. The expression of PLN in hiPSC-CMs is comparable to adult human cardiomyocytes (Rao *et al.,* 2013), despite the reduction in SERCA, and this contributes to the reduction in rate of SR-mediated Ca^{2+} removal from the cytosol in hiPSC-CMs compared to adult cardiomyocytes. However, more recent reports indicate that protein expression of PLN is substantially lower than in adult human cardiomyocytes (Chen *et al.,* 2015). Studies must be done to determine the modulators for PLN expression and confirm the role it plays in hiPSC-CM Ca^{2+} cycling.

Studies have indicated that the hiPSC-CM lusitropic response to adrenaline is mediated by phosphorylation of PLN, which increases the rate of Ca^{2+} uptake by the SR Ca^{2+} stores (Yokoo *et al.*, 2009; Xi *et al.*, 2010; Germanguz *et al.*, 2011). However, in conflict with this is the finding that hiPSC-CMs do not demonstrate a positive inotropic response to adrenergic stimulation, which is normally partly attributed to an increase in the $[Ca^{2+}]_{SR}$ as a result of faster uptake into the SR Ca^{2+} stores (Chen *et al.,* 2015). The lack of inotropic response in hiPSC-CM, despite a chronotropic response to adrenergic stimulation, suggests that hiPSC-CMs have a neonatal-like SR. It must be noted that there are contrasting reports of inotropic effects of noradrenaline (mixed α- and β-agonist) in studies that use atomic force microscopy or video-edge detecting systems to investigate single hiPSC-CMs (Brito-Martins, Harding and Ali, 2008; Yokoo *et al.*, 2009; Germanguz *et al.*, 2011; Liu *et al.*, 2012). These contrasting results may be due to the stem cell-derived cardiomyocytes being at different stages of development when used *in vitro*, as foetal heart tissue also demonstrates low numbers of β-adrenergic receptors (Slotkin, Lau and Seidler, 1994). hiPSC-CMs also have a reduction in essential components of the β-adrenergic signalling cascade, such as G-proteins that couple receptors to adenylate cyclase, which contributes to a reduced adrenergic response compared to adult cardiomyocytes (Slotkin, Lau and Seidler, 1994).

1.10.2.5 Na^+/Ca^{2+} exchanger (NCX)

NCX, expressed as the NCX1 isoform in the myocardium, has a key role in maintaining Ca^{2+} homeostasis. The exchanger moves Ca^{2+} out across the sarcolemma during systole in exchange for Na^+ influx into the cell, at a ratio of 3 Na^+ ions in for each Ca^{2+} ion out. This ionic exchange generates a substantial inward current, I_{NCX}, contributing to cardiomyocyte

depolarisation, pacemaker activity and the action potential duration (Blaustein and Lederer, 1999). Due to its role in both Ca^{2+} cycling and regulating cell membrane potential, NCX dysfunction is a key contributor to afterdepolarisation-based arrhythmogenesis. Consequently, regulation and function of NCX is of great interest both as a therapeutic target and as a source of pharmacological toxicity (Pott, Eckardt and Goldhaber, 2011). The expression of NCX in hiPSC-CMs has been shown to be comparable to that of adult human cardiomyocytes (Rao *et al.*, 2012). However, to date, there has been no assessment of NCX contribution to $[Na^+]_i$ or the reversal potential of the exchanger in hiPSC-CMs, so quantification of the significance of Ca^{2+} influx via reverse mode NCX remains undetermined.

1.10.3 Cardiomyocyte contraction

A key feature of mature cardiomyocytes in the human myocardium is a positive force-frequency relationship (FFR; Bowditch phenomenon), characterised by an increase in contractile force in response to an increase in beating frequency (Endoh, 2004). Loss of this mechanism, along with the changes that occur in EC-coupling, are important features of heart failure, such that the myocardium becomes unable to cope with energetic demands (Bers, 2002). hiPSC-CMs, unlike healthy cardiomyocytes in the adult myocardium, demonstrate a negative FFR; a reduction in Ca^{2+} availability to the myofilaments, and subsequently a reduction in contractile force, with increased frequency of contraction. The FFR is thought to be intrinsically dependent on the maturation of mechanisms utilising intracellular Ca^{2+} stores (Olivetti, Anversa and Loud, 1980). Rat and mouse cardiomyocytes have a flat FFR but also have transverse (T)-tubule structures, indicating that these invagination structures are not solely responsible for the positive FFR in adult human cardiomyocytes. However, negative FFR is indicative of inefficient utilisation of SR Ca^{2+} associated with, but may not be solely due to, absence of sarcolemma invaginations in hiPSC-CMs and neonatal cardiomyocytes and adult cardiomyocytes that have undergone detubulation during disease remodelling (Itzhaki *et al.*, 2011; Hwang *et al.*, 2015).

1.11 Applications for hiPSC-CMs

1.11.1 Disease modelling

The recent advancements in the development of hiPSC-derived cell types has broadened a valuable avenue for the development and utilisation of more accurate models of human cardiac disease. Much progress has been made in the use of hiPSCs to better understand cardiomyopathies (Tse *et al.*, 2013), rhythm disorders (Veerman *et al.*, 2016), valvular and vascular disorders (Kehl, Weber and Hoerstrup, 2016), and metabolic risk factors for heart disease (Wen *et al.*, 2015). Various human pathologies have also been investigated using hiPSC-CMs; long-QT syndrome (LQTS), Brugada syndrome, Timothy syndrome (also called LQT8), and catecholaminergic polymorphic ventricular tachycardia have been modelled and these have all been shown to recapitulate key features of the cardiac phenotypes observed in patients, as outlined in **Table 1.4**.

***Table 1.4 Available hiPSC-derived cells**. Both healthy and diseased lines have been made for many cell types. CM = cardiomyocyte, EC = Endothelial cell, RBC = Red blood cell, SMC = Smooth muscle cell (reproduced from Wang, Kit-Anan and Terracciano, 2018).*

Pathology	Cell Type Involved	Mutation	(Drug/Treatment) Test	Reference
Endothelial				
Healthy	EC	N/A	Flow-induced disease and simvastatin	(Adams *et al.*, 2013)
Hutchison-Gilford Progeria Syndrome	EC	Patient-derived	N/A	(Zhang *et al.*, 2011)
Smooth muscle cells				
Supravalvular aortic stenosis	SMC	Elastin (ELN)	Elastin recombinant protein	(Ge *et al.*, 2012)
Marfan syndrome	SMC	FBN1	Gene editing and drugs	(Granata *et al.*, 2017)
Lymphocytes				
Healthy	B-cell lymphoid lineage	N/A	N/A	(French *et al.*, 2015)
Red blood cells				
Healthy	CM and RBC	N/A	Toxicity of RBC	(Fan *et al.*, 2018)
Cardiomyocytes				
Hypoplastic left heart syndrome	CM	Patient-derived (GM12601)	Isoproterenol	(Jiang *et al.*, 2014)
Familial hypertrophic cardiomyopathy	CM	MYH7 Arg663His	Verapamil, Diltiazem, Mexiletine among 15 drugs	(Lan *et al.*, 2013)
LEOPARD syndrome	CM & 3 germ layers	PTPN11	N/A	(Carvajal-Vergara *et al.*, 2010)
Catecholaminergic polymorphic ventricular tachycardia type 1	CM	Ryanodine Receptor 2 (RYR2)	Isoproterenol	(Biochemistr *et al.*, 2011; Novak *et al.*, 2012)
LQT1,2,3,5,8,14	CM	Patient-derived	Common drugs	(Moretti *et al.*, 2010; Yazawa *et al.*, 2011; Davis *et al.*, 2012; Lahti *et al.*, 2012; Limpitikul *et al.*, 2017; Rocchetti *et al.*, 2017)
Barth syndrome	CM	Tafazzin (TAZ)	Genetic rescue	(G. Wang *et al.*, 2014)
Ischemic heart damage	CM	Aldehyde dehydrogenase 2 (ALDH-2) deficiency	siRNA knockdown	(Ebert *et al.*, 2014)
Brugada syndrome	CM	SCN5A-1795insD mutation	N/A	(Veerman *et al.*, 2016)

1.11.2 Cell transplantation

The limited regenerative capacity of adult cardiomyocytes leads to irreversible loss of cardiomyocytes following any initial myocardial injury or insult that prevents sufficient myocardial function to meet the contractile demands such as following myocardial infarction, valve disease, hypertension or familial cardiomyopathy (Bergmann *et al.*, 2009). The chronic overload on the surviving myocardium causes a positive feedback loop whereby the cumulative damage to the myocardium ultimately resulting in heart failure. We are currently unable to reproducibly introduce viable cardiomyocytes into the native myocardium to preserve cardiac function. The progressive loss of cardiac function leads to end stage heart failure, at which point the only treatment is cardiac transplantation. However, there are insufficient human donor organs to meet the demand (Gridelli and Remuzzi, 2000; Taylor *et al.*, 2007). Numerous studies have investigated the potential for introducing viable hiPSC-CMs to prevent deterioration of cardiac function by preventing mechanical overload for existing cardiomyocytes after cardiac injury (Chen et al. 2015; Emmert et al. 2014). hiPSC-CMs offer huge potential in cell transplantation (Park and Yoon, 2018). Their autologous properties suppress the risk of rejection and infection such that diseases caused by single gene defects could be addressed by made-to-order gene replacement in cells and allogenic cells from healthy people could be used.

Cell therapy utilising hiPSC-CMs can broadly be categorised as applying these cells either in suspension (Kadota *et al.*, 2017) or incorporated hiPSC-CMs in tissue engineering techniques (Zwi-Dantsis *et al.*, 2019). The inflamed, hostile environment into which cells are injected may, at least in part, contribute to the low retention of viable cells (Balsam *et al.*, 2004; Dohmann *et al.*, 2005). To combat this, tissue engineering has been used to modify the extracellular environment at the site of implantation or injection (Black *et al.*, 2009; Li and Guan, 2011; Zhang, 2015; Hansen *et al.*, 2016).

The ECM is the scaffold in the native myocardium and is likely to play a critical role in retention of these newly-introduced hiPSC-CMs. Ban and colleagues first demonstrated the potential of integrin ligands in promoting hiPSC-CM retention in engraftment (Ban *et al.*, 2014). They encapsulated mouse embryonic stem cell-derived cardiomyocytes (mESC-CMs) in an injectable nanomatrix gel consisting of peptide amphiphiles incorporating Arginine-Glycine-Aspartate-Serine (PA-RGDS) in experimental myocardial infarction. RGDS is an

integrin ligand motif expressed by ECM protein fibronectin that binds to integrins expressed by the mESC-CMs as well as cardiomyocytes and cardiac fibroblasts in the recipient mouse. Their study found a 3-fold higher engraftment in mice receiving the mESC-CMs with the PA-RGDS compared to those without PA-RGDS and higher cardiac function in the PA-RGDS mESC-CMs up to 12 weeks following engraftment (Ban *et al.*, 2014).

1.11.3 Drug development

Up to 90% of compounds that pass the pre-clinical screening stage then fail at the highly-expensive clinical trial level and up to a third of compounds show unforeseen side effects at this stage (Kraljevic, Stambrook and Pavelic, 2004). Beyond this, of the compounds that have been approved, cardiotoxicity accounts for 45% of post-approval withdrawal (Stevens and Baker, 2009). Improving the pre-clinical screening of novel compounds for efficacy and toxicity would be hugely beneficial to the pharmaceutical industry by reducing the attrition rates as well as improving drug safety.

Current models for drug discovery and disease modelling do not sufficiently reproduce human physiology and disease, and are therefore limited in their capacity to detect human cardiotoxicity. Current models that include forced expression of hERG channels in genetically transformed CHO or human embryonic kidney (HEK) cells, or animal models, do not accurately model crucial genetic, cellular or biochemical characteristics of the human heart and can lead to false results (Zhou *et al.*, 1998; Braam, Passier and Mummery, 2009). In particular, blockade of single ion channels is an imperfect measure of QT prolongation as cardiomyocyte electrophysiology is regulated by concurrent activity of multiple ion channels (Braam *et al.,* 2009).

The development of hiPSC-CMs has opened new possibilities for generating continuous supplies of progenitor cells for toxicity screening (Denning *et al.*, 2016). hiPSC-CMs with arrhythmogenic diseases can be treated with a subset of known arrhythmogenic drugs (Guo *et al.*, 2011; Lahti *et al.*, 2012). A re-entrant arrhythmia model was developed by Kadota and colleagues using hiPSC-CM sheets monitored by optically recording the Ca^{2+} signalling (Kadota *et al.*, 2013). Their study observed that treatment of the hiPSC-CMs with Na^{+} channel current blockers e.g. lidocaine and tetrodotoxin, as well as changing the time in culture or frequency of hiPSC-CM stimulation could alter the velocity and pattern of optically

recorded Ca^{2+} waves. High frequency stimulation of hiPSC-CMs could induce re-entrant spiral wave propagation that could be terminated by treatment with current anti-arrhythmic drugs (Nifekalant, E-4031, Sotalol, and Quinidine) (Kadota *et al.*, 2013). These results could not be recapitulated in models that use cardiac-cell sheets derived from rodent hearts but were comparable to treatment for ventricular tachycardia in the clinic. This demonstrates the need to develop accurate human models for drug development.

1.12 Hypotheses

The heterocellular environment of the myocardium is fundamental in the development and maintenance of cardiomyocyte physiology and the changes that occur in disease. Studies have identified that the cardiomyocyte extracellular environment, through mechanical, electrical and chemical interactions modulate cardiomyocyte structure and function. Cardiac fibroblasts are a key non-myocyte cell type in the myocardium and form critical interactions with cardiomyocytes through intercellular interactions and via the ECM scaffold. However, the interactions important in the regulation of Ca^{2+} cycling, a critical aspect of EC-coupling, are yet to be delineated. Understanding the role of these interactions using a stem cell-based model allows us to understand how we can produce hiPSC-CM phenotype closer to the adult cardiomyocyte morphology, increasing the potential use of this cell type in therapeutics, disease modelling and drug discovery.

We address the hypothesis that:

Human cardiac fibroblasts regulate intracellular Ca^{2+} cycling of human induced pluripotent stem cell-derived cardiomyocytes

This study aims to understand this hypothesis by investigating these more specific hypotheses in each chapter.

1. **hiPSC-CM cytosolic Ca^{2+} cycling is modulated by human cardiac fibroblasts.**

This hypothesis was tested by using different co-culture platforms to individually investigate the paracrine interactions between hiPSC-CMs and cardiac fibroblasts in the absence of direct contact interactions, as well as investigating the differences between unidirectional and bidirectional paracrine interactions. We also try to overcome the limitation to current platforms for investigating paracrine interactions by validating a reconfigurable, elastic co-culture setup that enables accurate investigation into the spatial dependency of intercellular paracrine interactions between cardiac fibroblasts and hiPSC-CMs (Chapter 3).

2. **hiPSC-CM cytosolic Ca^{2+} cycling is modulated by ECM-derived integrin ligands**

This hypothesis was tested by treating hiPSC-CMs with soluble and fibril-forming integrin ligands with the principal integrin-binding motif and investigating the changes in Ca^{2+}

transient parameters, including the contribution of SR and sarcolemma mechanisms of increasing Ca^{2+} availability and extrusion. The changes in hiPSC-CM structure were also assessed (Chapter 4).

3. **hiPSC-CM cytosolic Ca^{2+} cycling is modulated, at least in part, by EV interactions with cardiac fibroblasts**

This hypothesis was tested by treating hiPSC-CM–cardiac fibroblast co-cultures with GW4869, an inhibitor of ceramide-mediated exosome synthesis. We validate an ultrafiltration- and chromatography-based EV isolation protocol to separate fibroblast-secreted EVs from soluble contaminating proteins. The role of fibroblast-secreted EVs was investigated by treating hiPSC-CMs with fibroblast EVs and assessment of Ca^{2+} transient parameters (Chapter 5).

1.13 Study Design

Chapter 3: *modulation of hiPSC-CM Ca^{2+} cycling by human cardiac fibroblasts*

In initial co-culture studies investigating paracrine and direct physical interactions between the two cell types, hiPSC-CMs and cardiac fibroblasts are cultured in various setups:

1. Control condition was serum-free media used to culture 160,000 hiPSC-CMs for 24 hours before transferring the media to a new dish of 80,000 hiPSC-CMs (**Figure 1.10A**)
2. Fibroblast-conditioned media – serum-free media was used to culture 160,000 fibroblasts for 24 hours before the media was transferred and used to culture monolayer of 80,000 hiPSC-CMs (**Figure 1.10B**)
3. Fibroblasts-seeded on porous tissue culture suspensions – serum-free media was used to culture co-cultures of 160,000 fibroblasts suspended above the monolayer of 80,000 hiPSC-CMs (**Figure 1.10C**)
4. Fibroblasts seeded directly on cardiomyocytes – serum-free media was used to culture 160,000 fibroblasts seeded directly on top of the monolayer of 80,000 hiPSC-CMs (**Figure 1.10D**)
5. Fibroblast and cardiomyocytes were cultured together in one dish as distinct monocellular cultures so distance of paracrine interactions can be accurately measured (**Figure 1.10E**)

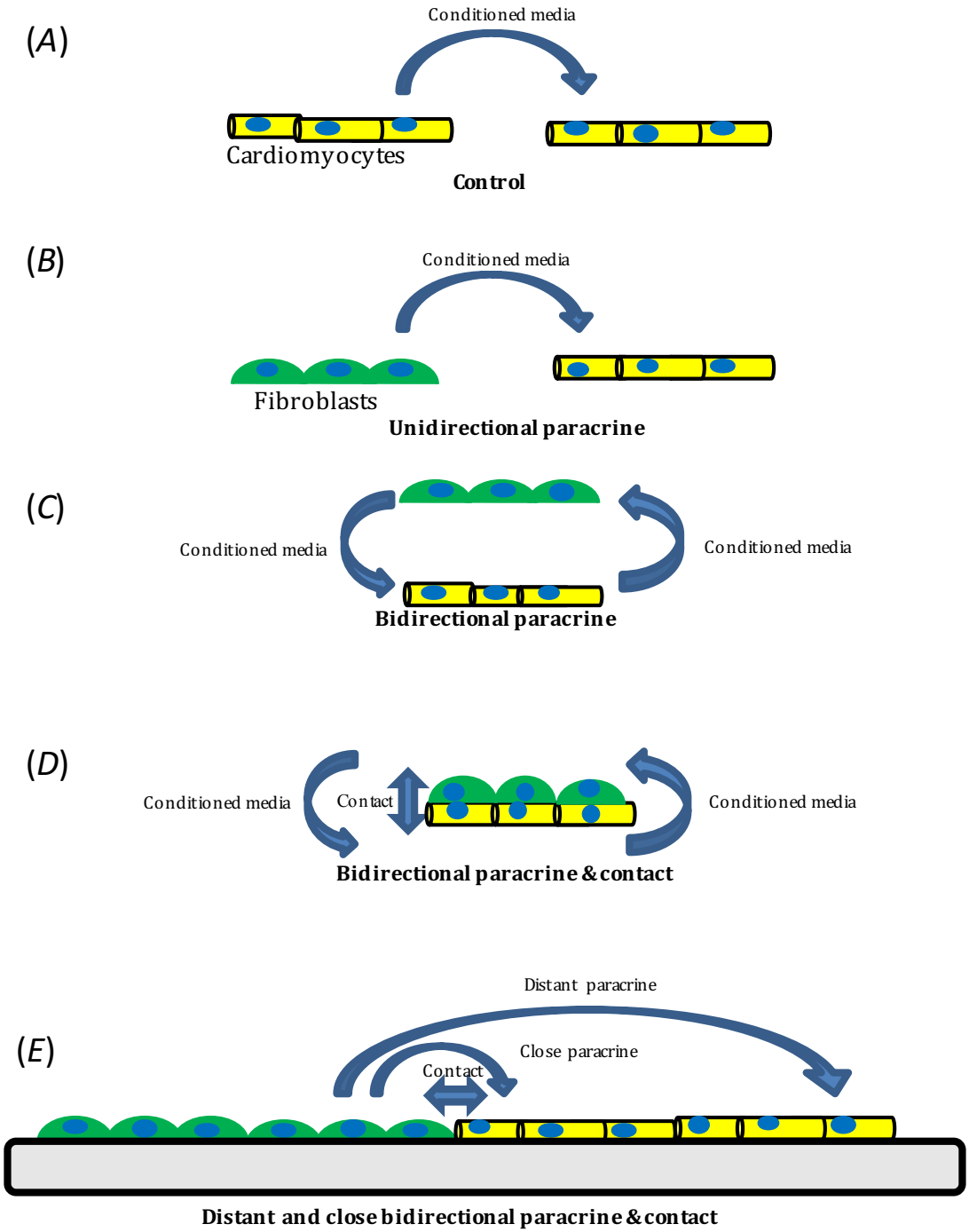

Figure 1.10 Study design for chapter 3*. Cardiomyocytes and cardiac fibroblasts were cultured in several platforms to investigate intercellular interactions. All platforms used serum-free media for conditioning and maintain the cardiomyocytes, to negate the effects of serum content. (A) Cardiomyocyte-conditioned media to culture a dish of cardiomyocytes, (B) unidirectional paracrine communication from fibroblasts to cardiomyocytes, (C) bidirectional paracrine communication between fibroblasts and cardiomyocytes, (D) bidirectional paracrine and direct contact communication between fibroblasts and cardiomyocytes. (E) cardiomyocyte and fibroblast monolayers cultured side-by-side on a reconfigurable substrate to allow accurate measure of distance for paracrine interactions.*

Chapter 4: *modulation of hiPSC-CM Ca^{2+} cycling by integrin ligands*

The role of ECM integrin ligands in modulating hiPSC-CM structure and function is investigated by treating hiPSC-CMs with soluble integrin ligands (**Figure 1.11A**), integrin antibodies (**Figure 1.11B**) or the two concomitantly (**Figure 1.11C**). Treatment with self-assembling, fibril-forming integrin ligands would more closely recapitulate the extracellular scaffold, preventing cell detachment (**Figure 1.11D)**.

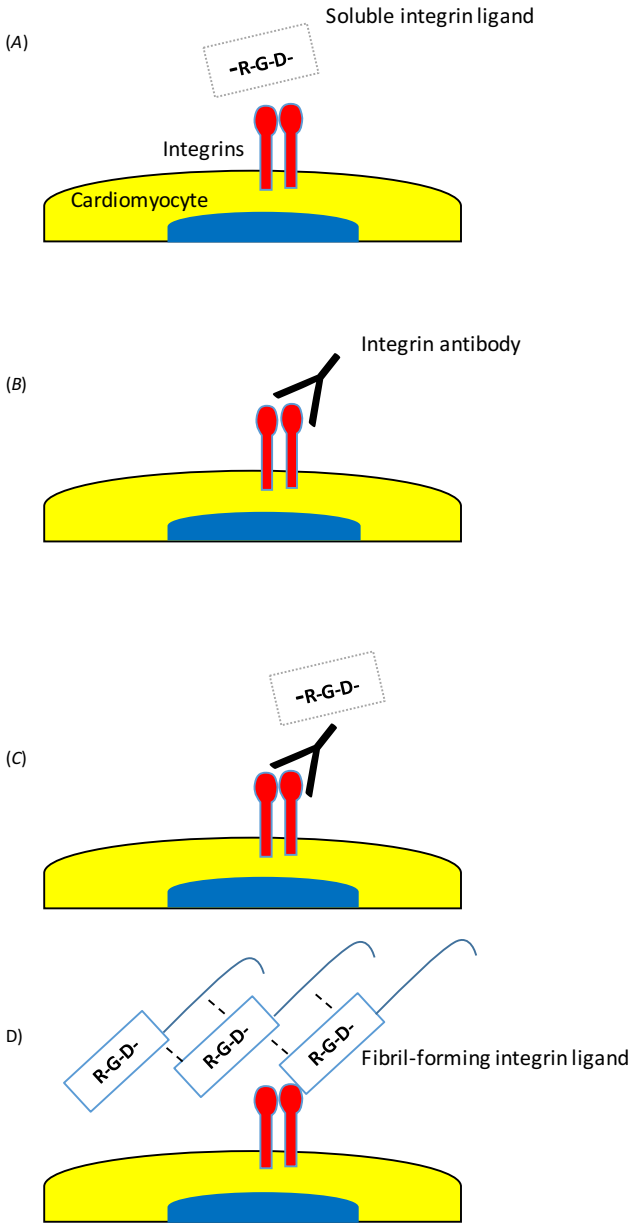

Figure 1.11 Study design for chapter 4*. Cardiomyocytes were treated with (A) soluble integrin ligands, (B) integrin antibodies, (C) integrin antibodies and soluble integrin ligands, (D) self-assembling, fibril-forming integrin ligands.*

Chapter 5: *modulation of hiPSC-CM Ca^{2+} cycling by cardiac fibroblast-derived EVs*

Chapter 5 investigates the role of EVs in mediating the crosstalk between cardiac fibroblasts and hiPSC-CMs. EVs from cardiac fibroblasts in culture were collected and purified by an ultrafiltration- and chromatography-based technique. The presence of EVs was investigated by identifying the presence of immunogold-linked EV markers (**Figure 1.12A**) and dot-blot analysis of EV markers (**Figure 1.12B**). The role that fibroblast-derived EVs have in the regulation of hiPSC-CM Ca^{2+} cycling was also investigated by optical recording intracellular Ca^{2+} transients (**Figure 1.12C**).

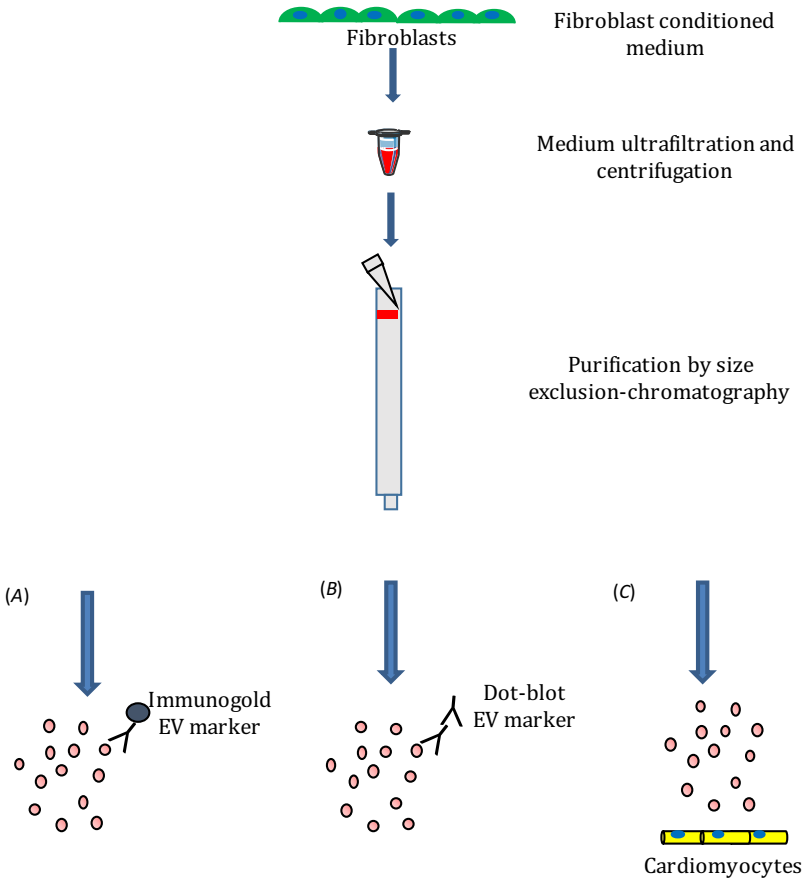

Figure 1.12 Study design for chapter 5. *Fibroblast-conditioned media was collected using exosome-depleted fibroblast culture media (2% exosome-depleted foetal bovine serum in Dulbecco's Modified Eagle Medium). Fibroblast-conditioned media was purified and filtered through a 0.45 µm bottle-top filter and then by ultrafiltration through centrifugal filter with a 100 kDa Molecular Weight Cut Off (approximately 7 nm) pore size. Samples were then purified by size exclusion-chromatography (SEC), collecting samples as 1mL fractions. The presence of extracellular vesicle markers was detected by (A) transmission electron microscopy imaging of immunogold labelled samples, or (B) dot blot imaging of extracellular vesicle markers in all (SEC) fractions. Samples were also used to investigate (C) effects of 150 µg fibroblast-secreted extracellular vesicles on cardiomyocyte Ca^{2+} cycling.*

2 Methods

All consumable items were purchased from Sigma-Aldrich unless otherwise stated.

2.1 Buffer preparation

Standard Tyrode's solution 140 mM sodium chloride (NaCl) (Scientific Lab Supplies), 4.5 mM potassium chloride (KCl), 10 mM glucose, 10 mM 4-(2-hydroxyethyl)-1-piperazineethanesulfonic acid (HEPES), 1 mM magnesium chloride ($MgCl_2$), 1 mM calcium chloride ($CaCl_2$); pH 7.4.

Na^+/Ca^{2+}-free Tyrode's solution: 140 mM Lithium chloride (LiCl), 4.5 mM KCl, 10 mM glucose, 10 mM HEPES, 1 mM $MgCl_2$, 1 mM EGTA; pH 7.4.

Tris-Buffered Saline (TBS): 20 mM tris, 150 mM NaCl; pH 7.6.

TBS with Tween (TBS-T): 20 mM tris, 150 mM NaCl, 0.1% v/v tween 20; pH 7.6.

2.2 Cell culture

All biological procedures were carried out under sterile conditions in a Biomat 2 class II microbial safety cabinet. Cells were maintained in an incubator (Sanyo, MCO-5M) at 37^oC and 5% CO_2.

2.2.1 Culture media preparation

Standard fibroblast culture media: Dulbecco's Modified Eagle Medium (DMEM), 10% v/v Foetal Bovine Serum (FBS), 1% v/v Penicillin-Streptomycin.

Exosome-depleted fibroblast culture media: DMEM, 2% v/v Exosome-depleted FBS (Gibco), 1% v/v Penicillin-Streptomycin.

Serum-free media: Medium-199, Insulin-Transferrin-Selenium (ITS), 1% v/v Penicillin-Streptomycin.

HiPSC-CM plating media: Roswell Park Memorial Institute (RPMI) 1640 (Life Technologies) media supplemented with B27 (RB + INS) (Life Technologies), 10% v/v FBS, 10 µM Rho-associated protein kinase (ROCK) inhibitor (Y-27632, Tocris), 1% v/v Penicillin-Streptomycin.

2.2.2 Cardiac fibroblast isolation and culture

Human cardiac ventricular fibroblasts were obtained from explanted hearts of patients with dilated or hypertrophic cardiomyopathy at Harefield Hospital or rejected human donor hearts undergoing transplant surgery at Addenbrooke's Hospital. Tissue samples from Harefield Hospital were provided by the Cardiovascular Research Centre Biobank at the Royal Brompton and Harefield NHS Foundation Trust, UK. (NRES ethics number for biobank samples: 09/H0504/104+5; Biobank approval number: NP001- 06-2015 & MED_CT_17_079). The inferior 1/3rd of the heart was received. Tissue samples from Addenbrooke's Hospital were provided by NHS Blood and Transplant, UK (REC reference 16/LO/1568). The whole heart was received.

A culture-based approach was used to isolate cardiac fibroblasts. Tissue culture-treated Petri dishes were coated with fibronectin in Phosphate-Buffered Saline (PBS) (Thermo Fisher Scientific) (10 µg/mL) at 37^{o}C for 1 hour during explant isolation and sterilisation. Left ventricular free wall samples were collected in cold cardioplegia. Tissue pieces were trimmed of excess fat and connective tissue, before being washed in sterile PBS containing 5% v/v Penicillin-Streptomycin and maintained in fresh sterile PBS containing 5% v/v Penicillin-Streptomycin while they were cut into small pieces (<10 mm^3). Tissue pieces were then transferred into a new dish of sterile PBS with 5% v/v Penicillin-Streptomycin and minced to smaller pieces (<1 mm^3). The PBS was aspirated, and the samples were maintained in 0.05% Trypsin- Ethylenediaminetetraacetic acid (EDTA) for 2 minutes. Trypsin was quenched with the same volume of fibroblast culture media. Fibronectin solution in the prepared Petri dishes was removed and replaced with 0.5 mL standard fibroblast culture media. Tissue pieces were transferred to the dishes and arranged with a distance of at least 5 mm between pieces to allow for outgrowth. These were incubated at 37^{o}C for 2 hours to allow for explant attachment before additional standard fibroblast culture media was added to submerge the explants. The cultures were incubated for 4 days before the supernatant was changed for new fibroblast culture media, and from this point, the explant supernatant was changed every 2 days while cell outgrowth was monitored. At confluence, approximately 2 weeks following explant formation, fibroblasts were trypsinised with 0.05% Trypsin-EDTA and incubated for 7 minutes at 37^{o}C, before the fibroblast suspension was transferred to a tissue culture flask. Trypsin was quenched with the same volume of standard fibroblast culture media.

2.2.3 Thawing, maintenance and plating of iCell cardiomyocytes

Commercially-available iCell (Cellular Dynamic International (CDI)) hiPSC-CMs were utilised for experiments described in chapter 4. Cryovials (CDI) were stored in liquid nitrogen until immediately before thawing and maintained as per manufacturer's instructions and previous studies (Lee *et al.*, 2012; Rao *et al.*, 2012).

To thaw, the cryovial of iCell hiPSC-CMs was immersed in a water bath at 37^{o}C for 3 minutes. To resuspend the cells, the cryovial content was transferred to a 50 mL centrifuge tube using a P1000 pipette. The empty cryovial was rinsed with 1 mL of room temperature iCell Plating Medium (CDI) to recover any residual cells from the vial, and this 1 mL was then added drop-wise to the cell suspension. The total cell suspension was topped up with iCell Plating Medium up to the final volume of 10 mL then adjusted to the final viable cell density based on the assay using the equation:

$$viable\ cell\ density = \frac{viable\ cells\ per\ vial\ x\ plating\ efficiency\ x\ viability}{cell\ suspension\ volume}$$

***Equation 1 viable cell density of iCell cardiomyocytes**. Online certificate of analysis has lot-specific values of viable cells per vial, plating efficiency and viability.*

If a higher cell density was required the cell suspension was centrifuged at 180 g for 5 minutes, the supernatant removed and the cells re-suspended in the required volume of iCell Plating Medium. 48 hours after plating, the plating medium was replaced with iCell Maintenance Medium (CDI) to remove cell debris and non-adherent cells. The maintenance medium was replaced every 2-3 days thereafter and all studies were carried out 10-14 days post-thawing and seeding of the hiPSC-CMs unless otherwise stated.

2.2.4 GCamp6f Stem cell dissociation and maintenance

HiPSC line Wild Type C (WTC) GCamp6f (Professor Bruse Conklin, Gladstone Institutes) was used for Chapter 3 and 5. These were maintained and differentiated with the help of Oisin King, Dr Worrapong Kit-Anan and Thusharika Kodagoda (Imperial College London). Significant days are outlined in **Figure 2.1**.

IMR90-4 and WTC GCamp6f hiPSC-CMs were maintained in tissue culture dishes coated overnight with 0.125% v/v Matrigel (Corning) diluted in Knockout DMEM (Life Technologies). Dissociation was performed when the cells reached 80% confluence. Cells were washed with PBS then incubated with 0.5 mM EDTA in PBS at room temperature for 5 minutes. The solution was removed and replaced with Essential 8™ Medium supplemented with 10 µM ROCK inhibitor to remove the cells from the tissue culture plate. The cells in suspension were replated on tissue culture dishes coated overnight with 10 µg/mL Matrigel (Corning) diluted in Knockout DMEM (Life Technologies). The cells were incubated in Essential 8™ Medium (Thermo Fisher Scientific) supplemented with 10 µM ROCK inhibitor for the first 24 hours after replating before maintained in Essential 8™ Medium replaced daily until cells reached 80% confluence. At this point (day 0), the stem cells were dissociated or underwent differentiation.

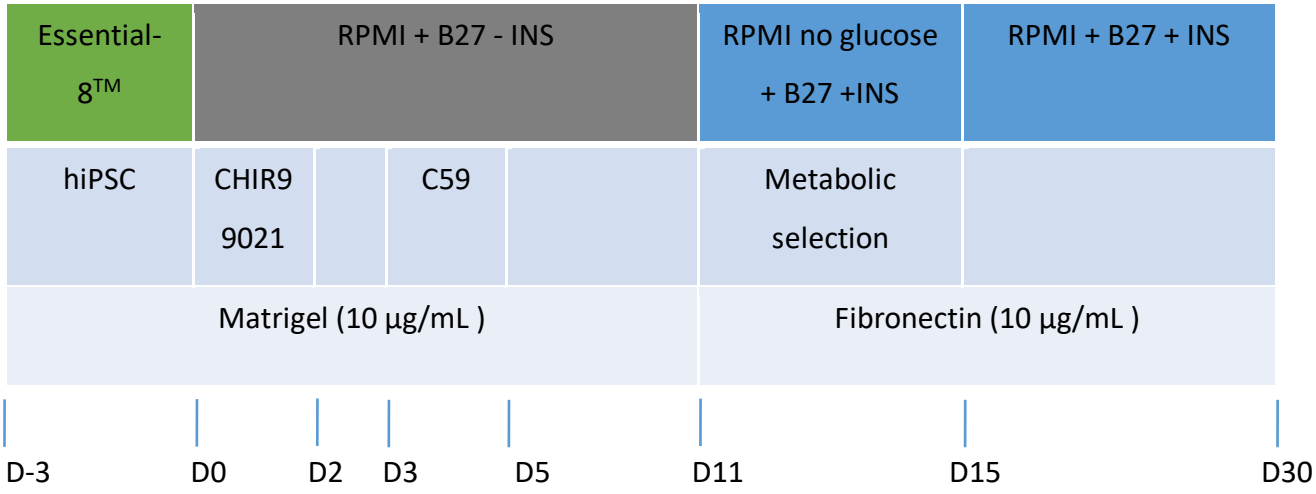

Figure 2.1 Timeline of human induced pluripotent stem cell differentiation into cardiomyocytes. *Schematic protocol for the production of human induced pluripotent stem cell-derived cardiomyocytes by modulation of Wnt signalling (Lian et al., 2012). Coloured bars depict the basal medium. Significant days (D) with supplements noted below this bar.*

2.2.5 GCamp6f stem cell differentiation

The hiPSCs were induced to differentiate by biphasic modulation of Wnt signalling (Lian *et al.*, 2012). The Wnt signalling pathway has emerged as a key regulator of cardiogenesis in vivo and in vitro. During embryonic development, inhibition of glycogen synthase kinase 3 (Gsk3) causes nuclear accumulation of β-catenin, which activates gene transcription that triggers cardiogenesis. In some species, including mouse embryos and mouse ES cells, Wnt signalling was shown to have a biphasic effect on cardiac development, with late signalling repressing the development of heart muscle. Therefore, a biphasic technique was established for hESCs and hiPSCs and shown to generate populations of up to 98% cardiomyocytes before cell sorting (Lian *et al.*, 2012)

On Day 0, cells were exposed to 8 μM Wnt-activator CHIR99021 (MERCK Millipore) in RPMI-1640 media supplemented with B27 minus insulin (RB – INS) (Life Technologies) for 24 hours. On day 1, the culture media was replaced with fresh RB – INS and maintained incubated for 48 hours. On day 3, the RB – INS was removed, and cells were then incubated in 2.5 μM Wnt-inhibitor C59 (Biorbyt) in RB – INS for 48 hours. On Day 5, this was changed to fresh RB – INS, which was changed every 2 days, until areas of beating cells became evident (~ Day 9-11).

2.2.6 GCamp6f hiPSC-CM purification

Once populations of hiPSCs have undergone differentiation induction, the mixed population of hiPSC-CMs and non-cardiomyocytes underwent purification before replating. Once areas of beating cells became evident, metabolic selection by glucose depletion was used to purify the cell population as the hiPSC-CMs rely on oxidative phosphorylation rather than glycolysis (Tohyama *et al.*, 2013). During these 96 hours, the cells were maintained in RPMI-1640 with no glucose, supplemented with B27. Following metabolic selection, cultures were maintained in RPMI-1640 supplemented with B27 (RB + INS) for 2 days before replating.

Tissue culture dishes were prepared with fibronectin in PBS (10 μg/mL) and incubated for at least 30 minutes to allow for fibronectin attachment to the tissue culture plate. During this time, cultures were washed in PBS then incubated in 1 mL of 1X TrypLE per tissue culture plate well for 7 minutes before agitated using a P1000 pipette and transferred to a fresh 50 mL centrifuge tube. 1 mL of RPMI-1640 + 10% FBS was added to the cells per 1 mL of TrypLE

before centrifugation at 200G for 5 minutes. The supernatant was removed before resuspension of the cell pellet in hiPSC-CM plating media for the desired density of 2.5 million live cells per 2 mL of media. PBS in the tissue culture dishes incubated with fibronectin in PBS (10 μg/mL) was aspirated before 2.5 million live cells were added per well of a 6-well plate. 24 hours following replating, the media was changed for RB + INS and 1% v/v Penicillin-Streptomycin and maintained from this second round of purification until D25-26 in RB + INS and 1% v/v Penicillin-Streptomycin, replaced every 2 days.

2.2.7 Plating of hiPSC-CMs on glass substrate

On D25-26, hiPSC-CMs were washed twice in PBS before being detached by 1 mL of TrypLE then incubated at 37^{o}C and 5% CO_2 for 8 minutes. Following incubation, a P1000 pipette was used to dislodge cells from the surface and gently mix to form a single-cell suspension. The dissociation solution was quenched by adding 5 mL RPMI 1640 + 10% v/v FBS. Cells suspensions were then centrifuged for 200 G for 5 minutes. The supernatant was removed, and the cell pellet was resuspended in hiPSC-CM plating media.

Cells were stained with acridine orange/propidium iodide (Logos Biosystems) and counted using a Logos Luna dual fluorescence cell counter, before plating onto 35 mm dishes with a 7 mm diameter glass bottomed well at a density of 80,000 GCaMP6f hiPSC-CMs per dish. Dishes were pre-coated with fibronectin in PBS (10 μg/mL) for 1 hour before cell plating, and PBS was aspirated before cells were plated. After incubation at 37^{o}C for 24 hours, the media was replaced with RB + INS and 1% v/v Penicillin-Streptomycin, replaced every 2-3 days. Cells were used for experiments 5-7 days after plating.

2.3 Co-culture design

GCamp6f hiPSC-CMs were used to study cardiac fibroblast co-culture with cardiomyocytes. All cultures were performed over 24 hours maintained at 37°C and 5% CO_2, at a ratio of 2:1 cardiac fibroblasts: hiPSC-CMs. The four culture designs used were as follows:

1. **Cardiomyocyte-conditioned control (Figure 2.2*a*).**

To control for effects owing to the metabolism and depletion of the medium by incubation with human cells, controls were cultured in hiPSC-CM-conditioned media, generated by culturing 160,000 hiPSC-CMs in serum-free medium for 24 hours. A separate dish of hiPSC-CMs was then washed in sterile PBS before the conditioned serum-free media was added to this second dish for a further 24 hours before electrophysiological assessment.

2. **Fibroblast-conditioned media – unidirectional paracrine interaction (Figure 2.2*b*).**

In order to assess the unidirectional effect of soluble factors secreted by fibroblasts in isolation on naïve hiPSC-CMs, cardiac fibroblast-conditioned media was generated from cardiac fibroblasts. 160,000 fibroblasts were plated on a semi-permeable 0.4 µm pore Transwell® (Corning, NY, USA) suspended over a petri dish containing 2 mL of serum-containing fibroblast culture media and incubated for 2 hours at 37°C to allow for fibroblast attachment. Following incubation, the membranes were washed in sterile PBS, transferred to a new petri dish containing 2 mL of serum-free media and incubated for a further 24 hours at 37°C. Following incubation, the conditioned medium was transferred to 37mm dishes with a 7mm glass-bottomed centre seeded with 80,000 hiPSC-CMs and incubated for 37°C for 24 hours before electrophysiological assessment.

3. **Co-culture – bidirectional paracrine interactions (Figure 2.2*c*).**

As hiPSC-CMs may secrete soluble factors that modulate fibroblast paracrine function, we co-cultured the two cell types in a set up that allowed bidirectional paracrine signalling. Cardiac fibroblasts were prepared as above in the fibroblast-conditioned media set up and then suspended over hiPSC-CMs in 2 mL of serum-free media and incubated for 24 hours before electrophysiological assessment. The suspension using Transwells designed for 24-well plates required placing the Transwells in plastic cuffs.

4. **Direct contact – bidirectional physical and paracrine interactions (Figure 2.2d).**

The third co-culture set-up allowed direct physical interaction between the two cell types. In this setup, cardiac fibroblasts were seeded directly on top of hiPSC-CM monolayers. Fibroblasts in culture flasks were trypsinised in 0.05% Trypsin-EDTA and resuspended at a concentration of 160,000 fibroblasts per 100 µL of fibroblast culture media. HiPSC-CM monolayers on glass-bottomed dishes were washed with PBS before 160,000 fibroblasts were pipetted within the recessed area of the dish, on top of the hiPSC-CM monolayer. This was incubated for 2 hours at 37^{o}C to allow for fibroblast attachment, washed in sterile PBS to remove debris and dead cells before culturing for 24 hours in 2 mL of serum-free media.

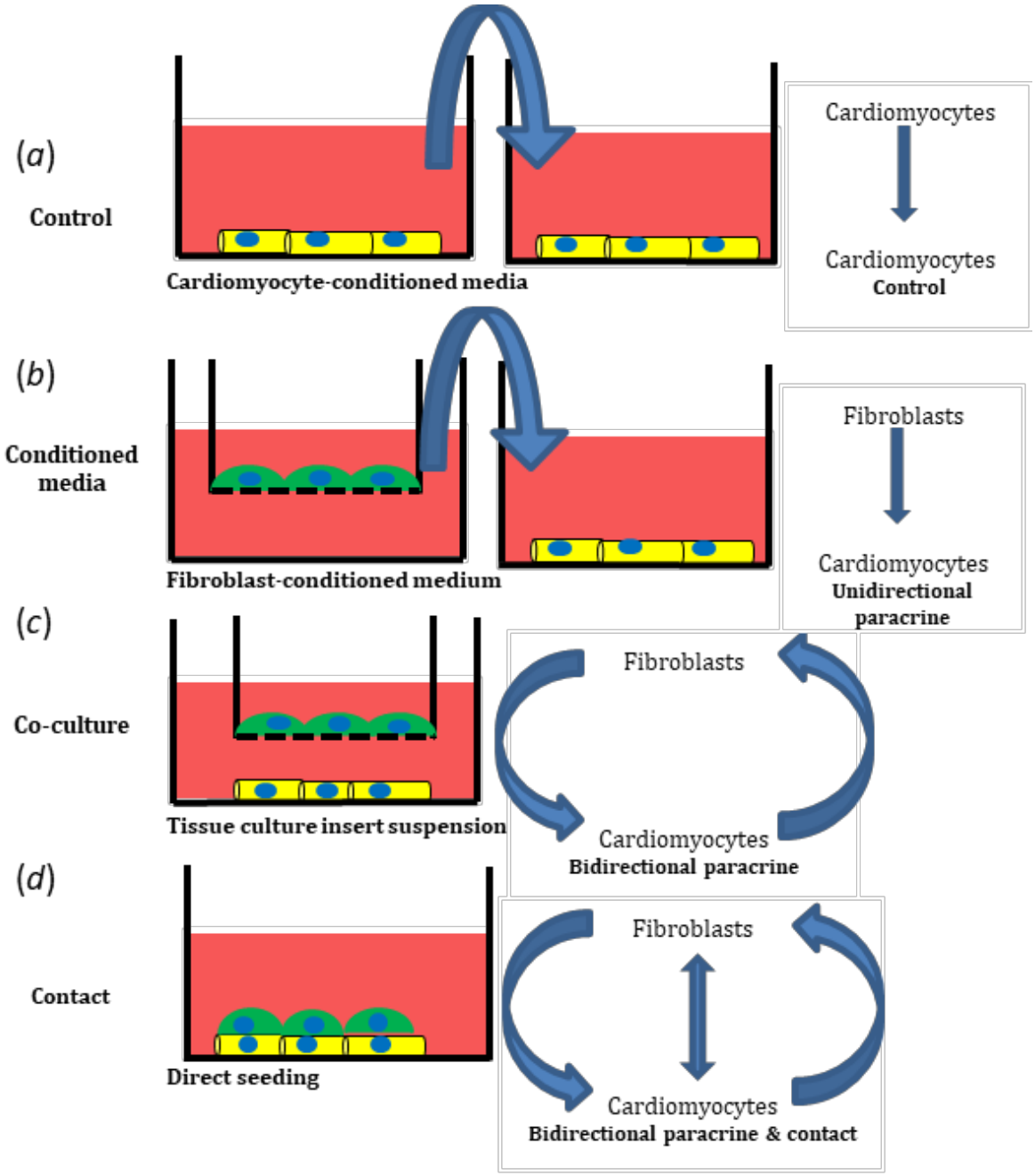

Figure 2.2 Cardiomyocyte and cardiac fibroblast culture platforms. *Cardiomyocytes and cardiac fibroblasts were cultured in separate platforms to investigate methods of intercellular interaction. All platforms used serum free media for conditioning and maintaining the cardiomyocytes for 24 hours before electrophysiological assessment. (a) Cardiomyocyte-conditioned serum-free media used to culture a fresh dish of cardiomyocytes for 24 hours as control, (b) Unidirectional paracrine communication from fibroblast to cardiomyocyte by culturing myocytes in fibroblast-conditioned serum-free media. (c) Fibroblasts were cultured in a Transwell tissue culture insert to allow for bidirectional paracrine communications only in the serum-free media. (d) Fibroblasts were seeded directly on top of cardiomyocytes to allow for bidirectional paracrine and direct contact interactions in the serum-free media. Adapted from Christopher Kane's thesis, Imperial College London.*

2.4 Elastic, reconfigurable co-culture setup

Lacking in the co-culture setup used above is a reproducible means of measure intercellular distance for paracrine communications. In chapter 3, we aim to develop and validate an elastic, reconfigurable substrate made out of Polydimethylsiloxane (PDMS). A schematic of the cell patterning approach is given in **Figure 2.3**.

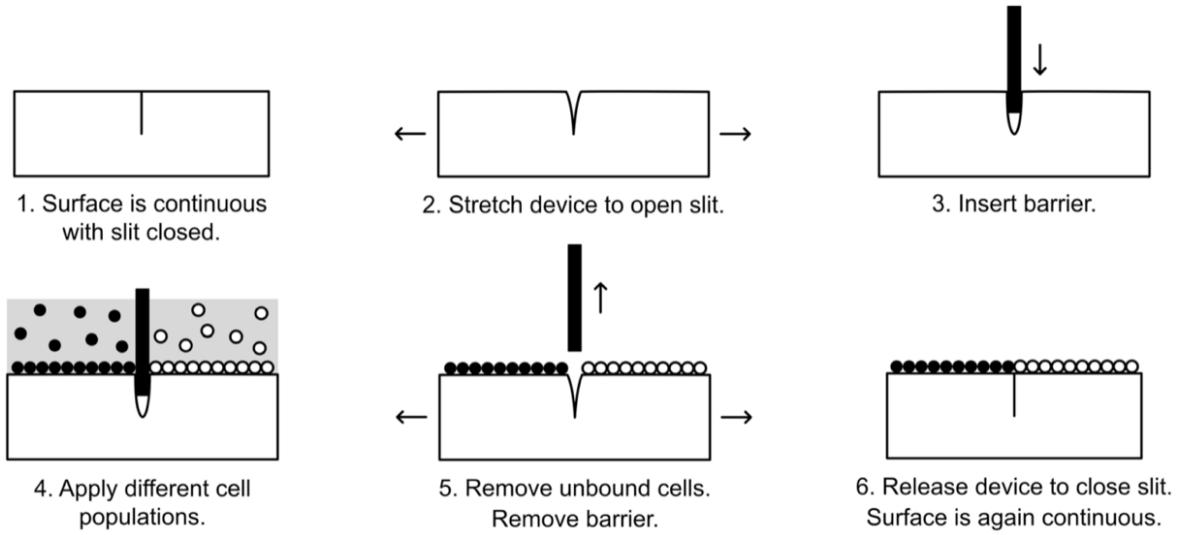

***Figure 2.3 Cell patterning approach**. A shallow slit can be formed on the elastic substrate. The substrate can be stretched open to allow insertion of a thin barrier. Different cell populations can be seeded onto separate sides of the barrier. Once the cells have adhered, the barrier can be removed to allow intercellular interactions between the two cell populations. (Curtis et al., 2017)*

2.4.1 Synthesis of an Elastic PDMS substrate

A mould for PDMS co-culture substrate fabrication was kindly provided by Dr Allison Curtis (University of California, Irvine). Moulds were created by attaching laser-cut acrylic parts (10 mm diameter squares x 6 mm) to the bottom of a square 100 mm polystyrene dish (Thermo Fisher Scientific) using cyanoacrylate glue (Gorilla Glue Company) (**Figure 2.4A**) (Curtis *et al.*, 2017). Two-part polymer Sylgard 184 (Dow Corning), base elastomer and curing agent were mixed at 1:10 weight ratio then poured into the mould. The mould was placed in a vacuum chamber for 120 minutes for degasification before incubation in an oven at 60°C overnight.

Following overnight incubation, the PDMS was removed from the mould and washed three times with PBS (**Figure 2.4B**). A shallow slit was cut across the bottom of each mould well by using a razor blade (**Figure 2.4C**). Devices were submerged in 70% ethanol for 15

minutes then air dried before UV-sterilisation for 30 minutes. The wells were then washed once with sterile PBS. To open the slit, the device was bent, and a #1 glass coverslip (Thermo Fisher Scientific) was inserted (**Figure 2.4D**).

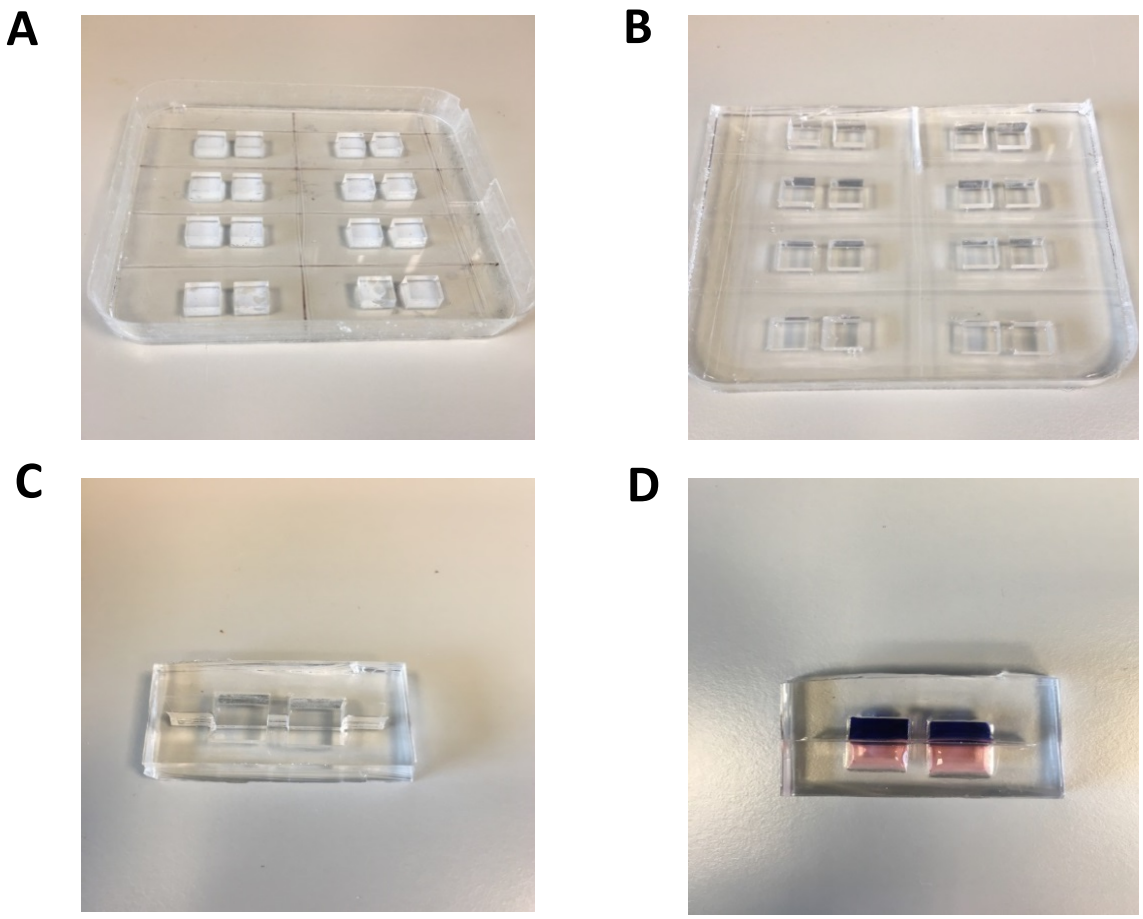

Figure 2.4 Reconfigurable elastic substrate device. *(A) Substrate mould composed of acrylic parts attached to a polystyrene dish. (B) Devices removed following degasification and incubation at 60°C overnight. (C) An individual device consists of two moulded elastic wells. Razor blade cut a slit extending partially through the bottom of the wells. (D) The device seals around an inserted coverslip to form two separate chambers from each well.*

2.4.2 hiPSC-CM and cardiac fibroblast plating on PDMS device

With the coverslip barrier in place, device wells were then incubated in 200 µL of fibronectin in PBS (10 µg/mL) at 37°C for 1 hour. The PBS was removed and hiPSC-CMs (1.5 x 10^5 cells in 200 mL hiPSC-CM plating media) and cardiac fibroblasts (0.5 x 10^5 in 200 mL fibroblast culture media) were seeded into the two separate chambers and incubated overnight to allow for adhesion. The wells were then gently aspirated, and the hiPSC-CMs and

cardiac fibroblasts were cultured with RB + INS and fibroblast culture media, respectively. Media was then changed every 2-3 days to allow hiPSC-CM maturation and fibroblast proliferation.

5 days after seeding, the wells were gently aspirated and washed three times with warm PBS. The device was then stretched to open the slit, and the coverslip barrier was removed. The cells were washed another 3 times with warm PBS to remove unattached cells, and finally, 500 µL of serum-free media was added. The cells were then incubated for 24 hours before electrophysiological assessment.

2.5 Integrins

2.5.1 Soluble Integrin ligands

The Arginine-Glycine-Aspartate (RGD)-tripeptide repeat has been shown to be sufficient and indispensable for integrin-binding activity. Several RGD-containing peptides were used to assess the effect of structural variations on hiPSC-CM electrophysiological changes. we investigate the effects of integrin ligands RGD, GRGDS and GRGDSP on hiPSC-CM structure and function. Compounds employed were RGD, GRGDS and GRGDSP (Sigma Aldrich). We also use the negative control RGES (Sigma-Aldrich) to identify that the effect is mediated by RGD. Amino acid structures of each compound are shown in Table 2.1. All peptides were used in their linear forms.

Table 2.1 Amino acid structures of RGD-containing peptides.

Compound	Structure
RGD	Arg-Gly-Asp
RGES	Arg-Gly-Glu-Ser
GRGDS	Gly-Arg-Gly-Asp-Ser
GRGDSP	Gly-Arg-Gly-Asp-Ser-Pro

Arg = arginine; Gly = glycine; Asp = aspartic acid; Ser = serine; Pro = proline and Glu = glutamic acid.

24 hours before optical mapping the RGD peptides were dissolved in sterile MΩ water and added to the cells at a concentration of 2mM and incubated at 37°C for 24 hours.

2.5.2 Integrin ligands antibodies

Mouse monoclonal against integrin β1 (P5D2) (Abcam) and mouse monoclonal antibody against β1 (F11) (Thermo Fisher Scientific) were either added individually or added together to hiPSC-CM monolayers at 10 μg/mL in PBS. Alternatively, the antibodies were added to hiPSC-CMs for 1 hour at 4°C then added concomitantly with 2mM soluble RGD-containing peptides and incubated at 37°C for 24 hours.

2.5.3 Self-assembling integrin ligands

The following synthetic peptides were studied: (a) NH_3^+-RGDSGAITIGA-$CONH_2$ (RGD_A), (b) NH_3^+-RGDSGAITIGC-$CONH_2$ (RGD_C) (Genecust). Both synthetic peptides possessed a degree of purity higher than 95%. These synthetic lyophilised peptide powders were dissolved in serum-free media (2mM) before vortexing to mix and sonication for 1 minute. Samples were then incubated at 37°C for 3 hours to allow for self-assembly. Media was removed from the hiPSC-CMs before a PBS wash. 80 μL of peptides (2mM) was added above the hiPSC-CM monolayer and incubated for 24 hours before assessment.

2.6 EV Isolation, purification and quantification

2.6.1 Fibroblast EV-conditioned media production & processing

Hyperflasks (Corning) were used to grow cardiac fibroblasts in fibroblast culture media until at least 70% confluence. Fibroblast culture media contains Foetal Bovine Serum, a blood product with very high concentration of bovine EVs (Shelke *et al.*, 2014). It would therefore be important to omit FBS from the cell culture medium for the duration of EV collection to avoid contamination. Fibroblasts are heavily dependent on FBS-content, and omission of FBS could change EV composition and cell survival, so collecting fibroblast-secreted EVs in media void of FBS risks substantial contamination with apoptotic bodies and other cellular debris. For the purposes of this study, we chose to limit the EV collections time to 48 hours and use EV-depleted FBS during the collection period. After washing with PBS, cell cultures were incubated for 48 hours in exosome-depleted fibroblast culture media. Following conditioning of the media, the media was removed and filtered through a 0.45 μm bottle-top filter.

2.6.2 EV-conditioned media purification by ultrafiltration

Ultrafiltration was then used to concentrate the filtered conditioned media, prior to additional purification steps.

By this method, the initial sample is forced against a membrane containing nano-scale pores that allow the passage of water and smaller biomolecules, but not EVs. Current opinion in the field holds that this process is less damaging to EVs than ultracentrifugation, as the EVs are never taken out of solution and there is little evidence of aggregation. By contrast, aggregation is a known consequence of ultracentrifugation (Nordin *et al.*, 2015). However, EVs are lost during this process. It is thought that this at least partially due to adherence to the membrane itself. Use of centrifugal concentrators with low membrane surface areas increases the EV recovery compared to pressure-driven, high surface area devices (Lobb *et al.*, 2015). The same study also found that ultrafiltration recovered approximately twice as many particles from the original sample as ultracentrifugation. Other studies have confirmed that ultrafiltration has a good recovery efficiency and does not damage EVs (Nordin *et al.*, 2015; Benedikter *et al.*, 2017; Mol *et al.*, 2017).

A pore size of 100 kDa (~ 7 nm) was used for routine purification of EVs. Filtered conditioned media were then concentrated by ultrafiltration using an Amicon Ultra-15 Centrifugal Filter (Merck) with a 100 kDa MWCO (Molecular Weight Cut-Off) (~ 7 nm) pore size, at 4000 x g, 4^{o}C for 3 minutes. This was repeated, topping up with additional media between centrifugations to a volume of 12 mL. In this way, each concentrator processed 500 mL of starting conditioned-media to a final volume of 500 µL.

2.6.3 Purification by SEC

SEC is an EV-purification method that has been shown to provide highly pure (Boing *et al.*, 2014; Benedikter *et al.*, 2017), physically intact, EVs with improved functionality (Gámez-Valero *et al.*, 2016; Mol *et al.*, 2017), compared to vesicles isolated by ultracentrifugation, the most common method for EV isolation. Differential centrifugation, unlike SEC, risks protein complex formation and vesicle aggregation. Previous studies have also reported that the viscosity of concentrated conditioned-media affects vesicle recovery in differential centrifugation, but does not affect vesicle recovery by SEC (O'Brien, 1969; Momen-Heravi *et al.*, 2012).

2.6.4 SEC column packing and preparation

To exchange the buffer before column packing, 60 mL of Sepharose CL-2B Slurry was transferred to a wide, shallow container and the gel beads were allowed to settle. The solvent was aspirated off and the beads resuspended in 120 mL of particle-free 18.2 MΩ water. This was repeated, before resuspending the slurry and pouring the suspension into a 30 cm Econo-Column (Bio-Rad) with a 50 mL syringe barrel attached as a reservoir. The slurry was allowed to sit to allow for any large air bubbles to be removed by tapping the side of the column before the bottom tap was opened to allow the column to pack under gravity. The column was allowed to pack until a final depth of 28 cm (**Figure 2.5**).

The packed SEC column was opened, and the PBS was allowed to drain through until the top of the beads in the separation media was dry. Loading of the sample into the column was carried out by gently applying 500 µL of sample to the top of the column using a 1 mL manual pipette. The column spout was then opened so sample could enter the column. Fraction collection began at this point. As soon as the media had wholly entered the separation media, PBS was gently added to the top of the column into the column headspace, avoiding disturbing the separation media. Once at least 3 cm of PBS was added on top of the separation media, a PBS reservoir was connected to the column. The first time a column was used, 1 mL fractions were collected, and the particle concentration analysed on a Nanosight to determine peak fractions. The protein content of the fractions was also analysed by microBCA assay to check for efficient separation of EV from soluble proteins.

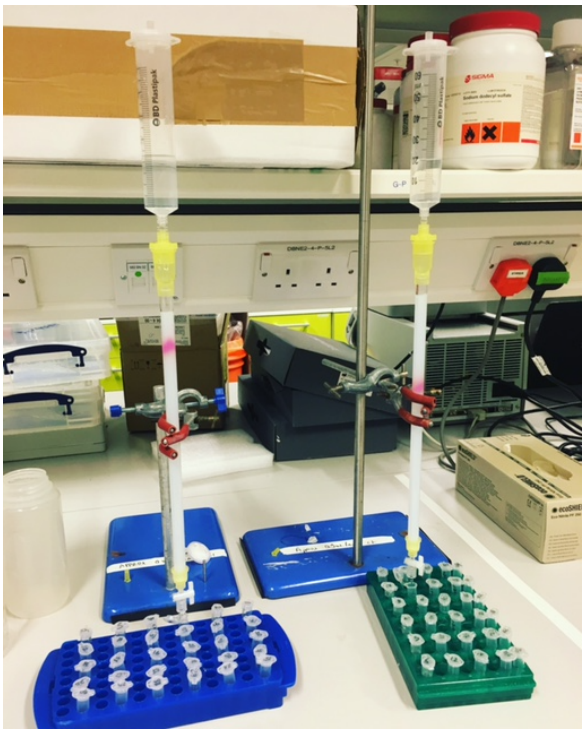

***Figure 2.5 Size-exclusion chromatography column**. Two 30 mL columns stacked with Sepharose CL-2B for isolation of vesicles from fibroblast-conditioned media. 50 mL syringe attached as a PBS reservoir once sample was added. 1 mL fractions collected at the tap.*

2.6.5 Nanoparticle Tracking Analysis (NTA)

The range of EV purification methods means that EV quantification and assessment of purity is of critical importance. Particle concentration in the fractions was quantified by NTA. This is the most widely used method for EV quantification and single particle analysis. NTA relies on the light scattering properties of particles in a solution by illuminating these particles with a laser light. The Brownian motion of particles is analysed from a video, and this motion of individual particles in the solution is analysed using the Stokes-Einstein equation to estimate the hydrodynamic diameter of the particles (Gardiner *et al.*, 2013). As such, the NTA covers the EV size spectrum and provides information on both the size distribution and concentration of particles in the solution.

The concentration and size distribution of particles in solution was measured using a Nanosight NS300 with an SCMOS (Scientific Complimentary Metal-Oxide Semiconductor) camera module and a 532 nm diode laser module. Samples were diluted 10-1,000 fold in particle-free water from a Select Fusion Milli-Q water purifier (Suez Water UK) to a concentration within the range of 10^8-10^9 particles/mL, such that the number of particles in

the field of view was below 200/image. Using NTA V3.0 software, three 60-second videos were recorded and analysed per sample, with software parameters Camera Level 15, Detection Threshold 5 used. The Finite Track Length smoothing algorithm was disabled.

2.6.6 Protein quantification

The microBCA (Bicinchoninic Acid) protein assay kit (Thermo Fisher Scientific) is a detergent-compatible BCA formulation for the colourimetric detection and quantification of total protein. It has been optimised for use with dilute protein samples (0.5 – 20 µg/mL). Cu^{2+} is reduced by protein in an alkaline environment, producing Cu^{+}, which is detected by BCA, causing the chelation of two molecules of BCA with one Cu^{1+}, a reaction that produces a purple-coloured water-soluble complex. This complex exhibits a strong absorbance at 562nm that is linear with increasing protein concentration. Preparation of a standard curve using BSA standards allows the researcher to determine the protein concentration of unknown samples.

Standard and working reagents were prepared as per manufacturer's instructions. Briefly, the working reagent was made by mixing components A, B and C in a 25:24:1 ratio and used immediately. Both samples and BSA standards were added with working reagent in clear-bottomed 96-well plates (50 µl of sample + 150 µL working reagent/well). Adhesive plate seals (Thermo Fisher Scientific) covered the top of the wells to prevent evaporation then plates were mixed thoroughly on a plate shaker for 30 seconds before incubation at 37^{o}C for 2 hours. Colour change was assessed by measuring absorbance at 562 nm wavelength light on a µQuantTM micro-plate reader (Bio-Tek Instruments Inc.). The average absorbance measured in the blank standard replicates was subtracted from the standard absorbance, and the concentrations of unknown samples were determined using a linear regression fitted to the standards.

One ampule of Albumin Standard solution was diluted into several clean vials using PBS to form the standard solutions (**Table 2.2**):

Table 2.2 Standard solutions for micro BCA.

Vial	Vial of Diluent	Volume and Source of BSA	Final BSA Concentration
A	4.5 mL	0.5 mL of Stock	200 µg/mL
B	8.0 mL	2.0 mL of vial A dilution	40 µg/mL
C	4.0 mL	4.0 mL of vial B dilution	20 µg/mL
D	4.0 mL	4.0 mL of vial C dilution	10 µg/mL
E	4.0 mL	4.0 mL of vial D dilution	5 µg/mL
F	4.0 mL	4.0 mL of vial E dilution	2.5 µg/mL
G	4.8 mL	3.2 mL of vial F dilution	1 µg/mL
H	4.0 mL	4.0 mL of vial G dilution	0.5 µg/mL
I	8.0 mL	0	0 µg/mL = blank

2.7 Structural characterisation

2.7.1 Dot blotting

2.7.1.1 Set up

It is important to note that these particles isolated by SEC may not exclusively be EVs; lipoprotein complexes, protein aggregates and other debris will also be counted. The presence of EVs was confirmed by detection of EV marks CD9, CD63 and CD81.

A 0.45 µm nitrocellulose membrane (Bio-Rad 162-0117) was submerged in Tris-buffered saline (TBS, Bio-Rad 170-6435) for 10 minutes. The Bio-Dot apparatus (Bio-Rad 170-6545) was assembled around the wetted membrane (**Figure 2.6**).

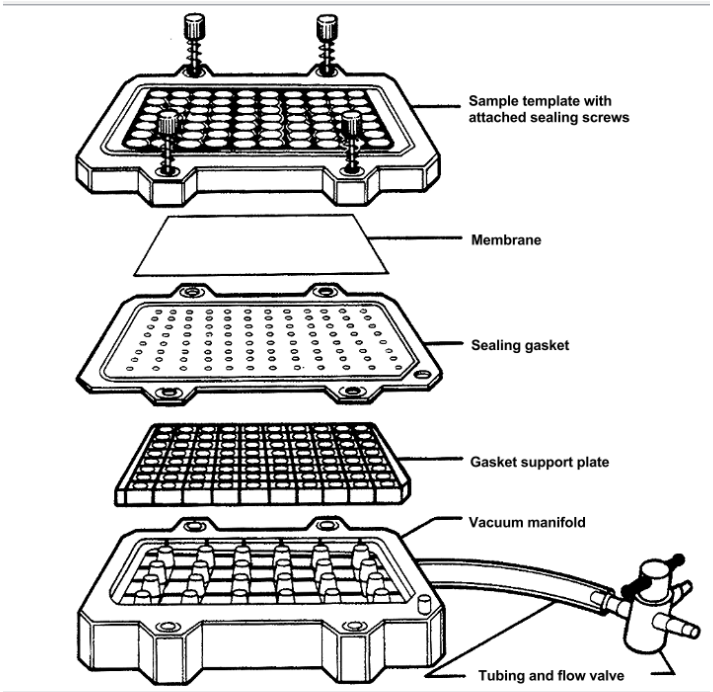

Figure 2.6 diagram of proper Bio-Dot apparatus assembly *(Bio-Rad Laboratories Inc. 2000).*

2.7.1.2 Membrane blocking

The four screws were tightened to prevent sample contamination between wells. All wells were rehydrated with 200 µL TBS and allowed to drain. 50 µL samples were added to a 96-well plate before transferred to the sample template using a multi-channel pipette. The sample was allowed to pass through under gravity. All wells were washed three times with TBS and allowed to drain. The BioDot was then disassembled before blocking of the membrane. The membrane was cut for orientation, marked with pencil for identification and then incubated in a solution of 5 % w/v BSA in TBS-T for 1 hour at room temperature.

2.7.1.3 Primary incubation

The dot blot membrane was then washed three times in TBS-T for 10 minutes each round at room temperature before incubation overnight at 4°C with the primary antibody in the desired dilution (**Table 2.3**) in TBS-T.

Table 2.3 Primary antibodies for dot blot.

Primary antibody	Dilution factor	Species	Manufacturer	Product code
Anti-CD9	800	Mouse	Thermo Fisher Scientific	10626D
Anti-CD63	400	Mouse	Thermo Fisher Scientific	10628D
Anti-CD81	400	Mouse	Thermo Fisher Scientific	10630D

2.7.1.4 Secondary incubation and imaging

Following the overnight incubation, membranes were washed three times in TBS-T for 10 minutes each time at room temperature, before incubation for 1 hour at room temperature with the secondary antibody in the desired dilution (1:15000) in TBS-T. The secondary antibody used was goat anti-mouse 800 CW (LI-COR 926-32210) Membranes were then washed three times in TBS-T for 10 minutes at room temperature and imaged using an LI-COR Odyssey imager.

2.7.1.5 Imaging of dot blots

Dot blots were quantified using Image Studio Lite V5.2 software (LI-COR). For each image, background was subtracted with a rolling ball radius set to 25 pixels before a rectangle was fitted around each lane and the profile plot was viewed. The intensity of each dot was measured using the gel analysis procedure. The Integrated Density for each fraction was then expressed as a percentage of the total of all the dots.

2.7.2 EV Electron Microscopy

2.7.2.1 Cryo-Electron Microscopy (CryoEM)

Holen Carbon Grids (HC200-Cu, Electron Microscopy Sciences) were plasma treated (15 s, O_2/H_2) on a Gatan Solaris Plasma Cleaner. Samples of EVs in PBS were prepared using a Leica EM GP automatic plunge freezer. 4µL of sample was added onto the carbon coated side of the grid while in an environmental chamber (relative humidity: 90%, temperature: 20°C). Excess sample was blotted on filter paper and the obtained film was vitrified in liquid ethane. Samples were then stored under liquid nitrogen until imaged. Samples were imaged using a JEOL 2100 plus with 200kV and the Minimum Dose System. Imaging temperature was -170°C in a Gatan914 cryoholder. Micrographs were taken using a Gatan Orius SC1000 camera at a magnification of 30k.

2.7.2.2 Transmission electron microscopy (TEM) processing of EVs

Isolated EVs were fixed in 2% paraformaldehyde (W/V) for 60 minutes, 10 µl of fixed EVs were placed on formvar-coated grid for 60 minutes, blot dry the grid and examined in JEOL 1200 EX transmission electron microscope. Digital micrographs were taken using Gatan digital micrograph.

2.7.2.3 Immunogold labelling

Isolated EVs were fixed in 2% paraformaldehyde (W/V) for 60 minutes, 10 µl of fixed EVs were placed on formvar-coated grid for 60 minutes. Each grid was placed in three droplets of 0.5M sodium cacodylate buffer (pH 7.4) for 5 minutes each followed by placing on a droplet of 1% Bovine serum albumin (BSA) for 30 minutes. Grids were then placed on 10 µl of CD63 (abcam) at 1:10 dilution for 60 minutes. Unbound antibody was removed by floating the grids on three droplets of 1% BSA for 5 minutes each. Grids we then placed on gold conjugated goat anti- mouse IgG (10 nm) at 1:50 dilution for further 60 minutes followed by 3 washes in PBS and final wash in distilled water. Grids were stained with 2% Uranyl acetate for 3 minutes, washed in distilled water, viewed in JEOL 1200 EX transmission electron microscope. Digital micrographs were taken using Gatan digital micrograph.

2.7.3 hiPSC-CM Electron Microscopy

hiPSC-CMs were attached to 1 x 1 cm Aclar film squares treated with 10 µg/mL Matrigel in serum free medium and cultured in maintenance medium. To prepare specimens for electron microscopy, samples were fixed in 2.5% glutaraldehyde and 2% paraformaldehyde in 100 mM sodium cacodylate buffer. After washing in sodium cacodylate buffer, samples were subsequently stained in: 1% osmium tetroxide and 1.5% potassium ferrocyanide; 1% tannic acid, 1% osmium tetroxide and 1% uranyl acetate, with washings in water after each staining step. After staining, samples were dehydrated in an ethanol ascending series (50%, 70%, 90%, 100%, 100%) followed by a further dehydration in pure acetone. Increasing concentrations of TAAB 812 hard resin (25%, 50%, 75%, 100%) mixed with acetone were used for infiltration. To finish, samples were embedded in pure resin and cured at 75^{o}C for 36 hours.

Resin blocks were sectioned with a diamond knife at 80 nm on a Leica Ultracut UCT and sections imaged on an FEI Tecnia12 BioTwin opened at 80 kV. Images were collected with a Gatan Microscoy Suit in dm3 format and analysed in Image J (Schneider, Rasband and Eliceiri, 2012; Rueden *et al.*, 2017) or IMOD (Kremer, Mastronarde and McIntosh, 1996).

2.8 Functional characterisation

2.8.1 Treatment of hiPSC-CMs with cardiac fibroblasts and GW4869

To investigate the effects of exosome inhibition by GW4869 in hiPSC-CM: cardiac fibroblast contact cultures, GW4869 was dissolved in DMSO to a stock concentration of 20 mM. hiPSC-CMs were pre-treated with 20µM GW4869 (1µL GW4869 in 1000µL of serum-free media) for 2 hours before this was washed with PBS cardiac fibroblasts were seeded directly on top of hiPSC-CMs with 20µM GW4869 using the fibroblast-contact setup method described in Section 2.3. Cultures were incubated at 37°C and 5% CO_2 for 2 hours before being washed and incubated at 37°C and 5% CO_2 for a further 22 hours in serum free media with 20µM GW4869.

2.8.2 Treatment of hiPSC-CMs with EVs

EVs were concentrated before treatment of the hiPSC-CM monolayers in glass-bottomed tissue culture dishes. Particle in SEC fractions 7-11 in solution were combined with 7 mL serum-free media and placed in a 100 kDa MWCO Amicon Ultra-15 Centrifugal Filter and ultrafiltrated in a centrifuge at 4000 x g, 4^{o}C for 3 minutes. Serial ultrafiltration at varying durations was carried out until a concentration of 150 µg per 100 µL of the sample remained. One hyperflask produced approximately 300 µg of protein in SEC fractions 7-11. 150 µg was added to the hiPSC-CMs. This 150 µg of protein is from an original starting volume of approximately 250 mL of fibroblast-conditioned media.

To investigate the contribution of the non-EV content of the exosome-depleted serum-containing media, the same starting volume of the exosome-depleted media (500 mL) was processed in the same manner as the fibroblast-conditioned media. Particle in SEC fractions 7-11 were concentrated to a volume of 200 µL. 100 µL was added to the hiPSC-CM monolayer.

The effects of exosome-depleted serum media with and without fibroblast conditioned EV content were compared to serum-free media.

2.8.3 Cytokine profiler

Fibroblast EV fractions following the SEC purification were pooled for cytokine analysis then further concentrated by ultrafiltration using a 100 kDa MWCO Ultra-15 Centrifugal Filter at 4000 x g, 4^{o}C until the sample reaches a volume of 250 µl. Sample was transferred to an Eppendorf before EV membranes were lysed with 250 µl RIPA solubilisation buffer containing a 1:500 dilution of protease inhibitor cocktail. Sample was then sonicated for 60 seconds before the content was analysed with a proteome array containing antibodies against 36 human cytokines following the manufacturer's instructions.

2.9 Electrophysiological techniques

2.9.1 Optical recording of twitch Ca^{2+} transients

IMR90-4 hiPSC-CM cytoplasmic [Ca^{2+}] transients were visualised by loading cells with Fluo-4-acetoxymethyl ester (Fluo-4 AM) (Invitrogen, Thermo Fisher Scientific); a cell-permeable Ca^{2+}-sensitive fluorescent molecule. Fluo-4 AM rapidly increases in fluorescence by 100-fold in the presence of cytoplasmic Ca^{2+-}, owing to the K_d[Ca^{2+}] of 350nM. Cells were loaded with 4 µL of Fluo-4 AM (50 µg Fluo-4 AM in 50µL DMSO + 1.5 µL Pluronic Acid) in 1 mL DMEM and incubated for 20 minutes. The media was replaced with fresh DMEM and incubated for a further 20 minutes to allow for dye de-esterification. Otherwise, genetically modified hiPSC line (WTC GCaMP6f) was used without Fluo-4AM incubation.

During optical mapping, the samples were maintained in standard Tyrode's. The samples were mounted on the stage of an upright Nikon Eclipse FN1 microscope or an inverted Nikon Eclipse TE2000 microscope in the 7mm glass bottom dishes and observed through a 40x water immersion or 40X oil objective, respectively. Samples were kept in 37^{o}C standard Tyrode's solution. Cells were excited using a 470nm wavelength LED light and emitted fluorescence collected through a 530 nm long-pass filter (Green channel). The cells were typically stimulated at 1 Hz using an external stimulator (IonOptix) and platinum electrodes with a biphasic stimulus consisting of a 10 ms pulse width and 20 V amplitude.

The fluorescence signal on the upright microscope was recorded using an ORCA-Flash 4.0 V2 Digital CMOS camera (4 ms frame rate) and WinFluor software (University of Strathclyde electrophysiology software) and acquired at 250 frames/second. On the inverted

camera, the recordings were captured using a NeuroCMOS camera (Redshirt) and acquired at 250 frames/second. LED intensity was kept constant throughout experiments at a level that minimised photo-bleaching.

The Ca^{2+} transients were analysed offline. For optical mapping carried out on the Upright microscope, both the analogue and image series were extracted in Tif format then opened in the software FIJI. A profile plot of the region of interest was generated and saved as a text file. For optical recording carried out on the inverted microscope, the region of interest was spatially averaged to produce an analogue series that was exported as an ASCII file, in the text file form. These text files were then analysed using Clampfit software (Molecular Devices).

The following parameters were then measured: normalised fluorescence amplitude (F1/F0), which is the transient peak amplitude (F1) divided by the baseline value of the signal (F0); time to peak (Tp) calculated as the time taken from the start of the transient to reach the peak amplitude; time to 50% decay (T50) and time to 80% decay (T80), calculated as the time taken for the transient to decrease from peak fluorescence to 50% and 80% of the transient peak amplitude, respectively, during the recovery phase of the transient (**Figure 2.7**). Alternatively, the text files were analysed using a custom MatLab © code (Mathworks). The custom MatLab © code, written by Ilona Sunyovszki (Imperial College London) and Bryan Hassell (Harvard University) determined the parameters: F1/F0, Tp, T50 and T80.

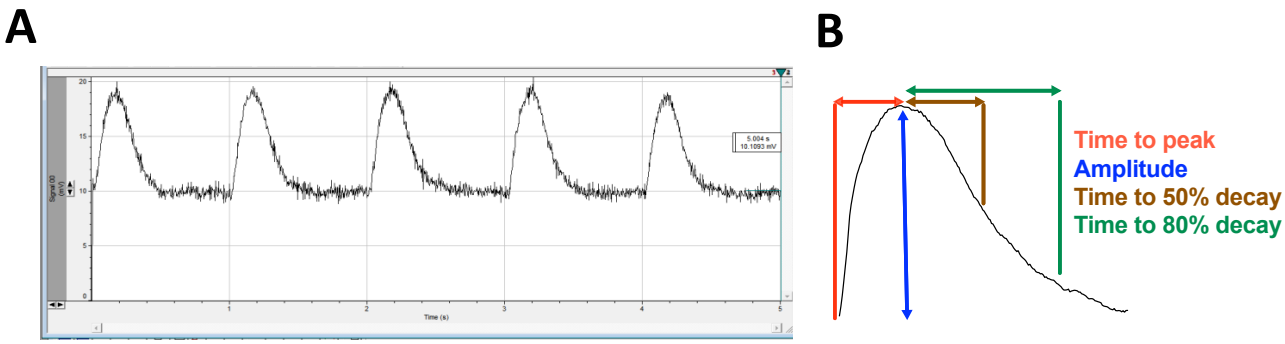

Figure 2.7 Ca^{2+} transient analysis. *(A) Ca^{2+} transient in Clampfit, (B) Ca^{2+} parameters.*

2.9.2 Caffeine application

Caffeine was applied locally to hiPSC-CMs to assess SR Ca^{2+} content and Ca^{2+} removal mechanisms. A solution of 40mM caffeine in standard Tyrode's or Na^{+}/Ca^{2+}-free Tyrode's solution was loaded into borosilicate glass micropipettes (Harvard Apparatus) and mounted

onto a 3-axis micromanipulator. The pipette tip was positioned just above the surface of the cells. The cells were field-stimulated at a pace of 1 Hz before stimulation was ceased and caffeine was applied simultaneously by applying positive pressure with a syringe pump.

2.9.3 Analysis of SR Ca^{2+} content, Fractional release and Ca^{2+} removal mechanisms

Amplitude (F1/F0) of caffeine-induced Ca^{2+} transient was used to determine the total SR Ca^{2+} content. Calculation of relative contribution of Ca^{2+} removal mechanisms has previously been set out by Bassani and colleagues as (Bassani, Yuan and Bers, 1995):

$$K_{twitch} = K_{SR} + K_{NCX} + K_{slow}$$

Equation 2 Contribution of mechanisms to Ca^{2+} removal in cardiomyocytes

Rate of Ca^{2+} decay was calculated following the fitting of a monoexponential curve with the function:

$$f(t) = \sum_{i=1}^{n} A_i e^{-t/Ti} + C$$

Equation 3 Rate of Ca^{2+} decay calculated using a monoexponential curve function

In this way, the fit identifies the Amplitude (A), the time constant T and the constant y-offset C for each input value (i) in the decline phase of the Ca^{2+} transient. Rate is calculated as 1/ τ (s^{-1}) for the transients triggered by field stimulation in standard Tyrode's (κ_{twitch}) (**Figure 2.8A**). The rate of SR Ca^{2+} uptake (κ_{SR}) was calculated as κ_{twitch} minus the rate of decline phase for the transient triggered by Caffeine in standard Tyrode's ($\kappa_{caffeine}$).

Slow mechanisms of Ca^{2+} removal were contributed to by sarcolemmal Ca^{2+}-ATPase and mitochondrial Ca^{2+} uniporter uptake. To measure the contribution of sarcolemmal Ca^{2+} flux, bath solution was switched to a Na^+/Ca^{2+}-free Tyrode's solution, where Na^+ is substituted for Li^+. 40 mM caffeine in Na^+/Ca^{2+}-free Tyrode's solution was applied to cells bathed in Na^+/Ca^{2+}-free Tyrode's. In this way, the rate of decline of the caffeine-induced Ca^{2+} transient is only contributed to by the slow mechanism (κ_{slow}), as NCX activity is negated (**Figure 2.8B**).

The contribution of NCX to the decay phase (κ_{NCX}) is calculated as the difference between this Na^+/Ca^{2+}-free Tyrode's solution caffeine-induced decline (κ_{slow}) and standard Tyrode's solution caffeine-induced decline ($\kappa_{caffeine}$).

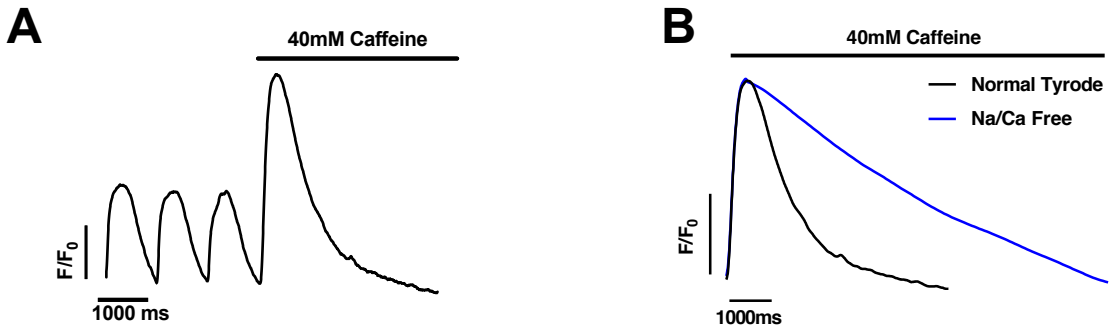

Figure 2.8 Assessment of Ca^{2+} extrusion mechanisms. *(A) Representative trace of field stimulated (twitch) Ca^{2+} transients followed by caffeine response in standard Tyrode's solution. (B) Representative traces showing response to caffeine in Na^+/Ca^{2+}-free and standard Tyrode's conditions.*

2.10 Imaging

2.10.1 Bright field imaging

Bright field images of hiPSC-CMs were obtained by using 40x objective mounted on a Zeiss Axio Observer Inverted Widefield Microscope at 20 frames per second. The samples were kept in 37^{o}C standard Tyrode's solution. All the acquired images were processed by ImageJ (NIH).

2.10.2 Immunofluorescence staining and imaging

Following optical mapping, hiPSC-CMs and cardiac fibroblasts were washed three times in PBS for 5 minutes each time then fixed with 4% paraformaldehyde (PFA) at room temperature for 15 minutes. The samples were washed three times in PBS for 5 minutes then samples were permeabilised with 0.2% Triton-X in PBS for 15 minutes at room temperature. After 3 further washes in PBS for 5 minutes each wash, samples were blocked for 1 hour using a blocking solution (10% v/v donkey serum (VWR International), 5% w/v BSA, and 10% FBS). The blocking solution was removed, and the primary antibody (Table 2.4) was added in 10% blocking solution in PBS overnight at 4^{o}C.

Following overnight incubation, the antibody was removed, and samples washed with PBS for 15 minutes another 3 times before the secondary antibody donkey anti-mouse immunoglobulin G (IgG) (H + L) (Thermo Fisher Scientific), donkey anti-rabbit IgG (H + L) (Thermo Fisher Scientific) and donkey anti-goat IgG (H + L) (Thermo Fisher Scientific) diluted 1:400 v/v in PBS were added for 1 hour at room temperature. The excitation wavelengths of secondary antibodies were selected among 488 (Green), 555 (Red) and 647 (Far red) nm. Nuclei were visualised using 1:1000 v/v DAPI (4', 6-diamino-2-phenylindole) (Thermo Fisher Scientific) in PBS for 1 minute. The samples were mounted in Fluoromount Aqueous Mounting Medium under a coverslip and imaged using a Zeiss LSM-780 confocal microscope unless stated otherwise.

Table 2.4 Primary antibodies for immunofluorescence.

Primary antibody	Dilution factor	Species	Manufacturer	Product code
Monoclonal anti-α-actinin	1500	mouse	Sigma-Aldrich	a7811
Polyclonal anti-cardiac troponin T	400	rabbit	Abcam	ab45932
Monoclonal anti-fibronectin	200	mouse	Thermo Fisher Scientific	3F12
Polyclonal anti-α-SMA	50	goat	Sigma-Aldrich	ab21027
Polyclonal anti-vimentin	5000	chicken	Thermo Fisher Scientific	PA1-10003
Polyclonal anti-collagen I	500	rabbit	Abcam	ab34710
Monoclonal anti-fibroblast surface protein	50	mouse	Sigma-Aldrich	F4771

2.10.3 Wheat Germ Agglutinin (WGA) staining

WGA staining was carried out to label the cell membranes. Cells on dishes were washed three times in PBS for 5 minutes each time and then fixed with 3.7 % PFA for 15 minutes. The samples were washed three times for 5 minutes to ensure any remaining fixative was removed to prevent over fixation. According to the manufacturer's protocol, the samples were incubated with 5 µg/mL WGA solution for 10 minutes at room temperature (Wright, 1984; Wang, Ho and Lim, 2010). After washing in PBS, nuclei were counterstained with Vectashield mounting medium containing DAPI (Vectorlabs), mounted and kept refrigerated protected from light until imaged using an inverted Zeiss LSM-780 confocal microscope.

2.10.4 Confocal Image Acquisition

Confocal microscopy was carried out at the Facility for Imaging by Light Microscopy, Imperial College London with the assistance of Mr. Stephen Rothery. A Zeiss LSM780 confocal laser scanning microscope with 7 laser lines (Diode 405nm 30mW, Argon multiline 458/488/514nm 25mW, HeNe 543nm 1mW, HeNe 594 2mW and HeNe 633nm 5mW) and 34 detectors (34 Channel GaAsP Detection System) was used for all imaging. During all experiments, laser intensity was optimised to enhance resolution, but minimise photo-bleaching and saturation. Z-stacks of images were acquired if cell volume was required for analysis.

2.11 Confocal Image Analysis

2.11.1 Analysis of sarcomere length

Sarcomere length was measured in image processing software FIJI by separating the α-actinin channel and viewing the profile plot of a line drawn perpendicularly across the α-actinin bands. Each peak on the graph corresponds with the increased fluorescence caused by an α-actinin band, so the distance between the 5 peaks was measured and averaged to give sarcomere length (**Figure 2.9**) (Jeziorowska *et al.*, 2017).

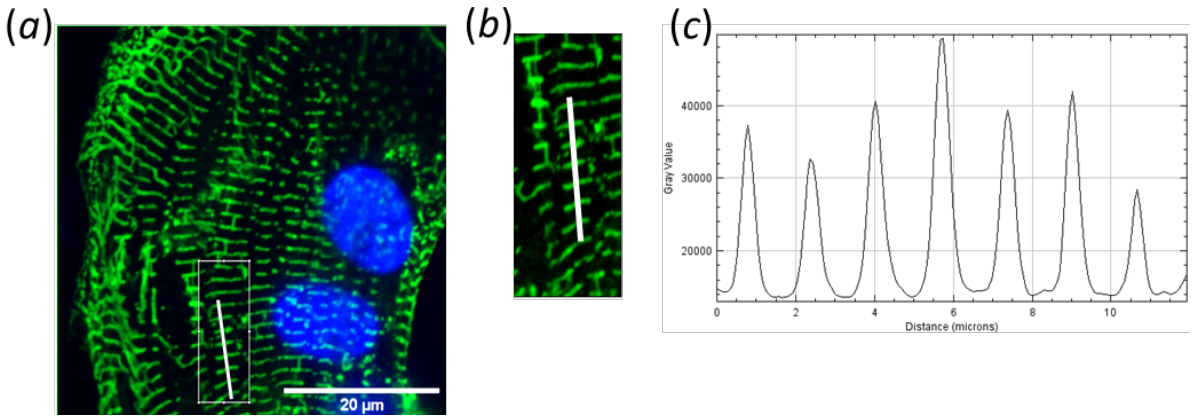

Figure 2.9 : Sarcomere length measurement*. (a) Representative image of human induced pluripotent stem cell-derived cardiomyocytes on glass. Green = α-actinin and blue = Hoechst, with a line drawn perpendicularly through the α-actinin bands. (b) A magnified version of the area highlighted by the white box. (c) The intensity fluorescence across the line was translated into a profile plot and the distance between the peaks measured to calculate the sarcomere length.*

2.11.2 Analysis of cell area

Analysis of average cardiomyocyte area was performed using WGA staining acquired using a 20x objective. A region of interest was drawn around the border of individual cardiomyocytes and the area was then measured digitally using image processing software FIJI.

2.11.3 Analysis of aspect ratio

The same WGA images as described above were used to calculate aspect ratio of the cell and nucleus. The ratio of the major axis to minor axis was measured digitally using the software FIJI and aspect ratio was calculated as major axis/minor axis.

2.11.4 Analysis of cell volume

Z-stacks of hiPSC-CMs stained with WGA were used to calculate cell volume. Individual images were acquired at 0.73µm intervals. Area of the lowest and highest images in the stack were measured, as well as the image in the middle of the stack series. These areas were averaged and multiplied by the stack height to give the cell volume.

2.11.5 Analysis of cell number

Analysis of cell number was performed using DAPI staining acquired using a 40x objective. The number of nuclei was measured digitally using FIJI software and the number of nuclei per mm^2 was calculated to indicate the number of adherent cells following RGD_A or RGD_C treatment.

2.12 Statistical analysis

All statistical analysis was performed using GraphPad Prism 8. Before statistical tests, all data were subjected to the D'Agostino & Pearson omnibus normality test. For parametric distribution, when comparing the means of two sample groups, a two-way paired t-test was used. For comparisons of three or more sample groups, where observations were linked, a one-way within-subject ANOVA (Analysis of Variance) was used. Post-hoc tests used with ANOVA were either Tukey's test (for comparison of all means) or Dunnett's (for comparison to a single control value). For non-parametric distribution, a statistical test was performed using Mann-Whitney (2 sample groups) or Krustal-Wallis (Three or more sample groups). Unless otherwise stated, the data is expressed as the mean ± standard error of the mean (SEM), n = number of technical replicates in each group (each dish of replated cells at day 26-30 of maturation is n of 1), and N = number of biological replicates in each group (each cardiomyocyte is N of 1). Statistical significance is highlighted by * p-value < 0.05; ** p-value < 0.01; *** p-value < 0.001; **** p-value < 0.0001.

3 Fibroblast-mediated regulation of human cardiomyocyte Ca^{2+} cycling

3.1 Introduction

In the last few decades, there has been growing evidence that cardiac fibroblasts play a significant role in the maintenance of the healthy cardiomyocyte phenotype and the remodelling that occurs in disease. They form extensive interactions with cardiomyocytes and are the key regulators of the ECM (Porter and Turner, 2009). The mechanisms by which fibroblasts affect EC-coupling and cytoplasmic Ca^{2+} cycling, fundamental mechanisms of normal cardiac function universally altered during disease, remain largely unexplored.

Intercellular communication between cardiomyocytes and cardiac fibroblasts in the myocardium can occur through three main broad pathways: direct physical, mechanical and electrical intercellular connections between the two cell types, secretion of soluble mediators that interact in a paracrine manner between the cells, or indirect interactions by modulating the composition of the ECM (Kakkar and Lee, 2010).

In this chapter, we first identify the effects of cardiac fibroblasts on the Ca^{2+} transients of the GCaMP6f hiPSC-CMs, to determine if the GCaMP6f hiPSC-CMs are appropriate for studying the intercellular crosstalk between human cardiomyocytes and cardiac fibroblasts. We then validated the use of an elastic, reconfigurable co-culture platform for accurately studying the spatial dependence of intercellular interactions between pure populations of hiPSC-CMs and cardiac fibroblasts.

3.2 Methods

3.2.1 Cell culture

Human ventricular cardiac fibroblasts were isolated from explanted human hearts, as described in section 2.2.2. GCamp6f hiPSCs were maintained and differentiated into hiPSC-CMs as described in Chapter 2 (Section 2.2.4-2.2.6) and plated onto glass-bottomed dishes as described in section 2.2.7.

3.2.2 Co-culture

To investigate the paracrine and physical interactions between cardiomyocytes and cardiac fibroblasts, GCaMP6f hiPSC-CMs and passage 3-6 human ventricular cardiac fibroblasts were cultured in three different conditions, as outlined by Section 0 (Kane and Terracciano, 2018):

- Fibroblast conditioned media – mediating unidirectional paracrine interactions (**Figure 2.2B**)
- Co-culture – mediating bidirectional paracrine interactions (**Figure 2.2C**).
- Direct contact – mediating bidirectional physical and paracrine interactions (**Figure 2.2D**)

Cardiomyocyte-conditioned media was used as control (**Figure 2.2A**).

3.2.3 PDMS substrate fabrication

Plastic moulds for the synthesis of the elastic PDMS substrates were kindly provided by Dr Allison Curtis, and elastic substrate was formed using the method outlined in section 2.4.1. GCamp6f hiPSC-CMs and passage 3-6 human ventricular cardiac fibroblasts were seeded either side of a coverslip partition as described in 2.4.2.

3.2.4 Optical recording techniques

Optical recordings of twitch Ca^{2+} transients were performed on hiPSC-CMs submerged in 37^{o}C standard Tyrode's solution field stimulated at 1 Hz and visualised on an inverted microscope as described in section 2.9.1. SR Ca^{2+} content and the contributions of

mechanisms to Ca^{2+} transient decay were assessed using caffeine application in standard Tyrode's solution and Na^{+}/Ca^{2+}-free Tyrode's solution as described in 2.9.2. Transients were analysed as outlined in section 2.9.3.

Alternatively, to investigate the spatial dependency of intercellular interactions, the partition separating cell populations of GCaMP6f hiPSC-CMs and cardiac fibroblasts in the PDMS co-culture substrates was removed, and cell cultures were incubated for 24 hours. Then, the wells were cut out of the substrate using a razor blade to allow focusing with a 40X water-immersion lens, before the PDMS well with the cells attached was submerged in 37^{o}C standard Tyrode's solution and cytoplasmic [Ca^{2+}] transients were visualised on an upright microscope as described in section 2.9.1.

3.2.5 Immunofluorescence

hiPSC-CMs and cardiac fibroblasts plated in PDMS co-culture substrates were treated for immunofluorescence imaging as described in section 2.6. Samples were incubated with primary antibodies against cardiac troponin T (ab45932; Abcam) and fibroblast surface protein (F4771; Sigma-Aldrich). Wells were cut out from the substrate before mounting and imaging using an inverted confocal microscope (Section 2.10.4).

3.3 Results

3.3.1 Fibroblast contact reverse hiPSC-CM Ca^{2+} transient prolongation caused by fibroblast-secreted factors

We investigated the effect of fibroblast paracrine and physical interactions on the GCaMP6f hiPSC-CM cell line used in this project. Our group has previously studied the impact of cardiac fibroblasts on commercially available hiPSC-CMs (Cellular Dynamic International) but maintaining and differentiating hiPSCs into hiPSC-CMs in-house has provided a cheaper and easier alternative to the commercially available hiPSC-CMs (Lian *et al.*, 2012; Kane and Terracciano, 2018). In this study, we utilised an isogenic hiPSC-CM cell line harbouring a genetically encoded Ca^{2+} indicator, GCaMP6f, to perform optical mapping of intracellular Ca^{2+}. GCaMP binds to 2 free Ca^{2+} ions in the stimulated state, and upon stimulation with a blue light emits a green fluorescent signal. hiPSC-CMs without a genetically encoded Ca^{2+} indicator require a dye such as Fluo4 to be loaded into the cytosol and this has toxic effects.

Due to differences in hiPSC-CM EC-coupling between cell lines, the Ca^{2+} cycling parameters of the GCaMP6f hiPSC-CMs were assessed in the various culture setups to identify the effects that paracrine and physical communication with cardiac fibroblasts have on hiPSC-CM Ca^{2+} handling. We used co-culture setups that investigated the changes that occur to hiPSC-CM Ca^{2+} transients by unidirectional paracrine interactions from fibroblasts (**Figure 2.2B**), the bidirectional paracrine interactions of hiPSC-CMs and cardiac fibroblasts (**Figure 2.2C**) and two-way physical and paracrine interactions (**Figure 2.2D**), as described in Section 2.3 (Kane and Terracciano, 2018).

We found that cardiac fibroblasts modulate the Ca^{2+} transients of hiPSC-CMs. Paracrine-only interactions cause prolongation of the hiPSC-CM Ca^{2+} transients and this is reversed in conditions where there is physical contact between the two cell types, such that the hiPSC-CM Ca^{2+} transients are abbreviated compared to control. This is shown in the representative Ca^{2+} transient traces in **Figure 3.1A**.

When investigating the Ca^{2+} transient parameters, no changes were identified in Ca^{2+} transient amplitude in any of the setups vs control (**Figure 3.1B**). Direct contact with cardiac fibroblasts significantly reduces the amplitude compared to fibroblast conditioned-media (**Figure 2.2B** – $p < 0.01$). Both fibroblast-conditioned media and co-culture cause prolongation

of Ca^{2+} transient time to peak vs control (**Figure 3.1C**). Fibroblast contact causes abbreviation of time to transient peak vs control and vs co-culture and conditioned media (**Figure 3.1C**– $p < 0.0001$). Similarly, the fibroblast conditioned-media and co-culture setups, which allow unidirectional and bidirectional paracrine interactions, respectively, prolong the time from Ca^{2+} transient peak to 50% decay (**Figure 3.1D** - $p < 0.001$) and time to 80% decay (**Figure 3.1E**– $p < 0.001$). Fibroblast contact abbreviates the time to 50% decay vs control (**Figure 3.1D**– $p < 0.05$) but there was no significant change in time to 80% decay vs control (**Figure 3.1E)**.

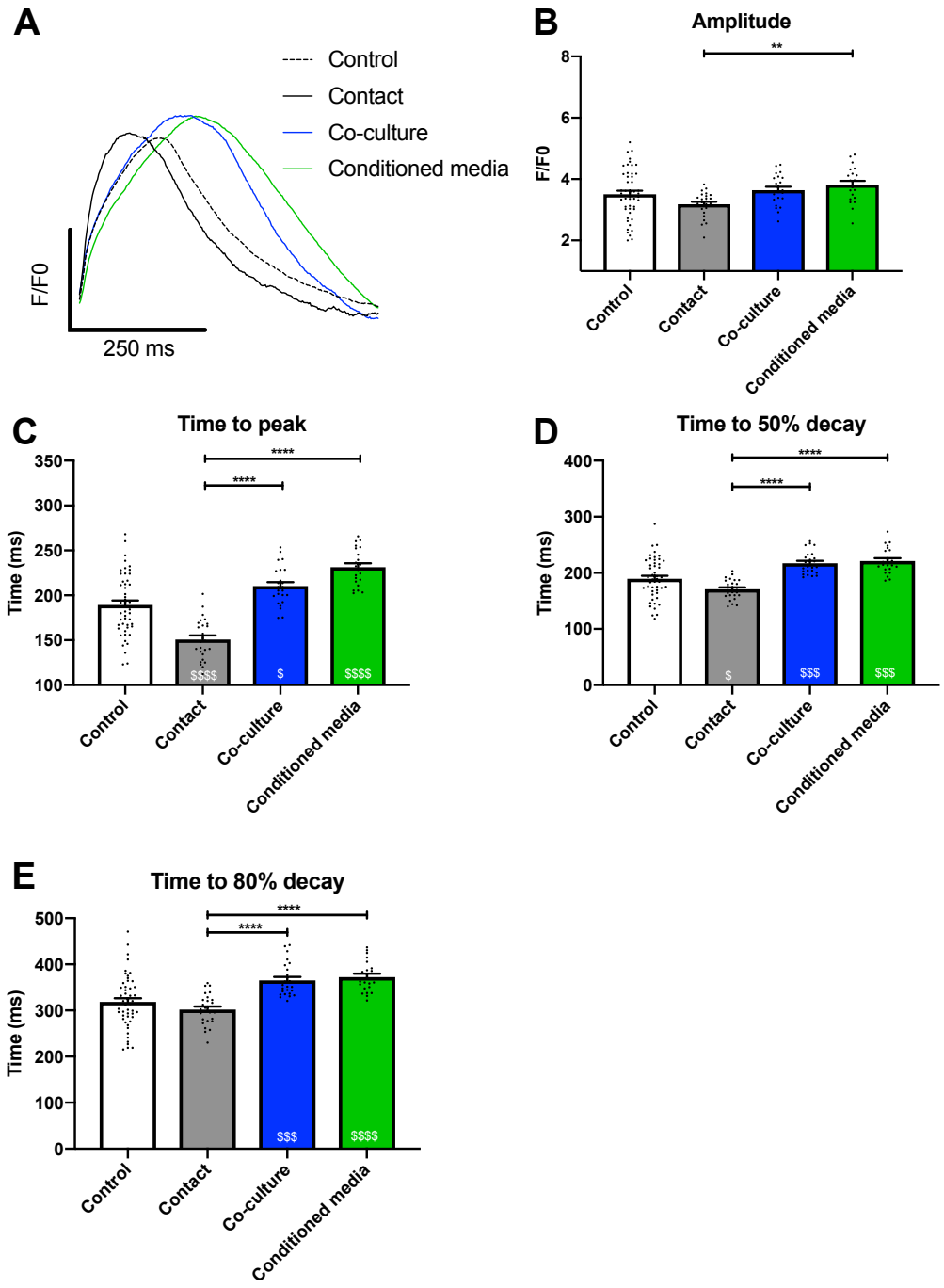

Figure 3.1 Assessment of Ca^{2+} handling properties of human cardiomyocytes after 24 hours culture with human cardiac fibroblasts. *Human induced pluripotent stem cell-derived cardiomyocytes were placed in different co-culture configurations with human cardiac fibroblasts for 24 hours. (A) Representative Ca^{2+} traces show that indirect co-culture and fibroblast-conditioned media prolonged transient duration and contact abbreviated duration compared to control. Parameters measured were Ca^{2+} transient (B) amplitude, (C) time to peak, (D) time from peak to 50% decay and (E) time from peak to 80% decay. Error bars represent SEM. N = 6-12 preparations. ** = p < 0.01, **** = p < 0.0001 between non-control conditions. $ = p < 0.05, $$$ = p < 0.001, $$$$ = p < 0.0001 vs control.*

3.3.2 Contact with cardiac fibroblasts increases the SR Ca^{2+} content

Given that the fibroblast contact setup caused significant abbreviation of the Ca^{2+} transient time to peak, we then investigated the changes that this condition may have on the SR Ca^{2+} stores, an important determinant of Ca^{2+} availability for contraction. The time to peak of the twitch Ca^{2+} transient gives an indicator of the efficiency of CICR – the release of Ca^{2+} from the SR Ca^{2+} stores. Caffeine-induced Ca^{2+} transients in standard Tyrode's solution gives a measure of the Ca^{2+} content in the SR (**Figure 3.2A**), which was seen to be increased in the fibroblast contact setup (**Figure 3.2B** – $p < 0.0001$). The fractional release, measured as the twitch transient amplitude (**Figure 3.1B**) as a proportion of the SR content (**Figure 3.2B**), was decreased in fibroblast-contact conditions (**Figure 3.2C** – $p < 0.05$). This assumes that SR Ca^{2+} is the greatest contributor to twitch Ca^{2+} transient in both control and fibroblast contact conditions, and transmembrane Ca^{2+} entry from outside the hiPSC-CM is equal between both conditions. Our study demonstrates that despite a greater SR Ca^{2+} content in fibroblast contact conditions, there is tighter control over SR Ca^{2+} content release such that a lower proportion of SR Ca^{2+} is released during twitch Ca^{2+} transients.

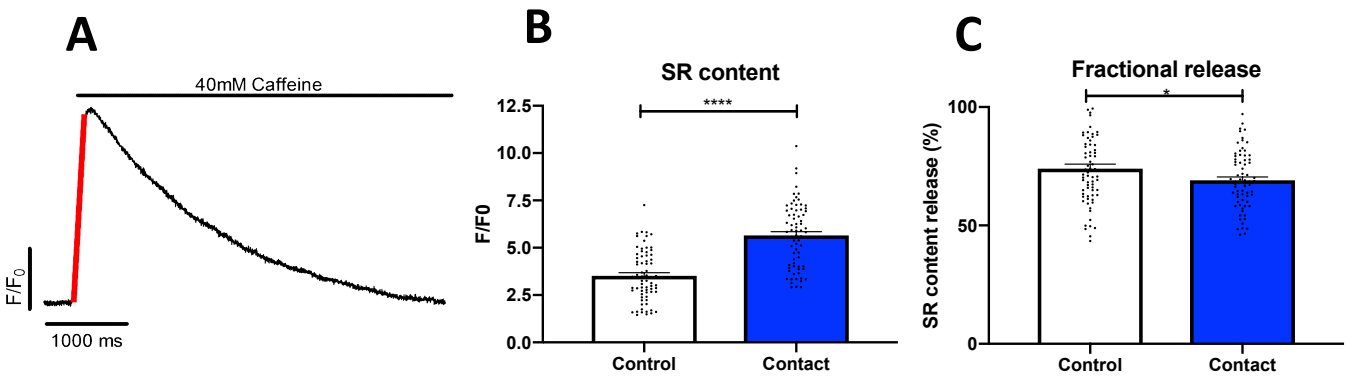

Figure 3.3 Assessment of human cardiomyocyte sarcoplasmic reticulum (SR) Ca^{2+} content and fractional release. *Caffeine application was used to investigate SR parameters of human induced pluripotent stem cell-derived cardiomyocyte monolayers. (A) Representative trace of caffeine-induced Ca^{2+} transient where amplitude (Red) indicates the SR Ca^{2+} content. (B) Caffeine-induced Ca^{2+} transient amplitude. (C) Fractional release of SR Ca^{2+} content, measured as a percentage of SR content released with each twitch transient. Error bars represent SEM. n = 70-71 cells. *= $p < 0.05$, **** = $p < 0.0001$.*

3.3.3 Cardiac fibroblasts increase the rate of Ca^{2+} extrusion by recruiting the SR

Given that direct fibroblast contact abbreviated the time at which the twitch Ca^{2+} transient reached 50% decay, we investigated changes in the contribution of mechanisms, including the SR, to Ca^{2+} removal from the cytosol. As outlined by Bassani and colleagues, the difference between twitch Ca^{2+} transient decay and caffeine-induced Ca^{2+} transient decay in standard Tyrode's solution is a measure of the SR contribution to Ca^{2+} removal (**Figure 2.9A**) (Bassani, Yuan and Bers, 1995). The contribution of the NCX to cytosolic Ca^{2+} removal is calculated as the difference in rate constant between the caffeine-induced Ca^{2+} transient in standard Tyrode's and Na^{+}/Ca^{2+}-free Tyrode's solutions; the latter is a measure of the rate constant for the slow mechanisms of Ca^{2+} removal (**Figure 2.9B**).

The rate of decay of the twitch Ca^{2+} transient is significantly increased in fibroblast direct contact vs. control (**Figure 3.3A** – $p < 0.0001$). We identify that there is a significant increase in the SR rate constant in fibroblast-contact setups (**Figure 3.3B** – $p < 0.001$) and a concomitant reduction in the NCX rate constant (**Figure 3.3C** – $p < 0.05$) but no change in the slow rate constant (**Figure 3.3D**). These changes in the contribution of Ca^{2+} removal mechanisms indicate that the hiPSC-CMs are NCX-dominant, but culture setups that allow direct contact with cardiac fibroblasts causes the recruitment of the SR to EC-coupling such that the hiPSC-CMs Ca^{2+} extrusion becomes SR-dominant (**Figure 3.3E**).

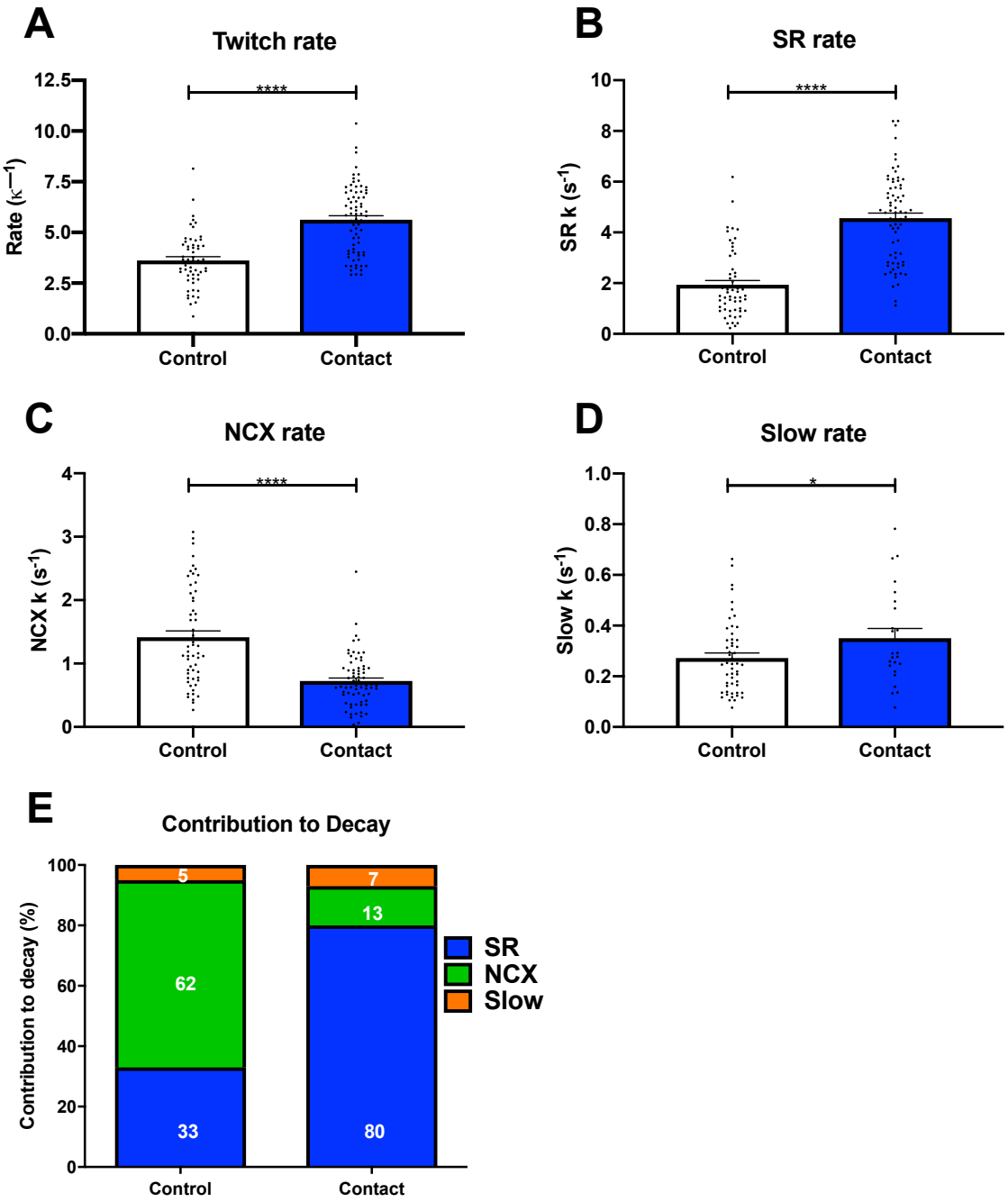

Figure 3.3 Assessment of human cardiomyocyte Ca^{2+} extrusion mechanism in fibroblast contact setup*. Human induced pluripotent stem cell-derived cardiomyocytes were maintained in culture in contact with cardiac fibroblasts and optical recording was performed with cultures maintained in standard Tyrode's and Na^{+}/Ca^{2+} free Tyrode's solutions. Caffeine application was used to determine the contributions of Ca^{2+} decay mechanisms. Parameters measured were rate of (A) twitch Ca^{2+} transient decay, and relative contributions by (B) sarcoplasmic reticulum (SR) Ca^{2+} removal, (C) sodium-calcium exchanger (NCX)-mediated Ca^{2+} removal and (D) Ca^{2+} removal mediated via mitochondria Ca^{2+}-uniporter and sarcolemma Ca^{2+}-ATPase activity. (E) Percentage contribution of Ca^{2+} removal mechanisms. Error bars represent SEM. n = number of cells = 57-73 for (A-C), 24-52 for (D). * = $p < 0.05$, **** = $p < 0.0001$ vs control.*

3.3.4 Seeding distinct cell-populations using a reconfigurable elastic substrate

Having identified that cardiac fibroblasts influence hiPSC-CMs with paracrine mechanisms that cause prolongation of hiPSC-CM Ca^{2+} transients, we utilised a co-culture platform that allows for an accurate and reproducible investigation of the cell-cell interactions over a spatial gradient. In the co-culture setup used in Sections 3.3.1-3.3.3, cardiac fibroblasts were seeded on semi-porous tissue culture inserts that were suspended above the hiPSC-CM monolayers. However, the distance between the two cell types could not be accurately measured or manipulated. We fabricated elastic, reconfigurable substrates to investigate the cell-cell interactions between pure populations of cardiac fibroblasts and hiPSC-CMs over a measurable, spatial gradient. Cardiac fibroblasts and hiPSC-CMs were seeded and cultured in PDMS wells either side of a barrier, which was then removed to allow for the two cell types to interact. Immunofluorescence of substrates seeded with hiPSC-CMs and cardiac fibroblasts show distinct populations of cells expressing cardiac Troponin-T and fibroblast surface protein on either side of the partition (**Figure 3.4**).

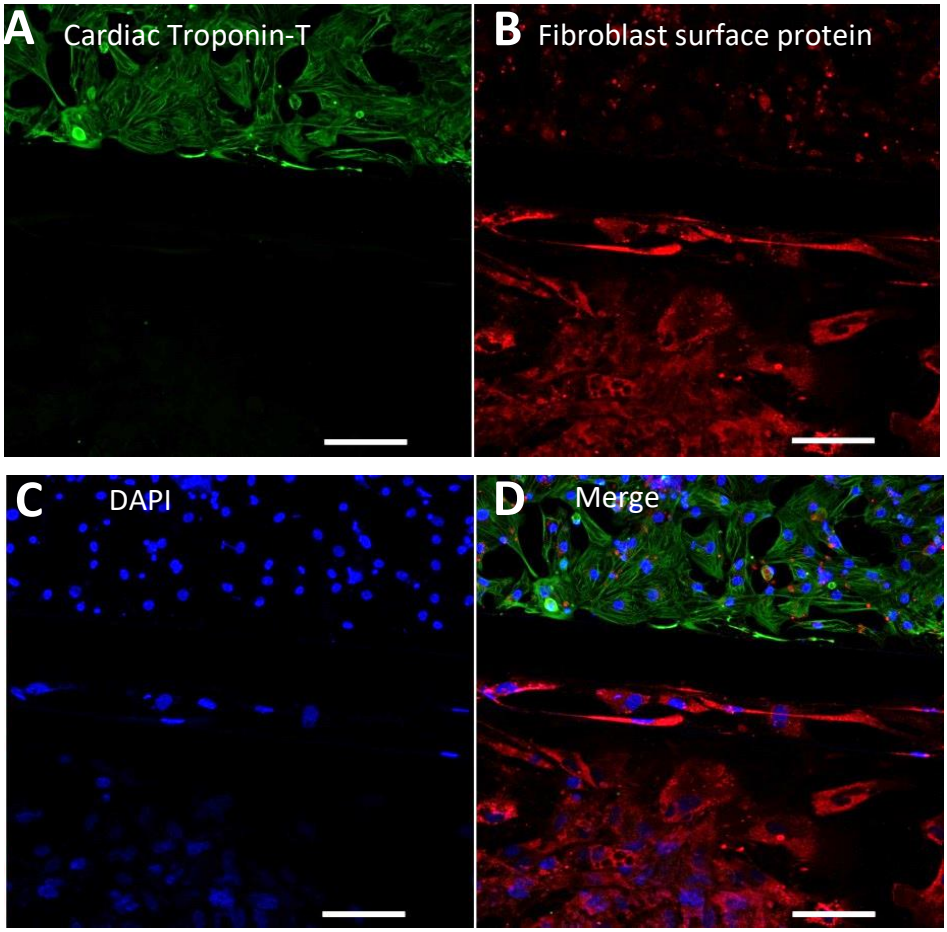

Figure 3.4 Human cardiac fibroblast: cardiomyocyte co-culture on a polydimethylsiloxane (PDMS) substrate. *Human induced pluripotent stem cell-derived cardiomyocytes and cardiac fibroblasts were seeded and cultured on a PDMS substrate as distinct populations on either side of a partition. Representative confocal images of (A) Cardiac Troponin-T (green), (B) fibroblast surface protein (red) and (C) DAPI (blue). In merge image (D), there is a central rectangular area absent of either cell type, showing that the two sides could not fully return to allow fibroblast-cardiomyocyte contact following removal of the partition. Scale bar = 100 µm.*

3.3.5 Spatial dependence of intercellular interactions between cardiomyocytes and cardiac fibroblasts

We utilised the reconfigurable elastic substrate to investigate the hiPSC-CM Ca^{2+} transient parameters in co-culture. The partition was removed to allow for cell-cell communication between the hiPSC-CM and cardiac fibroblast populations for 24 hours before Ca^{2+}-sensitive fluorescence of the GCamp6f hiPSC-CMs was investigated on an upright microscope. After removal of the barrier, the surface was often not continuous as the slit in which the barrier was placed did not close perfectly. The gap was often visible during microscopy and even when the gap was not present, we could not be confident that this remained closed during the whole period in which the partition was removed. As a result, the substrate could not be used to investigate direct contact interactions in this study. However, as paracrine factors could still cross the gap and a distinct area between the two cell types could be discerned, the setups could be used to investigate close, bi-directional paracrine interactions, and importantly, any differences between the hiPSC-CM Ca^{2+} at measurable intercellular distances from the cardiac fibroblasts.

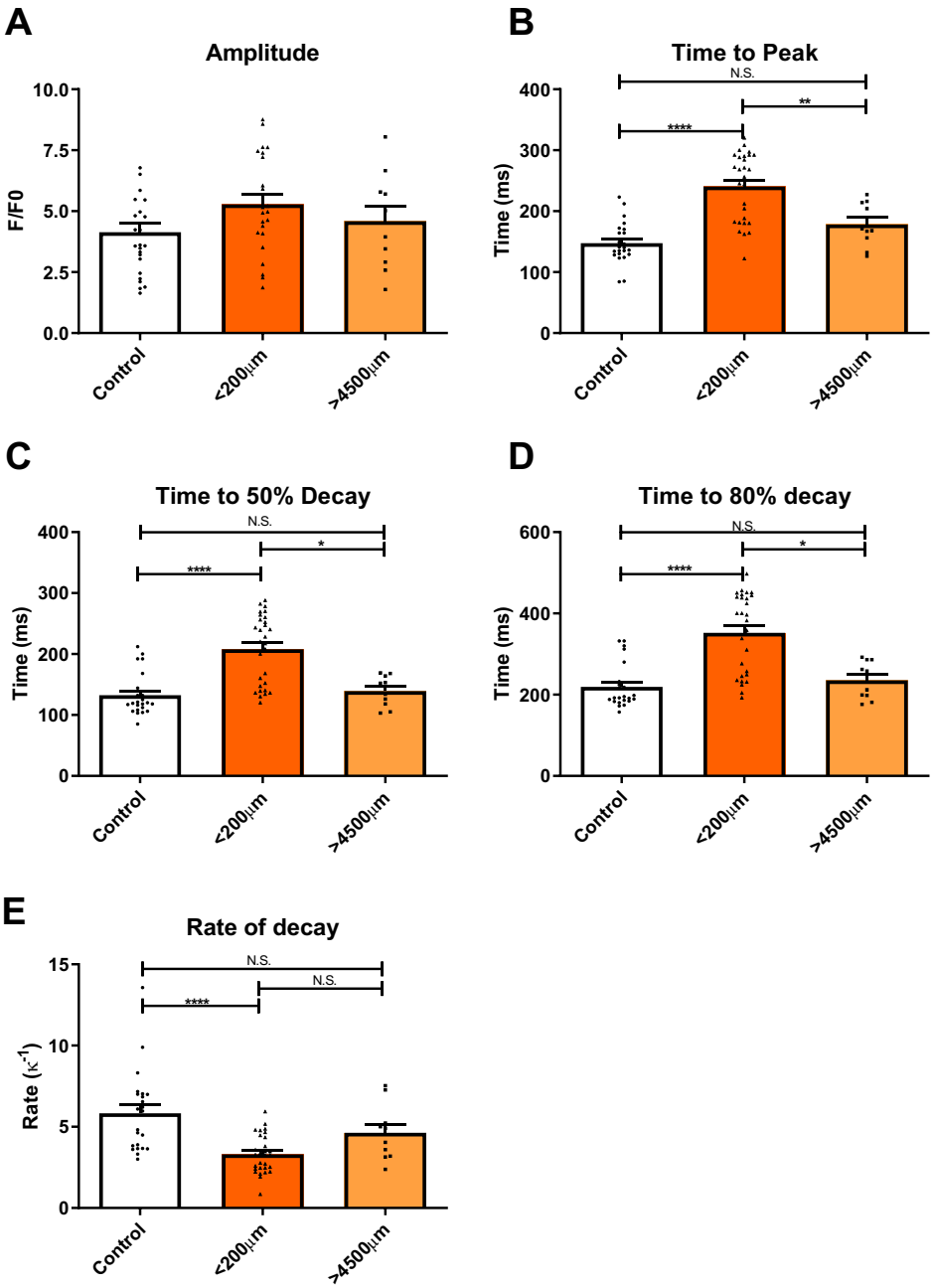

Figure 3.5 Ca^{2+} handling properties of human cardiomyocytes in culture with cardiac fibroblasts over a spatial gradient*. Human induced pluripotent stem cell-derived cardiomyocytes (hiPSC-CMs) and human cardiac fibroblasts were cultured on either side of a glass partition. The partition was removed for 24 hours before Ca^{2+} transient parameters were measured on an upright microscope. Ca^{2+} transients were recorded for hiPSC-CMs within 200μm and greater than 4500μm from the cardiac fibroblasts. Parameters measured were Ca^{2+} transient (A) amplitude, (B) time to peak, (C) time from peak to 50% decay, (D) time from peak to 80% decay, (E) rate of decay. Error bars represent SEM. N = 8 preparations. * = p<0.05, ** = p < 0.01, **** = p < 0.0001.*

We investigated the Ca^{2+} transients of hiPSC-CMs within 200 µm of the cardiac fibroblasts, and hiPSC-CMs greater than 4500 µm away from the cardiac fibroblasts. There was no difference in the Ca^{2+} transient amplitude in either of these hiPSC-CM populations compared to control (**Figure 3.5A**), but there was a significant prolongation in the time to peak in hiPSC-CMs less than 200 µm away from the cardiac fibroblasts (**Figure 3.5B** – $p < 0.0001$). The hiPSC-CMs greater than 4500 µm away from the cardiac fibroblasts showed no significant changes in Ca^{2+} transients' time to peak compared to control.

We also measured the decay phase of the Ca^{2+} transients. hiPSC-CMs less than 200 µm from the cardiac fibroblasts had a prolonged decay phase; both the time from Ca^{2+} transient peak to 50% decay (**Figure 3.5C**– $p < 0.0001$) and to 80% decay (**Figure 3.5D** – $p < 0.0001$) were longer compared to control. The time to 50% decay (**Figure 3.5C**) and time to 80% decay (**Figure 3.5D**) were not significantly different in hiPSC-CMs greater than 4500µm from the cardiac fibroblasts vs control. The prolongation of the decay phase of hiPSC-CMs less than 200 µm from cardiac fibroblasts is reflected in a significantly reduced rate of decay compared to control (**Figure 3.5E** – $p < 0.0001$). The Ca^{2+} transients rate of decay of hiPSC-CMs greater than 4500 µm from the cardiac fibroblasts were not significantly changed compared to control.

These findings with hiPSC-CMs from the GCamp6f cell line less than 200µm from the cardiac fibroblasts are consistent with the co-culture findings in Fig 3.1 which identified that paracrine interactions between cardiac fibroblasts and hiPSC-CMs causes prolongation of hiPSC-CM Ca^{2+} transients. We have been able to validate the use of this elastic, reconfigurable co-culture setup to accurately measure the spatial dependence of intercellular interactions. The bidirectional paracrine co-culture setup used earlier in this chapter, and outlined in Fig. 2.3B, does not allow accurate measurements of distance between the pure cell populations. We find in our culture setup that the hiPSC-CMs closer to the cardiac fibroblasts are subject to more significant paracrine modulation by cardiac fibroblasts than the hiPSC-CMs further away and can accurately measure the distance between the hiPSC-CMs and cardiac fibroblasts.

3.4 Discussion

Ca^{2+} handling is a critical component of EC-coupling, a fundamental function of cardiomyocytes that is universally altered in cardiovascular disease (Bers, 2002). Cardiac fibroblasts are known to be major regulators of the remodelling that happens in disease, but the mechanisms of intercellular crosstalk important in regulating Ca^{2+} cycling, and EC-coupling, are poorly defined (Camelliti, Borg and Kohl, 2005; Civitarese *et al.*, 2017). We show in this chapter that cultures allowing contact between cardiac fibroblasts and hiPSC-CMs, which display a phenotype akin to the diseased adult human cardiomyocyte (Kane *et al.*, 2015), cause abbreviation of the Ca^{2+} transient time to peak and time to decay, indicating more efficient CICR and Ca^{2+} removal mechanisms. SR dysfunction is thought to play a major role in the inefficient Ca^{2+} cycling in disease, and we show that physical contact with cardiac fibroblasts causes an increase in the SR Ca^{2+} stores and an increase in the SR rate constant for Ca^{2+} extrusion of the cytosol, which underlies the increased rate of Ca^{2+} removal required for cessation of cardiomyocyte contraction. These findings are consistent with published studies from our group using other hiPSC-CM lines and demonstrate that the sensitivity of hiPSC-CMs to cardiac fibroblasts is reproducible (Kane and Terracciano, 2018). As a result, GCaMP6f hiPSC-CMs are an appropriate cell line for use in further studies of fibroblast-mediated modulation of cardiomyocyte Ca^{2+} cycling.

3.4.1 CICR

There are two main differences between hiPSC-CMs and adult human C cardiomyocyte M Ca^{2+} handling: 1) Slower time to peak Ca^{2+} transient and 2) significantly slower SERCA and NCX Ca^{2+} transport (Hwang *et al.*, 2015). We show that paracrine interactions between cardiac fibroblasts and cardiomyocytes cause further prolongation of the hiPSC-CM Ca^{2+} time to peak and physical contact causes an abbreviation. The twitch Ca^{2+} transient is predominantly made up of Ca^{2+} release from the SR through RyRs in CICR, and an abbreviation in the time to peak indicates more efficient CICR (Koivumäki *et al.*, 2018). Factors such as the lack of T-tubules in the hiPSC-CMs lead to an inefficient CICR (Kane *et al.*, 2015). The rise in $[Ca^{2+}]_i$ in hiPSC-CMs during a Ca^{2+} transient has been attributed to Ca^{2+} availability initially increasing at the sarcolemma before spreading inwards (Koivumäki *et al.*,

2018). This propagative signalling is a more inefficient form of CICR, as the internal, non-coupled RyRs are activated by the rise in [Ca^{2+}] closer to the sarcolemma, rather than being as a result of direct activation by sarcolemma Ca^{2+} channels. This is also found in neonatal cardiomyocytes from other species as well as adult atrial cardiomyocytes that lack T-tubules (Ibrahim *et al.*, 2011).

The change in Ca^{2+} transient time to peak is likely to be attributed to changes in SR Ca^{2+} regulation, given the importance of the SR Ca^{2+} to CICR (Eisner *et al.*, 2017). Increased SR Ca^{2+} load, as we report to be the case when cardiac fibroblasts are in physical contact with hiPSC-CMs, has been shown to increase the rate of SR Ca^{2+} release in the guinea pig and rat cardiomyocytes (Terracciano, Naqvi and MacLeod, 1995; Venetucci, Trafford and Eisner, 2006). This abbreviation in time to peak could also be attributed to increased RyR sensitivity and opening to Ca^{2+} triggers (Ramay, Liu and Sobie, 2011). It is also possible that this increase in CICR efficiency is due to changes in the contribution of Ca^{2+} entry through the sarcolemma. Studies have suggested that there is a considerable contribution of NCX to Ca^{2+} transients in hiPSC-CMs (Zhang *et al.*, 2013). This is consistent with findings in developing and neonatal mammalian cardiomyocytes (Chen *et al.*, 1995). There is evidence that NCX activity can be increased, unchanged or even down-regulated during cardiac remodelling (Laughlin *et al.*, 1991; Palmer *et al.*, 1999; Despa and Bers, 2013). This is important in the context of utilising the hiPSC-CMs as models of disease, as Ca^{2+} entry in the absence of I_{CaL} has been shown to trigger SR Ca^{2+} release in feline (Bradley *et al.*, 2019) and guinea pig (Vornanen, Shepherd and Isenberg, 2017) cardiomyocytes and there is evidence that this NCX activity is a significant source of Ca^{2+} entry in hiPSC-CMs (Zhang and Morad, 2016).

Although not investigated in this chapter, the abbreviation of time to Ca^{2+} transient peak could be due to changes in the composition of caveolae – microdomains in which essential scaffolding proteins and ion channels and transporters have been identified (Balijepalli and Kamp, 2008). Another potential mechanism could be changes in the SR localisation or sensitivity to Ca^{2+} trigger (Ji *et al.*, 2006). It has been reported that hiPSC-CMs display SR localisation to the sarcolemma to form functional RyRs (Gherghiceanu *et al.*, 2011). However, our group has reported that hiPSC-CMs display poor co-localisation between $Ca_v1.2$ and RyR2 (Rao *et al.*, 2013). The change in CICR efficiency could, therefore, be as a result of ultrastructural changes such as SR rearrangement within the cardiomyocytes. The role of integrins, the key cardiomyocyte receptors for communication between the extracellular

stimuli and intracellular cytoskeleton, in modulating SR localisation to the sarcolemma and in modulating the presence of caveolae will be investigated in Chapter 4.

3.4.2 Ca^{2+} removal

The second major difference between hiPSC-CMs and adult human cardiomyocytes Ca^{2+} handling is the significantly slower SERCA and NCX Ca^{2+} transport (Kane *et al.*, 2015). Piacentino and colleagues reported that the Ca^{2+} transient decay rate constant of 5.88 s^{-1} in non-failing cardiomyocytes is attributed to by an SR rate constant of 4.5 s^{-1} and NCX rate constant of 1.38 s^{-1}, and there is no measurable contribution of slow mechanisms to the decay (Piacentino *et al.*, 2003). This is in contrast to the hiPSC-CMs utilised here, which shows a much slower rate constant (3.62 s^{-1}), contributed to an SR and NCX rate constants of 2.08 s^{-1} and 1.41 s^{-1} respectively, and the remainder (0.279 s^{-1}) by the slow mechanisms, the mitochondrial Ca^{2+}-ATPase uniporter and the sarcolemmal Ca^{2+}-ATPase. SR Ca^{2+} uptake is driven by the SERCA pump, the cardiac isoform of which is SERCA2a. Our lab has previously shown that SERCA2a expression in hiPSC-CMs are substantially lower than in the adult heart (Rao *et al.*, 2013), while in development there is a steady increase of SERCA2a mRNA and a decrease in NCX-1 from the embryonic heart to adulthood (Liu *et al.*, 2002). The complexity of the mechanisms in intercellular interactions between the two cell types and the Ca^{2+} cycling ultrastructure means that a true understanding of the regulation of hiPSC-CM Ca^{2+} cycling by cardiac fibroblasts requires investigations into key modalities of intercellular communication, which is the focus of the remaining chapters of this study.

3.4.3 Co-culture setups

We show that paracrine interactions between cardiac fibroblasts and hiPSC-CMs significantly prolong the hiPSC-CM Ca^{2+} transient time to peak and time to decay. The configuration used to investigate the bidirectional paracrine interactions is unable to manipulate the intercellular distance between the two cell types accurately. The myocardium consists of a complex architecture that relies on precise positioning of myocytes and non-myocyte within the extracellular scaffold formed by ECM proteins, and thus the spatial proximity between cell populations is fundamental to tissue and organ function (Kofron and

Mende, 2017). However, investigation of the spatial dependency of intercellular communications is limited.

Sequential seeding is the most common patterning method for creating micro-patterned co-cultures used for investigating these dependencies. In this way, one cell population is first patterned before a second population is seeded around the first pattern (Bhatia *et al.*, 1999; Stine *et al.*, 2012). With both of these sequential seeding approaches, it is difficult to avoid cross-contamination between the two cell populations, and there is a lack of a sharp interface between these populations. We utilised an elastic PDMS substrate to create co-cultures with sharp borders and less cross-contamination than the common alternative patterning strategies.

We demonstrate that the reconfigurable elastic substrate can be utilised to investigate cell-cell interactions over a spatial gradient accurately. Although the slit in which the barrier was placed could not close up perfectly, we do identify a sharp interface between the two cell types such that the cell-cell interactions could be accurately measured over a spatial gradient.

3.4.4 Spatial dependence of paracrine interactions

There is strong evidence that cardiac fibroblasts regulate cardiomyocyte phenotype through paracrine pathways (Tian and Morrisey, 2012; Bang *et al.*, 2014; Cartledge *et al.*, 2015). We use the elastic PDMS co-culture substrates to show that the Ca^{2+} transients of hiPSC-CMs less than 200µm from the cardiac fibroblasts are significantly prolonged compared to control, consistent with the prolongation identified in the co-culture setups using tissue culture inserts in Figure 3.1. However, the hiPSC-CMs more than 4500 µm away from the cardiac fibroblasts have Ca^{2+} transient parameters that are not significantly different to control. This indicates that the spatial organisation of the cell types in co-culture is important for intercellular interactions. One possible explanation for these results is that the paracrine factors from the cardiac fibroblasts interact with, and therefore modulate, the hiPSC-CMs closest to the cardiac fibroblasts and therefore do not reach the hiPSC-CMs further away. Another possible explanation is that the paracrine factors important in regulating Ca^{2+} cycling in the hiPSC-CMs only act over a short distance. Future study could incorporate two barriers and seeding the cell populations at the far ends of the well. This would form a defined space

between the cell populations void of cells. Changing the diameter of this space would allow us to identify if there are any changes in hiPSC-CM Ca^{2+} cycling of the hiPSC-CMs closest to the cardiac fibroblasts as the distance between the cell population changes. If increasing the shortest distance between the cell populations causes changes in the Ca^{2+} transient parameters, this would indicate that the paracrine factors that modulate the Ca^{2+} transient parameters work over very short distances.

We must also consider that the number or density of cardiac fibroblasts is important in determining the effects on hiPSC-CMs. The density is different between our co-culture setups using tissue culture inserts (Figure 2.2C) and co-cultures with the elastic mould (Figure 2.4). The differences in substrate stiffness may explain why the co-culture setups with tissue culture inserts have an effect on hiPSC-CMs despite having a distance between the hiPSC-CMs and cardiac fibroblasts greater than 200 µm. We have shown here that the use of the PDMS substrate allows for a distinct, sharp interface between cell populations and the spatial composition of cardiomyocytes and cardiac fibroblasts is important in modulating hiPSC-CM Ca^{2+} cycling.

3.4.5 Direct contact setup – cell-cell contact, close paracrine or ECM?

In the direct contact setup, intercellular physical interactions and close paracrine interactions could determine the abbreviation in Ca^{2+} transients identified in the hiPSC-CMs. Alternatively, the production of ECM proteins could present an indirect mechanism by which cardiac fibroblasts can influence hiPSC-CM Ca^{2+} cycling. The complex, bidirectional interplay between different cell populations means that the different modalities by which cardiac fibroblasts regulate cardiomyocyte structure and function are regulated or conditioned by factors from the recipient cell types - the cardiomyocytes.

It is important to consider that the direct cell-cell contact in the contact culture setup can affect the secretory profile of both cell types. The complexity of the secretory profile of cardiac fibroblasts has been extensively explored elsewhere and has been shown to be sensitive to the stiffness of culture setups. Cells cultured on top of feeder cells adopt a phenotype reflecting the stiffness of the feeder layer (Llames *et al.*, 2015). In the culture setups, the fibroblasts in the contact scenario, seeded on top of hiPSC-CM monolayers, are

therefore likely to display a secretory profiled different to the fibroblasts seeded on the stiffer semi-porous tissue culture inserts (Co-culture) or in the culture dishes (conditioned-media).

Mechanical load exerts predominantly pro-fibrotic effects on cardiac fibroblasts but the response of cardiac fibroblasts, whether it be predominantly proliferative or synthetic, is dependent on the stimulus cue: paracrine signalling from stretched cardiomyocytes induces cardiac fibroblast proliferation, whereas direct stretching of the fibroblasts induces an increase in ECM production. Herum and colleagues identified that progressive stiffening of the gel matrix used in the study causes the formation of α-SMA, and upregulation of collagen I and downregulation of collagen III, changing the composition of the ECM (Herum *et al.*, 2017).

As well as cell-cell physical and paracrine interactions, the ECM could play a critical role as an indirect modality by which cardiac fibroblasts can modulate cardiomyocyte Ca^{2+} cycling. We hypothesise that there is deposition of ECM proteins in the contact culture set up, promoted by intercellular communication between the cardiac fibroblasts and cardiomyocytes, and this deposition is reduced in the indirect co-culture setup, in which the ECM proteins would need to cross the semi-porous tissue culture insert membrane, and absent in the fibroblast-conditioned setup. Studies have shown that angiotensin II, through the angiotensin type I receptor, induces matrix protein synthesis only when fibroblasts are co-cultured with cardiomyocytes (Pathak *et al.*, 2001; Sarkar *et al.*, 2019). The ECM could, therefore, play a significant role in producing the different effects of the culture conditions and will be investigated later in this project (Chapter 4).

There is increasing evidence to suggest that EVs play an essential role in cardiac function. EVs have been shown to transfer genetic material such as RNA, mRNA and miRNA as well as proteins, including components of the ECM (Paolillo and Schinelli, 2017). Fibroblast-derived exosomes, a subtype of EVs, have been shown to carry miRNAs that act as potent paracrine-acting molecules inducing changes in mice cardiomyocyte structure (Bang *et al.*, 2014). Therefore, EVs may also play a vital role in the human cardiac fibroblast: cardiomyocyte interactions and will be investigated in Chapter 5.

3.5 Summary

In this chapter, we have presented an assessment of the effects of human ventricular cardiac fibroblasts on Ca^{2+} cycling in hiPSC-CMs through various modalities. While soluble mediators caused prolongation of the hiPSC- cardiomyocyte Ca^{2+} transients, physical contact with cardiac fibroblasts induced substantial abbreviation in these transients. We have shown that physical contact engages the SR in hiPSC-CM Ca^{2+} cycling, increasing the efficiency of CICR and Ca^{2+} removal, essential features of Ca^{2+} cycling in human cardiomyocytes altered in disease. This is consistent with previous studies in our group utilising hiPSC-CMs from a different cell line, indicating that the sensitivity of hiPSC-CMs is consistent across cell lines. These GCaMP6f hiPSC-CMs are therefore appropriate for the studies described in the following chapters, in which we will attempt to identify the mechanisms by which human cardiac fibroblasts bring about these fundamental changes in hiPSC-CMs.

4 Integrin-mediated modulation of human cardiomyocyte structure and function

4.1 Introduction

In the previous chapter, we showed that hiPSC-CMs display plasticity and can develop features of the adult, human cardiomyocyte when cultured with cardiac fibroblasts *in vitro,* including recruitment of the SR to the EC-coupling process (Kane and Terracciano, 2018). Cardiac fibroblasts play a key role in the production, maintenance and remodelling of the ECM (Fan *et al.*, 2012; Howard and Baudino, 2014). In this chapter, we aim to delineate how the ECM can modulate hiPSC-CM Ca^{2+} handling, including the recruitment of the SR to EC-coupling.

In this study, we use soluble integrin ligands to investigate the role of integrin activity in EC-coupling and, in particular, the recruitment of the SR to Ca^{2+} cycling. A potential limitation to the use of soluble RGD-containing peptides is that these have been shown to induce cell detachment in non- cardiomyocyte cell types (Hayman, Pierschbacher and Ruoslahti, 1985). To overcome this, we investigated the effects of RGD-linked peptides with fibril-forming and self-assembling properties on the SR recruitment to Ca^{2+} cycling.

Here, we investigated a mechanism by which proteins in the ECM may modulate cardiomyocyte EC-coupling. We used soluble and self-assembling RGD-containing peptides to investigate the role of integrin activity in the recruitment of the SR to EC-coupling in hiPSC-CMs.

4.2 Methods

4.2.1 Cell culture

Commercially-available hiPSC-CMs (CDI) were prepared, maintained then plated on 35mm dishes with a 7mm glass-bottomed well as described in section 2.2.3.

4.2.2 Integrin peptides and antibodies

Integrin-binding peptide sequences RGD, GRGDS, and GRGDSP as well as negative control RGES, which does not bind to integrins, were solubilised as described in section 2.5.1 before hiPSC-CMs were treated with soluble integrin ligands (2mM) and anti-integrin antibodies (10 μg/mL) prepared and applied as described in section 2.5.2. Integrin ligands RGDSGAITIGA (RGD_A) and RGDSGAITIGC (RGD_C) were prepared by suspension of the peptide in powder form into serum-free media before incubation at 37^{o}C for 3 hours to allow for self-assembly into fibrils (section 2.5.3). hiPSC-CMs were then treated with the RGD_A or RGD_C (2mM) as described in section 2.5.3.

4.2.3 Structural characterisation

Electron microscopy of hiPSC-CMs treated with RGD_A and RGD_C was carried out by Dr. Christian Pinali (University of Manchester). Analysis of electron microscopy images was carried out by Ms. Laura Nicastro (Imperial College London) as described in chapter 2.7.3.

4.2.4 Optical recording techniques

Optical recording of twitch Ca^{2+} transients were performed on hiPSC-CMs submerged in 37^{o}C standard Tyrode's solution field stimulated at 1 Hz and visualised on an inverted microscope as described in section 2.9.1.

Investigation of SR Ca^{2+} content and contribution of mechanisms to Ca^{2+} transient decay was measured using caffeine application in standard Tyrode's solution and Na^{+}/Ca^{2+}-free Tyrode's solution as described in 2.9.2 and transients were analysed as outlined in section 2.9.3.

4.2.5 Imaging

Bright field images of hiPSC-CMs were obtained on a Widefield microscope as described in section 2.10.1. Following optical mapping, samples were fixed and permeabilised before immunofluorescence staining (section 2.10.2-3). Images were then acquired on a confocal microscope as described in 2.10.4. Immunofluorescent images acquired on the confocal microscope were then used to analyse morphology parameters: sarcomere length, cell area, cell volume and both cell and nucleus aspect ratio, as described in section 2.11.1-2.11.4.

4.3 Results

4.3.1 Soluble integrin ligands abbreviate Ca^{2+} transient duration

In this chapter, we investigated the regulation of cardiomyocyte cytosolic Ca^{2+} by ECM integrin ligands. Soluble RGD-containing peptides have been used to investigate the role of integrin signalling in studies utilising non-myocytes and so were used in this study to investigate the effect on human cardiomyocytes. In line with a study by our group (Kane and Terracciano, 2018), hiPSC-CMs were plated on glass-bottomed dishes and maintained for 5 days, at which point they form a spontaneously beating monolayer. This hiPSC-CM monolayer was then treated with soluble RGD, GRGDS or GRGDSP, or negative control RGES. After 24 hours of incubation at 37^{o}C, the hiPSC-CMs were loaded with Fluo4-AM before optical mapping of Ca^{2+} transients.

Figure 4.1A shows representative Ca^{2+} transients of hiPSC-CMs treated with soluble integrin ligands, using the values for Ca^{2+} transient amplitude, time to peak and time to 50% decay and 80% decay. We identify significant differences in the Ca^{2+} transients induced by GRGDS or GRGDSP compared to control. The most striking finding was that treatment with either soluble GRGDS or GRGDSP significantly abbreviated the Ca^{2+} transient duration by abbreviating the time to peak and time to decay.

Figure 4.1B shows the Ca^{2+} transient of hiPSC-CM monolayers 24 hours after the onset of treatment of the hiPSC-CMs with soluble integrin ligands RGD, GRGDS or GRGDSP or the negative control RGES. We identify that soluble GRGDS induced a significant increase in Ca^{2+} transient amplitude (**Figure 4.1B** – $p < 0.05$) vs. control, but there were no significant changes upon application of soluble RGD, RGES or GRGDSP (**Figure 4.1B**) against control.

An important observation was that while the hiPSC-CMs were initially utilised in the form of monolayers, GRGDS or GRGDSP application caused these monolayers to detach from their glass dishes and formed a cluster of hiPSC-CMs (not shown). There was no detachment observed following RGD or RGES treatment. The clustering of hiPSC-CMs treated with GRGDS may underlie the increase in amplitude and the greater range of amplitudes in GRGDS-treated hiPSC-CMs than other groups. Clustering may increase the peak amplitude due to overlapping of multiple hiPSC-CMs in the z-plane rather than an increase in Ca^{2+} availability in a single cell. This overlapping of signals does not occur in monolayers of hiPSC-CMs but is a crucial

limitation in interpreting changes in amplitude in hiPSC-CMs that are clustered or non-adherent to the cell culture substrate.

We then analysed the time from Ca^{2+} transient onset to peak. The duration of Ca^{2+} transient time to peak is an indicator of CICR efficiency, which improves during cardiomyocyte maturation. We identified that application of soluble GRGDS or GRGDSP induced abbreviation of Ca^{2+} transient time to peak (**Figure 4.1C** – $p < 0.0001$) vs. control, indicating more efficient CICR. There was no significant effect induced by the negative control, RGES, compared to control and the RGD-tripeptide caused only a small decrease in the time to Ca^{2+} transient peak, but this was not statistically significant (**Figure 4.1C**).

Following contraction, relaxation is then mediated by removal of Ca^{2+} from the cytosol. Time to 50% decay and time to 80% decay are indicators of the Ca^{2+} removal efficiency. Soluble GRGDS and GRGDSP both abbreviated the time 50% to decay (**Figure 4.1D** – $p < 0.001$) compared to control, indicating more efficient Ca^{2+} extrusion mechanisms, but again there was no change induced by RGD or RGES. Despite the changes to the time to 50% decay caused by GRGDS and GRGDSP, none of the soluble peptides studied induced any significant change in time to 80% decay vs control (**Figure 4.1E**). A possible explanation for this is the accumulation of variability at time to 80% decay. It must be considered that the detachment from the glass substrate following treatment with GRGDS or GRGDSP is a crucial limitation to attributing the changes in Ca^{2+} transient parameters to integrin-binding activity.

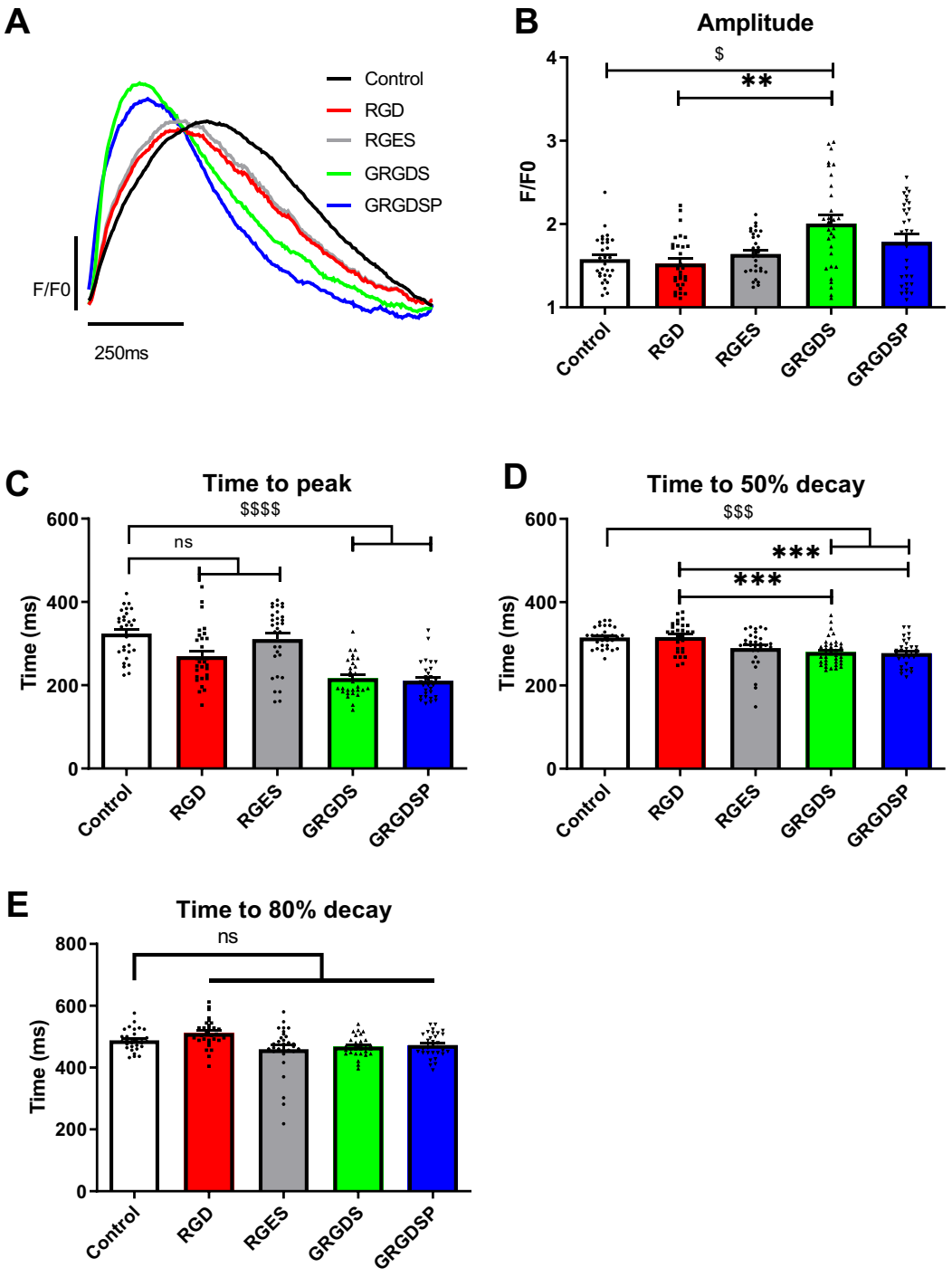

Figure 4.1 Effect of soluble integrin ligands on cardiomyocyte Ca^{2+} handling parameters. *Human induced pluripotent stem cell-derived cardiomyocyte (hiPSC-CM) monolayers were incubated for 24 hours with soluble RGD, RGES, GRGDS or GRGDSP. HiPSC-CMs were then maintained in standard Tyrode's solution and subject to 1 Hz field-stimulation during optical recording on an inverted microscope at 40x magnification. Representative Ca^{2+} transients are shown in (A). Ca^{2+} transient parameters analysed were (B) amplitude, (C) time to peak, (D) time from peak to 50% decay and (E) time from peak to 80% decay. Error bars represent SEM. N = 8 preparations, n = 30 images. ** = p < 0.01, *** = p < 0.001, **** = p < 0.0001. $ = p < 0.05, $$$ = p < 0.001, $$$$ = p < 0.0001 vs control.*

4.3.2 Anti-β1- and anti-β3-integrin antibodies abbreviate Ca^{2+} transient duration

After identifying the changes in hiPSC-CM Ca^{2+} transients following soluble integrin ligand treatment, we investigated the integrin subtypes responsible for these changes. Integrins are a family of heterodimeric receptors, composed of α and β subunits. The β1 and β3 subunits are the predominantly expressed types expressed in the human cardiomyocyte so we investigated the effects of antibodies against the β1 or β3 subunits on hiPSC-CM Ca^{2+} transients to investigate if antibody-mediated inhibition of integrins would have the opposite effect of integrin ligands and cause prolongation of Ca^{2+} transients and reduce Ca^{2+} availability.

Concomitant treatment of hiPSC-CM monolayers with anti-β1 and anti-β3 integrin antibodies caused an increase in Ca^{2+} transient amplitude (**Figure 4.2A**). Individually, the antibodies abbreviated the time to Ca^{2+} transient peak, an effect also observed when antibodies against β1 and β3 were added together (**Figure 4.2B**). Abbreviation in time from Ca^{2+} transient peak to 50% decay was only observed in conditions where anti-β3 integrin antibody was present, but not significant when both anti-β1 and β3 integrin antibodies were present (**Figure 4.2C**). There were no changes in time to 80% decay (**Figure 4.2D**). These results indicate that anti-integrin antibodies cause abbreviation in Ca^{2+} transient parameters, similar to soluble GRGDS or GRGDSP peptides.

An important observation in this study is that unlike the soluble integrin ligands GRGDS and GRGDSP, the antibodies modulated Ca^{2+} transients in the hiPSC-CMs without causing cell detachment from the substrate. This indicates that the effects are independent of the changes to mechanical stimulation caused by cell detachment.

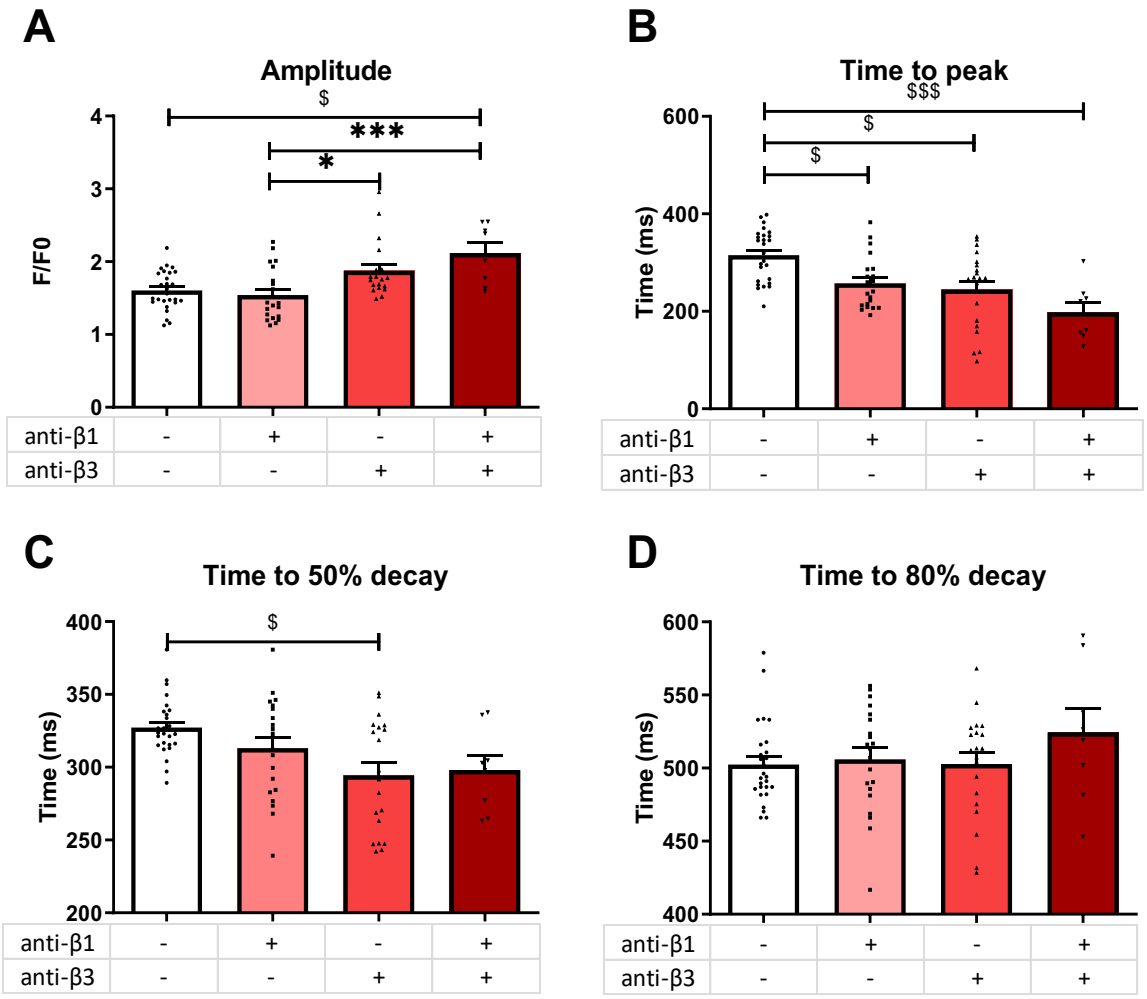

Figure 4.2 Effect of anti-integrin antibodies on human induced pluripotent stem cell-derived cardiomyocyte (hiPSC-CM) Ca^{2+} handling parameters*. anti-β-integrin antibodies potentiate soluble GRGDS- or GRGDSP-mediated abbreviation of Ca^{2+} transient decay. HiPSC-CM monolayers were incubated for 24 hours with anti-β1-integrin antibody and anti-β3-integrin antibody. HiPSC-CMs were then maintained in standard Tyrode's solution and subject to 1 Hz field-stimulation during optical mapping on an inverted microscope at 40x magnification. Ca^{2+} transient parameters analysed were (A) amplitude, (B) time to peak, (C) time from peak to 50% decay, (D) time from peak to 80% decay. Error bars represent SEM. N/n = number of preparations/images = 7/27 for Control, 6/21 for anti-β1 integrin, 5/20 for anti-β3 integrin, and 2/8 for anti-β1+β3-integrin antibodies. * = p < 0.05, *** = p < 0.001 between non-control conditions. $ = p < 0.05, $$$ = p < 0.001 vs control.*

4.3.3 anti-β-integrin antibodies potentiate soluble GRGDS- or GRGDSP-mediated abbreviation of Ca^{2+} transient decay

The observation that antibodies against the hiPSC-CM integrin subunits causes changes in Ca^{2+} transients is important to consider when they are used in electrophysiological

studies. Surprisingly, the abbreviation of the Ca^{2+} transients is similar to that induced by soluble GRGDS and GRGDSP. This indicates that integrin-binding may cause conformational changes that modulate Ca^{2+} transients, rather than downstream pathway activation.

We then repeated the GRGDS and GRGDSP treatment, but on hiPSC-CM monolayers pre-treated with the anti-β1 or anti-β3 integrin antibodies. Cultures were pre-incubated for an hour with 50mM antibodies then 2mM RGD-motif containing peptides were added concomitantly with 50mM antibodies in solution. These were incubated for 24 hours before Ca^{2+} transients were optically recorded.

In all hiPSC-CM dishes in which soluble GRGDS or GRGDSP were present, there was still formation of a spontaneously beating cluster of cells even with anti-β integrin subunit antibodies, indicating that the soluble GRGDS and GRGDSP were still able to cause cellular detachment despite anti-integrin antibody pre-treatment. There were also significant changes in the hiPSC-CM Ca^{2+} transients induced by the anti-integrin antibodies. The increase in Ca^{2+} transient amplitude with GRGDS treatment was further increased when hiPSC-CMs were treated with anti-β1 integrin antibodies (**Figure 4.3A**) but there were no changes in time to peak (**Figure 4.3B**). The abbreviation in time to 50% induced by GRGDS was further shortened in the presence of anti- β1 or anti- β3 integrin antibodies (**Figure 4.3C**). Addition of antibodies against either integrin subunit with GRGDS caused an abbreviation in time to 80% decay (**Figure 4.3D**) vs GRGDS without antibodies and vs control.

Investigation of hiPSC-CM Ca^{2+} transient was repeated with soluble GRGDSP and anti-integrin antibodies treatment. Amplitude was significantly increased by the presence of anti-β3 integrin antibodies compared to just GRGDSP (**Figure 4.3E**– $p < 0.001$). Presence of anti-β1 or β3 subunit antibodies did not cause any change to the abbreviation in time to peak induced by GRGDSP (**Figure 4.3F**) – a similar observation to the time to peak when hiPSC-CMs were treated with GRGDS instead of GRGDSP (**Figure 4.3B**). Anti- β3 subunit antibodies further abbreviated the time to 50% decay induced by GRGDSP, but no change was observed in the presence of anti- β1 integrin subunit antibodies with GRGDSP treatment (**Figure 4.3G**). GRGDSP did not cause any abbreviation in time to 80% decay unless anti- β3 integrin subunit antibody was present (**Figure 4.3H**). Our data indicate that the binding of peptides that recognise integrins causes changes in Ca^{2+} transients, rather than activation of downstream pathways.

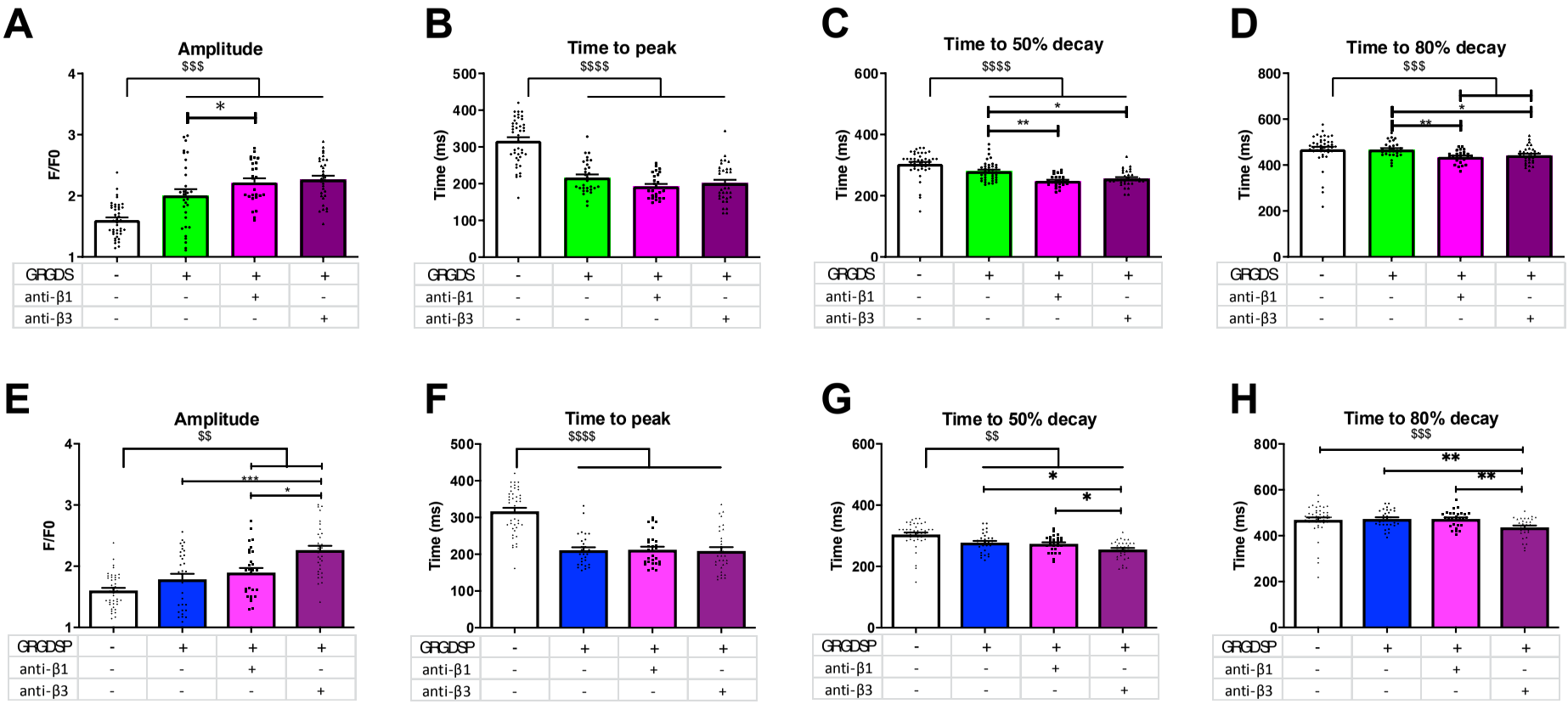

*Figure 4.3 Effect of anti-integrin antibodies on soluble integrin ligand-mediated changes in human induced pluripotent stem cell-derived cardiomyocyte (hiPSC-CM) Ca^{2+} handling parameters. HiPSC-CM monolayers were incubated with anti-β1 (pink) or anti-β3 (purple) integrin antibody and then incubated for 24 hours with soluble integrin ligands GRGDS (green) or GRGDSP (blue) added with anti-β1- or anti-β3-integrin antibody concentration. HiPSC-CMs were then maintained in standard Tyrode's solution and subject to 1 Hz field-stimulation during optical mapping on an inverted microscope at 40x magnification. Ca^{2+} transients were measured for GRGDS (A-D) or GRGDSP (green)-treated hiPSC-CM monolayers. Ca^{2+} transient parameters analysed were (A & E) amplitude, (B & F) time to peak, (C & G) time from peak to 50% decay, (D & H) time from peak to 80% decay. Error bars represent SEM. N/n = number of preparations/images = 11/42 for control, 6-8/22-32 for GRGDS conditions (A-D), 6-8/20-32 for GRGDSP conditions (E-H). * = p < 0.05, ** = p < 0.01, *** = p < 0.001, **** = p < 0.0001. $$ = p < 0.01, $$$ = p < 0.001, $$$$ = p < 0.0001 vs control.*

4.3.4 Self-assembling integrin peptides do not induce cell detachment from the glass substrate

While integrin stimulation achieved through soluble GRGDS or GRGDSP treatment resulted in robust changes in hiPSC-CM electrophysiology, the phenomenon of substrate detachment cell clustering represented a significant confounding factor. Cardiomyocytes in a free-floating cluster are subject to different mechanical stimuli to a monolayer of cardiomyocytes attached to a glass substrate. To address this issue of cell detachment caused by soluble integrin ligands, we utilised the fibril-forming properties of self-assembling peptides synthesised with integrin and substrate-binding properties.

NSGAITIG is an amyloid-forming amino acid sequence extracted from the fibre shaft of the adenovirus (Deidda *et al.*, 2017). This sequence consists of a β-sheet-forming GAITIG core. The exposed NS terminal has been replaced with an RGDS sequence, such that the RGD tripeptide repeat at the N-terminus then remains exposed to cells post-assembly (Jonnalagadda *et al.*, 2017). The two peptide sequences investigated were RGDSGAITIGC (RGD_C) and RGDSGAITIGA (RGD_A). The exchanged cysteine and alanine residues at the C-terminus have been shown to modulate the stability of the fibrils once assembled and provide substrate-attachment properties, mimicking fibril-forming ECM proteins that form the native myocardial extracellular environment (Deidda *et al.*, 2017). RGD_A and RGD_C sequences in powder form were suspended in serum free media and allowed to self-assemble into fibrils before application onto the hiPSC-CM monolayers.

We wanted to ensure that treatment of hiPSC-CM monolayers with these fibril-forming, self-assembling integrin ligands does not induce cell detachment. Glass dishes seeded with hiPSC-CMs and treated with RGD_A or RGD_C were stained with anti-cardiac Troponin T antibody and DNA-binding DAPI (**Figure 4.4A-C**). We identified that following treatment with these self-assembling integrin ligands, there was no change the density of nuclei detected by immunofluorescence, indicating that there was no cell detachment induced by these fibril-forming integrin ligands (**Figure 4.4D**).

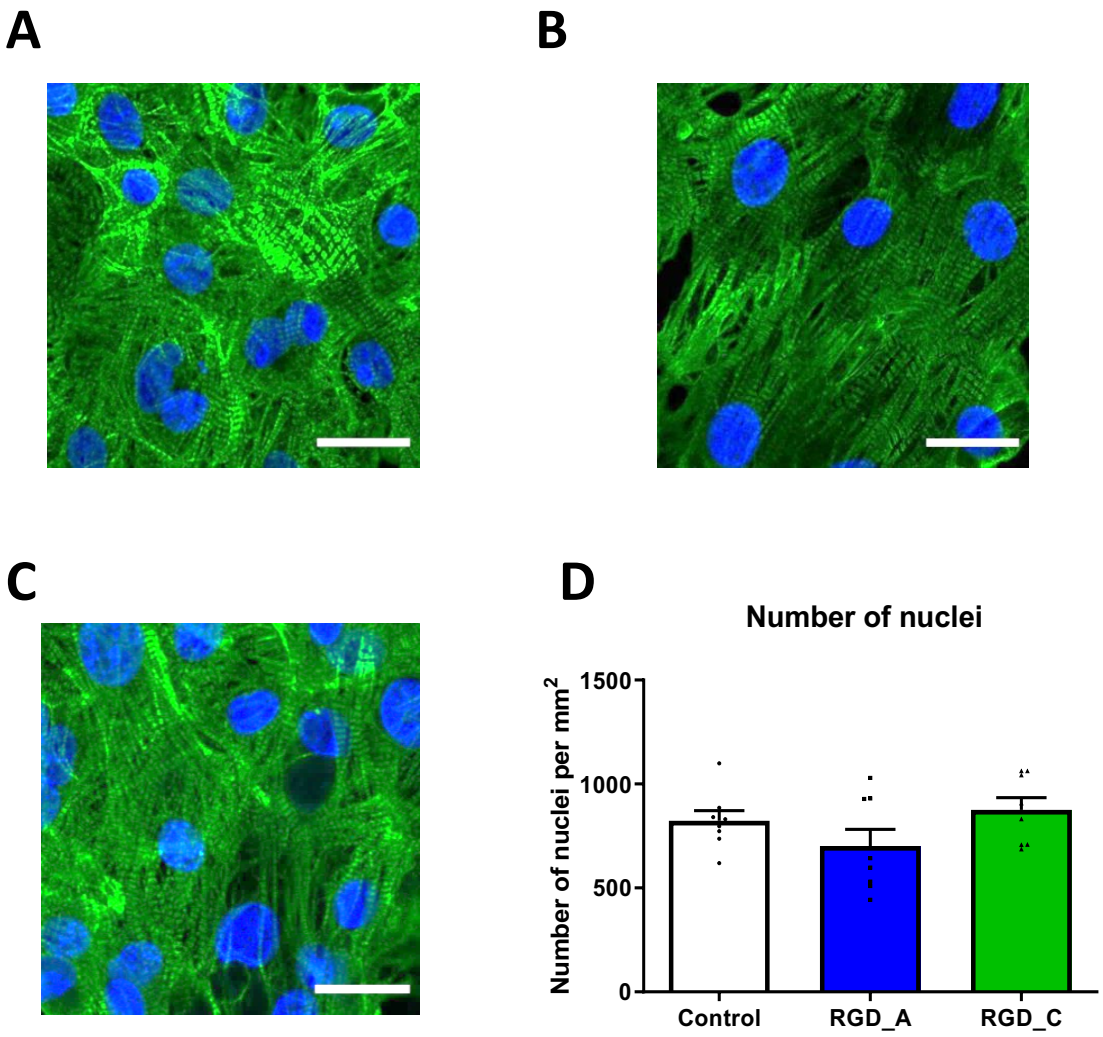

Figure 4.4: Effect of self-assembling integrin ligands on human induced pluripotent stem cell-derived cardiomyocyte (hiPSC-CM) attachment to glass substrate. *Representative confocal images of hiPSC-CMs monolayers cardiac Troponin-T (green) and DAPI (blue). Conditions shown are (A) control, (B) RGD_A (RGDSGAITIGA) or (C) RGD_C (RGDSGAITIGC). Scale bar = 25µm. Confocal images were used to investigate the (D) number of nuclei attached to the glass substrate, as an indicator of cell density. Error bars represent SEM. N/n = number of preparations/images = 2/8.*

4.3.5 Self-assembling integrin ligands increase hiPSC-CM spontaneous beating rate

The finding that these self-assembling integrin ligands RGD_A and RGD_C do not induce cardiomyocyte detachment allows for electrophysiological studies into the effect of integrin ligands independent of the change in mechanical stimulus induced by detachment from the glass substrate. HiPSC-CMs remained as a spontaneously beating monolayer on the

glass substrate. Representative brightfield images are shown in **Figure 4.5A-C**. These show that there are more areas of the glass substrate exposed without cell attachment. As we reported that there was no change in nuclei number (**Figure. 4.4D**), the observation of increased areas without cells is as a result of change in cell shape rather than fewer cells. This could be due to rearrangement of integrins such that cells do not spread on the glass. The beating frequency of these monolayers increased after self-assembling integrin-ligand treatment vs. control (**Figure 4.5D**), indicating changes in the excitability of these cardiomyocytes.

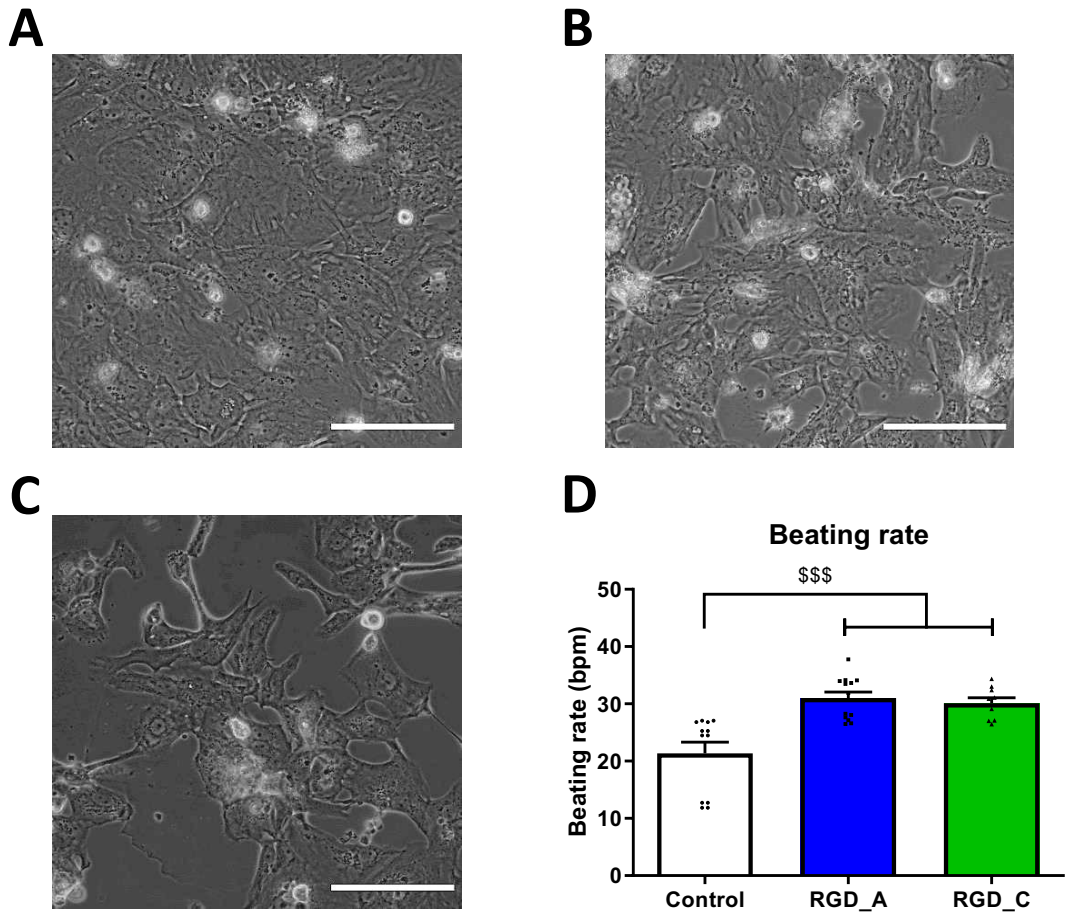

Figure 4.5 Effect of fibril-forming, self-assembling integrin ligands on human cardiomyocyte structure and beating rate*. Representative bright field images of human induced pluripotent stem cell-derived cardiomyocyte monolayers following 24-hour treatment with self-assembling, fibril-forming integrin ligands RGD_A (RGDSGAITIGA) or RGD_C (RGDSGAITIGC). Conditions shown are (A) control, (B) RGD_A or (C) RGD_C. Scale bar = 100µm. Confocal images were used to investigate the beating rate (D). Error bars represent SEM. N = 9-12 preparations. $$$ = p < 0.001 vs control.*

4.3.6 Self-assembling integrin ligands abbreviate Ca^{2+} transient duration

We then investigated the changes in Ca^{2+} transient parameters induced self-assembling integrin ligands. This would allow us to determine if the more efficient Ca^{2+} cycling induced by soluble RGD peptides reported in section 4.3.1 can be observed by integrin ligands without the phenomenon of cell detachment. To investigate this, we treated the hiPSC-CMs with RGD_A or RGD_C and fluorescently labelled the cells with the Ca^{2+}-sensitive dye Fluo4-AM. The dishes were then maintained in standard Tyrode's solution during optical mapping. Due to morphological differences shown in Figure 4.5 A-C, both RGD_A and RGD_C were investigated for the rest of this study.

The Ca^{2+} transients were recorded at 1 Hz field stimulation on an inverted microscope at 40x magnification and these transients were then analysed. We identified that both RGD_A and RGD_C induced significant abbreviation of the Ca^{2+} transients, shown by the representative traces in **Figure 4.6A**. We identified no change in Ca^{2+} transient amplitude in hiPSC-CMs treated with RGD_A or RGD_C vs. control (**Figure 4.6B**). Both of these self-assembling, integrin-binding peptides induced a significant abbreviation in time to transient peak and time from transient peak to 50% decay and 80% decay compared to control (**Figure 4.6C-E**). These changes in Ca^{2+} transient parameters caused an abbreviation of whole transient duration compared to control. The representative Ca^{2+} transients are shown in Figure 4.6E.

These findings show that the self-assembling, fibril-forming integrin ligands RGD_A and RGD_C can recapitulate the Ca^{2+} transient abbreviation caused by soluble GRGDS or GRGDSP. This indicates two major findings. Firstly, as the abbreviation caused by RGD_A and RGD_C is independent of cellular detachment from the substrate, we deduce that the effects seen by GRGDS and GRGDSP are also independent from cell detachment. Secondly, the abbreviation in Ca^{2+} transient caused by soluble GRGDS and GRGDSP together with the abbreviation caused by RGD_A and RGD_C indicate that the abbreviation is integrin-mediated.

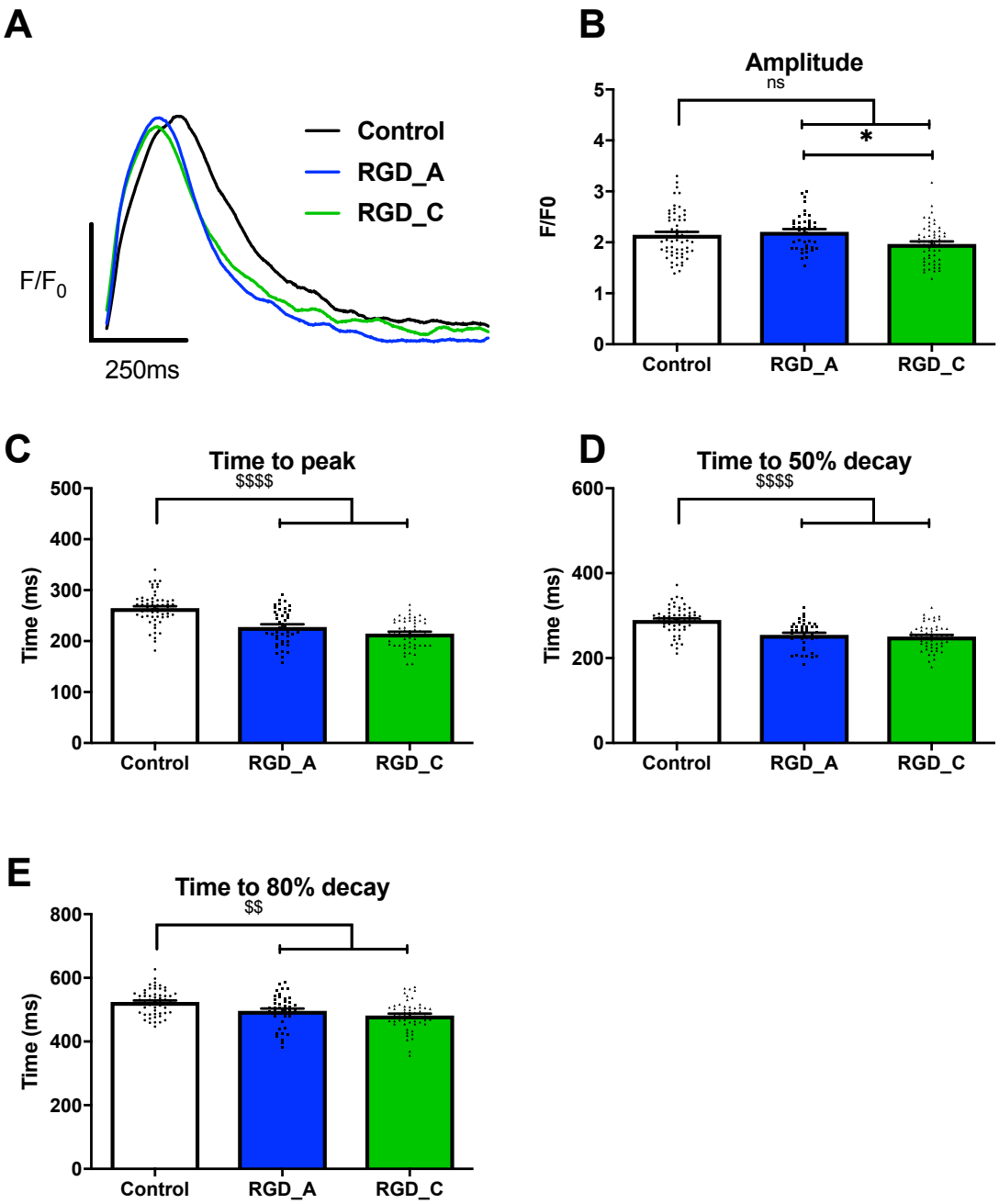

Figure 4.6 Effect of fibril-forming, self-assembling integrin ligands on human cardiomyocyte Ca^{2+} handling properties*. human induced pluripotent stem cell-derived cardiomyocyte (hiPSC-CM) monolayers were cultured for 24-hour with self-assembling, fibril-forming integrin ligands RGD_A (RGDSGAITIGA) or RGD_C (RGDSGAITIGC). hiPSC-CMs were then maintained in standard Tyrode's solution and subject to 1 Hz field-stimulation during optical recording on an inverted microscope at 40x magnification. Representative Ca^{2+} transients are shown in (A). Ca^{2+} transient parameters analysed were (B) amplitude, (C) time to peak, (D) time from peak to 50% decay and (E) time from peak to 80% decay. Error bars represent SEM. N = 4 preparations, n = 60 cells for control, 42 cells for RGD_A and 56 cells for RGD_C. * = p < 0.05. $$= p < 0.01, $$$$ = p < 0.0001 vs control.*

4.3.7 Self-assembling integrin ligands recruit the SR to Ca^{2+} cycling

The prevention of cell detachment from the substrate with preservation of the Ca^{2+} transient abbreviation following self-assembling integrin ligand treatment afforded us to assess, using caffeine application, the Ca^{2+} extrusion mechanisms as previously described (Varro *et al.*, 1993; Maier *et al.*, 2003). Locally applied caffeine induces a robust Ca^{2+} response in both standard bath solutions as well as Na^{+}-Ca^{2+} free conditions, as described in Chapter 2 (**Figure 2.7A & B**).

In keeping with the reduced time to 50% decay (**Figure 4.6C**) and time to 80% decay (**Figure 4.6D**), rate of twitch Ca^{2+} transient decay was significantly faster following application with either RGD_A or RGD_C compared to control (**Figure 4.7A**). When the constituent parts of Ca^{2+} removal were assessed, the increased rate of transient decay was attributed to an approximately 100% increase in the rate of SR Ca^{2+} uptake (**Figure 4.7B**). Treatment with RGD-A and RGD-C had no effect on NCX or slow Ca^{2+} removal mechanisms (**Figure 4.7C-D**). When determining the relative contributions of these decay mechanisms to the total rate of Ca^{2+} decay during the twitch Ca^{2+} transient, this study shows that integrin ligands induce hiPSC-CM cytosolic Ca^{2+} removal to be from a predominantly NCX-mediated process, to one that is predominantly dependent on the SR (**Figure 4.7E**).

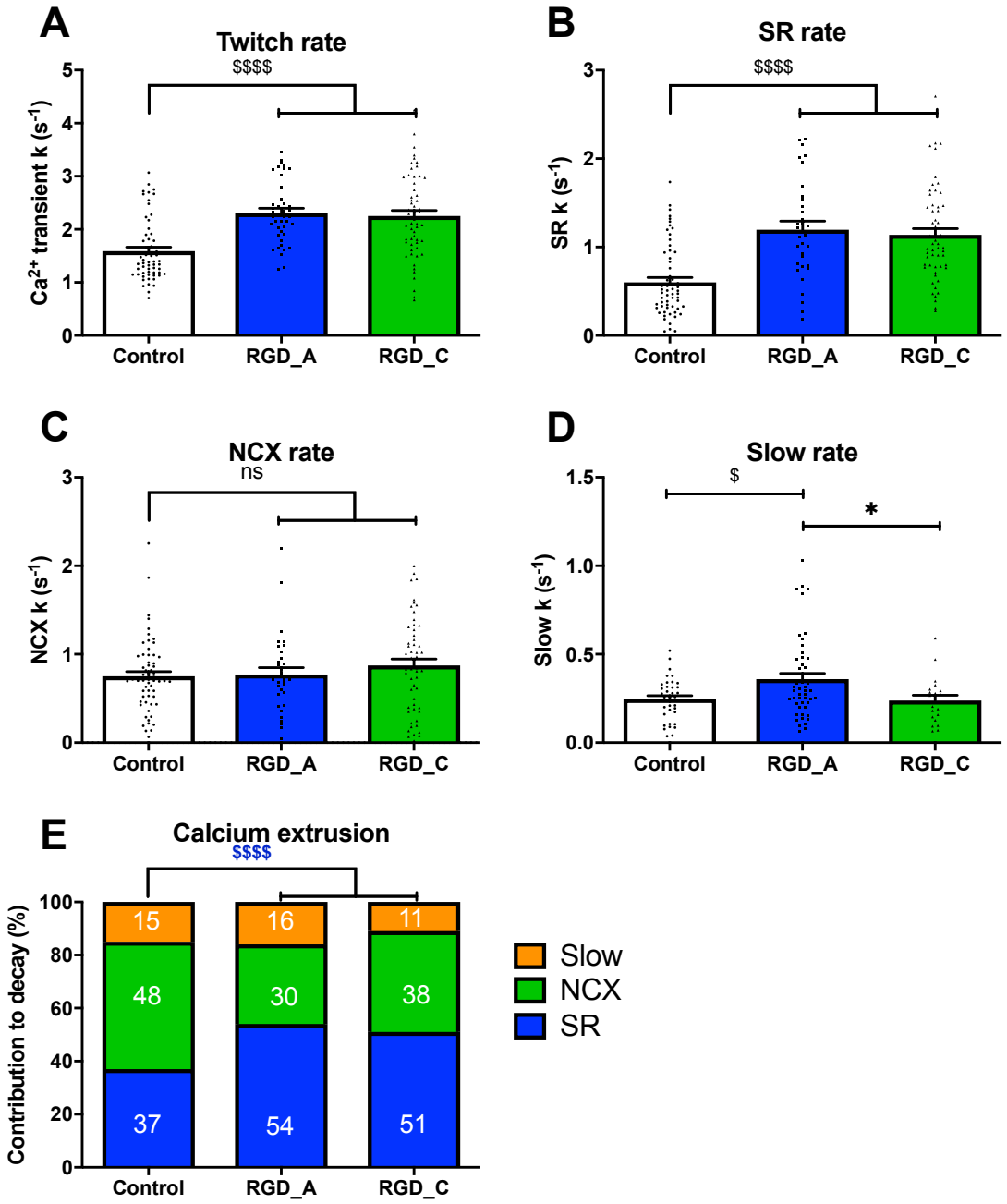

Figure 4.7 Effect of fibril-forming, self-assembling integrin ligands on human cardiomyocyte cytosolic Ca^{2+} extrusion mechanisms. *Human induced pluripotent stem cell-derived cardiomyocyte (hiPSC-CM) monolayers were treated for 24 hours with RGD_A (RGDSGAITICA) or RGD_C (RGDSGAITIGC) (2mM). Ca^{2+} transients from optical recording of hiPSC-CM monolayers in standard Tyrode's solution or Na^{+}/Ca^{2+}-free Tyrode's solution were used to calculate contribution of Ca^{2+} extrusion mechanisms. Rate of (A) twitch Ca^{2+} transient decay, and contributions by (B) SR-mediated Ca^{2+} uptake, (C) NCX-mediated Ca^{2+} removal and (D) Ca^{2+} removal mediated via mitochondria Ca^{2+}-uniporter and sarcolemma Ca^{2+}-ATPase activity. (E) Percentage contribution of Ca^{2+} removal mechanisms. Error bars represent SEM. N = number of preparations = 6-8. n = number of cells = 33-60 for (A-C), 24-52 for (D). * = $p<0.05$. $ = $p < 0.05$, $$$$ = $p < 0.0001$ vs control.*

4.3.8 Self-assembling integrin-mediated induce a more rod-like cardiomyocyte morphology

Having identified that the fibril-forming integrin ligands RGD_A and RGD_C were able to induce the changes in electrophysiology, we then investigated the structural changes that could underlie the improved Ca^{2+} cycling efficiency. The fibril-forming integrin ligands did not cause cell detachment but did cause changes in the hiPSC-CM morphology (**Figure 4.8A-C**). There was a significant reduction in the cell area (**Figure 4.8D**) and volume (**Figure 4.8E**). These changes were not uniform, such that the cell aspect ratio was significantly increased with either integrin ligand (**Figure 4.8F**), inducing a more rod-like morphology that is characteristic of adult human cardiomyocytes (Yang, Pabon and Murry, 2014).

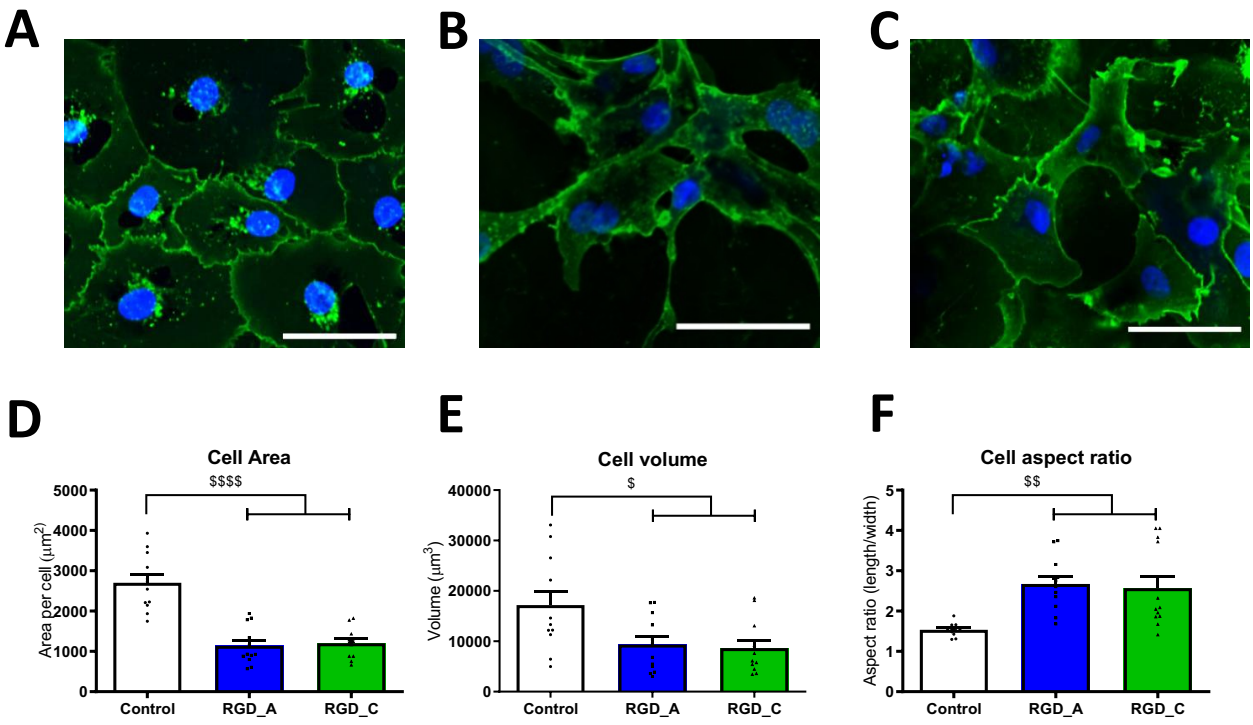

***Figure 4.8 Effect of fibril-forming, self-assembling integrin ligands on human cardiomyocyte morphology**. Human induced pluripotent stem cell-derived cardiomyocyte (hiPSC-CM) monolayers were treated for 24 hours with self-assembling, fibril-forming RGD_A (RGDSGAITIGA) or RGD_C (RGDSGAITIGC) (2mM). hiPSC-CMs were then fixed and permeabilised. Non-specific binding was blocked before samples were stained. Representative confocal images of hiPSC-CMs monolayers WGA (green) and DAPI (blue) staining. Conditions are (A) control, (B) RGD_A or (C) RGD_C. Scale bar = 50µm. Confocal images were used to investigate the (D) cell area, (E) cell volume and (F) Cell aspect ratio. Error bars represent SEM. N/n = number of preparations/number of cells = 3/12. $ = p < 0.05, $$ = p<0.01 and $$$$ = p < 0.0001 vs control.*

4.3.9 Integrin ligands increase cardiomyocyte sarcomere length and nucleus aspect ratio

We then investigated the changes in cell cytoskeleton or nucleus that could indicate a phenotype more akin to the healthy, adult cardiomyocyte. Control and RGD_A or RGD_C-treated hiPSC-CMs were stained for α-sarcomeric actinin and DAPI, shown in **Figure 4.9 A-I.** The nucleus aspect ratio is used as a measure of cardiomyocyte maturation (**Figure 4.9J**), as this increases during the development of the adult cardiomyocyte phenotype. We identify that both RGD_A (**Figure. 4.9D**) and RGD_C (**Figure 4.9G**) increase the aspect ratio of the nucleus compared to control (**Figure 4.9A**).

Common to hiPSC-CMs and immature cardiomyocytes is a disarrayed sarcomere structure compared to the highly organised sarcomeres in the adult cardiomyocytes. The length of sarcomeres in hiPSC-CMs is typically of 1.6 μm (Lundy *et al.*, 2013). The expression of α-sarcomeric actinin in immunofluorescent images were used to analyse the sarcomere length (Fig 4.9K), which increased from 1.63 ± 0.070 μm in control (**Figure 4.9B & C**) to 1.74 ± 0.066 μm with RGD_A (**Figure 4.9E & F**) or 1.747 ± 0.107 μm with RGD_C (**Figure 4.9 H & I**). Measurements of sarcomere length and nucleus aspect ratio, as indicators of cardiomyocyte maturation, suggest that the hiPSC-CMs display a more mature phenotype following treatment with self-assembling integrin ligands.

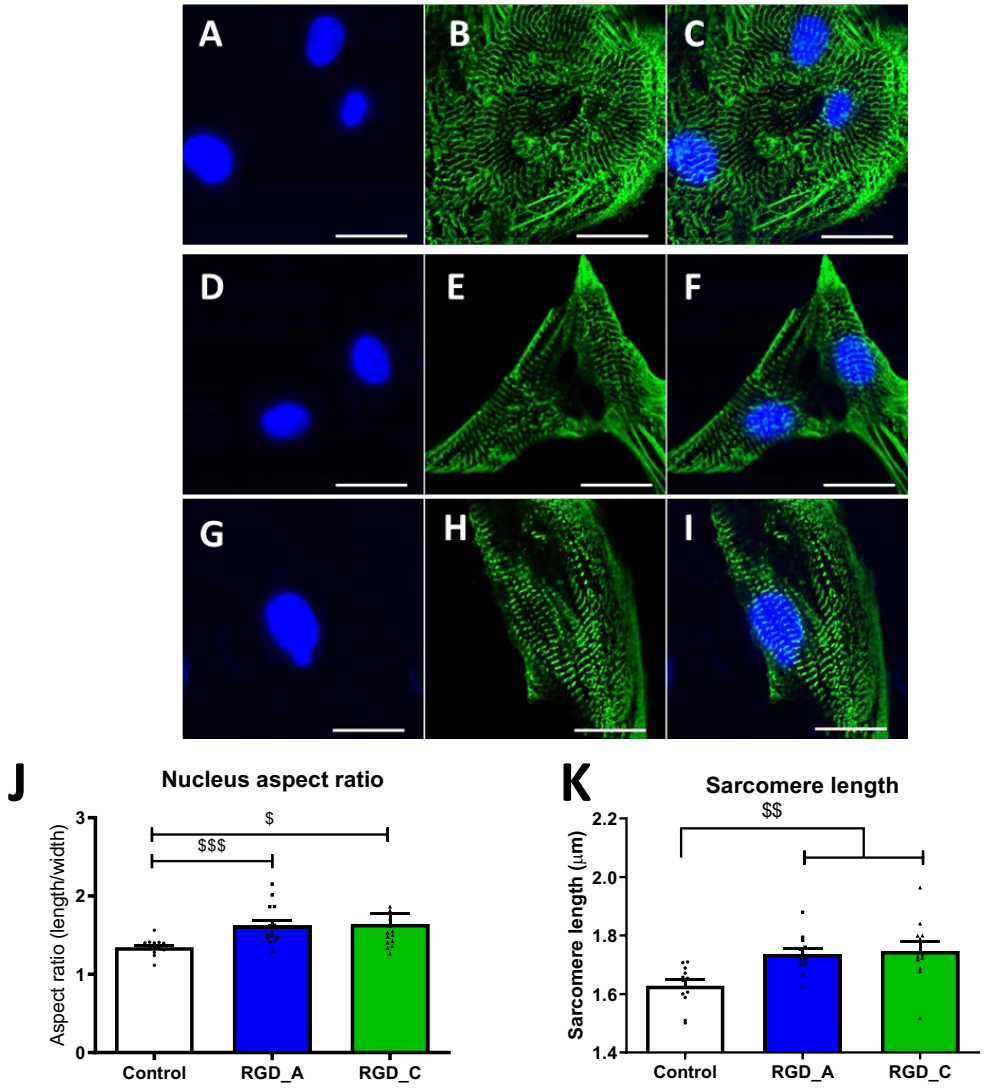

Figure 4.9 Effect of fibril-forming, self-assembling integrin ligands on the sarcomere and nucleus morphology of human cardiomyocytes*. Human induced pluripotent stem cell-derived cardiomyocyte (hiPSC-CM) monolayers were treated for 24 hours with self-assembling RGD_A (RGDSGAITIGA) or RGD_C (RGDSGAITIGC) (2mM). hiPSC-CMs were then fixed and permeabilised. Non-specific binding was blocked before samples were stained. DAPI (Blue) and α-sarcomeric actinin (green) staining of the hiPSC-CMs in (A-C) Control and following (D-F) RGD_A and (G-I) RGD_C treatment. The images on the right (C, F and I) are merged images of the images on the left (A, D and G) and middle (B, E and H) columns. Scale bar = 20μm. DAPI was used to measure (J) nucleus aspect ratio. α-sarcomeric actinin used to measure (K) sarcomere length. Error bars represent SEM. N/n = number of preparations/number of cells = 3/12. $ = p < 0.05, $$ = p<0.01 and $$$ = p < 0.001 vs control.*

4.3.10 Integrin ligand RGD_C increases cardiomyocyte sarcolemma: SR junctional gap.

Having identified these changes in Ca^{2+} cycling parameters and cardiomyocyte structure, we then investigated the potential changes in Ca^{2+} handling ultrastructure that could underlie the Ca^{2+} cycling changes induced by the integrin ligands. The SR is a critical organelle in Ca^{2+} cycling. During maturation, there is progressive recruitment of associated proteins that link the SR to the sarcolemma. This is reported to increase the sensitivity of RyRs on the SR to the Ca^{2+} influx through sarcolemmal Ca^{2+} channels, increasing the efficiency of CICR.

This distance between the SR and sarcolemma is determined by the size of the accessory proteins and is reported to be around 12nm in the healthy, adult human cardiomyocyte due to the size of the RyR foot processes linking the SR to the sarcolemma being of this length (Franzini-Armstrong, Protasi and Ramesh, 1999). We analysed the SR parameters from EM images (**Figure 4.10A & F**) of hiPSC-CMs treated with RGD_A or RGD_C. We separated the sides into the apical **(Figure 4.10A-E)** and basal aspects **(Figure 4.10F-J)** of the hiPSC-CMs. The apical side is the sarcolemma exposed to the media and treatment conditions and the basal side is the sarcolemma that is directly opposed to the cell culture substrate and pre-plated substrates.

When measuring the SR parameters, there were no changes in SR area, perimeter or length of the functional side of the SR on the apical side of the hiPSC-CMs when exposed to either RGD_A or RGD_C (**Figure 4.10B-D**). There was an increase in the junctional gap of functional SRs found on the apical side following treatment with RGD_C but not RGD_A (**Figure 4.10E**). Similarly, there were no changes in SR area, perimeter or length of functional SR on the basal side of the hiPSC-CMs, in close apposition to the fibronectin preplated on the substrate surface, following treatment with either RGD_A or RGD_C (**Figure 4.10G-I**).

There was an increase in the junctional gap on the basal aspect of the hiPSC-CMs when hiPSC-CMs were treated with RGD_C but no significant change when treated with RGD_A (**Figure 4.10J**). The lack of significant increase following RGD_A treatment despite observing abbreviation in Ca^{2+} transient duration indicates that the rearrangement in SR following RGD_C treatment, at most, only partially explains the SR recruitment.

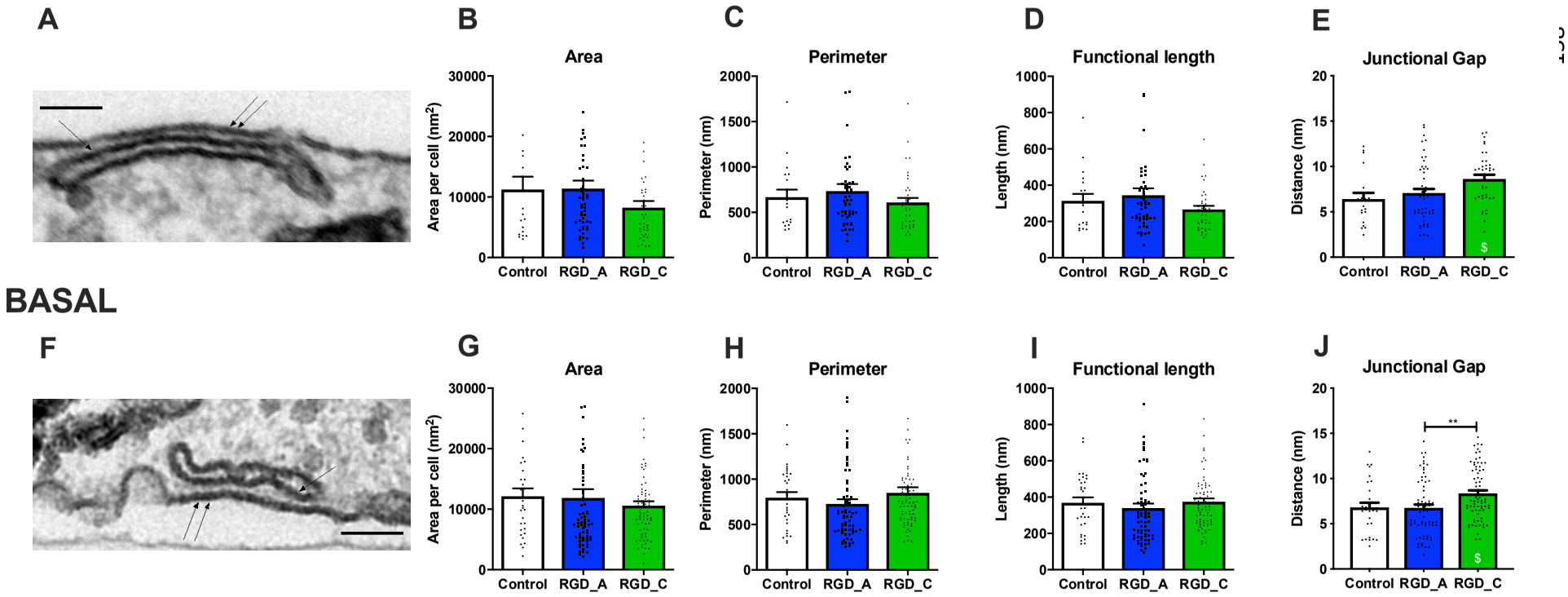

*Figure 4.10 Effect of fibril-forming, self-assembling integrin ligands on the sarcoplasmic reticulum (SR) parameter of hiPSC-CMs. hiPSC-CM monolayers were treated for 24 hours with self-assembling, fibril-forming RGD_A or RGD_C (2mM). hiPSC-CMs were then fixed and processed for EM imaging. SR parameters were measured for functional SR on the side exposed to the media and integrin ligand treatment (apical (A-E)) and side closest to the fibronectin-coated dish (basal (F-J)). SR parameters measured were (B & G) Area, (C & H) Perimeter, (D & I) Functional length and (E & J) Junctional gap. Error bars represent SEM. N/n = number of preparations/number of SR= 2/49-2/111. ** = p<0.01. $ = p < 0.05.*

4.4 Discussion

Extracellular mechanical stimuli from the ECM communicate via integrins on the cardiomyocyte membrane to modulate cardiomyocyte structure and function, but the role of integrins in the modulation of SR-recruitment to Ca^{2+} cycling in human cardiomyocytes was unknown (Civitarese *et al.*, 2017). In this chapter, we demonstrate important aspects of the integrin-mediated regulation of Ca^{2+} cycling. Soluble integrin ligands abbreviate hiPSC-CM Ca^{2+} transients in a manner dependent on the flanking sequence on either side of the RGD-tripeptide sequence. The Ca^{2+} transient abbreviation following treatment with fibril-forming integrin ligands is independent of cell detachment, and is associated with a recruitment of the SR to the Ca^{2+} removal mechanism. These fibril-forming integrin ligands induce changes in cardiomyocyte shape, into a more rod-like morphology, closer to the adult human cardiomyocyte. There are also changes to the hiPSC-CM ultrastructure – an increase in junctional gap distance closer to the values previously reported for healthy, adult cardiomyocytes, and a change in sarcomere length, which is known to affect Ca^{2+} sensitivity and cardiomyocyte contraction. It is clear that the integrin-mediated pathways are complex, but we have demonstrated key changes in cardiomyocyte structure that can influence Ca^{2+} handling in hiPSC-CMs and could underlie the effects of ECM-mediated modulation of cardiomyocyte Ca^{2+} cycling.

4.4.1 Integrin-mediated modulation of Ca^{2+} cycling

Treatment of cardiomyocytes with soluble peptides containing the RGD-tripeptide sequence has been shown to activate cytoskeletal assembly of integrin-associated signalling proteins as well as downstream pathways in a manner mirroring that seen *in vivo* under conditions of increased mechanical load (Harston and Kuppuswamy, 2011; Yu *et al.*, 2011). We identified that soluble peptides GRGDS and GRGDSP caused significant abbreviation of the hiPSC-CM Ca^{2+} transients through an abbreviation of time to peak and time to decay, indicating more efficient CICR and Ca^{2+} removal, respectively. RGD tripeptide and negative control RGES did not cause any change in Ca^{2+} cycling in the hiPSC-CMs. It is known that GRGDS has a 1000-fold lower affinity for fibronectin receptors, as multiple neighbouring domains influence the binding of the ligand to the receptor (Hautanen *et al.*, 1989). This study indicates that the flanking sequences around the RGD-tripeptide are important in

determining the efficacy of soluble RGD-containing peptides in modulating cardiomyocyte Ca^{2+} cycling. This is supported by a study in rat pulmonary arterial smooth muscle cells that identified that the potency of the effect of soluble integrin ligands on intracellular Ca^{2+} concentration was dependent on the flanking sequences, such that cyclo-RGD had a much less potent effect that soluble integrin ligands with flanking sequences (Umesh *et al.*, 2006). Therefore, the differences in affinity of binding could underlie the lack of significant effect seen with RGD tripeptide.

Important to consider is that integrins incorporate a large family of heterodimer combinations (Ginsberg, Partridge and Shattil, 2005). The family of integrins in mammals consists of more than 18 α and 18 β integrin subunits, which heterodimerise to form 24 receptors. Cardiomyocytes mainly express the heterodimers α1β1, α5β1 and α7β1, which are predominantly collagen, fibronectin and laminin binding receptors, respectively. Previous studies have reported unique integrin profiles in normal vs. pathological hearts; α5 subunit is predominantly expressed in foetal or neonatal cardiomyocytes but is replaced by α7 subunits post-natally such that it is the predominant subunit expressed by mature, adult cardiomyocytes (Brancaccio *et al.*, 1998). It is therefore likely that not all integrin heterodimers play a role in modulating hiPSC-CM Ca^{2+} cycling and that the relative expression of the subunits is important for cardiomyocyte function.

4.4.2 Anti-integrin antibodies

We identified that a limitation to the use of anti-integrin antibodies is that these antibodies caused changes in the Ca^{2+} cycling. This was surprising but does indicate that binding and possibly clustering of integrins by integrin antibodies can mediate some of the effects induced by integrin ligands. Morphological changes in the hiPSC-CMs were not measured but could underlie the change in Ca^{2+} transients observed. As hiPSC-CMs are contractile, there may be changes in the exposure of integrins during contraction. This would allow some antibody binding that would induce morphological changes or even detachment over a period greater than the 24 hours measured here. Future work needs to determine the structural effects induced by integrin-binding antibodies to determine if these, despite not causing recruitment of downstream accessory proteins or activation of kinase pathways, may cause structural changes to cardiomyocytes that alter function.

We observe that antibodies against the β1 or β3 integrin subunits did not prevent cellular detachment induced by GRGDS or GRGDSP or attenuate the effects of these soluble integrin ligands on hiPSC-CM Ca^{2+} transients; instead, we show evidence of potentiating GRGDS and GRGDSP-mediated Ca^{2+} transient amplitude amplification and abbreviation of the time to 50% decay or time to 80% decay. A possible explanation for why the detachment still occurred is that the soluble integrin ligands can preferentially bind to integrins compared to the much larger anti-integrin antibodies. As integrins are a family of heterodimeric receptors, integrins that do not express the β1 or β3 integrin subunits may mediate the detachment when antibodies against these subunits are present (Le Gat *et al.*, 2001; Johnston *et al.*, 2009; Suryakumar *et al.*, 2010).

4.4.3 Integrin-mediated modulation of SR Ca^{2+} release

Although reports have implicated integrins in modulating cytosolic Ca^{2+} availability, this is the first study to identify that integrin ligands increase the efficiency of Ca^{2+} cycling in human cardiomyocytes. In rat pulmonary arterial smooth muscle cells, soluble integrin ligands contributes to Ca^{2+} release from RyR-gated stores (Umesh *et al.*, 2006). This study also identified that soluble GRGDSP increase cyclic ADP-ribose, the endogenous activator of RyRs, by 70% in rat pulmonary arterial smooth muscle cells. Immunological studies with mouse cardiomyocytes identified localisation of β1 integrins to T-tubules, co-localising with RyR2s and stabilising RyR2 opening (Umesh *et al.*, 2006). This increase in RyR activation could be a mechanism by which CICR is increased in the presence of integrin ligands in our study; future studies should identify changes in cyclic ADP-ribose in human cardiomyocytes. However, the lack of ultrastructural features for the development of T-tubules and dyadic formation in hiPSC-CMs could prevent this mechanism from acting.

To determine the ultrastructural changes that could contribute to the increase efficiency of CICR, we then investigated the apposition of the SR to the sarcolemma, which forms the calcium release units (CRUs). CRUs contain two proteins essential to EC-coupling: dihydropyridine receptors (DHPRs) or L-type Ca^{2+} channels of exterior membranes, and RyRs, the Ca^{2+} release channels of the SR (Protasi, Sun and Franzini-Armstrong, 1996; Franzini-Armstrong, Protasi and Tijskens, 2005). The CRUs are restricted by two geometrical factors. One is the size of the junctional gap separating the SR from the exterior membranes (12nm),

which is determined by the size of the RyR cytoplasmic domain or foot; the other is the tight, ordered clustering of feet, which an arrangement approximately 29nm apart (Franzini-Armstrong, Protasi and Ramesh, 1999). This enables Ca^{2+} released into the junctional gap to be temporarily trapped, such that there is a brief rise in $[Ca^{2+}]_i$ greater than in the surrounding cytoplasm, promoting CICR.

The parameters of the sarcolemma and jSR membrane also affect the CRU properties; as larger and more rounded membrane domains are more likely to trap the Ca^{2+} (Franzini-Armstrong, Protasi and Ramesh, 1999). We see that treatment of hiPSC-CMS with self-assembling RGD-containing peptides induces an increase in junctional gap distance, closer to the value of 12nm reported in healthy, adult cardiomyocytes (Fig. 4.10) (Olivetti *et al.*, 1996). This was a surprising result, as functionally, an increase in junctional gap distance would be thought to reduce CICR efficiency. Due to the insufficient resolution of the EMs, whether the increase in junctional gap distance was accompanied by the presence of normal CRUs-containing juxtaposed RyRs and DHPRs could not be established; however, the rearrangement of the SR-sarcolemma junction could be operated by structural recruitment of the SR to EC-coupling. As the molecular machinery of CRUs is assembled in a series of sequential steps, further studies would need to investigate the effects of integrin ligands on the assembly of the junctional complex proteins to identify if this increase in junctional gap distance is indicative of recruitment of accessory CRU scaffold proteins.

4.4.4 Integrin-mediated modulation of Ca^{2+} removal

This study used micropipette caffeine application to identify integrin ligands induce hiPSC-CMs to change from an NCX-dominant cytosolic Ca^{2+} extrusion to an SR-dominant Ca^{2+}extrusion. Based on previous studies using human myocytes, in non-failing myocytes the contribution of NCX and SR Ca^{2+}-ATPase to $[Ca^{2+}]_i$ decline are 23% and 77%, respectively. In the hiPSCs used in this study, these contributions are 37% by SR and 48% by NCX, driven mainly by weaker intrinsic SR Ca^{2+}-ATPase function due to reduced SERCA expression and maintained expression of the negative regulator, PLN (Kane *et al.*, 2015). We show that RGD_A and RGD_C increase the relative contribution of SR (54% and 51%, respectively) compared to control. This indicates that the Ca^{2+} decay in these hiPSC-CMs becomes SR-dominant and more closely resembling the values in adult human control cardiomyocytes.

Although not studied here, the expression of key modulators of SR activity can be investigated in future investigations. For example, downregulation of negative regulator PLN would increase the activity of SERCA a change in SERCA expression. Beyond protein expression, changes in small proteins may also regulate activity of SERCA. Umesh and colleagues identified that soluble GRGDS causes an increase in cyclic ADP-ribose in mouse cardiomyocytes, and cyclic ADP-ribose has been identified in other studies to accelerate the activity of SERCA pumps (Umesh *et al.*, 2006; Yamasaki-Mann, Demuro and Parker, 2010). The heterogeneity in integrin receptor subtypes and the role of flanking sequences on ligand affinity must be considered when attributing integrin-mediated effects.

4.4.5 Integrin-mediated cytoskeletal changes

Classical integrin pathways involve the recruitment and activation of kinases, but the effects of soluble integrin ligands in this study informs us that these pathways are not required for the changes in Ca^{2+} cycling. Unlike the receptor tyrosine kinase family, integrins do not possess intrinsic kinase activity but rather promote signalling by facilitating the activation of kinases such as src or focal adhesion kinase. The adaptor proteins assembled following integrin ligation can be divided into three groups: (1) structural adaptors (E.g. alpha-actinin) that bind integrins to F-actin and therefore to the cytoskeleton, (2) scaffold adaptors that provide binding sites for additional focal adhesion proteins, and (3) catalytic adaptors (E.g. FAK, Src) that facilitate signal propagation (Fa *et al.*, 2009). Importantly, only RGD-containing peptides applied within a collagen gel, as opposed to in solution, recruit and activate focal adhesion molecules to form the focal adhesion complex (FAC) (Laser *et al.*, 2000; Balasubramanian and Kuppuswamy, 2003; Rauch *et al.*, 2011). Therefore, application of peptides in the absence of collagen gel allows us to determine that the observed effect on Ca^{2+} cycling parameters are independent of FAC formation.

4.4.6 Implications for *in vitro* models

A major aim of the biomaterials field is the development of biocompatible and biodegradable scaffolds for tissue engineering. Lacking in current 2D models are structures that represent the mechanical, extracellular stimuli that are known to play a crucial role in

modulating cardiomyocyte structure and function. In this study, we utilise a self-assembling, fibril-forming peptide that displays integrin-binding activity. We demonstrate that the cell-binding properties of these fibril-forming, self-assembling peptides together with their substrate-adhesive properties presents them as an attractive scaffold for tissue engineering.

4.4.7 Clinical implications in modelling heart failure

This study implicates the ECM as a critical extracellular modulator of SR recruitment to cardiomyocyte Ca^{2+} cycling. Terracciano *et al*. previously showed that functional improvement of heart function in human patients treated with left ventricular assist devices is linked to a more efficient SR Ca^{2+} cycling (Terracciano *et al.*, 2004). We identify the integrin ligand-receptor interactions between the ECM proteins and cardiomyocytes as a potential target for modulation of SR recruitment to Ca^{2+} cycling.

It is important to remember that in many cardiac pathological conditions, fibroblast expansion and accumulation of ECM proteins is not the primary cause of disease, but represents activation of a reparative process in response to cardiomyocyte injury (Chen and Frangogiannis, 2013). In humans, repair of diseased myocardium requires generation of a well-organised scar. In this study, we have exploited the developing phenotype of hiPSC-CMs in culture, which reproduces, with low and poorly synchronised SR Ca^{2+} release and predominant sarcolemma Ca^{2+} cycling, the developing and diseased myocardium. By using hiPSC-CMs which rely on NCX-dominant Ca^{2+} cycling mechanisms, this study indicates that manipulating the composition of the integrin ligands in the ECM can be a target for future therapeutics aimed at recruiting the SR to Ca^{2+} cycling (Frangogiannis, 2008; Kong, Christia and Frangogiannis, 2014).

4.5 Summary

Ca^{2+} handling is a significant feature of electrophysiology that differs between human hiPSC-CMs and non-failing adult cardiomyocytes. The former reflects morphology and electrophysiology akin to neonatal cardiomyocytes or adult human cardiomyocytes in disease or in culture. We show that integrin ligands change hiPSC-CM Ca^{2+} handling and cellular morphology to closer reflect that of the adult cardiomyocytes; namely a more efficient SR-dominated Ca^{2+} cycling and a more rod-like morphology. It is essential to integrate all the aspects of electrophysiology and Ca^{2+} handling into a comprehensive model but this study shows the importance of understanding the role of integrin ligands, and more widely the role of ECM proteins, in modulating human cardiomyocyte structure and function.

5 Extracellular vesicle crosstalk between cardiac fibroblasts and cardiomyocytes

5.1 Introduction

In the previous chapter, we identified that integrin-mediated communications are a modality by which we can recruit the SR Ca^{2+} stores of hiPSC-CMs to Ca^{2+} cycling *in vitro*. This built on our findings in chapter 3 and published findings that cardiac fibroblasts induced more efficient Ca^{2+} cycling in hiPSC-CMs when the two cell types are co-cultured in direct contact (Kane and Terracciano, 2018). It is important to note that direct contact co-cultures, as well as allowing direct physical contact, allow close paracrine intercellular interactions. As we know cardiomyocytes and cardiac fibroblasts interact bi-directionally, the secretory profiles of cell populations may also change in direct contact co-cultures.

Much of the work investigating the intercellular interactions between cardiomyocytes and non-myocytes has investigated paracrine interactions that occur via a classic factor secretion-receptor binding modality (Cartledge *et al.*, 2015). In recent years, another way of cell-cell paracrine communication has been proposed: EVs, and in particular, exosomes (Vlassov *et al.*, 2012; Bang *et al.*, 2014). In this chapter, we investigate the potential that EVs have in the communication between cardiomyocytes and cardiac fibroblasts.

In this chapter, we compile a rapid ultrafiltration- and chromatography-based approach for EV isolation from biological samples (Lobb et al., 2015; Nordin et al., 2015; Benedikter et al., 2017). Since it is spin-based and dependent on size exclusion, the method has broad application with regards to sample volume and/or type, but for this project we focus on its use for isolating and purifying fibroblast-secreted EVs in order to understand the role they may have in the intercellular interactions between cardiomyocytes and cardiac fibroblasts.

5.2 Methods

5.2.1 Cell culture

WTC GCamp6f HiPSCs were differentiated into hiPSC-CMs and plated onto 35mm dishes with a 7 mm diameter glass bottomed-well as outlined in section 2.2.1. Cardiac fibroblasts were isolated from explanted human hearts as described in section 2.2.4.

5.2.2 Conditioned-media production and processing

Hyperflasks with cardiac fibroblasts were cultured with exosome-depleted fibroblast culture media for 48 hours. Conditioned media was collected and content was concentrated as described in section 2.2.6. Self-packed 30 cm Econo-Columns for SEC were prepared and packed as described in section 2.3.1 and used for purification of samples as described in section 2.3.2. Particle content were quantified by NTA as described in section 2.3.3, and protein quantification was carried out by using a micro-BCA protein assay kit as per manufacturer's instructions (Thermo Fisher Scientific).

It is important to consider that fibroblasts cultured *in vitro* are thought to display a secretory profile that is distinct from quiescent fibroblasts in the myocardium and active, disease-phenotype myofibroblasts. Conditioned media from fibroblasts negative for the marker of myofibroblast phenotype have been shown to increase adult rat Ca^{2+} transient amplitude, whereas the media from cultured fibroblasts and myofibroblasts from pressure-overloaded hearts reduced Ca^{2+} transient amplitude (Cartledge *et al.*, 2015). It is therefore important when interpreting the results of this study to consider that the conditioned media from these fibroblasts isolated from dilated cardiomyopathy patients and maintained for 3-7 passages in culture have different secretory profiles to the quiescent fibroblasts in the myocardium and acutely active diseased fibroblasts in the myocardium.

5.2.3 Presence of EV particles and protein markers

The morphology of cardiac fibroblast EVs eluting from the column were assessed by cryo-TEM (Cryogenic Transmission Electron Microscopy). Cryo-TEM sample preparation and imaging was performed by Dr. Ulrike Kauscher and Valeria Nele (both Imperial College

London). Immuno-gold localisation of CD63 in EM imaging was carried out by Padmini Sarathchandra (Imperial College London). Dot blot identified the presence of exosome markers CD9, CD63 and CD81 in fibroblast-conditioned media, standard fibroblast media and exosome-depleted fibroblast culture media as described in section 2.7.1 and dot blots were quantified using Image Studio Lite V5.2 software (LI-COR) as described in section 2.7.1.5.

5.2.4 EV treatment to hiPSC-CMs

hiPSC-CM monolayers were treated with fibroblast-secreted extracellular EVs as described in section 2.8.2 for 24 hours before electrophysiological assessment. Following culture, Ca^{2+} transients were visualised by optical mapping as described in section 2.9.1.

5.2.5 Cytokine array

The presence of cytokines in the EV fractions following SEC was assessed using a Proteome Profiler™ Human Cytokine Array Kit (R&D), UK). Supernatant samples were concentrated and incubated with the array kit antibody mixture as described in section 2.8.3. Bound complexes on the nitrocellulose membranes were detected by subsequent incubation in a Streptavidin-HRP secondary antibody at room temperature for 30 minutes. The membranes were developed with a chemiluminescent substrate and densitometric quantification performed using ImageJ.

5.3 Results

5.3.1 GW4869 attenuates fibroblast-mediated changes in Ca^{2+} transients

To first determine the contribution of exosomes, a subtype of EVs, in the intercellular crosstalk between cardiac fibroblasts and hiPSC-CMs *in vitro*, we utilised a chemical inhibitor of exosome generation. GW4869 inhibits exosome synthesis by blocking ceramide-mediated inward budding of MVBs and release of mature exosomes from MVBs.

We observed that GW4869 caused a reduction in the amplitude of hiPSC-CM Ca^{2+} transients (Fig 5.1A). This reduction in Ca^{2+} transient amplitude was also present when cardiac fibroblasts were in contact with the hiPSC-CM, as well as when contact co-cultures between hiPSC-CMs and cardiac fibroblasts were treated with GW4869. (**Figure 5.1A**). There is no significant difference between the three treatment groups. Direct co-culture conditions in chapter 3 did not cause any change in hiPSC-CM monolayers and we find a significant decrease here in fibroblast-hiPSC-CM direct contact culture. This may be due to differences in the experimental conditions – unlike chapter 3, all conditions in figure 5.1 had 0.1% DMSO in the serum-free media for the 24 hours before electrophysiological assessment. This could change fibroblast secretory or mechanical activity and further demonstrates that hiPSC-CMs are highly sensitive to their environment. The difference between control and GW4869-treated hiPSC-CMs in Fig 5.1A indicates that exosomes play a significant role in the cytosolic Ca^{2+} amplitude of hiPSC-CM populations but ceramide-mediated exosomes do not have a role in the cardiac fibroblast-mediated effects on Ca^{2+} transient amplitude.

Time to Ca^{2+} transient peak was not significantly changed with GW4869 treatment compared to control, but did show a slight decrease (**Figure 5.1B**). This decrease in time to peak could be accounted for by the GW4869-mediated reduction in amplitude – a reduced amplitude despite a consistent rate of CICR would lead to a reduced time to peak. Time to Ca^{2+} transient peak was significantly attenuated when cultured with cardiac fibroblasts – an observation also reported in contact co-culture studies in section 3 (Figure 3.1). This fibroblast-mediated abbreviation was significantly attenuated when exosome-inhibitor GW4869 was also present in the culture (**Figure 5.1B**– $p < 0.01$). This indicates that exosomes,

at least in part, mediate the abbreviation in time to Ca^{2+} transient peak observed in cardiac fibroblast-cardiomyocyte contact co-cultures.

We then measured the Ca^{2+} decay mechanisms to investigate the contribution of EVs to cytosolic Ca^{2+} removal in cardiac fibroblast-cardiomyocyte contact co-cultures. We identify that GW4869 application to hiPSC-CM monolayers does cause a slight attenuation of the fibroblast-mediated abbreviation the time to 50% decay (**Figure 5.1C**) and time to 80% decay (**Figure 5.1D**), but this was not significantly different from fibroblast-hiPSC-CM co-cultures in the absence of GW4869. This lack of EV contribution to the fibroblast-hiPSC-CM crosstalk is reflected in the rate of Ca^{2+} decay, which shows that fibroblast-mediated increase in hiPSC-CM Ca^{2+} transient decay is not significantly affected by fibroblast EVs (**Figure 5.1E**).

We demonstrate that EVs play a role in cardiac fibroblast-mediated abbreviation in Ca^{2+} transient time to peak. However, we also observe that EVs play a role in the Ca^{2+} transient amplitude in hiPSC-CM monolayers in the absence of any fibroblasts, indicating that exosomes play a critical role in hiPSC-CM Ca^{2+} availability. As intercellular crosstalk between these two cell types is known to be bidirection, changes in hiPSC-CM function due to GW4869 may affect cardiac fibroblast activity. The selectivity of GW4869 for certain pathways in EV production is also a limitation in attributing the effects of the chemical to complete EV cessation. We therefore then investigated the role of cardiac fibroblast-secreted EVs in modulating cardiomyocyte Ca^{2+} cycling.

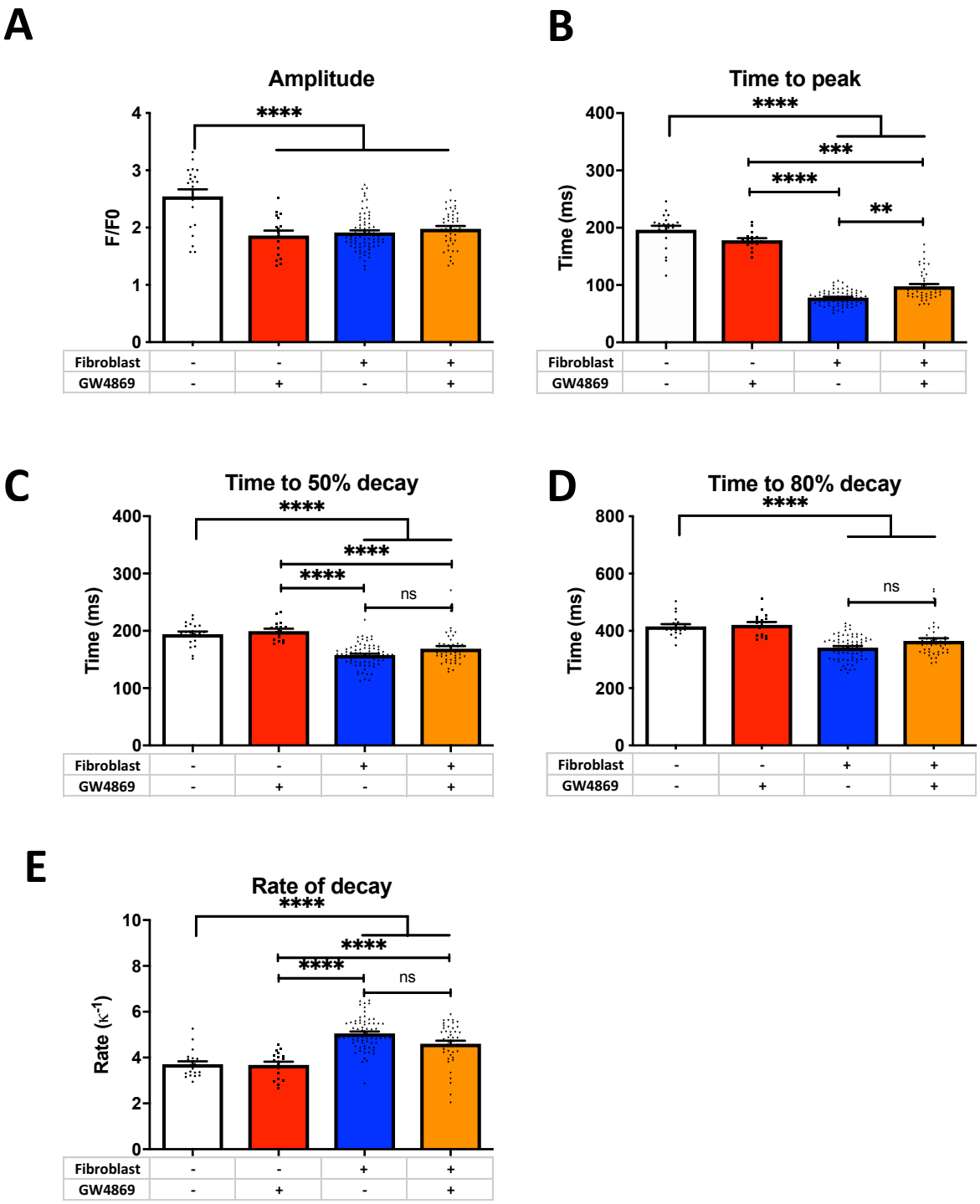

Figure 5.1 Exosome inhibition by GW4869 attenuates cardiac fibroblast-mediated increase in human cardiomyocyte Ca^{2+}-induced Ca^{2+}-release efficiency. *Human induced pluripotent stem cell-derived cardiomyocyte (hiPSC-CM) monolayers and hiPSC-CM-fibroblasts contact co-cultures were treated with exosome inhibitor, GW4869. Parameters measured were Ca^{2+} transient (A) amplitude, (B) time to peak, (C) time from peak to 50% decay, (D) time from peak to 80% decay. (E) Rate of decay was measured as 1/tau. Error bars represent SEM. n = number of cells from at least 3 preparations= 17-73. ** = p < 0.01, *** = p < 0.001, **** = p < 0.0001.*

5.3.2 Particle Isolation and purification by ultrafiltration and SEC

The most commonly used method for EV isolation is precipitation-based ultracentrifugation, but this has been criticised for producing EV samples that have high contamination from soluble content (Lobb *et al.*, 2015; Gudbergsson *et al.*, 2016). Practically, ultracentrifugation is also resource- and time-intensive for repeated isolations. In this project, we utilise ultrafiltration and SEC-based EV isolation, which is widely agreed to be more robust in producing EV samples with lower amounts of contaminating proteins but this technique does require more initial validation (Nordin *et al.*, 2015; Gámez-Valero *et al.*, 2016; Mol *et al.*, 2017). Fibroblast EVs were collected from hyperflasks of human cardiac fibroblasts maintained for 48 hours in exosome-depleted serum-containing media, as described in Methods section 2.6.1. Samples were then subjected to ultrafiltration and SEC as described in 2.6.2-2.6.6. The elution produced by SEC using a self-packed 28 x 1 cm chromatography column was collected as 30 individual 1mL fractions. In SEC, the larger particles are unable to enter the column beads so elute in earlier fractions and smaller, soluble proteins are held within the beads, taking the tortuous route so requiring longer to elute.

SEC has been shown to present a characteristic profile of protein content with two peaks – one smaller, earlier peak high in EV content, and a much larger peak consisting of soluble protein contaminants. We therefore first validated the efficiency of SEC for particle separation by quantifying the protein content in each SEC fraction using a micro-BCA assay. From this, we reproducibly identified a protein profile with two distinct peaks. One smaller peak in protein content, thought to be the EVs, was consistently found at fraction 8 and a much larger peak composed of soluble contaminating proteins that eluted at fraction 21 (**Figure 5.2A**). This does not confirm the presence of EVs in our earlier fractions so we then investigated the presence of particles with EV morphology and expression of markers.

EVs have a diameter ranging from 30-1000nm so we utilised NTA to analyse the distribution of particles in the SEC fractions. Fractions 4-13 were analysed as these have been shown to be the fractions with the highest purity of EVs. Fractions outside of this range were excluded because no EV content is expected in fractions 1-5 as this represents the column void volume and there are high levels of contaminating proteins in fractions greater than 13. Fractions 7-13 show particle content with a modal distribution between 50-150nm, within the expected range for EVs.

There are low levels particles detected to have a diameter greater than 200nm. This could be accounted for by the aggregation of EVs, which has been reported to occur over time, without affect EV activity. When plotting the EV concentration against the protein content, there is a clear peak of particle-associated protein at fraction 8. Representative elution profiles are shown in figure 5.2.

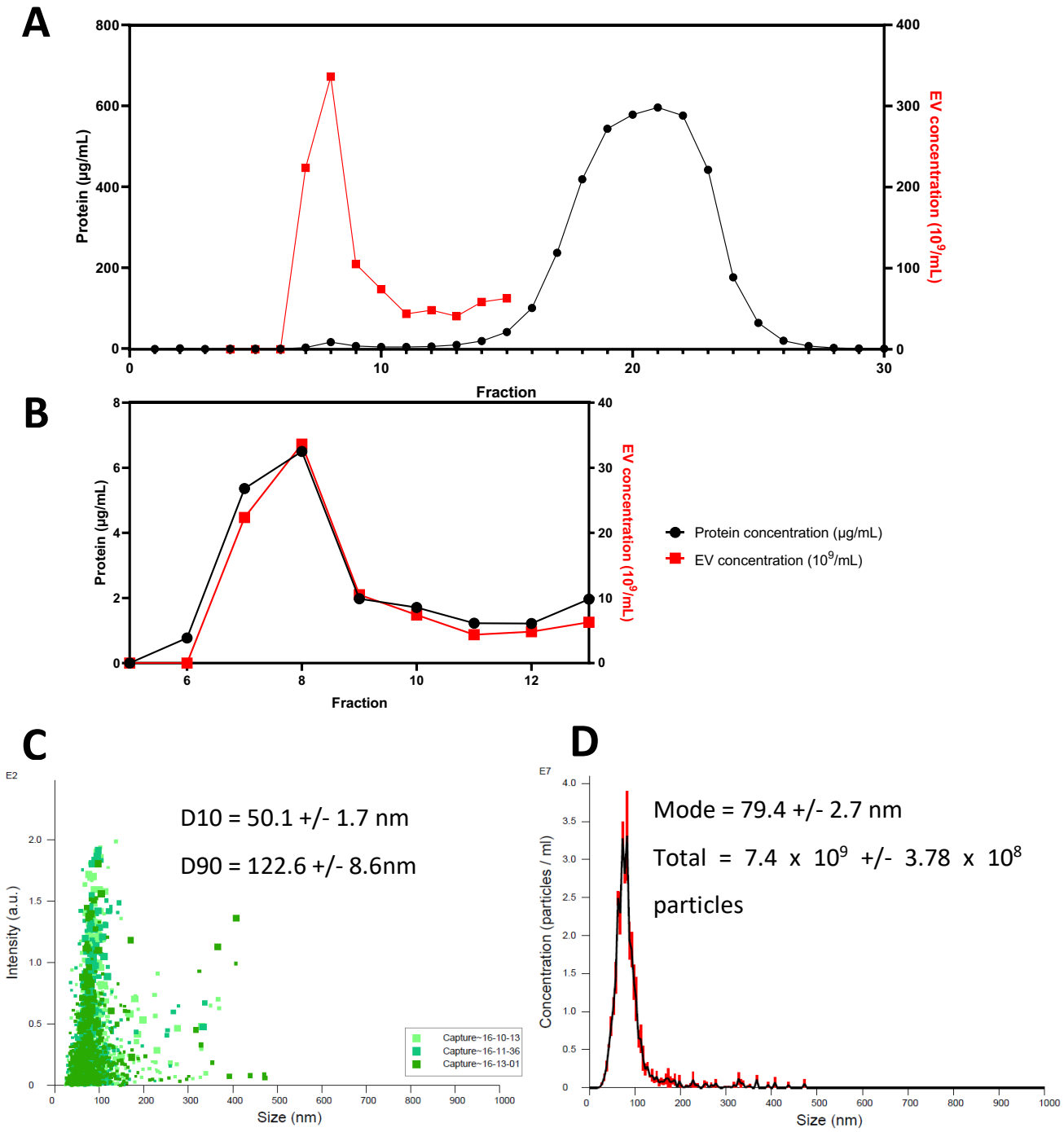

Figure 5.2 Elution profile of fibroblast extracellular vesicles from size-exclusion chromatography and particle concentration*. (A) Following size exclusion chromatography (SEC) of fibroblast extracellular vesicle (EV) samples into 30 fractions of 1mL, micro-BCA assay quantified protein content of the fractions (black) (N=4, n = 4). Nanosight NS300 with a 532 nm laser measured particle concentration in fractions 5-13 (red) (N=1, n = 1). (B) Zoomed in distribution of SEC fractions 5-13. (C) and (D) Representative Nanocyte Tracking Analysis (NTA) detection of particles in fraction 10 with a 1:25 dilution. Total particle count was calculated as NTA particle count multiplied by 25 to account for the dilution (N=1, n = 1 for B-D).*

5.3.3 Direct correlation between protein weight and particle concentration

Studies that use EV treatments quantify the sample content by using particle concentration or protein content. The variety of EV isolation and purification techniques together with the high levels of impurities with the most common technique, ultracentrifugation, makes the inconsistencies in EV studies a significant caveat when interpreting studies. The ratio of particle concentration to protein concentration was proposed by Webber and Clayton to be a good reference for assessing sample purity (Webber and Clayton, 2013). The ratio of particles to protein content in our isolation technique was detected as 4.67 x 10^9 particles/µg of protein (**Figure 5.3**), considered to be of intermediate purity by the standards set out by Webber and Clayton. By plotting the two values against each other for fractions 7-12 from the SEC elution, we identify that the two values are closely correlated (r^2 = 0.9581). This close correlation indicates that the two values can be used interchangeably.

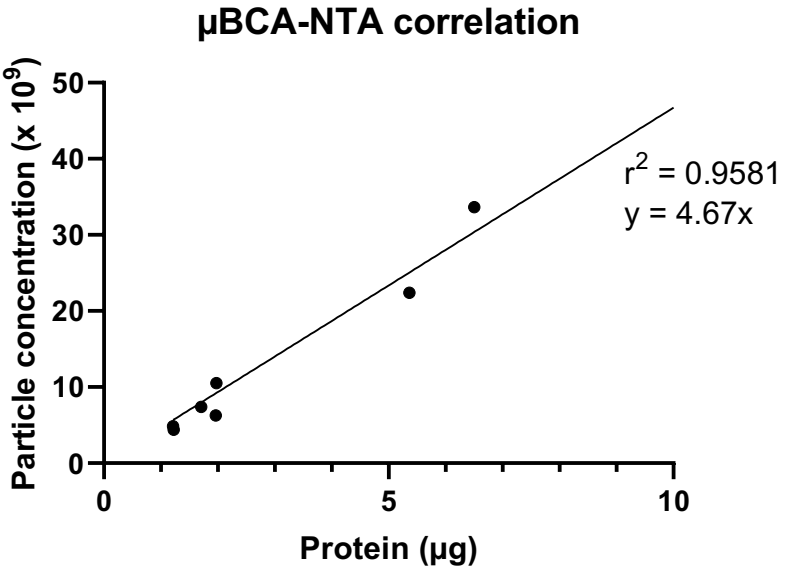

Figure 5.3 Correlation between particle concentration and protein content in fibroblast extracellular vesicle samples following size exclusion chromatography*. Following SEC, the particle concentration and protein content in fractions 7-12 were plotted and a line of best fit blotted to identify the correlation. Straight line of best fit identifies the presence of 4.67 x 10^9 particles/µg of protein (N=1, n = 1).*

5.3.4 Electron Microscopy of chromatography-purified EVs

The morphology of particles eluting from the column were assessed by cryo-TEM to identify the presence of cardiac fibroblast EVs. Cryo-TEM sample preparation and imaging was performed by Dr. Ulrike Kauscher and Valeria Nele. Cryo-TEM imaging shows liposome-like particles vesicles between 50-200 nm diameter (**Figure 5.4**). This indicates the presence of exosomes and microvesicles. Alternatively, exosomes may merge to form larger lipid structures. Nevertheless, we identify the presence of lipid structures with the characteristic EV morphology in the fibroblast-conditioned media.

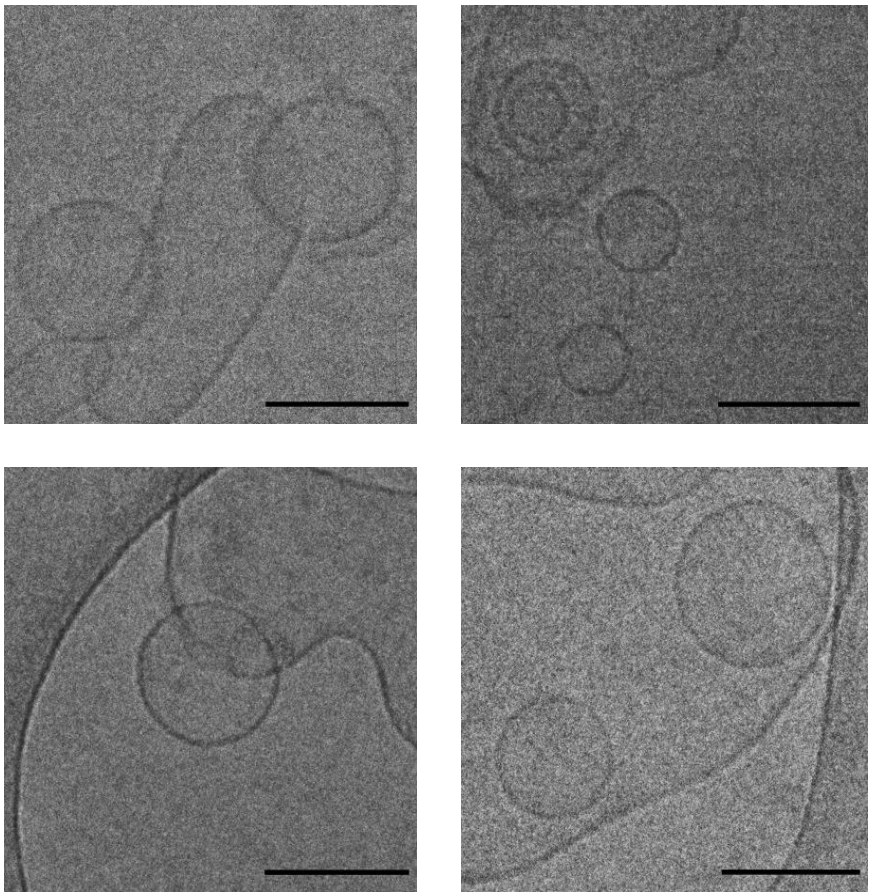

Figure 5.4 Transmission electron microscopy (TEM) of size exclusion chromatography (SEC)-purified fibroblast extracellular vesicles (EVs)*. Fibroblast EV samples were purified by SEC then prepared for TEM as described in methods. Scale bar = 200nm. TEM was performed by Dr. Ulrike Kauscher.*

5.3.5 Expression of EV markers CD9, CD63 & CD81

So far, we observed liposome-like particles of the characteristic EV structure to elute from SEC. It was important to validate these liposome-like particles as EVs by confirming the presence of EV marker proteins. Immunogold-EM of EV marker CD63 in SEC fraction 8 identified that the lipophilic particles with EV characteristic morphology had high expression of EV marker CD63 (**Figure 5.5A**). This does not quantitatively measure the expression of EV markers in the SEC fraction and is low throughput in measuring the presence of EV markers. We therefore carried out dot blot of the 30 individual 1 mL elution fractions following SEC, probing for EV markers CD9, CD63 and CD81. All fractions from SEC were prepared for dot blot as described in materials and methods section 2.7.1.

For markers CD9 and CD81, the highest signal intensity was detected in fraction 8 (**Figure 5.5B**). This fraction was shown by the NTA and microBCA to have the highest particle and protein content, respectively (Figure 5.2A). The finding that CD63 is most highly expressed in fraction 11 indicates that the expression of the three EV markers is not homogenous within the EV population, such that there are subpopulations of EVs that highly express CD63 that are a different size to the EVs with high CD9- or CD81-expression. As the highest expression of CD63 was in a later SEC fraction than CD9 or CD81, the dot blot indicates that the subpopulation with high CD63 expression are smaller than those with high CD9 or CD81 expression.

The cardiac fibroblast EVs were collected in exosome-depleted serum. The absence of EV markers in the serum is shown in **Figure 5.5C-E** – the expression of EV markers were no more than 2 SDs away from the mean in any of the SEC fractions, except for CD9 in Fraction 8 and CD81 in Fraction 29, but these may be attributed to the low N number (2), which causes a low power and high variability. The presence of the peak expression of EV markers CD9, CD63 and CD81 in SEC fractions 8-12 can therefore be attributed to fibroblast-secreted EVs.

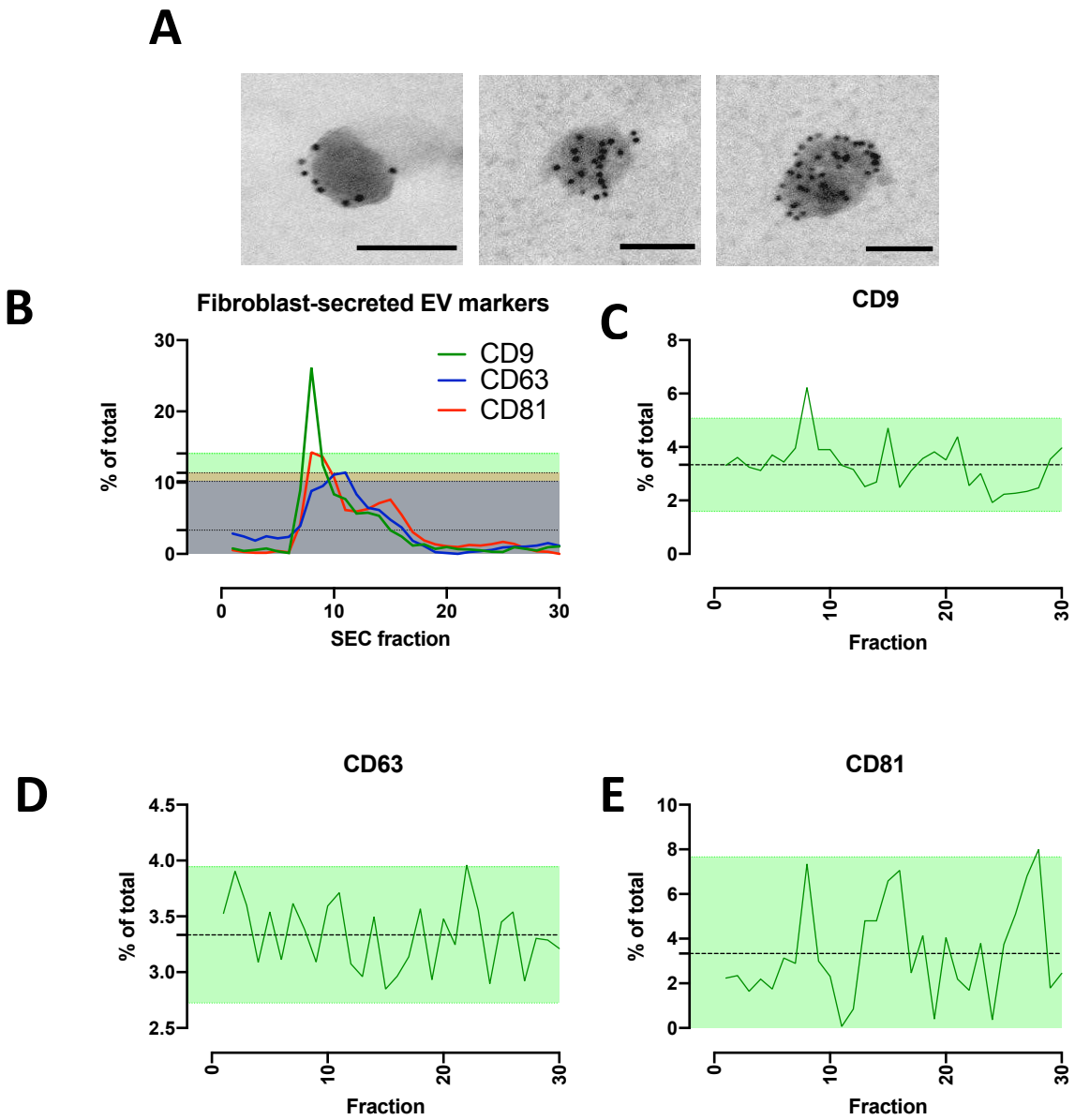

Figure 5.5 Expression of extracellular vesicle (EV) markers of size exclusion chromatography fractions from fibroblast-conditioned media, exosome-depleted and standard FBS. Immunogold-EM tagging for CD63 identified lipophilic particles with high CD63 expression. Representative images shown in (A). Scale bar = 100nm. (B) Quantification of dot blots of fibroblast-secreted EV samples against CD9, CD63 and CD81 as percentage of total signal. N = number of preparations = 2. (C-E) Expression of exosome markers in exosome-depleted serum-containing fibroblast media without fibroblast-conditioning. Shaded area represents 2 standard deviations from the mean (3.33). N = 2 preparations.

5.3.6 Fibroblast EVs abbreviate hiPSC-CM Ca^{2+} transient time to peak

Having determined that the fractions with high EV content are fractions 7-9, the content in these fractions were applied to hiPSC-CM monolayers to assess the effect on hiPSC-CM Ca^{2+} cycling. The Ca^{2+} transients were compared against serum-free conditions, which is known to not have any EV or serum content, and the EV-depleted serum-containing media that is used to collect fibroblast EVs. This is to identify if the non-EV content of FBS serum could account for changes in Ca^{2+} cycling. We identify that there was no change to Ca^{2+} transient amplitude caused by EV-depleted serum-containing media in the presence or absence of fibroblast-conditioning (**Figure 5.5A**).

Ca^{2+} transient time to peak was significantly abbreviated by application of 120µg of fibroblast EVs compared to serum-free control (**Figure 5.6B**). However, we identify that the serum-containing control also caused an abbreviation in time to peak. Despite this, the abbreviation in time to peak was still significantly reduced by the presence of fibroblast-secreted EVs.

We also investigated the time from the Ca^{2+} transient peak to 50% decay (**Figure 5.6C**) and 80% decay (**Figure 5.6D**). We identify that, compared to serum-free control, 120µg of fibroblast-secreted EVs caused a significant abbreviation in both. However, this abbreviation could be accounted for by the exosome-depleted serum, as there was no difference between the fibroblast-secreted EV condition and exosome-depleted serum condition.

We therefore identify that Fibroblast EVs could account for an abbreviation in time to peak when collected in EV-depleted serum, but changes in decay are accounted for by non-EV serum content. This demonstrates the importance of appropriate control when determining EV-mediated effects.

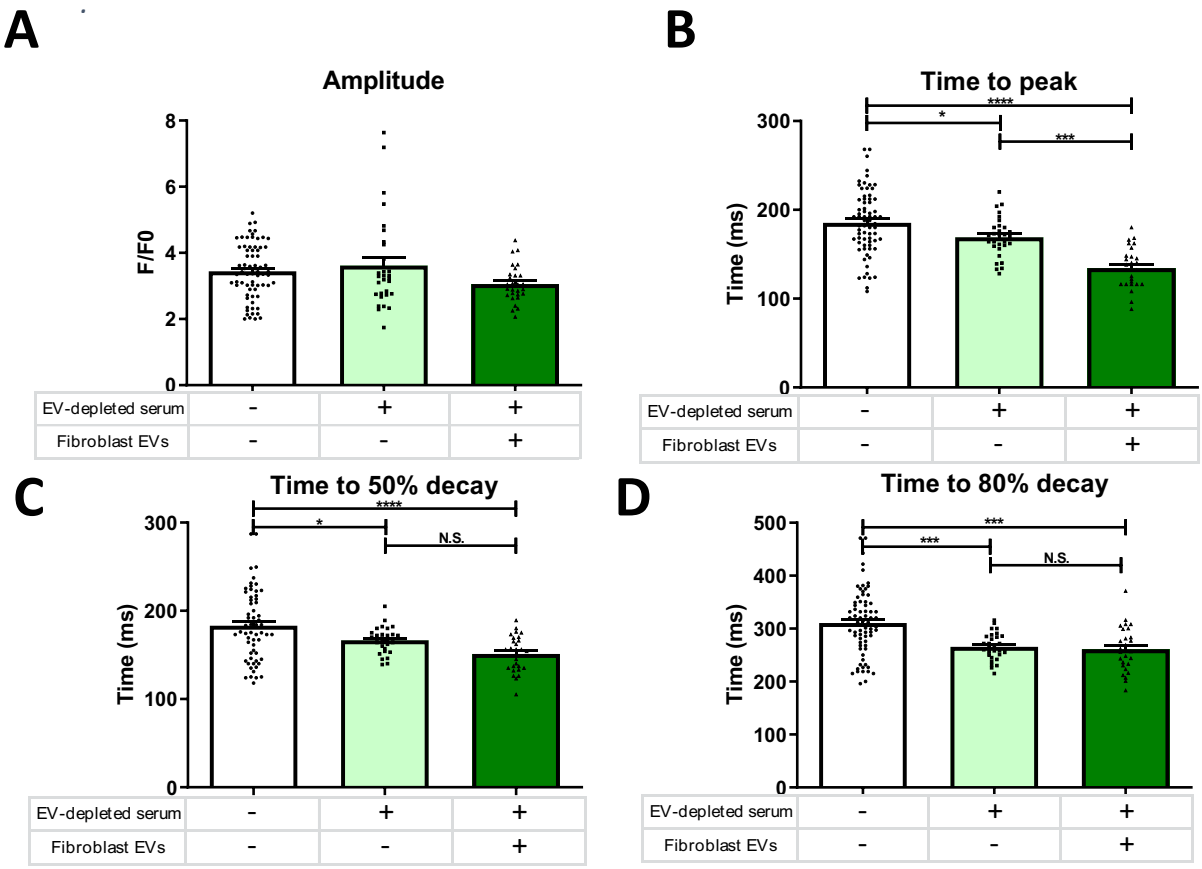

Figure 5.6 Modulation of human cardiomyocyte Ca^{2+} cycling by fibroblast-secreted extracellular vesicles*. Human induced pluripotent stem cell-derived cardiomyocyte (hiPSC-CM) monolayers were maintained for 24 hours in culture media consisting of serum-free media (white bar), media containing 1% Exosome-depleted serum without fibroblast conditioning (light green), or media containing 1% Exosome-depleted serum conditioned with cardiac fibroblast-secreted extracellular vesicles (EVs) (150 µL) (dark green). Ca^{2+} transient parameters measured were Ca^{2+} transient (A) amplitude, (B) time to peak, (C) time from peak to 50% decay, (D) time from peak to 80% decay, Error bars represent SEM. N = 4 preparations, n = 17-73 number of cells. * = p < 0.05, *** = p < 0.001, **** = p < 0.0001.*

5.3.7 ECM protein fibronectin in EV-concentrated SEC fractions

We demonstrate in the previous chapter that integrins modulate cytosolic Ca^{2+} transients in hiPSC-CMs. Dot blots of SEC fractions show a distribution of fibronectin in the dot blots with two peaks, similar to the microBCA assay reported in figure 5.2. This distribution is shown in **figure 5.7**. As expected, there is a large peak in fibronectin detected in the soluble contaminant fractions from fractions 13 onwards. We also identify a smaller peak at fractions 9-10. Future studies must identify the presence of these ECM proteins on the EVs but this does indicate that fibronectin may be associated with fibroblast EVs.

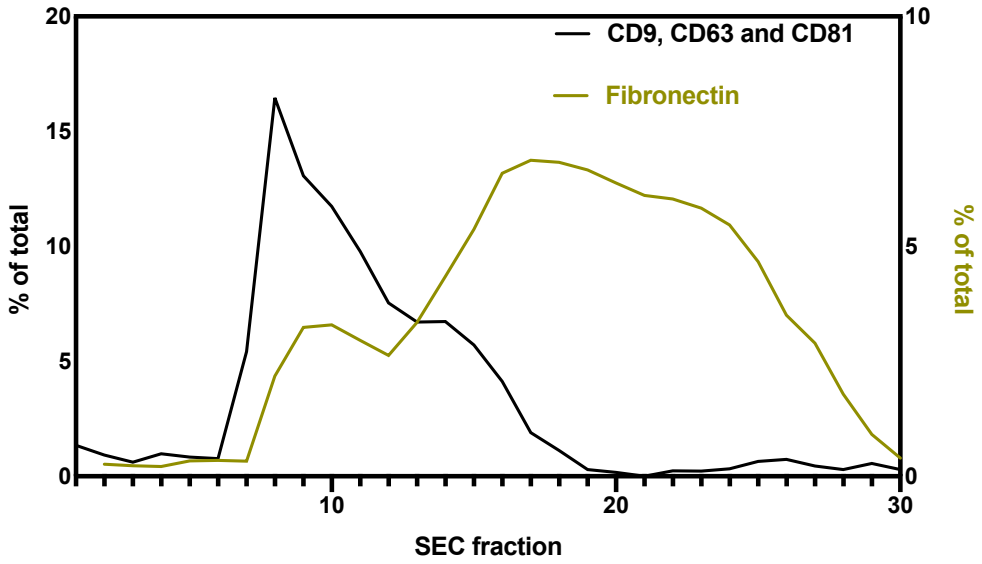

***Figure 5.7 Presence of fibronectin in extracellular vesicle fractions**. Expression of exosome markers CD9, CD63 and CD81 (black line) and fibronectin (green line) from fibroblast-conditioned media after separation by size exclusion chromatography (SEC) into 30 consecutive 1mL fractions. Small fibronectin peak around SEC fractions 8-10 before higher expression of fibronectin in the fractions with numerous soluble contaminants (fraction 13-28). N = number of preparations = 6 for EV markers and 2 for fibronectin.*

5.3.8 EV content – CCL5 and CXCL12/SDF-1

To identify potential factors in the EVs that may be involved in fibroblast-CM signalling, the EV fractions were assessed with a cytokine profiler array as described in Methods section 2.8.3. SEC fractions 7-11 were combined and the EV content was lysed with RIPA buffer treatment and sonication before array assessment. Two cytokines were identified as being present in the cardiac fibroblast EVs – CCL5 and CXCL12/SDF1 (**Figure 5.8**). Time constrain prevented assessment of the effects of these cytokines on the hiPSC-CMs and future studies on these effects are warranted.

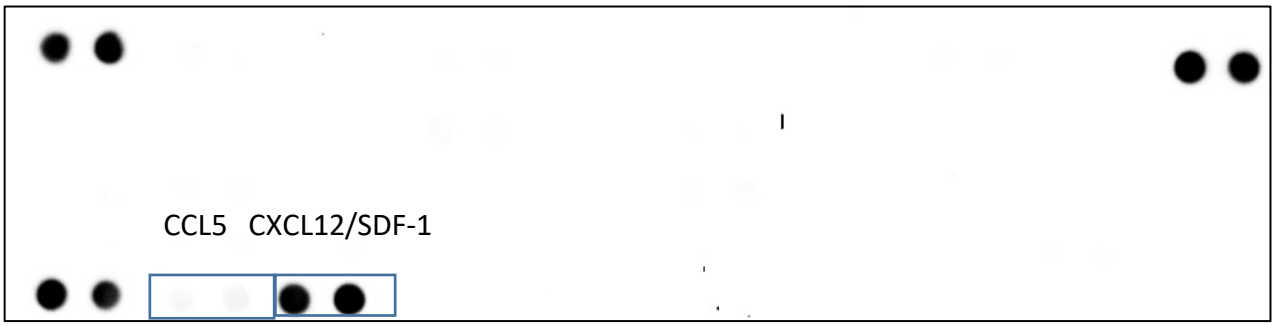

Figure 5.8 Fibroblast extracellular vesicle content screening for cytokines*. Example image of cytokine array positive for CXCL12/SDF-1. Non-boxed dots are reference spots to align the transparency overlay demonstrate and also to indicate that the array has been incubated with Streptavidin-HRP during the assay procedure.*

5.4 Discussion

In this chapter, we identified a role for EVs in the intercellular crosstalk between cardiac fibroblasts and hiPSC-CMs *in vitro*. We identified that chemical inhibition of ceramide-mediated exosome production by GW4869 attenuates the cardiac fibroblast-mediated abbreviation in hiPSC-CM Ca^{2+} transient time to peak, implicating these exosomes in the intercellular crosstalk between cardiac fibroblasts and hiPSC-CMs. We validated a technique for purification of EVs from cardiac fibroblast-conditioned media, utilising a combination of ultrafiltration and SEC. These cardiac fibroblast EVs have high expression of cytokine CXCL12. The purified fibroblast-secreted EV samples, when compared to serum-free controls, caused a significant abbreviation of hiPSC-CM Ca^{2+} transient time to peak and time to decay. However, much of the abbreviation in time to decay can be contributed to non-EV serum content. This is an important caveat when interpreting EV studies, which is still yet to demonstrate a standardised isolation technique.

5.4.1 Exosome inhibition by GR4869 in co-culture

We investigated the role of exosomes in cardiac fibroblast-hiPSC-CM direct contact co-cultures by using the chemical inhibitor of ceramide-mediated exome release, GW4869. We identify that 20 μM GW4869 causes a significant attenuation in the abbreviation in Ca^{2+} transient time to peak induced by cardiac fibroblast co-cultures. This concentration is in line with previous studies that use the compound as a chemical inhibitor of N-SMase activity to inhibit EV production (Essandoh *et al.*, 2015; Park *et al.*, 2018). However, there are criticisms to the use of GW4869 as a chemical inhibitor of exosome release. The effect of this concentration of GW4869 has, to the best of the author's knowledge, not been formally assessed for hiPSC-CMs or cardiac fibroblasts. There are reports that the compound also interferes with apoptosis pathways, interfering with the production of EVs produced by apoptotic bodies, in addition to the microvesicles and exosomes studies here (Park *et al.*, 2018)

GW4869 is used to inhibit the ceramide-mediated inward budding of MVBs and release of mature exosomes from MVBs, but not all exosome synthesis is ceramide-mediated (X. Wang *et al.*, 2014). As described in Chapter 1, exosomes are generated by a complex, multi-step process, progressing from the invagination of late endosomal vesicles, which capsulates cytosolic content into internal vesicles, to the production of MVBs. This process can occur by three different mechanisms: either ESCRT (Endosomal sorting complexes required for transport)-dependent, ceramide-dependent or tetraspanin-dependent mechanisms. Blocking of ceramide-mediated activity does not therefore show us the complete effects of exosome inhibition.

In addition, some studies that have investigated the effects of ceramide formation have shown that inhibition of ceramide formation does not affect exosome secretion (Phuyal *et al.*, 2014). Similarly, inhibition of neutral sphingomyelinase 3, an enzyme that catalyses the formation of ceramide from sphingomyelin, has been shown to not inhibit the secretion of exosomes in PC-3 (Phuyal *et al.*, 2014). One explanation could be that GW4869 is ineffective in blocking ceramide-mediated exosome production.

Alternatively, the hiPSC-CMs and cardiac fibroblasts may combat the chemical inhibition of ceramide-mediated exosome synthesis by upregulating other pathways of exosome production. This is important to consider as there is evidence that the pathway of exosome production affects the cargo content. A study by Colombo et al identified that silencing of the ESCRT gene causes a reduction in EV secretion but changed the content of the EVs that remained (Colombo, Raposo and Théry, 2014). There were similar findings when ceramide-synthesis was inhibited (Trajkovic *et al.*, 2008) or when the expression of tetraspanins is changed (Nazarenko *et al.*, 2010). Therefore, a possible effect of GW4869 treatment is that alternative pathways are upregulated, changing the secretory profile of the EVs.

In addition, cardiac fibroblasts and cardiomyocytes may rely on microvesicles, rather than exosomes, as the predominant EV subtype for intercellular communication. The exact mechanisms of EV production and secretion are still poorly understood and it is not clear why different cell types would be dependent on different mechanisms or whether multiple mechanisms may act simultaneously. The notion that microvesicles are the EV subtype preferentially released from fibroblasts is supported by the cryo-TEM images. Microvesicles are larger than exosomes – exosomes exist as lipid structures between 30-150nm in diameter,

whereas microvesicles have been reported to be 100nm-1µm in diameter. Lipid structures between 80-200nm in diameter were identified in EMs, indicating that microvesicles are a prominent EV subtype secreted by cardiac fibroblasts. The mechanisms of microvesicle formation and release are even less understood than exosomes. The pathway is known to require molecular machinery that is common to other endolysosomal and intracellular pathways – including the rely on Rab-family GTPases, Snare-family membrane-fusing proteins and the cytoskeleton (actin and myosin, and microtubules and kinesins) (Cai, Reinisch and Ferro-Novick, 2007). It is therefore very difficult to target these pathways without having deleterious effects on hiPSC-CMs or cardiac fibroblasts. It is therefore clear that although GW4869 can be used as a chemical inhibitor of some EV production pathways, possible off-target effects of the chemical, as with any other chemical inhibitor without a fully delineated activity pathway, could mediate the effects seen.

5.4.2 Purification technique – Ultracentrifugation vs chromatography and Ultrafiltration

When considering EV isolation techniques, it is important to note that the choice of isolation method impacts the purity and yield of collected EV samples (Nordin *et al.*, 2015; Gámez-Valero *et al.*, 2016; Li *et al.*, 2017). Before 2015, ultracentrifugation was used in 90% of studies with EV isolation (Gudbergsson *et al.*, 2016). This EV isolation procedure generate higher yields than the more labour-intensive procedures, but the resulting sample purity is often compromised due to the presence of abundant contaminating proteins. Furthermore, this procedure often also causes extensive damage to the EVs (Webber and Clayton, 2013). Ultracentrifugation also demonstrates very low reproducibility compared to other emerging techniques (Thery *et al.*, 2006; Livshts *et al.*, 2015). As a result, the proportion of studies utilising ultracentrifugation dropped to 62.1% of studies between 2015-2018. Only 44.9% of studies during this period utilise ultracentrifugation as the sole isolation technique without incorporating modifications (Lobb *et al.*, 2015; Monguió-Tortajada *et al.*, 2019).

In this project, we setup and used a method based on ultrafiltration followed by SEC. It is difficult to quantify EV content in samples, as the presence of EV markers does not quantitatively determine EV content, but we have been able to demonstrate that vesicles can be purified from human cardiac fibroblast-conditioned media by Sepharose CL-2B SEC.

Studies have reported a lower quantity of exosome proteins recovered using ultrafiltration and SEC techniques compared to ultracentrifugation, but SEC is credited to form very pure samples compared to ultracentrifugation (Salih, Zietse and Hoorn, 2014; Lobb *et al.*, 2015; Taylor and Shah, 2015).

The principle of SEC is separation of proteins based on difference in size. The Sepharose beads packed into the column have pores with a diameter of approximately 75 nm (Hagel, Ostberg and Andersson, 1996) and a tortuous path through the beads. An increased path length for particles that can enter the beads delays the point at which they elute at the bottom of the column. All particles larger than 75nm, including exosomes, cannot enter the beads so only travel along with the void volume fluid, eluting in the earlier fractions than the proteins that enter the beads. Based on our NTA results, the largest size of particles in the lowest decile (D10) for fractions 7 and 8, have a diameter of 97.9 ± 2.2 and 80.6 ± 2.2nm, respectively. Fraction 8 also showed the highest CD9 and CD81 content by dot blot, which coincides with the highest EV fractions. SEC fraction 9 has a D10 of 54.3 ± 0.3 nm, and this decreases as the fraction number increases. This confirms the theoretical separation of components above and below 75nm in diameter into fractions 7-8, and 9 onwards, respectively. The finding that the highest expression of exosome marker CD63 is in Fraction 12 indicates that there are exosomes present in fractions 9 onwards, and CD63 may be a marker for smaller EVs than those expressing CD9 and CD81. This demonstrates the importance of using several markers when identifying the presence of EVs.

5.4.3 EV isolation purity

The quantification of EV markers does not provide a measure of EV content, as there are no consistencies in EV marker expression on exosomes. Webber and Clayton proposed an integration of quantification methods to assess the purity of samples following EV purification, by calculating the ratio of particle concentration to protein concentration (Webber and Clayton, 2013). Less stringent purification methods produce samples with fewer particles per µg of protein, as these methods are unable to remove all contaminating proteins. They proposed that samples with 3×10^{10} particles/ µg or greater should be considered highly pure, samples with less than 1.5×10^{9} particles/ µg are to be considered impure, and samples with particle counts per µg of protein between these values are of intermediate purity. In our

study, the ratio was detected as 4.67 x 10^9 particles/µg of protein, indicating an intermediate purity. It is important to consider that this ratio may vary between cell lines. However, this does provide a useful reference point and as the ultrafiltration-SEC system has already been validated, this ratio was not considered a cause for concern.

5.4.4 Cardiac fibroblast EVs and their role in paracrine signalling

We investigated the effects of fibroblast-secreted EVs on hiPSC-CM Ca^{2+} cycling. Hyperflasks of cardiac fibroblasts were maintained in exosome-depleted serum-containing fibroblast media for 48 hours. Foetal bovine serum has vast amounts of EVs so we utilised a commercially-available FBS that has undergone EV depletion. Serum was present during the exosome-isolation period, rather than maintaining the cardiac fibroblasts in serum free media, because serum starvation may have led to cell stress. Cell stress has been shown to induce phenotypic changes that are reflected in the content of EVs (de Jong *et al.*, 2012).

Furthermore, cardiac fibroblasts were maintained throughout culture and passaging in the presence of serum in the culture media. An abrupt change in culture conditions induces changes in cardiac fibroblast metabolism (Pirkmajer and Chibalin, 2011). As cellular stress and changes in metabolism can be reflected in the EVs, any functional characterisation of EVs collected in serum-free conditions would have been affected and therefore not reflected the native cardiac fibroblast secretory profile.

We also maintained serum content to maintain a relatively high level of EV release. The health of cardiac fibroblasts in culture is reflected in their secretory profile. Comparing the protein yields from studies that use EV-depleted serum and studies that abruptly changed culture media to serum-free conditions showed that studies using EV-depleted serum reported a significantly higher average yield than the serum-free conditions (Gudbergsson *et al.*, 2016). This indicates that starved cells secrete fewer EVs and changes the secretome.

5.4.5 Effects of cardiac fibroblast EVs on CICR but none on removal of cytosolic Ca^{2+}

We identify that although the majority of the effect in conditions with fibroblast-secreted EVs can be attributed to non-EV content of serum, there is a significant abbreviation

in time to peak induced by the presence of fibroblast EVs. The plethora of bioactive content that have been identified in EVs makes it difficult to discern the factors that are significant in this abbreviation. However, it does show that the mechanisms that affect CICR and Ca^{2+} removal are independent, such that cardiac fibroblast EVs can increase CICR efficiency, without causing a significant change in the Ca^{2+} removal mechanisms.

Exogenous stimulation of cells is known to alter their phenotype, including their EV secretome. As we now know that cardiac fibroblasts and cardiomyocytes interact in a bidirectional manner, such that cardiac fibroblast secretory profile is influenced by cardiomyocytes, the cardiac fibroblast EVs may be different to those secreted when cardiac fibroblasts are in direct contact co-culture with hiPSC-CMs. To date, there is no way to independently inhibit the EV secretion from one cell population in co-culture setups. Proteomics and transcriptomic profiling of EVs are dependent on method of isolation (Eldh *et al.*, 2012; Yáñez-Mó *et al.*, 2015) and many –omics studies of vesicular content draws conclusions from a single replicate. Therefore, the abbreviation of hiPSC-CM Ca^{2+} cycling following the application of the fibroblast EVs does rely on the assumption that these EVs are representative of those in co-culture.

5.4.5.1 Bioactive components of fibroblast EVs

We explored possible cargo that could mediate the fibroblast EV effect on hiPSC-CM Ca^{2+} cycling. Fibronectin and other ECM proteins have been identified on circulating EVs and this may be a mechanism by which fibroblast-derived ECM proteins may interact with cardiomyocyte integrins (Purushothaman *et al.*, 2016). The EV cargo can also be taken up by recipient cells following initial membrane recognition between the EV and cell surface. We identified one chemokine in the EV fractions – namely, CCL5 and stroma-cell-derived factor-1α (SDF-1α)/CXCL12.

CCL5 is a pro-inflammatory chemoattractant for monocytes and neutrophils (Yabluchanskiy *et al.*, 2016). The effect of CCL5 on cardiomyocytes is unknown. Future studies could identify the effects this proinflammatory factor may have on cardiomyocyte function. This indicates that fibroblast EVs are a source of pro-inflammatory chemokines to recruit inflammatory cells but there is no evidence that the chemokine plays a direct role in modulating hiPSC-CM Ca^{2+} cycling.

CXCL12 has been identified as a cardio-protective chemokine, acting through its G-protein coupled receptor CXCR4. Treatment of rat neonatal cardiomyocytes with CXCL12 increased cytoplasmic Ca^{2+} release and increased cardiomyocyte beating frequency in an IP_3-dependent manner (Hadad *et al.*, 2013). In vivo, treatment of rats with CXCL12 increased left ventricular dP/dtmax, suggesting that CXCL12 plays a positive chronotropic and ionotropic effect (Hadad *et al.*, 2013). In this manner, cardiac fibroblasts may mediate the abbreviation in hiPSC-CM Ca^{2+} transient time to peak, but this is to be determined in future studies. In a murine study investigating the role of CXCL12 and its receptor CXCR4 in inflammation, they identified that the presence of AMD3100, a specific CXCR4 inhibitor, abrogated the reduction in calcium transient amplitude and resultant negative inotropic effect of CXCL12 (Pyo *et al.*, 2006).

The role of CXCL12 in normal heart function has been investigated in animal studies. In isolated adult rat cardiomyocytes, CXCL12 treatment prevented isoproterenol-induced hypertrophy and interrupted the calcineurin/NFAT pathway (Larocca *et al.*, 2013). Cardiac-specific knockout of CXCR4 in mice led to significant hypertrophy and cardiac dysfunction in an isoproterenol-induced heart failure model (Larocca *et al.*, 2013). Even in models without exogenous stress, cardiomyocyte specific-CXCR4 knockout (CXCR4 cKO) mice demonstrated a progressive cardiac dysfunction leading to cardiac failure (LaRocca *et al.*, 2019). These CXCR4cKO mice had significant tissue fibrosis vs. wild-type, indicating that CXCR4 function plays a role as a negative regulator for cardiac fibroblast proliferation and secretory activity (LaRocca *et al.*, 2019). These indicate that CXCR4, a cytokine we have identified to be released by the cardiac fibroblasts, plays a non-developmental role in regulating normal cardiac function and is vital in prevention of progression to clinical heart failure.

Although we have identified a role for the fibroblast EVs in in vitro co-cultures with hiPSC-CMs, the relevance of these EVs *in vivo* is yet to be determined. To date, we have been unable to accurately determine the relevant levels of EVs or these chemokines in vivo. However, the finding of EV mediated effects in vitro and the presence of these cytokines may suggest a role for these factors in vivo, and warrants further investigations.

5.5 Summary

We validated an effective EV isolation and purification protocol. Assessment of the contribution of fibroblast EVs to hiPSC-CM monolayers and using a chemical inhibitor of exosomes in cardiac fibroblast-hiPSC-CM co-cultures indicate that fibroblast EVs are involved, at least in part, in the abbreviation of hiPSC-CM Ca^{2+} transient time to peak, indicating an abbreviation in CICR efficiency. Experimental techniques that do not consider the non-EV serum content of culture media could lead to misleading results and erroneous identification of EVs as major signalling effectors. Further research could clarify if these results are limited to the in vitro studies or are more widely relevant within the native myocardium.

6 Conclusions and future perspectives

This chapter provides suggestions for future investigations and provides a summary of the conclusions of the study, including recommendations for the field.

6.1 Highlights

- Reconfigurable, elastic PDMS co-culture substrate used to identify a spatial relationship of interactions between cardiac fibroblasts and hiPSC-CMs

- Integrin ligands induced functional recruitment of the SR Ca^{2+} stores to increase hiPSC-CM Ca^{2+} cycling efficiency

- Fibril-forming, self-assembling peptides with cell- and substrate-binding properties induce SR recruitment without cell detachment from substrate

- ultrafiltration- and SEC-based EV isolation technique efficiently isolate fibroblast EVs from contaminating proteins

- Fibroblast EVs increase the rate of hiPSC-CM $[Ca^{2+}]_i$ rise *in vitro*

6.2 Overview of key findings

The aim of this project was to investigate mechanisms by which hiPSC-CM Ca^{2+} cycling is regulated by human cardiac fibroblasts and the ECM. In chapter 3, our initial co-culture studies identified that human cardiac fibroblasts modulated hiPSC-CM Ca^{2+} cycling *in vitro*. Co-cultures that only allow paracrine interactions but not physical interactions between the two cell types significantly prolonged Ca^{2+} transient duration, whereas, direct contact co-cultures between cardiac fibroblasts and hiPSC-CMs significantly abbreviated Ca^{2+} transient time to peak and time to decay, indicating more efficient CICR and Ca^{2+} removal mechanisms, respectively. This increase in Ca^{2+} cycling efficiency was attributed to an increase in contribution of SR Ca^{2+} stores to Ca^{2+} cycling, as this is a more efficient mechanism for Ca^{2+} cycling than sarcolemma NCX, the latter being the prominent mechanism in hiPSC-CMs, as well as neonatal and diseased cardiomyocytes. This is in line with the findings from our group's study using commercially available hiPSC-CM (CDI), lending support for the findings (Kane and Terracciano, 2018). We utilised a PDMS-based co-culture substrate to identify that

the paracrine effects by cardiac fibroblasts on hiPSC-CMs Ca^{2+} cycling is spatially dependent, with the prolongation of hiPSC-CM Ca^{2+} transient declining as the distance between the two cell types extends. These paracrine and contact-mediated effects must be considered when developing multicellular, tissue-engineered constructs with hiPSC-CMs and cardiac fibroblasts.

In chapter 4, we built on the hypothesis that the deposition of ECM proteins may play a prominent role in the SR-dominant Ca^{2+} cycling in hiPSC-CMs, and investigated the integrin-mediated interactions between hiPSC-CMs and ECM proteins. We identified that both soluble and fibril-forming, self-assembling integrin ligands abbreviate Ca^{2+} cycling by increasing the efficiency of CICR and cytosolic Ca^{2+} removal. Fibril-forming, self-assembling integrin ligands functionally recruited the SR Ca^{2+} stores to cytosolic Ca^{2+} cycling in the hiPSC-CMs, recapitulating the effects observed in cardiac fibroblast direct contact co-cultures.

We showed structural changes in the hiPSC-CMs following treatment with fibril-forming, self-assembling integrin ligands; a more rod-like hiPSC-CM morphology and increase in sarcomere length, closer to the adult cardiomyocyte phenotype. The hiPSC-CMs treated with the integrin ligands also showed an increase in the junctional gap distance between the SR and sarcolemma at the CRUs, closer to the values of the healthy, adult cardiomyocyte. Our findings indicate that integrin ligands present in the ECM play a pivotal role in the development of features of the healthy, adult cardiomyocyte. We show that integrating integrin ligands into hiPSC-CM cultures can be used to induce a morphology and electrophysiology in hiPSC-CMs closer to the healthy, adult cardiomyocyte.

In chapter 5, we built on the knowledge that all mammalian cells secrete EVs to investigate the role of EVs in the intercellular interaction between cardiac fibroblasts and cardiomyocytes. We identified that a chemical inhibitor of ceramide-mediated exosome synthesis and release, GW4869, attenuated the abbreviation in hiPSC-CM Ca^{2+} transient time to peak induced by cardiac fibroblasts, implicating the EVs as a mediator of intercellular crosstalk between cardiac fibroblasts and hiPSC-CMs. We then validated an ultrafiltration and SEC-based EV isolation technique to isolate fibroblast EVs from soluble contaminating proteins. The fibroblast EVs could abbreviate the hiPSC-CM Ca^{2+} transient time to peak. This study implicates the fibroblast EVs as important mediators of the cardiac fibroblast-induced abbreviation in Ca^{2+} transient time to peak. Human cytokine arrays identified the presence of CCR5 and CXCL12 in the fibroblast EV samples. CXCL12 has previously been shown in animal

studies to play a pivotal role in preventing the onset of heart failure in animals even without exogenous stress, indicating that cardiac fibroblast-derived CXCL12 delivered by EVs could play a prominent role in the maintenance of the healthy, adult cardiomyocyte phenotype.

6.3 Implications

6.3.1 Human hiPSC-CM EC-coupling

hiPSC-CMs have huge potential for applications in disease modelling, cell transplantation and in drug discovery. However, a major limitation to their use, as we have mentioned throughout the study, is that their phenotype closely resembles the neonatal or diseased, adult cardiomyocyte. A key issue to the used of hiPSC-CMs is inefficient EC-coupling, which is heavily reliant on sarcolemma NCX for Ca^{2+} cycling (Kane *et al.*, 2015). We have built on previous cardiac fibroblast-hiPSC-CM co-culture studies to implicate integrin ligand-receptor interactions as a key pathway for the recruitment of the SR Ca^{2+} stores to hiPSC-CM Ca^{2+} cycling and EC-coupling. Integrin ligands induce a phenotype resembling the adult cardiomyocyte and more efficient Ca^{2+} cycling. This goes some way to enabling greater application of the hiPSC-CMs by enabling a more accurate representation of the adult cardiomyocyte phenotype. Current models of disease lack many of the extracellular interactions and often utilise a monocellular population of hiPSC-CMs, but models must recapitulate the extracellular environment if we are to develop more accurate models of the native myocardium (Wang, Kit-Anan and Terracciano, 2018). In this study, we have implicated the ECM in the development of a hiPSC-CM phenotype with more efficient EC-coupling, more akin to the adult cardiomyocyte phenotype.

It is well documented that in disease there is an increase in fibroblast activity, contributing to accumulation of ECM proteins. This resultant fibrosis is initially compensatory for insufficient heart function and maintains myocardial integrity following loss of viable cardiomyocytes. However, the excessive fibrosis adversely influences the stiffness of tissue and thus ventricular function, eventually leading to heart failure. The accumulation of ECM proteins is an initial attempt to recover cardiomyocyte contractile function in the native myocardium, and manipulating the turnover of ECM proteins may be a useful target for therapeutic strategies against excessive fibrosis.

6.3.2 Cell- and substrate-binding scaffold for tissue engineering

One of the major potential uses for hiPSC-CMs is as a therapeutic which can be applied to the native myocardium, broadly as either a suspension of cells or within a tissue construct such as an engineered heart tissue. However, a significant barrier is poor cell retention *in vivo*. Ban and colleagues first demonstrated the potential of integrin ligands in promoting hiPSC-CM retention in engraftment (Ban *et al.*, 2014). They encapsulated cardiomyocytes derived from mouse embryonic stem cells (mESCs) in an injectable nanomatrix gel consisting of peptide amphiphiles incorporating RGDS (PA-RGDS) in experimental myocardial infarction. They found a 3-fold higher engraftment in mice receiving the mESC-CMs with the PA-RGDS compared to those without PA-RGDS and higher cardiac function in the PA-RGDS mESC-CMs up to 12 weeks following engraftment. The fibril-forming properties of the RGD-linked self-assembling peptides used in our study could aid retention of the cardiomyocytes even more than the PA-RGDS incorporating mESC-CMs used by Ban and colleagues (Ban *et al.*, 2014). The substrate-binding properties also opens the avenue for using these fibril-forming, self-assembling integrin ligands as an intermediate scaffold for attaching hiPSC-CMs to substrates which by themselves have poor cell-binding properties.

6.3.3 EVs modulate human hiPSC-CM EC-coupling

We identified that fibroblast EVs increase the efficiency of Ca^{2+} cycling in the hiPSC-CMs and are implicate in carrying CXCL12, a chemokine with cardioprotective effects in animal studies. As EVs have been shown to express ECM proteins on their surface, these may mediate the transfer of integrin ligands from human fibroblasts to human cardiomyocytes. In this way, fibroblast-derived integrin ligands can interact with and modulate the cardiomyocyte phenotype. Both EV surface proteins and EV cargo may play a role in the modulation of hiPSC-CM Ca^{2+} cycling by cardiac fibroblasts physiologically and in disease. It is clear that EVs are multi-target messengers that may have a prominent role in the native myocardium. Although much focus has been on the use of exogenous EVs as a vector for drug delivery, the ability to identify subpopulations of EVs and the role that patient morbidity has on EV function indicates that manipulation of the EV cargo in the native myocardium could be a potential therapeutic target.

6.4 Limitations

The immaturity of the hiPSC-CM phenotype is a crucial limitation to the translatability of findings from hiPSC-based studies to adult human physiology. Studies have shown that the contractile function of hiPSC-CMs improves with prolonged culture periods, as a result of more efficient EC-coupling parameters. In our study, we used hiPSC-CMs over a narrow period of culture (D30-32) to limit the biological variability. The plasticity of the hiPSC-CMs and dependence on culture conditions had to be considered when determining the experimental techniques for this project. Our group previously identified density-dependent changes in hiPSC-CM electrophysiology (Du *et al.*, 2015). This prevented us from employing electrophysiological studies that required sparse densities or hiPSC-CM detachment form substrates.

There is difficulty in identifying appropriate control cardiomyocytes for disease modelling. It is ethically difficult to justify isolation of human cardiomyocytes from a healthy control patient. Cardiomyocytes are available from healthy donor hearts that are rejected for transplantation but, as described in the introduction, these undergo rapid dedifferentiation when isolated from the myocardium. Therefore, much of the work in disease modelling uses adult animal cardiomyocytes as a control. However, animal controls were not used in this project.

Despite the limitations of hiPSC-CMs, they have advantages over adult human and animal cardiomyocytes. The ability to form a confluent electrically-coupled syncytia of cardiomyocytes is similar to that of native cardiomyocytes but not possible with isolated adult human cardiomyocytes. Their human origin is hugely beneficial over models utilising animal cardiomyocytes. By utilising hiPSC-CMs, we are able to construct a humanised model substantially more beneficial in recapitulating the native environment than alternative animal or adult cardiomyocyte models.

There are also limitations to the use of cardiac fibroblasts in this study. Despite their human origin providing a more accurate representation of cardiomyocyte-cardiac fibroblast interactions of the human adult heart than animal fibroblasts, there are criticisms as to the relevance of cultured fibroblasts as a model for the native fibroblast phenotype. Our group reported that fresh and cultured rat fibroblasts have different effects on cardiomyocyte properties (Cartledge *et al.*, 2015). Paracrine factors from fresh, physiological fibroblasts

increased cardiomyocyte Ca^{2+} transient amplitude, whereas pathological myofibroblasts maintained in culture secrete paracrine factors that decrease the Ca^{2+} transient amplitude of cardiomyocytes. The need to passage the cardiac fibroblasts to achieve a large enough population for the study may therefore induce changes in the cardiac fibroblast phenotype that does not represent the native active cardiac fibroblast phenotype.

We should consider the cardiac fibroblasts as a heterogeneous population of cells, rather than just a quiescent vs active phenotype. In the native myocardium, cardiac fibroblast secretome changes over the course of pathological activation. Mouton et al., recently identified that following myocardial infarction, fibroblasts shift from a pro-inflammatory secretome on day 1 post-myocardial infarction, to a pro-angiogenic secretome on day 3 (Mouton *et al.*, 2019). There is also a lack of consensus on the classification of cardiac fibroblast phenotype, as discussed in the Introduction. Despite these limitations, the overarching changes that occur following cardiac fibroblast activation still lends support to the findings of our study – integrin signalling is the major enriched process for the pan fibroblast phenotype following myocardial injury and remains enriched up to a week post injury, indicating that fibroblasts selectively express integrins to adapt to the changing ECM environment (Mouton *et al.*, 2019).

In our study, inclusion of results from other cell types could strengthen claims that the effects seen are specific to the fibroblast cell type. In the co-culture experiments of chapter 3, cardiomyocyte-conditioned serum was used as a control for the cardiomyocytes that underwent optical recording. However, non-myocyte cellular controls different to cardiac fibroblasts should be used to strengthen the claims that the effects are cardiac fibroblast-specific. Even with non-myocyte cellular controls, we would still need to consider the myocardium as a multicellular organ containing all the components shown in table 1.1 and described in section 1.4.

The purity of fibroblasts and cardiomyocytes used in this study were not formally assessed. There is general consensus that the techniques for human fibroblast isolation and hiPSC-CM differentiation and purification generate populations of cells with the characteristics of fibroblasts and cardiomyocytes, respectively. The explant technique relies on the expansion of proliferative cells and the assumption is that non-fibroblastic cells are removed during the passaging of the cultured cells (Huschtscha *et al.*, 2012). The biphasic manipulation of the Wnt pathway and glucose depletion during stem cell differentiation into

cardiomyocytes assumes the production of cells with measurable calcium transients are all cardiomyocytes. However, whether this feature is sufficient to attribute these cells to be cardiomyocytes is debated (Kane and Terracciano, 2015b).

Currently, there is a lack of agreement on the optimal EV isolation technique. Differences in the techniques accounts for variable impurities form the same sample but isolated with different techniques. In our study, we use cultured cardiac fibroblasts that have undergone passaging. Isolation of fibroblast EVs in the native myocardium would allow us to investigate if the effects we see in our study are representative of the effects of the native cardiac fibroblast EVs. However, the high number of EVs required for studies and difficulties in identifying fibroblast-specific EV markers may be a limiting factor.

6.5 Future directions

There are several substantial avenues of further investigation following the work of this project:

In chapter 3, we demonstrated the potential that an elastic, reconfigurable PDMS co-culture substrate has in investigating the spatial relationship between pure cell populations. This study used one barrier to investigate the two cell types – cardiac fibroblasts and hiPSC-CMs- in co-culture. As we know that the two cell types interact bidirectionally, this substrate can be used to investigate the changes in cardiac fibroblast structure induced by bidirectional paracrine interactions with hiPSC-CMs, independent from physical contact.

Previous studies have reported a change in cardiac fibroblast phenotype over the course of injury (Mouton *et al.*, 2019). Future studies could investigate the temporal dependency in fibroblast phenotype when co-cultured with hiPSC-CMs over different time periods. This is not possible with the co-culture substrates using porous tissue culture inserts as this would require fibroblast detachment from the inserts and replating, which would change the hiPSC-CM phenotype. In addition, our study investigated the co-culture between two cell types but future studies can utilise more than one barrier to investigate more complex intercellular interactions e.g. triculture. This would enable us to gain a deeper understanding of the interactions that occur in multicellular tissue preparations.

The use of fibril-forming integrin ligands with substrate binding properties offers the opportunity to investigate the effects of integrin binding on cell ultrastructure. We identified a significant increase in the junctional gap at the CRUs, closer to the values in the healthy adult cardiomyocyte. This indicates progression in the development of the CRUs, but future studies should investigate the development and recruitment of accessory proteins to the CRU to confirm whether the integrin ligands are promoting development of these ultrastructural domains towards an adult phenotype.

We have implicated fibroblast EV surface proteins and cargo in the fibroblast-mediated modulation of hiPSC-CM Ca^{2+} cycling in vitro. The relevance of EVs in the intercellular crosstalk in vivo is yet to be determined. However, we've identified that EVs could be a potential mediator of crosstalk between these two cells and manipulating the surface proteins and cargo content offers the potential for use as a therapeutic for human cardiac disease.

In this project, we have focused on the cardiac fibroblasts and the ECM. However, endothelial cells and smooth muscle cells also make up a large bulk of the non-myocyte composition of the native myocardium. Understanding the intercellular interactions in co-culture with these different cell types, combined with tissue engineering techniques to implement ECM proteins would enable us to produce a more physiological mechanical and structural extracellular environment for the cardiomyocytes.

The findings of this study have important implications in the use of hiPSC-CMs in disease modelling and cell transplantation, as well as identifying therapeutic targets in the native myocardium. Future work investigating these findings in an *in vivo* setting would enable us to determine the implications for these findings for translational medicine.

6.6 Conclusion

In this project, we have demonstrated that human cardiac fibroblasts cause functional recruitment of the SR Ca^{2+} stores to hiPSC-CM Ca^{2+} cycling, and identified comparable effects when cultured with integrin ligands, as well as inducing a morphology closer to the healthy, adult cardiomyocyte. In demonstrating that EVs secreted from human cardiac fibroblast abbreviate hiPSC-CM CICR, we implicate these as a form of intercellular crosstalk between the two cell types. We highlight the importance of the cell extracellular environment in regulating cardiomyocyte function. Future work will delineate the mechanisms by which these effects are achieved and determine the importance of these in mediating maturation and maintenance of the mature phenotype and the changes that occur in disease.

7 Bibliography

Aalberts, M., van Dissel-Emiliani, F. M. ., van Adrichem, N. P. ., van Wijnen, M., Wauben, M. H. ., Stout, T. A. . and Stoorvogel, W. (2012) 'Identification of Distinct Populations of Prostasomes That Differentially Express Prostate Stem Cell Antigen, Annexin A1, and GLIPR2 in Humans1', *Biology of Reproduction*, 86(3), pp. 1–8. doi: 10.1095/biolreprod.111.095760.

Abi-Gerges, N., Szabo, G., Otero, A. S., Fischmeister, R. and Méry, P. F. (2002) 'NO donors potentiate the β-adrenergic stimulation of ICa,L and the muscarinic activation of IK,ACh in rat cardiac myocytes', *Journal of Physiology*, 540(2), pp. 411–424. doi: 10.1113/jphysiol.2001.012929.

Adams, W. J., Zhang, Y., Cloutier, J., Kuchimanchi, P., Newton, G., Sehrawat, S., Aird, W. C., Mayadas, T. N., Luscinskas, F. W. and García-Cardeña, G. (2013) 'Functional vascular endothelium derived from human induced pluripotent stem cells', *Stem Cell Reports*, 1(2), pp. 105–113. doi: 10.1016/j.stemcr.2013.06.007.

Akar, F. G., Nass, R. D., Hahn, S., Cingolani, E., Shah, M., Hesketh, G. G., DiSilvestre, D., Tunin, R. S., Kass, D. a and Tomaselli, G. F. (2007) 'Dynamic changes in conduction velocity and gap junction properties during development of pacing-induced heart failure.', *American journal of physiology. Heart and circulatory physiology*, 293(2), pp. H1223–H1230. doi: 10.1152/ajpheart.00079.2007.

Akpolat, N., Yahsi, S., Godekmerdan, A., Yalniz, M. and Demirbag, K. (2005) 'The value of alpha-SMA in the evaluation of hepatic fibrosis severity in hepatitis B infection and cirrhosis development: a histopathological and immunohistochemical study.', *Histopathology*. England, 47(3), pp. 276–280. doi: 10.1111/j.1365-2559.2005.02226.x.

Ali, S. R., Ranjbarvaziri, S., Talkhabi, M., Zhao, P., Subat, A., Hojjat, A., Kamran, P., Müller, A. M. S., Volz, K. S., Tang, Z., Red-Horse, K. and Ardehali, R. (2014) 'Developmental heterogeneity of cardiac fibroblasts does not predict pathological proliferation and activation', *Circulation Research*, 115(7), pp. 625–635. doi: 10.1161/CIRCRESAHA.115.303794.

van Amerongen, M. J., Bou-Gharios, G., Popa, E., van Ark, J., Petersen, A. H., van Dam, G. M., van Luyn, M. J. A. and Harmsen, M. C. (2008) 'Bone marrow-derived myofibroblasts contribute functionally to scar formation after myocardial infarction.', *The Journal of*

pathology. England, 214(3), pp. 377–386. doi: 10.1002/path.2281.

van Amerongen, M. J., Harmsen, M. C., van Rooijen, N., Petersen, A. H. and van Luyn, M. J. A. (2007) 'Macrophage depletion impairs wound healing and increases left ventricular remodeling after myocardial injury in mice.', *The American journal of pathology*. United States, 170(3), pp. 818–829. doi: 10.2353/ajpath.2007.060547.

Amos, G. J., Wettwer, E., Metzger, F., Li, Q., Himmel, H. M. and Ravens, U. (1996) 'Differences between outward currents of human atrial and subepicardial ventricular myocytes.', *The Journal of physiology*. England, 491 (Pt 1, pp. 31–50. doi: 10.1113/jphysiol.1996.sp021194.

Anderson, K. R., Sutton, M. G. and Lie, J. T. (1979) 'Histopathological types of cardiac fibrosis in myocardial disease.', *The Journal of pathology*. England, 128(2), pp. 79–85. doi: 10.1002/path.1711280205.

Ardell, J. L., Andresen, M. C., Armour, J. A., Billman, G. E., Chen, P. S., Foreman, R. D., Herring, N., O'Leary, D. S., Sabbah, H. N., Schultz, H. D., Sunagawa, K. and Zucker, I. H. (2016) 'Translational neurocardiology: preclinical models and cardioneural integrative aspects', *Journal of Physiology*, 594(14), pp. 3877–3909. doi: 10.1113/JP271869.

Armstrong, E. J. and Bischoff, J. (2004) 'Heart valve development: endothelial cell signaling and differentiation.', *Circulation research*. United States, 95(5), pp. 459–470. doi: 10.1161/01.RES.0000141146.95728.da.

Azuma, K., Ichimura, K., Mita, T., Nakayama, S., Jin, W. L., Hirose, T., Fujitani, Y., Sumiyoshi, K., Shimada, K., Daida, H., Sakai, T., Mitsumata, M., Kawamori, R. and Watada, H. (2009) 'Presence of alpha-smooth muscle actin-positive endothelial cells in the luminal surface of adult aorta.', *Biochemical and biophysical research communications*. United States, 380(3), pp. 620–626. doi: 10.1016/j.bbrc.2009.01.135.

Bagley, R. G., Honma, N., Weber, W., Boutin, P., Rouleau, C., Shankara, S., Kataoka, S., Ishida, I., Roberts, B. L. and Teicher, B. A. (2008) 'Endosialin/TEM 1/CD248 is a pericyte marker of embryonic and tumor neovascularization.', *Microvascular research*. United States, 76(3), pp. 180–188. doi: 10.1016/j.mvr.2008.07.008.

Balasubramanian, S. and Kuppuswamy, D. (2003) 'RGD-containing peptides activate S6K1 through beta3 integrin in adult cardiac muscle cells.', *The Journal of biological chemistry*. United States, 278(43), pp. 42214–42224. doi: 10.1074/jbc.M303428200.

Balijepalli, R. C. and Kamp, T. J. (2008) 'Caveolae, ion channels and cardiac

arrhythmias.', *Progress in biophysics and molecular biology*, 98(2–3), pp. 149–160. doi: 10.1016/j.pbiomolbio.2009.01.012.

Balsam, L. B., Wagers, A. J., Christensen, J. L., Kofidis, T., Weissman, I. L. and Robbins, R. C. (2004) 'Haematopoietic stem cells adopt mature haematopoietic fates in ischaemic myocardium', *Nature*, 428(6983), pp. 668–673. doi: 10.1038/nature02460.

Ban, K., Park, H.-J., Kim, S., Andukuri, A., Hwang, J. W., Cho, K.-W., Cha, H., YoonKim, S., Kim, Woan-SangJun, H.-W. and Yoon, Y.-S. (2014) 'Cell Therapy with Embryonic Stem Encapsulated in Injectable Nanomatrix Gel Enhances Cell Engraftment and', *ACS Nano*, 8(10), pp. 10815–10825.

Banerjee, I., Fuseler, J. W., Price, R. L., Borg, T. K. and Baudino, T. A. (2007) 'Determination of cell types and numbers during cardiac development in the neonatal and adult rat and mouse.', *American journal of physiology. Heart and circulatory physiology*. United States, 293(3), pp. H1883-91. doi: 10.1152/ajpheart.00514.2007.

Bang, C., Batkai, S., Dangwal, S., Gupta, S. K., Foinquinos, A., Holzmann, A., Just, A., Remke, J., Zimmer, K., Zeug, A., Ponimaskin, E., Schmiedl, A., Yin, X., Mayr, M., Halder, R., Fischer, A., Engelhardt, S., Wei, Y., Schober, A., Fiedler, J. and Thum, T. (2014) 'Cardiac fibroblast-derived microRNA passenger strand-enriched exosomes mediate cardiomyocyte hypertrophy', *Journal of Clinical Investigation*, 124(5), pp. 2136–2146. doi: 10.1172/JCI70577.

Bassani, J. W., Yuan, W. and Bers, D. M. (1995) 'Fractional SR Ca release is regulated by trigger Ca and SR Ca content in cardiac myocytes.', *The American journal of physiology*, 268(5 Pt 1), pp. C1313–C1319.

Benedikter, B. J., Bouwman, F. G., Vajen, T., Heinzmann, A. C. A., Grauls, G., Mariman, E. C., Wouters, E. F. M., Savelkoul, P. H., Lopez-, C., Koenen, R. R., Rohde, G. G. U. and Stassen, F. R. M. (2017) 'Ultrafiltration combined with size exclusion chromatography efficiently isolates extracellular vesicles from cell culture media for compositional and functional studies', *Scientific Reports*. Springer US, (June), pp. 1–13. doi: 10.1038/s41598-017-15717-7.

Bergmann, O., Bhardwaj, R. D., Bernard, S., Zdunek, S., Barnabé-Heider, F., Walsh, S., Zupicich, J., Alkass, K., Buchholz, B. A., Druid, H., Jovinge, S., Frisén, J., Barnabe-Heider, F., Walsh, S., Zupicich, J., Alkass, K., Buchholz, B. A., Druid, H., Jovinge, S., Frisen, J., Barnabé-Heider, F., Walsh, S., Zupicich, J., Alkass, K., Buchholz, B. A., Druid, H., Jovinge, S., Frisén, J., Barnabe-Heider, F., Walsh, S., Zupicich, J., Alkass, K., Buchholz, B. A., Druid, H., Jovinge, S., Frisen, J., Barnabé-Heider, F., Walsh, S., Zupicich, J., Alkass, K., Buchholz, B. A., Druid, H.,

Jovinge, S. and Frisén, J. (2009) 'Evidence for cardiomyocyte renewal in humans.', *Science (New York, N.Y.)*, 324(5923), pp. 98–102. doi: 10.1126/science.1164680.

Bernardo, B. C., Weeks, K. L., Pretorius, L. and McMullen, J. R. (2010) 'Molecular distinction between physiological and pathological cardiac hypertrophy: experimental findings and therapeutic strategies.', *Pharmacology & therapeutics*. England, 128(1), pp. 191–227. doi: 10.1016/j.pharmthera.2010.04.005.

Bers, D. M. (2002) 'Cardiac excitation-contraction coupling.', *Nature*, 415(6868), pp. 198–205. doi: 10.1038/415198a.

Bers, D. M. (2002) 'Cardiac excitation–contraction coupling', *Nature*. Department of Physiology, Stritch School of Medicine, Loyola Unversity Chicago, IL 60153, USA. dbers@lumc.edu, 415(6868), pp. 198–205. doi: 10.1038/415198a.

Bhatia, S. N., Balis, U. J., Yarmush, M. L. and Toner, M. (1999) 'Effect of cell-cell interactions in preservation of cellular phenotype: cocultivation of hepatocytes and nonparenchymal cells.', *FASEB journal : official publication of the Federation of American Societies for Experimental Biology*. United States, 13(14), pp. 1883–1900.

Biochemistr, and, Fatima, A., Xu, G., Shao, K., Papadopoulos, S., Lehmann, M., Arnáiz-Cot, J. J., Rosa, A. O., Nguemo, F., Matzkies, M., Dittmann, S., Stone, S. L., Linke, M., Zechner, U., Beyer, V., Christian Hennies, H., Rosenkranz, S., Klauke, B., Parwani, A. S., Haverkamp, W., Pfitzer, G., Farr, M., Cleemann, L., Morad, M., Milting, H., Hescheler, J. and Šaric, T. (2011) 'Cellular Physiology Cellular Physiology Cellular Physiology Cellular Physiology Cellular Physiology In vitro Modeling of Ryanodine Receptor 2 Dysfunction Using Human Induced Pluripotent Stem Cells', *Original Paper Cell Physiol Biochem*, 28, pp. 579–592. doi: 10.1159/000335753.

Bird, S. D., Doevendans, P. A., Van Rooijen, M. A., Brutel De La Riviere, A., Hassink, R. J., Passier, R. and Mummery, C. L. (2003) 'The human adult cardiomyocyte phenotype', *Cardiovascular Research*, 58(2), pp. 423–434. doi: 10.1016/S0008-6363(03)00253-0.

Black, L. D. 3rd, Meyers, J. D., Weinbaum, J. S., Shvelidze, Y. A. and Tranquillo, R. T. (2009) 'Cell-induced alignment augments twitch force in fibrin gel-based engineered myocardium via gap junction modification.', *Tissue engineering. Part A*. United States, 15(10), pp. 3099–3108. doi: 10.1089/ten.TEA.2008.0502.

Blaustein, M. P. and Lederer, W. J. (1999) 'Sodium/calcium exchange: its physiological implications.', *Physiological reviews*. United States, 79(3), pp. 763–854. doi:

10.1152/physrev.1999.79.3.763.

Bobrie, A., Colombo, M., Krumeich, S., Raposo, G. and Thery, C. (2012) 'Diverse subpopulations of vesicles secreted by different intracellular mechanisms are present in exosome preparations obtained by differential ultracentrifugation.', *Journal of extracellular vesicles*. Sweden, 1. doi: 10.3402/jev.v1i0.18397.

Boing, A. N., van der Pol, E., Grootemaat, A. E., Coumans, F. A. W., Sturk, A., Nieuwland, R., Coumans, F. A. W., Böing, A. N., van der Pol, E. and Grootemaat, A. E. (2014) 'Single-step isolation of extracellular vesicles by size-exclusion chromatography.', *Journal of Extracellular Vesicles*. Sweden, 3, pp. 1–11. doi: 10.3402/jev.v3.23430.

Bonnin, C. M., Sparrow, M. P. and Taylor, R. R. (1981) 'Collagen synthesis and content in right ventricular hypertrophy in the dog.', *The American journal of physiology*. United States, 241(5), pp. H708-13. doi: 10.1152/ajpheart.1981.241.5.H708.

Bosman, F. T. and Stamenkovic, I. (2003) 'Functional structure and composition of the extracellular matrix.', *The Journal of pathology*. England, 200(4), pp. 423–428. doi: 10.1002/path.1437.

Boyer, L. A., Lee, T. I., Cole, M. F., Johnstone, S. E., Levine, S. S., Zucker, J. P., Guenther, M. G., Kumar, R. M., Murray, H. L., Jenner, R. G., Gifford, D. K., Melton, D. A., Jaenisch, R. and Young, R. A. (2005) 'Core transcriptional regulatory circuitry in human embryonic stem cells.', *Cell*. United States, 122(6), pp. 947–956. doi: 10.1016/j.cell.2005.08.020.

Braam, S. R., Passier, R. and Mummery, C. L. (2009) 'Cardiomyocytes from human pluripotent stem cells in regenerative medicine and drug discovery', *Trends in Pharmacological Sciences*. England, 30(10), pp. 536–545. doi: 10.1016/j.tips.2009.07.001.

Bracken, M. B. (2009) 'Why animal studies are often poor predictors of human reactions to exposure', *Journal of the Royal Society of Medicine*, 102(3), pp. 120–122. doi: 10.1258/jrsm.2008.08k033.

Bradley, H., Houser, R., Bradley, H. and Houser, S. R. (2019) 'Sodium-calcium in feline ventricular myocytes 2P I', (in mM).

Brancaccio, M., Cabodi, S., Belkin, A. M., Collo, G., Koteliansky, V. E., Tomatis, D., Altruda, F., Silengo, L. and Tarone, G. (1998) 'Differential onset of expression of alpha 7 and beta 1D integrins during mouse heart and skeletal muscle development.', *Cell adhesion and communication*. Switzerland, 5(3), pp. 193–205.

Brancaccio, M., Fratta, L., Notte, A., Hirsch, E., Poulet, R., Guazzone, S., De Acetis, M.,

Vecchione, C., Marino, G., Altruda, F., Silengo, L., Tarone, G. and Lembo, G. (2003) 'Melusin, a muscle-specific integrin β1–interacting protein, is required to prevent cardiac failure in response to chronic pressure overload', *Nature Medicine*, 9(1), pp. 68–75. doi: 10.1038/nm805.

Brancaccio, M., Guazzone, S., Menini, N., Sibona, E., Hirsch, E., De Andrea, M., Rocchi, M., Altruda, F., Tarone, G. and Silengo, L. (1999) 'Melusin is a new muscle-specific interactor for beta(1) integrin cytoplasmic domain [In Process Citation]', *J Biol Chem*, 274(41), pp. 29282–29288. doi: 10.1074/jbc.274.41.29282.

British Heart Foundation (2015) *Cardiovascular Disease Statistics 2015 - BHF*. British Heart Foundation. Available at: https://www.bhf.org.uk/publications/statistics/cvd-stats-2015.

Brito-Martins, M., Harding, S. E. and Ali, N. N. (2008) 'beta(1)- and beta(2)-adrenoceptor responses in cardiomyocytes derived from human embryonic stem cells: comparison with failing and non-failing adult human heart.', *British journal of pharmacology*. England, 153(4), pp. 751–759. doi: 10.1038/sj.bjp.0707619.

Bujak, M. and Frangogiannis, N. G. (2007) 'The role of TGF-beta signaling in myocardial infarction and cardiac remodeling.', *Cardiovascular research*. England, 74(2), pp. 184–195. doi: 10.1016/j.cardiores.2006.10.002.

Cai, H., Reinisch, K. and Ferro-Novick, S. (2007) 'Coats, Tethers, Rabs, and SNAREs Work Together to Mediate the Intracellular Destination of a Transport Vesicle', *Developmental Cell*, 12(5), pp. 671–682. doi: 10.1016/j.devcel.2007.04.005.

Camelliti, P., Borg, T. K. and Kohl, P. (2005) 'Structural and functional characterisation of cardiac fibroblasts', *Cardiovascular Research*. England, 65(1), pp. 40–51. doi: 10.1016/j.cardiores.2004.08.020.

Campbell, K. H., McWhir, J., Ritchie, W. A. and Wilmut, I. (1996) 'Sheep cloned by nuclear transfer from a cultured cell line.', *Nature*. England, 380(6569), pp. 64–66. doi: 10.1038/380064a0.

Cartledge, J. E., Kane, C., Dias, P., Tesfom, M., Clarke, L., Mckee, B., Al Ayoubi, S., Chester, A., Yacoub, M. H., Camelliti, P. and Terracciano, C. M. (2015) 'Functional crosstalk between cardiac fibroblasts and adult cardiomyocytes by solublemediators', *Cardiovascular Research*, 105(3), pp. 260–270. doi: 10.1093/cvr/cvu264.

Carvajal-Vergara, X., Sevilla, A., Dsouza, S. L., Ang, Y. S., Schaniel, C., Lee, D. F., Yang,

L., Kaplan, A. D., Adler, E. D., Rozov, R., Ge, Y., Cohen, N., Edelmann, L. J., Chang, B., Waghray, A., Su, J., Pardo, S., Lichtenbelt, K. D., Tartaglia, M., Gelb, B. D. and Lemischka, I. R. (2010) 'Patient-specific induced pluripotent stem-cell-derived models of LEOPARD syndrome', *Nature*. Nature Publishing Group, 465(7299), pp. 808–812. doi: 10.1038/nature09005.

Chaturvedi, R. R., Herron, T., Simmons, R., Shore, D., Kumar, P., Sethia, B., Chua, F., Vassiliadis, E. and Kentish, J. C. (2010) 'Passive stiffness of myocardium from congenital heart disease and implications for diastole.', *Circulation*. United States, 121(8), pp. 979–988. doi: 10.1161/CIRCULATIONAHA.109.850677.

Chen, C. H., Sereti, K. I., Wu, B. M. and Ardehali, R. (2015) 'Translational aspects of cardiac cell therapy', *Journal of Cellular and Molecular Medicine*, 19(8), pp. 1757–1772. doi: 10.1111/jcmm.12632.

Chen, F., Mottino, G., Klitzner, T. S., Philipson, K. D. and Frank, J. S. (1995) 'Distribution of the Na+/Ca2+ exchange protein in developing rabbit myocytes.', *The American journal of physiology*. United States, 268(5 Pt 1), pp. C1126-32. doi: 10.1152/ajpcell.1995.268.5.C1126.

Chen, G., Li, S., Karakikes, I., Ren, L., Zi-Ying Chow, M., Chopra, A., Keung, W., Yan, B., Chan, C. W. Y. Y., Costa, K. D., Kong, C.-W. W., Hajjar, R. J., Chen, C. S., Li, R. A., Chow, M. Z.-Y., Chopra, A., Keung, W., Yan, B., Chan, C. W. Y. Y., Costa, K. D., Kong, C.-W. W., Hajjar, R. J., Chen, C. S. and Li, R. A. (2015) 'Phospholamban as a crucial determinant of the inotropic response of human pluripotent stem cell-derived ventricular cardiomyocytes and engineered 3-dimensional tissue constructs', *Circulation: Arrhythmia and Electrophysiology*. United States, 8(1), pp. 193–202. doi: 10.1161/CIRCEP.114.002049.

Chen, Q., Zhang, H., Liu, Y., Adams, S., Eilken, H., Stehling, M., Corada, M., Dejana, E., Zhou, B. and Adams, R. H. (2016) 'Endothelial cells are progenitors of cardiac pericytes and vascular smooth muscle cells', *Nature Communications*. Nature Publishing Group, 7, pp. 1–13. doi: 10.1038/ncomms12422.

Chen, W. and Frangogiannis, N. G. (2013) 'Fibroblasts in post-infarction inflammation and cardiac repair.', *Biochimica et biophysica acta*. Netherlands, 1833(4), pp. 945–953. doi: 10.1016/j.bbamcr.2012.08.023.

Cheng, Q., Ross, R. S. and Walsh, K. B. (2004) 'Overexpression of the integrin beta(1A) subunit and the beta(1A) cytoplasmic domain modifies the beta-adrenergic regulation of the cardiac L-type Ca(2+)current.', *Journal of molecular and cellular cardiology*. England, 36(6), pp. 809–819. doi: 10.1016/j.yjmcc.2004.03.006.

Cheung, C., Bernardo, A. S., Trotter, M. W. B., Pedersen, R. A. and Sinha, S. (2012) 'Generation of human vascular smooth muscle subtypes provides insight into embryological origin–dependent disease susceptibility', *Nature Biotechnology*. Nature Publishing Group, 30(2), pp. 165–173. doi: 10.1038/nbt.2107.

Chilton, L., Giles, W. R. and Smith, G. L. (2007) 'Evidence of intercellular coupling between co-cultured adult rabbit ventricular myocytes and myofibroblasts.', *The Journal of physiology*. England, 583(Pt 1), pp. 225–236. doi: 10.1113/jphysiol.2007.135038.

Chin, I. L., Hool, L. and Choi, Y. S. (2019) 'A review of in vitro platforms for understanding cardiomyocyte Mechanobiology', *Frontiers in Bioengineering and Biotechnology*, 7(JUN), pp. 1–10. doi: 10.3389/fbioe.2019.00133.

Christoffels, V. M., Burch, J. B. E. and Moorman, A. F. M. (2004) 'Architectural plan for the heart: early patterning and delineation of the chambers and the nodes.', *Trends in cardiovascular medicine*. United States, 14(8), pp. 301–307. doi: 10.1016/j.tcm.2004.09.002.

Christoffels, V. M. and Moorman, A. F. M. (2009) 'Development of the cardiac conduction system: why are some regions of the heart more arrhythmogenic than others?', *Circulation. Arrhythmia and electrophysiology*. United States, 2(2), pp. 195–207. doi: 10.1161/CIRCEP.108.829341.

Civitarese, R. A., Kapus, A., Mcculloch, C. A. and Connelly, K. A. (2017) 'Role of integrins in mediating cardiac fibroblast – cardiomyocyte cross talk : a dynamic relationship in cardiac biology and pathophysiology', *Basic Research in Cardiology*. Springer Berlin Heidelberg. doi: 10.1007/s00395-016-0598-6.

Colombo, M., Raposo, G. and Théry, C. (2014) 'Biogenesis, Secretion, and Intercellular Interactions of Exosomes and Other Extracellular Vesicles', *Annual Review of Cell and Developmental Biology*, 30(1), pp. 255–289. doi: 10.1146/annurev-cellbio-101512-122326.

Cordeiro, J. M., Nesterenko, V. V, Sicouri, S., Goodrow, R. J. J., Treat, J. A., Desai, M., Wu, Y., Doss, M. X., Antzelevitch, C. and Di Diego, J. M. (2013) 'Identification and characterization of a transient outward K+ current in human induced pluripotent stem cell-derived cardiomyocytes.', *Journal of molecular and cellular cardiology*. England, 60, pp. 36–46. doi: 10.1016/j.yjmcc.2013.03.014.

Curtis, A., Li, D. J., DeVeale, B., Onishi, K., Kim, M. Y., Blelloch, R., Laird, D. J. and Hui, E. E. (2017) 'Patterning of sharp cellular interfaces with a reconfigurable elastic substrate', *Integr. Biol.* Royal Society of Chemistry, 9(1), pp. 50–57. doi: 10.1039/C6IB00203J.

Cyganek, L., Tiburcy, M., Sekeres, K., Gerstenberg, K., Bohnenberger, H., Lenz, C., Henze, S., Stauske, M., Salinas, G., Zimmermann, W.-H., Hasenfuss, G. and Guan, K. (2018) 'Deep phenotyping of human induced pluripotent stem cell–derived atrial and ventricular cardiomyocytes', *JCI Insight*, 3(12), pp. 1–17. doi: 10.1172/jci.insight.99941.

Dai, D.-F., Danoviz, M. E., Wiczer, B., Laflamme, M. A. and Tian, R. (2017) 'Mitochondrial Maturation in Human Pluripotent Stem Cell Derived Cardiomyocytes.', *Stem cells international*. United States, 2017, p. 5153625. doi: 10.1155/2017/5153625.

Davis, R. P., Casini, S., Van Den Berg, C. W., Hoekstra, M., Remme, C. A., Dambrot, C., Salvatori, D., Oostwaard, D. W. Van, Wilde, A. A. M., Bezzina, C. R., Verkerk, A. O., Freund, C. and Mummery, C. L. (2012) 'Cardiomyocytes derived from pluripotent stem cells recapitulate electrophysiological characteristics of an overlap syndrome of cardiac sodium channel disease', *Circulation*, 125(25), pp. 3079–3091. doi: 10.1161/CIRCULATIONAHA.111.066092.

Deb, K. and Sarda, K. (2008) 'Human embryonic stem cells: Preclinical perspectives', *Journal of Translational Medicine*, 6, pp. 1–8. doi: 10.1186/1479-5876-6-7.

Deidda, G., Jonnalagadda, S. V. R., Spies, J. W., Ranella, A., Mossou, E., Forsyth, V. T., Mitchell, E. P., Bowler, M. W., Tamamis, P. and Mitraki, A. (2017) 'Self-Assembled Amyloid Peptides with Arg-Gly-Asp (RGD) Motifs As Scaffolds for Tissue Engineering', *ACS Biomaterials Science and Engineering*, 3(7), pp. 1404–1416. doi: 10.1021/acsbiomaterials.6b00570.

Denning, C., Borgdorff, V., Crutchley, J., Firth, K. S. A. A., George, V., Kalra, S., Kondrashov, A., Hoang, M. D., Mosqueira, D., Patel, A., Prodanov, L., Rajamohan, D., Skarnes, W. C., Smith, J. G. W. W. and Young, L. E. (2016) 'Cardiomyocytes from human pluripotent stem cells: From laboratory curiosity to industrial biomedical platform.', *Biochimica et biophysica acta*. Netherlands, 1863(7 Pt B), pp. 1728–1748. doi: 10.1016/j.bbamcr.2015.10.014.

Despa, S. and Bers, D. M. (2013) 'Na^+ transport in the normal and failing heart - remember the balance.', *Journal of molecular and cellular cardiology*, 61, pp. 2–10. doi: 10.1016/j.yjmcc.2013.04.011.

Dezso, K., Jelnes, P., Laszlo, V., Baghy, K., Bodor, C., Paku, S., Tygstrup, N., Bisgaard, H. C. and Nagy, P. (2007) 'Thy-1 is expressed in hepatic myofibroblasts and not oval cells in stem cell-mediated liver regeneration.', *The American journal of pathology*. United States, 171(5), pp. 1529–1537. doi: 10.2353/ajpath.2007.070273.

Dhamoon, A. S. and Jalife, J. (2005) 'The inward rectifier current (IK1) controls cardiac

excitability and is involved in arrhythmogenesis.', *Heart rhythm*. United States, 2(3), pp. 316–324. doi: 10.1016/j.hrthm.2004.11.012.

Dispersyn, G. D., Geuens, E., Ver Donck, L., Ramaekers, F. C. S. and Borgers, M. (2001) 'Adult rabbit cardiomyocytes undergo hibernation-like dedifferentiation when co-cultured with cardiac fibroblasts', *Cardiovascular Research*, 51(2), pp. 230–240. doi: 10.1016/S0008-6363(01)00326-1.

Dohmann, H. F. R., Perin, E. C., Takiya, C. M., Silva, G. V, Silva, S. A., Sousa, A. L. S., Mesquita, C. T., Rossi, M.-I. D., Pascarelli, B. M. O., Assis, I. M., Dutra, H. S., Assad, J. A. R., Castello-Branco, R. V, Drummond, C., Dohmann, H. J. F., Willerson, J. T. and Borojevic, R. (2005) 'Transendocardial autologous bone marrow mononuclear cell injection in ischemic heart failure: postmortem anatomicopathologic and immunohistochemical findings.', *Circulation*. United States, 112(4), pp. 521–526. doi: 10.1161/CIRCULATIONAHA.104.499178.

Doppler, S. A., Carvalho, C., Lahm, H., Deutsch, M.-A., Dreßen, M., Puluca, N., Lange, R. and Krane, M. (2017) 'Cardiac fibroblasts: more than mechanical support', *Journal of Thoracic Disease*, 9(S1), pp. S36–S51. doi: 10.21037/jtd.2017.03.122.

Dorn, G. W., Vega, R. B. and Kelly, D. P. (2015) 'Mitochondrial biogenesis and dynamics in the developing and diseased heart', *Genes and Development*, 29(19), pp. 1981–1991. doi: 10.1101/gad.269894.115.

Du, D. T. M., Hellen, N., Kane, C. and Terracciano, C. M. N. (2015) 'Action potential morphology of human induced pluripotent stem cell-derived cardiomyocytes does not predict cardiac chamber specificity and is dependent on cell density', *Biophysical Journal*. Biophysical Society, 108(1), pp. 1–4. doi: 10.1016/j.bpj.2014.11.008.

Dumont, J., Euwart, D., Mei, B., Estes, S. and Kshirsagar, R. (2016) 'Human cell lines for biopharmaceutical manufacturing: history, status, and future perspectives', *Critical Reviews in Biotechnology*, 36(6), pp. 1110–1122. doi: 10.3109/07388551.2015.1084266.

Ebert, A. D., Kodo, K., Liang, P., Wu, H., Huber, B. C., Riegler, J., Churko, J., Lee, J., de Almeida, P., Lan, F., Diecke, S., Burridge, P. W., Gold, J. D., Mochly-Rosen, D. and Wu, J. C. (2014) 'Characterization of the molecular mechanisms underlying increased ischemic damage in the aldehyde dehydrogenase 2 genetic polymorphism using a human induced pluripotent stem cell model system', *Science Translational Medicine*, 6(255), p. 255ra130-255ra130. doi: 10.1126/scitranslmed.3009027.

Eisner, D. A., Caldwell, J. L., Kistamás, K. and Trafford, A. W. (2017) 'Calcium and

Excitation-Contraction Coupling in the Heart', *Circulation Research*, 121(2), pp. 181–195. doi: 10.1161/CIRCRESAHA.117.310230.

Eldh, M., Lötvall, J., Malmhäll, C. and Ekström, K. (2012) 'Importance of RNA isolation methods for analysis of exosomal RNA: Evaluation of different methods', *Molecular Immunology*. Elsevier Ltd, 50(4), pp. 278–286. doi: 10.1016/j.molimm.2012.02.001.

Elliott, E. B., Kelly, A., Smith, G. L. and Loughrey, C. M. (2012) 'Isolated rabbit working heart function during progressive inhibition of myocardial SERCA activity', *Circulation Research*, 110(12), pp. 1618–1627. doi: 10.1161/CIRCRESAHA.111.262337.

Emmert, M. Y., Hitchcock, R. W. and Hoerstrup, S. P. (2014) 'Cell therapy, 3D culture systems and tissue engineering for cardiac regeneration', *Advanced Drug Delivery Reviews*. Elsevier B.V., 69–70, pp. 254–269. doi: 10.1016/j.addr.2013.12.004.

Endemann, D. H. and Schiffrin, E. L. (2004) 'Endothelial dysfunction', *Journal of the American Society of Nephrology*, 15(8), pp. 1983–1992. doi: 10.1097/01.ASN.0000132474.50966.DA.

Endo, J., Sano, M., Fujita, J., Hayashida, K., Yuasa, S., Aoyama, N., Takehara, Y., Kato, O., Makino, S., Ogawa, S. and Fukuda, K. (2007) 'Bone marrow derived cells are involved in the pathogenesis of cardiac hypertrophy in response to pressure overload.', *Circulation*. United States, 116(10), pp. 1176–1184. doi: 10.1161/CIRCULATIONAHA.106.650903.

Endoh, M. (2004) 'Force-frequency relationship in intact mammalian ventricular myocardium: physiological and pathophysiological relevance.', *European journal of pharmacology*. Netherlands, 500(1–3), pp. 73–86. doi: 10.1016/j.ejphar.2004.07.013.

Epelman, S., Liu, P. P. and Mann, D. L. (2015) 'Role of innate and adaptive immune mechanisms in cardiac injury and repair', *Nature Reviews Immunology*, 15(2), pp. 117–129. doi: 10.1038/nri3800.

Erickson, R. P. (1988) 'Minireview: Creating Animal Models of Genetic Disease', *Am. J. Hum. Genet*, 43, pp. 582–586.

Ericsson, A. C., Crim, M. J. and Franklin, C. L. (2008) 'A brief history of animal modeling', *Missouri medicine*, 110(3), pp. 201–5. doi: 10.1021/nl061786.

Essandoh, K., Yang, L., Wang, X., Huang, W., Qin, D., Hao, J., Wang, Y., Zingarelli, B., Peng, T. and Fan, G.-C. (2015) 'Blockade of exosome generation with GW4869 dampens the sepsis-induced inflammation and cardiac dysfunction', *Biochimica et biophysica acta*. 2015/08/20, 1852(11), pp. 2362–2371. doi: 10.1016/j.bbadis.2015.08.010.

Evans, S. M., Yelon, D., Conlon, F. L. and Kirby, M. L. (2010) 'Myocardial lineage development', *Circulation research*, 107(12), pp. 1428–1444. doi: 10.1161/CIRCRESAHA.110.227405.

Fa, R., Legate, K. R., Wickstro, S. A., Wickstrom, S. A. and Fassler, R. (2009) 'Genetic and cell biological analysis of integrin outside-in signaling', *Genes and Development*. United States, 23(4), pp. 397–418. doi: 10.1101/gad.1758709.elegans.

Fan, D., Takawale, A., Lee, J. and Kassiri, Z. (2012) 'Cardiac fibroblasts, fibrosis and extracellular matrix remodeling in heart disease.', *Fibrogenesis & tissue repair*. Fibrogenesis & Tissue Repair, 5(1), p. 15. doi: 10.1186/1755-1536-5-15.

Fan, F., Yu, Y., Sun, L., Wang, S., Wang, R., Zhang, L., Li, C. and Wang, D. (2018) 'Induction of Pluripotent Stem Cell-Derived Cardiomyocyte Toxicity by Supernatant of Long Term-Stored Red Blood Cells in Vitro', *Cellular Physiology and Biochemistry*, 46(3), pp. 1230–1240. doi: 10.1159/000489073.

Feng, D., Zhao, W. L., Ye, Y. Y., Bai, X. C., Liu, R. Q., Chang, L. F., Zhou, Q. and Sui, S. F. (2010) 'Cellular internalization of exosomes occurs through phagocytosis', *Traffic*, 11(5), pp. 675–687. doi: 10.1111/j.1600-0854.2010.01041.x.

Frangogiannis, N. G. (2008) 'The immune system and cardiac repair.', *Pharmacological research*. Netherlands, 58(2), pp. 88–111. doi: 10.1016/j.phrs.2008.06.007.

Franke, W. W., Schmid, E., Osborn, M. and Weber, K. (1979) 'Intermediate-sized filaments of human endothelial cells.', *The Journal of cell biology*. United States, 81(3), pp. 570–580. doi: 10.1083/jcb.81.3.570.

Franzini-Armstrong, C., Protasi, F. and Ramesh, V. (1999) 'Shape, size, and distribution of Ca2+ release units and couplons in skeletal and cardiac muscles', *Biophysical Journal*, 77(3), pp. 1528–1539. doi: 10.1016/S0006-3495(99)77000-1.

Franzini-Armstrong, C., Protasi, F. and Tijskens, P. (2005) 'The assembly of calcium release units in cardiac muscle', *Annals of the New York Academy of Sciences*, 1047, pp. 76–85. doi: 10.1196/annals.1341.007.

French, A., Yang, C.-T., Taylor, S., Watt, S. M. and Carpenter, L. (2015) 'Human Induced Pluripotent Stem Cell-Derived B Lymphocytes Express sIgM and Can Be Generated via a Hemogenic Endothelium Intermediate', *Stem Cells and Development*, 24(9), pp. 1082–1095. doi: 10.1089/scd.2014.0318.

Fujita, J., Mori, M., Kawada, H., Ieda, Y., Tsuma, M., Matsuzaki, Y., Kawaguchi, H., Yagi,

T., Yuasa, S., Endo, J., Hotta, T., Ogawa, S., Okano, H., Yozu, R., Ando, K. and Fukuda, K. (2007) 'Administration of granulocyte colony-stimulating factor after myocardial infarction enhances the recruitment of hematopoietic stem cell-derived myofibroblasts and contributes to cardiac repair.', *Stem cells (Dayton, Ohio)*. United States, 25(11), pp. 2750–2759. doi: 10.1634/stemcells.2007-0275.

Gaborit, N., Le Bouter, S., Szuts, V., Varro, A., Escande, D., Nattel, S. and Demolombe, S. (2007) 'Regional and tissue specific transcript signatures of ion channel genes in the non-diseased human heart.', *The Journal of physiology*, 582(Pt 2), pp. 675–693. doi: 10.1113/jphysiol.2006.126714.

Gámez-Valero, A., Monguió-Tortajada, M., Carreras-Planella, L., Franquesa, M., Beyer, K. and Borràs, F. E. (2016) 'Size-Exclusion Chromatography-based isolation minimally alters Extracellular Vesicles' characteristics compared to precipitating agents', *Scientific Reports*. Nature Publishing Group, 6(September), pp. 1–9. doi: 10.1038/srep33641.

Gardiner, C., Ferreira, Y. J., Dragovic, R. A., Redman, C. W. G. and Sargent, I. L. (2013) 'Extracellular vesicle sizing and enumeration by nanoparticle tracking analysis', *Journal of extracellular vesicles*. Co-Action Publishing, 2, p. 10.3402/jev.v2i0.19671. doi: 10.3402/jev.v2i0.19671.

Le Gat, L., Bonnel, S., Gogat, K., Brizard, M., Van Den Berghe, L., Kobetz, A., Gadin, S., Dureau, P., Dufier, J. L., Abitbol, M. and Menasche, M. (2001) 'Prominent beta-5 gene expression in the cardiovascular system and in the cartilaginous primordiae of the skeleton during mouse development.', *Cell communication & adhesion*. England, 8(3), pp. 99–112.

Gaudesius, G., Miragoli, M., Thomas, S. P. and Rohr, S. (2003) 'Coupling of cardiac electrical activity over extended distances by fibroblasts of cardiac origin.', *Circulation research*. United States, 93(5), pp. 421–428. doi: 10.1161/01.RES.0000089258.40661.0C.

Ge, X., Ren, Y., Bartulos, O., Lee, M. Y., Yue, Z., Kim, K. Y., Li, W., Amos, P. J., Bozkulak, E. C., Iyer, A., Zheng, W., Zhao, H., Martin, K. A., Kotton, D. N., Tellides, G., Park, I. H., Yue, L. and Qyang, Y. (2012) 'Modeling supravalvular aortic stenosis syndrome with human induced pluripotent stem cells', *Circulation*, 126(14), pp. 1695–1704. doi: 10.1161/CIRCULATIONAHA.112.116996.

Gelinas, R., El Khoury, N., Chaix, M.-A., Beauchamp, C., Alikashani, A., Ethier, N., Boucher, G., Villeneuve, L., Robb, L., Latour, F., Mondesert, B., Rivard, L., Goyette, P., Talajic, M., Fiset, C. and Rioux, J. D. (2017) 'Characterization of a Human Induced Pluripotent Stem

Cell-Derived Cardiomyocyte Model for the Study of Variant Pathogenicity: Validation of a KCNJ2 Mutation.', *Circulation. Cardiovascular genetics*. United States, 10(5). doi: 10.1161/CIRCGENETICS.117.001755.

Germanguz, I., Sedan, O., Zeevi-Levin, N., Shtrichman, R., Barak, E., Ziskind, A., Eliyahu, S., Meiry, G., Amit, M., Itskovitz-Eldor, J. and Binah, O. (2011) 'Molecular characterization and functional properties of cardiomyocytes derived from human inducible pluripotent stem cells', *Journal of Cellular and Molecular Medicine*, 15(1), pp. 38–51. doi: 10.1111/j.1582-4934.2009.00996.x.

Gherghiceanu, M., Barad, L., Novak, A., Reiter, I., Itskovitz-Eldor, J., Binah, O. and Popescu, L. M. (2011) 'Cardiomyocytes derived from human embryonic and induced pluripotent stem cells: Comparative ultrastructure', *Journal of Cellular and Molecular Medicine*. England, 15(11), pp. 2539–2551. doi: 10.1111/j.1582-4934.2011.01417.x.

Gilbert, R. E., Connelly, K., Kelly, D. J., Pollock, C. A. and Krum, H. (2006) 'Heart failure and nephropathy: catastrophic and interrelated complications of diabetes.', *Clinical journal of the American Society of Nephrology : CJASN*, 1(2), pp. 193–208. doi: 10.2215/CJN.00540705.

Ginsberg, M. H., Partridge, A. and Shattil, S. J. (2005) 'Integrin regulation.', *Current opinion in cell biology*. England, 17(5), pp. 509–516. doi: 10.1016/j.ceb.2005.08.010.

Gittenberger-de Groot, A. C., Vrancken Peeters, M. P., Mentink, M. M., Gourdie, R. G. and Poelmann, R. E. (1998) 'Epicardium-derived cells contribute a novel population to the myocardial wall and the atrioventricular cushions.', *Circulation research*. United States, 82(10), pp. 1043–1052.

Goffin, J. M., Pittet, P., Csucs, G., Lussi, J. W., Meister, J.-J. and Hinz, B. (2006) 'Focal adhesion size controls tension-dependent recruitment of alpha-smooth muscle actin to stress fibers.', *The Journal of cell biology*. United States, 172(2), pp. 259–268. doi: 10.1083/jcb.200506179.

Granata, A., Serrano, F., Bernard, W. G., McNamara, M., Low, L., Sastry, P. and Sinha, S. (2017) 'An iPSC-derived vascular model of Marfan syndrome identifies key mediators of smooth muscle cell death', *Nature Genetics*, 49(1), pp. 97–109. doi: 10.1038/ng.3723.

Gray, M. O., Long, C. S., Kalinyak, J. E., Li, H. T. and Karliner, J. S. (1998) 'Angiotensin II stimulates cardiac myocyte hypertrophy via paracrine release of TGF-beta 1 and endothelin-1 from fibroblasts.', *Cardiovascular research*. England, 40(2), pp. 352–363. doi:

10.1016/s0008-6363(98)00121-7.

Gridelli, B. and Remuzzi, G. (2000) 'Strategies for making more organs available for transplantation.', *The New England journal of medicine*. United States, 343(6), pp. 404–410. doi: 10.1056/NEJM200008103430606.

Grubisic, Z., Rempp, P. and Benoit, H. (2011) 'A Universal Calibration for Gel Permeation Chromatography', *Rubber Chemistry and Technology*, 42(2), pp. 636–640. doi: 10.5254/1.3539243.

Gudbergsson, J. M., Johnsen, K. B., Skov, M. N. and Duroux, M. (2016) 'Systematic review of factors influencing extracellular vesicle yield from cell cultures', *Cytotechnology*. Springer Netherlands, 68(4), pp. 579–592. doi: 10.1007/s10616-015-9913-6.

Guo, L., Abrams, R. M. C., Babiarz, J. E., Cohen, J. D., Kameoka, S., Sanders, M. J., Chiao, E. and Kolaja, K. L. (2011) 'Estimating the risk of drug-induced proarrhythmia using human induced pluripotent stem cell-derived cardiomyocytes', *Toxicological Sciences*, 123(1), pp. 281–289. doi: 10.1093/toxsci/kfr158.

Guo, Y., Zeng, Q., Zhang, C., Zhang, X., Li, R., Wu, J., Guan, J., Liu, L., Zhang, X., Li, J. and Wan, Z. (2013) 'Extracellular matrix of mechanically stretched cardiac fibroblasts improves viability and metabolic activity of ventricular cells.', *International journal of medical sciences*. Australia, 10(13), pp. 1837–1845. doi: 10.7150/ijms.6786.

Gurtner, G. C., Werner, S., Barrandon, Y. and Longaker, M. T. (2008) 'Wound repair and regeneration.', *Nature*. England, 453(7193), pp. 314–321. doi: 10.1038/nature07039.

Hadad, I., Veithen, A., Springael, J. Y., Sotiropoulou, P. A., Mendes Da Costa, A., Miot, F., Naeije, R., de Deken, X. and Entee, K. M. (2013) 'Stroma Cell-Derived Factor-1α Signaling Enhances Calcium Transients and Beating Frequency in Rat Neonatal Cardiomyocytes', *PLoS ONE*, 8(2), pp. 2–11. doi: 10.1371/journal.pone.0056007.

Hagel, L., Ostberg, M. and Andersson, T. (1996) 'ik : l Apparent pore size distributions of chromatography media', 743, pp. 33–42.

Hanft, L. M. and McDonald, K. S. (2010) 'Length dependence of force generation exhibit similarities between rat cardiac myocytes and skeletal muscle fibres.', *The Journal of physiology*. England, 588(Pt 15), pp. 2891–2903. doi: 10.1113/jphysiol.2010.190504.

Hansen, K. J., Favreau, J. T., Guyette, J. P., Tao, Z.-W., Coffin, S. T., Cunha-Gavidia, A., D'Amore, B., Perreault, L. R., Fitzpatrick, J. P., DeMartino, A. and Gaudette, G. R. (2016) 'Functional Effects of Delivering Human Mesenchymal Stem Cell-Seeded Biological Sutures to

an Infarcted Heart.', *BioResearch open access*. United States, 5(1), pp. 249–260. doi: 10.1089/biores.2016.0026.

Harston, R. K. and Kuppuswamy, D. (2011) 'Integrins Are the Necessary Links to Hypertrophic Growth in Cardiomyocytes', *Journal of Signal Transduction*, 2011, pp. 1–8. doi: 10.1155/2011/521742.

Haudek, S. B., Trial, J., Xia, Y., Gupta, D., Pilling, D. and Entman, M. L. (2008) 'Fc receptor engagement mediates differentiation of cardiac fibroblast precursor cells.', *Proceedings of the National Academy of Sciences of the United States of America*. United States, 105(29), pp. 10179–10184. doi: 10.1073/pnas.0804910105.

Hautanen, A., Gailit, J., Mann, D. M. and Ruoslahti, E. (1989) 'Effects of modifications of the RGD sequence and its context on recognition by the fibronectin receptor.', *The Journal of biological chemistry*. United States, 264(3), pp. 1437–1442.

Hayman, E. G., Pierschbacher, M. D. and Ruoslahti, E. (1985) 'Detachment of cells from culture substrate by soluble fibronectin peptides.', *The Journal of cell biology*. United States, 100(6), pp. 1948–1954.

He, L., Huang, X., Kanisicak, O., Li, Y., Wang, Y., Li, Y., Pu, W., Liu, Q., Zhang, H., Tian, X., Zhao, H., Liu, X., Zhang, S., Nie, Y., Hu, S., Miao, X., Wang, Q. D., Wang, F., Chen, T., Xu, Q., Lui, K. O., Molkentin, J. D. and Zhou, B. (2017) 'Preexisting endothelial cells mediate cardiac neovascularization after injury', *Journal of Clinical Investigation*, 127(8), pp. 2968–2981. doi: 10.1172/JCI93868.

Henrique Franco, N. (2013) 'Animal experiments in biomedical research: A historical perspective', *Animals*, 3(1), pp. 238–273. doi: 10.3390/ani3010238.

Herum, K. M., Choppe, J., Kumar, A., Engler, A. J. and McCulloch, A. D. (2017) 'Mechanical regulation of cardiac fibroblast profibrotic phenotypes', *Molecular Biology of the Cell*, 28(14), pp. 1871–1882. doi: 10.1091/mbc.e17-01-0014.

Hirano, S., Suzuki, S. T. and Redies, C. (2003) 'The cadherin superfamily in neural development: diversity, function and interaction with other molecules.', *Frontiers in bioscience : a journal and virtual library*. United States, 8, pp. d306-55.

Hochedlinger, K. and Jaenisch, R. (2003) 'Nuclear transplantation, embryonic stem cells, and the potential for cell therapy.', *The New England journal of medicine*. United States, 349(3), pp. 275–286. doi: 10.1056/NEJMra035397.

Hofmann, U. and Frantz, S. (2015) 'Role of lymphocytes in myocardial injury, healing,

and remodeling after myocardial infarction', *Circulation Research*, 116(2), pp. 354–367. doi: 10.1161/CIRCRESAHA.116.304072.

Howard, C. M. and Baudino, T. a (2014) 'Dynamic cell-cell and cell-ECM interactions in the heart.', *Journal of molecular and cellular cardiology*. Elsevier Ltd, 70, pp. 19–26. doi: 10.1016/j.yjmcc.2013.10.006.

Hsieh, P. C. H., Davis, M. E., Lisowski, L. K. and Lee, R. T. (2006) 'ENDOTHELIAL-CARDIOMYOCYTE INTERACTIONS IN CARDIAC DEVELOPMENT AND REPAIR', *Annual Review of Physiology*, 68(1), pp. 51–66. doi: 10.1146/annurev.physiol.68.040104.124629.

Hulsmans, M., Clauss, S., Xiao, L., Aguirre, A. D., King, K. R., Hanley, A., Hucker, W. J., Wülfers, E. M., Seemann, G., Courties, G., Iwamoto, Y., Sun, Y., Savol, A. J., Sager, H. B., Lavine, K. J., Fishbein, G. A., Capen, D. E., Da Silva, N., Miquerol, L., Wakimoto, H., Seidman, C. E., Seidman, J. G., Sadreyev, R. I., Naxerova, K., Mitchell, R. N., Brown, D., Libby, P., Weissleder, R., Swirski, F. K., Kohl, P., Vinegoni, C., Milan, D. J., Ellinor, P. T. and Nahrendorf, M. (2017) 'Macrophages Facilitate Electrical Conduction in the Heart', *Cell*, 169(3), p. 510–522.e20. doi: 10.1016/j.cell.2017.03.050.

Huschtscha, L. I., Napier, C. E., Noble, J. R., Bower, K., Au, A. Y. M., Campbell, H. G., Braithwaite, A. W. and Reddel, R. R. (2012) 'Enhanced isolation of fibroblasts from human skin explants', *BioTechniques*, 53(4), pp. 239–244. doi: 10.2144/0000113939.

Hwang, H. S., Kryshtal, D. O., Feaster, T. K., Sánchez-Freire, V., Zhang, J., Kamp, T. J., Hong, C. C., Wu, J. C. and Knollmann, B. C. (2015) 'Comparable calcium handling of human iPSC-derived cardiomyocytes generated by multiple laboratories', *Journal of Molecular and Cellular Cardiology*. Elsevier B.V., 85, pp. 79–88. doi: 10.1016/j.yjmcc.2015.05.003.

Ibrahim, M., Gorelik, J., Yacoub, M. H. and Terracciano, C. M. (2011) 'The structure and function of cardiac t-tubules in health and disease.', *Proceedings. Biological sciences / The Royal Society*, 278(1719), pp. 2714–23. doi: 10.1098/rspb.2011.0624.

Ieda, M., Tsuchihashi, T., Ivey, K. N., Ross, R. S., Hong, T.-T., Shaw, R. M. and Srivastava, D. (2009) 'Cardiac fibroblasts regulate myocardial proliferation through beta1 integrin signaling.', *Developmental cell*. United States, 16(2), pp. 233–244. doi: 10.1016/j.devcel.2008.12.007.

Ikeuchi, M., Tsutsui, H., Shiomi, T., Matsusaka, H., Matsushima, S., Wen, J., Kubota, T. and Takeshita, A. (2004) 'Inhibition of TGF-beta signaling exacerbates early cardiac dysfunction but prevents late remodeling after infarction.', *Cardiovascular research*. England,

64(3), pp. 526–535. doi: 10.1016/j.cardiores.2004.07.017.

Inada, T., Fujiwara, H., Hasegawa, K., Araki, M., Yamauchi-Kohno, R., Yabana, H., Fujiwara, T., Tanaka, M. and Sasayama, S. (1999) 'Upregulated expression of cardiac endothelin-1 participates in myocardial cell growth in Bio14.6 Syrian cardiomyopathic hamsters.', *Journal of the American College of Cardiology*. United States, 33(2), pp. 565–571.

Inamdar, A. and Inamdar, A. (2016) 'Heart Failure: Diagnosis, Management and Utilization', *Journal of Clinical Medicine*, 5(7), p. 62. doi: 10.3390/jcm5070062.

Isoyama, S. and Nitta-Komatsubara, Y. (2002) 'Acute and chronic adaptation to hemodynamic overload and ischemia in the aged heart.', *Heart failure reviews*. United States, 7(1), pp. 63–69.

Israeli-Rosenberg, S., Manso, A. M., Okada, H. and Ross, R. S. (2014) 'Integrins and integrin-associated proteins in the cardiac myocyte', *Circulation Research*, 114(3), pp. 572–586. doi: 10.1161/CIRCRESAHA.114.301275.

Itzhaki, I., Rapoport, S., Huber, I., Mizrahi, I., Zwi-Dantsis, L., Arbel, G., Schiller, J. and Gepstein, L. (2011) 'Calcium handling in human induced pluripotent stem cell derived cardiomyocytes', *PLoS ONE*, 6(4). doi: 10.1371/journal.pone.0018037.

Janeway, C. A. J. and Medzhitov, R. (2002) 'Innate immune recognition.', *Annual review of immunology*. United States, 20, pp. 197–216. doi: 10.1146/annurev.immunol.20.083001.084359.

Jeziorowska, D., Fontaine, V., Jouve, C., Villard, E., Dussaud, S., Akbar, D., Letang, V., Cervello, P., Itier, J.-M., Pruniaux, M.-P. and Hulot, J.-S. (2017) 'Differential Sarcomere and Electrophysiological Maturation of Human iPSC-Derived Cardiac Myocytes in Monolayer vs. Aggregation-Based Differentiation Protocols.', *International journal of molecular sciences*. Switzerland, 18(6). doi: 10.3390/ijms18061173.

Ji, G., Feldman, M., Doran, R., Zipfel, W. and Kotlikoff, M. I. (2006) 'Ca2+ -induced Ca2+ release through localized Ca2+ uncaging in smooth muscle.', *The Journal of general physiology*. United States, 127(3), pp. 225–235. doi: 10.1085/jgp.200509422.

Jiang, Y., Habibollah, S., Tilgner, K., Collin, J., Barta, T., Al-Aama, J. Y., Tesarov, L., Hussain, R., Trafford, A. W., Kirkwood, G., Sernagor, E., Eleftheriou, C. G., Przyborski, S., Stojković, M., Lako, M., Keavney, B. and Armstrong, L. (2014) 'An Induced Pluripotent Stem Cell Model of Hypoplastic Left Heart Syndrome (HLHS) Reveals Multiple Expression and Functional Differences in HLHS-Derived Cardiac Myocytes', *STEM CELLS Translational*

Medicine, 3(4), pp. 416–423. doi: 10.5966/sctm.2013-0105.

Jiang, Z.-S., Jeyaraman, M., Wen, G.-B., Fandrich, R. R., Dixon, I. M. C., Cattini, P. A. and Kardami, E. (2007) 'High- but not low-molecular weight FGF-2 causes cardiac hypertrophy in vivo; possible involvement of cardiotrophin-1.', *Journal of molecular and cellular cardiology*. England, 42(1), pp. 222–233. doi: 10.1016/j.yjmcc.2006.09.002.

Johns, D. C., Nuss, H. B. and Marban, E. (1997) 'Suppression of neuronal and cardiac transient outward currents by viral gene transfer of dominant-negative Kv4.2 constructs.', *The Journal of biological chemistry*. United States, 272(50), pp. 31598–31603. doi: 10.1074/jbc.272.50.31598.

Johnston, R. K., Balasubramanian, S., Kasiganesan, H., Baicu, C. F., Zile, M. R. and Kuppuswamy, D. (2009) 'Beta3 integrin-mediated ubiquitination activates survival signaling during myocardial hypertrophy.', *FASEB journal : official publication of the Federation of American Societies for Experimental Biology*. United States, 23(8), pp. 2759–2771. doi: 10.1096/fj.08-127480.

de Jong, O. G., Verhaar, M. C., Chen, Y., Vader, P., Gremmels, H., Posthuma, G., Schiffelers, R. M., Gucek, M. and van Balkom, B. W. M. (2012) 'Cellular stress conditions are reflected in the protein and RNA content of endothelial cell-derived exosomes', *Journal of Extracellular Vesicles*, 1(1). doi: 10.3402/jev.v1i0.18396.

Jonnalagadda, S. V. R., Ornithopoulou, E., Orr, A. A., Mossou, E., Trevor Forsyth, V., Mitchell, E. P., Bowler, M. W., Mitraki, A. and Tamamis, P. (2017) 'Computational design of amyloid self-assembling peptides bearing aromatic residues and the cell adhesive motif Arg-Gly-Asp', *Molecular Systems Design & Engineering*. Royal Society of Chemistry, 2(3), pp. 321–335. doi: 10.1039/C7ME00016B.

Jourdan-LeSaux, C., Zhang, J. and Lindsey, M. L. (2010) 'Extracellular matrix roles during cardiac repair', *Life Sciences*, 87(13–14), pp. 391–400. doi: 10.1016/j.lfs.2010.07.010.

Kadota, S., Minami, I., Morone, N., Heuser, J. E., Agladze, K. and Nakatsuji, N. (2013) 'Development of a reentrant arrhythmia model in human pluripotent stem cell-derived cardiac cell sheets.', *European heart journal*. England, 34(15), pp. 1147–1156. doi: 10.1093/eurheartj/ehs418.

Kadota, S., Pabon, L., Reinecke, H. and Murry, C. E. (2017) 'In Vivo Maturation of Human Induced Pluripotent Stem Cell-Derived Cardiomyocytes in Neonatal and Adult Rat Hearts', *Stem Cell Reports*. ElsevierCompany., 8(2), pp. 278–289. doi:

10.1016/j.stemcr.2016.10.009.

Kahlenberg, J. M. (2016) ‘Anti-inflammatory panacea? The expanding therapeutics of interleukin-1 blockade.’, *Current opinion in rheumatology*. United States, 28(3), pp. 197–203. doi: 10.1097/BOR.0000000000000266.

Kai, H., Mori, T., Tokuda, K., Takayama, N., Tahara, N., Takemiya, K., Kudo, H., Sugi, Y., Fukui, D., Yasukawa, H., Kuwahara, F. and Imaizumi, T. (2006) ‘Pressure overload-induced transient oxidative stress mediates perivascular inflammation and cardiac fibrosis through angiotensin II.’, *Hypertension research : official journal of the Japanese Society of Hypertension*. England, 29(9), pp. 711–718. doi: 10.1291/hypres.29.711.

Kakkar, R. and Lee, R. T. (2010) ‘Intramyocardial Fibroblast-Myocyte Communication’, *Circulation Research*, 106(1), pp. 47–57. doi: 10.1161/CIRCRESAHA.109.207456.Intramyocardial.

Kamakura, T., Makiyama, T., Sasaki, K., Yoshida, Y., Wuriyanghai, Y., Chen, J., Hattori, T., Ohno, S., Kita, T., Horie, M., Yamanaka, S. and Kimura, T. (2013) ‘Ultrastructural maturation of human-induced pluripotent stem cell-derived cardiomyocytes in a long-term culture.’, *Circulation journal : official journal of the Japanese Circulation Society*. Japan, 77(5), pp. 1307–1314.

Kane, C., Couch, L., Terracciano, C. M. N. and M. N. Terracciano, C. (2015) ‘Excitation–contraction coupling of human induced pluripotent stem cell-derived cardiomyocytes’, *Frontiers in Cell and Developmental Biology*, 3(September), p. 59. doi: 10.3389/fcell.2015.00059.

Kane, C. and Terracciano, C. M. (2015a) ‘Induced pluripotent stem cell-derived cardiac myocytes to understand and test calcium handling: Pie in the sky?’, *Journal of Molecular and Cellular Cardiology*, 89, pp. 376–378. doi: 10.1016/j.yjmcc.2015.10.023.

Kane, C. and Terracciano, C. M. (2015b) ‘Induced pluripotent stem cell-derived cardiac myocytes to understand and test calcium handling: Pie in the sky?’, *Journal of Molecular and Cellular Cardiology*, 89, pp. 376–378. doi: 10.1016/j.yjmcc.2015.10.023.

Kane, C. and Terracciano, C. M. (2018) ‘Human Cardiac Fibroblasts Engage the Sarcoplasmic Reticulum in Induced Pluripotent Stem Cell-Derived Cardiomyocyte Excitation–Contraction Coupling’, *Journal of the American College of Cardiology*, 72(9), pp. 1061–1063. doi: 10.1016/j.jacc.2018.06.028.

Kane, C. and Terracciano, C. M. N. (2017) ‘Concise Review: Criteria for Chamber-

Specific Categorization of Human Cardiac Myocytes Derived from Pluripotent Stem Cells', *Stem Cells*, 35(8), pp. 1881–1897. doi: 10.1002/stem.2649.

Kania, G., Blyszczuk, P., Stein, S., Valaperti, A., Germano, D., Dirnhofer, S., Hunziker, L., Matter, C. M. and Eriksson, U. (2009) 'Heart-infiltrating prominin-1+/CD133+ progenitor cells represent the cellular source of transforming growth factor beta-mediated cardiac fibrosis in experimental autoimmune myocarditis.', *Circulation research*. United States, 105(5), pp. 462–470. doi: 10.1161/CIRCRESAHA.109.196287.

Kanisicak, O., Khalil, H., Ivey, M. J., Karch, J., Maliken, B. D., Correll, R. N., Brody, M. J., J. Lin, S.-C., Aronow, B. J., Tallquist, M. D. and Molkentin, J. D. (2016) 'Genetic lineage tracing defines myofibroblast origin and function in the injured heart', *Nature Communications*. The Author(s), 7, p. 12260. Available at: https://doi.org/10.1038/ncomms12260.

Karakikes, I., Ameen, M., Termglinchan, V. and Wu, J. C. (2015) 'Human Induced Pluripotent Stem Cell-Derived Cardiomyocytes: Insights into Molecular, Cellular, and Functional Phenotypes', *Circulation Research*, 117(1), pp. 80–88. doi: 10.1161/CIRCRESAHA.117.305365.

Kaur, H., Chaurasia, S. S., de Medeiros, F. W., Agrawal, V., Salomao, M. Q., Singh, N., Ambati, B. K. and Wilson, S. E. (2009) 'Corneal stroma PDGF blockade and myofibroblast development.', *Experimental eye research*. England, 88(5), pp. 960–965. doi: 10.1016/j.exer.2008.12.006.

Kehat, I., Kenyagin-Karsenti, D., Snir, M., Segev, H., Amit, M., Gepstein, A., Livne, E., Binah, O., Itskovitz-Eldor, J. and Gepstein, L. (2001) 'Human embryonic stem cells can differentiate into myocytes with structural and functional properties of cardiomyocytes.', *The Journal of clinical investigation*. United States, 108(3), pp. 407–414. doi: 10.1172/JCI12131.

Kehl, D., Weber, B. and Hoerstrup, S. P. (2016) 'Bioengineered living cardiac and venous valve replacements: current status and future prospects', *Cardiovascular Pathology*. Elsevier B.V. doi: 10.1016/j.carpath.2016.03.001.

Khan, S. A., Skaf, M. W., Harrison, R. W., Lee, K., Minhas, K. M., Kumar, A., Fradley, M., Shoukas, A. A., Berkowitz, D. E. and Hare, J. M. (2003) 'Nitric oxide regulation of myocardial contractility and calcium cycling: independent impact of neuronal and endothelial nitric oxide synthases.', *Circulation research*. United States, 92(12), pp. 1322–1329. doi: 10.1161/01.RES.0000078171.52542.9E.

Kim, H. S., Yoon, J. W., Li, H., Jeong, G. O., Park, J. J., Shin, S. E., Jang, I. H., Kim, J. H.

and Park, W. S. (2017) 'Functional expression and pharmaceutical efficacy of cardiac-specific ion channels in human embryonic stem cell-derived cardiomyocytes.', *Scientific reports*. England, 7(1), p. 13821. doi: 10.1038/s41598-017-14198-y.

Klocke, R., Tian, W., Kuhlmann, M. T. and Nikol, S. (2007) 'Surgical animal models of heart failure related to coronary heart disease', *Cardiovascular Research*, 74(1), pp. 29–38. doi: 10.1016/j.cardiores.2006.11.026.

Kofron, C. M. and Mende, U. (2017) '*In vitro* models of the cardiac microenvironment to study myocyte and non-myocyte crosstalk: bioinspired approaches beyond the polystyrene dish', *The Journal of Physiology*, 595(12), pp. 3891–3905. doi: 10.1113/JP273100.

Kohl, P. (2003) 'Heterogeneous cell coupling in the heart: an electrophysiological role for fibroblasts.', *Circulation research*. United States, pp. 381–383. doi: 10.1161/01.RES.0000091364.90121.0C.

Koivumäki, J. T., Naumenko, N., Tuomainen, T., Takalo, J., Oksanen, M., Puttonen, K. A., Lehtonen, Š., Kuusisto, J., Laakso, M., Koistinaho, J. and Tavi, P. (2018) 'Structural immaturity of human iPSC-derived cardiomyocytes: In silico investigation of effects on function and disease modeling', *Frontiers in Physiology*, 9(FEB), pp. 1–17. doi: 10.3389/fphys.2018.00080.

Kong, P., Christia, P. and Frangogiannis, N. G. (2014) 'The pathogenesis of cardiac fibrosis', *Cellular and Molecular Life Sciences*, 71(4), pp. 549–574. doi: 10.1007/s00018-013-1349-6.

Kopf, M., Baumann, H., Freer, G., Freudenberg, M., Lamers, M., Kishimoto, T., Zinkernagel, R., Bluethmann, H. and Kohler, G. (1994) 'Impaired immune and acute-phase responses in interleukin-6-deficient mice.', *Nature*. England, 368(6469), pp. 339–342. doi: 10.1038/368339a0.

Kraljevic, S., Stambrook, P. J. and Pavelic, K. (2004) 'Accelerating drug discovery', *EMBO reports*, 5(9), pp. 837–842. doi: 10.1038/sj.embor.7400236.

Kremer, J. R., Mastronarde, D. N. and McIntosh, J. R. (1996) 'Computer visualization of three-dimensional image data using IMOD.', *Journal of structural biology*. United States, 116(1), pp. 71–76. doi: 10.1006/jsbi.1996.0013.

Krenning, G., Zeisberg, E. M. and Kalluri, R. (2010) 'The origin of fibroblasts and mechanism of cardiac fibrosis.', *Journal of cellular physiology*, 225(3), pp. 631–7. doi: 10.1002/jcp.22322.

Kuppuswamy, D., Kerr, C., Narishige, T., Kasi, V. S., Menick, D. R. and Cooper, G. 4th (1997) 'Association of tyrosine-phosphorylated c-Src with the cytoskeleton of hypertrophying myocardium.', *The Journal of biological chemistry*. United States, 272(7), pp. 4500–4508. doi: 10.1074/jbc.272.7.4500.

Kyotani, Y., Takasawa, S. and Yoshizumi, M. (2019) 'Proliferative Pathways of Vascular Smooth Muscle Cells in Response to Intermittent Hypoxia.', *International journal of molecular sciences*. Switzerland, 20(11). doi: 10.3390/ijms20112706.

de la Peña, P., Domínguez, P. and Barros, F. (2018) 'Functional characterization of Kv11.1 (hERG) potassium channels split in the voltage-sensing domain', *Pflugers Archiv European Journal of Physiology*. Pflügers Archiv - European Journal of Physiology, 470(7), pp. 1069–1085. doi: 10.1007/s00424-018-2135-y.

Lahti, A. L., Kujala, V. J., Chapman, H., Koivisto, A.-P., Pekkanen-Mattila, M., Kerkela, E., Hyttinen, J., Kontula, K., Swan, H., Conklin, B. R., Yamanaka, S., Silvennoinen, O. and Aalto-Setala, K. (2012) 'Model for long QT syndrome type 2 using human iPS cells demonstrates arrhythmogenic characteristics in cell culture', *Disease Models & Mechanisms*, 5(2), pp. 220–230. doi: 10.1242/dmm.008409.

Lan, F., Lee, A. S. S., Liang, P., Sanchez-Freire, V., Nguyen, P. K. K., Wang, L., Han, L., Yen, M., Wang, Y., Sun, N., Abilez, O. J. J., Hu, S., Ebert, A. D. D., Navarrete, E. G. G., Simmons, C. S. S., Wheeler, M., Pruitt, B., Lewis, R., Yamaguchi, Y., Ashley, E. A. A., Bers, D. M. M., Robbins, R. C. C., Longaker, M. T. T. and Wu, J. C. C. (2013) 'Abnormal Calcium Handling Properties Underlie Familial Hypertrophic Cardiomyopathy Pathology in Patient-Specific Induced Pluripotent Stem Cells', *Cell Stem Cell*. Elsevier Inc., 12(1), pp. 101–113. doi: 10.1016/j.stem.2012.10.010.

de Lange, F. J., Moorman, A. F. M., Anderson, R. H., Manner, J., Soufan, A. T., de Gier-de Vries, C., Schneider, M. D., Webb, S., van den Hoff, M. J. B. and Christoffels, V. M. (2004) 'Lineage and morphogenetic analysis of the cardiac valves.', *Circulation research*. United States, 95(6), pp. 645–654. doi: 10.1161/01.RES.0000141429.13560.cb.

Langness, U. and Udenfriend, S. (1974) 'Collagen biosynthesis in nonfibroblastic cell lines.', *Proceedings of the National Academy of Sciences of the United States of America*. United States, 71(1), pp. 50–51. doi: 10.1073/pnas.71.1.50.

LaRocca, T. J., Altman, P., Jarrah, A. A., Gordon, R., Wang, E., Hadri, L., Burke, M. W., Haddad, G. E., Hajjar, R. J. and Tarzami, S. T. (2019) 'CXCR4 Cardiac Specific Knockout Mice

Develop a Progressive Cardiomyopathy.', *International journal of molecular sciences*, 20(9). doi: 10.3390/ijms20092267.

Larocca, T. J., Jeong, D., Kohlbrenner, E., Lee, A., Chen, J. and Roger, J. (2013) 'failure', 53(2), pp. 223–232. doi: 10.1016/j.yjmcc.2012.05.016.CXCR4.

Laser, M., Willey, C. D., Jiang, W., Cooper IV, G., Menick, D. R., Zile, M. R. and Kuppuswamy, D. (2000) 'Integrin activation and focal complex formation in cardiac hypertrophy', *Journal of Biological Chemistry*, 275(45), pp. 35624–35630. doi: 10.1074/jbc.M006124200.

Laughlin, M. H., Hale, C. C., Novela, L., Gute, D., Hamilton, N. and Ianuzzo, C. D. (1991) 'Biochemical characterization of exercise-trained porcine myocardium.', *Journal of applied physiology (Bethesda, Md. : 1985)*. United States, 71(1), pp. 229–235. doi: 10.1152/jappl.1991.71.1.229.

Lee, P., Klos, M., Bollensdorff, C., Hou, L., Ewart, P., Kamp, T. J., Zhang, J., Bizy, A., Guerrero-Serna, G., Kohl, P., Jalife, J. and Herron, T. J. (2012) 'Simultaneous voltage and calcium mapping of genetically purified human induced pluripotent stem cell-derived cardiac myocyte monolayers.', *Circulation research*. United States, 110(12), pp. 1556–1563. doi: 10.1161/CIRCRESAHA.111.262535.

Lee, Y. K., Ng, K. M., Lai, W. H., Chan, Y. C., Lau, Y. M., Lian, Q., Tse, H. F. and Siu, C. W. (2011) 'Calcium Homeostasis in Human Induced Pluripotent Stem Cell-Derived Cardiomyocytes', *Stem Cell Reviews and Reports*, 7(4), pp. 976–986. doi: 10.1007/s12015-011-9273-3.

Li, D., Wu, J., Bai, Y., Zhao, X. and Liu, L. (2014) 'Isolation and Culture of Adult Mouse Cardiomyocytes for Cell Signaling and in vitro Cardiac Hypertrophy', *Journal of Visualized Experiments*, (87), pp. 2–9. doi: 10.3791/51357.

Li, P., Kaslan, M., Lee, S. H., Yao, J. and Gao, Z. (2017) 'Progress in Exosome Isolation Techniques.', *Theranostics*. Australia, 7(3), pp. 789–804. doi: 10.7150/thno.18133.

Li, R., Wu, Y., Manso, A. M., Gu, Y., Liao, P., Israeli, S., Yajima, T., Nguyen, U., Huang, M. S., Dalton, N. D., Peterson, K. L. and Ross, R. S. (2012) 'beta1 integrin gene excision in the adult murine cardiac myocyte causes defective mechanical and signaling responses.', *The American journal of pathology*. United States, 180(3), pp. 952–962. doi: 10.1016/j.ajpath.2011.12.007.

Li, Z. and Guan, J. (2011) 'Hydrogels for cardiac tissue engineering', *Polymers*, 3(2), pp.

740–761. doi: 10.3390/polym3020740.

Lian, X., Hsiao, C., Wilson, G., Zhu, K., Hazeltine, L. B., Azarin, S. M., Raval, K. K., Zhang, J., Kamp, T. J. and Palecek, S. P. (2012) 'PNAS Plus: Robust cardiomyocyte differentiation from human pluripotent stem cells via temporal modulation of canonical Wnt signaling', *Proceedings of the National Academy of Sciences*, 109(27), pp. E1848–E1857. doi: 10.1073/pnas.1200250109.

Lian, X., Zhang, J., Azarin, S. M., Zhu, K., Hazeltine, L. B., Bao, X., Hsiao, C., Kamp, T. J. and Palecek, S. P. (2013) 'Directed cardiomyocyte differentiation from human pluripotent stem cells by modulating Wnt/beta-catenin signaling under fully defined conditions.', *Nature protocols*. England, 8(1), pp. 162–175. doi: 10.1038/nprot.2012.150.

Liang, P., Lan, F., Lee, A. S., Gong, T., Sanchez-Freire, V., Wang, Y., Diecke, S., Sallam, K., Knowles, J. W., Wang, P. J., Nguyen, P. K., Bers, D. M., Robbins, R. C. and Wu, J. C. (2013) 'Drug screening using a library of human induced pluripotent stem cell-derived cardiomyocytes reveals disease-specific patterns of cardiotoxicity', *Circulation*. 2013/03/21, 127(16), pp. 1677–1691. doi: 10.1161/CIRCULATIONAHA.113.001883.

Liang, X., Wang, G., Lin, L., Lowe, J., Zhang, Q., Bu, L., Chen, Y., Chen, J., Sun, Y. and Evans, S. M. (2013) 'HCN4 dynamically marks the first heart field and conduction system precursors.', *Circulation research*. United States, 113(4), pp. 399–407. doi: 10.1161/CIRCRESAHA.113.301588.

Lie-Venema, H., van den Akker, N. M. S., Bax, N. A. M., Winter, E. M., Maas, S., Kekarainen, T., Hoeben, R. C., deRuiter, M. C., Poelmann, R. E. and Gittenberger-de Groot, A. C. (2007) 'Origin, fate, and function of epicardium-derived cells (EPDCs) in normal and abnormal cardiac development.', *TheScientificWorldJournal*. United States, 7, pp. 1777–1798. doi: 10.1100/tsw.2007.294.

Liepins, A. (1983) 'Possible role of microtubules in tumor cell surface membrane shedding, permeability, and lympholysis.', *Cellular immunology*. Netherlands, 76(1), pp. 120–128. doi: 10.1016/0008-8749(83)90354-4.

Limpitikul, W. B., Dick, I. E., Tester, D. J., Boczek, N. J., Limphong, P., Yang, W., Choi, M. H., Babich, J., Disilvestre, D., Kanter, R. J., Tomaselli, G. F., Ackerman, M. J. and Yue, D. T. (2017) 'A Precision Medicine Approach to the Rescue of Function on Malignant Calmodulinopathic Long-QT Syndrome', *Circulation Research*, 120(1), pp. 39–48. doi: 10.1161/CIRCRESAHA.116.309283.

Lindahl, P., Johansson, B. R., Leveen, P. and Betsholtz, C. (1997) 'Pericyte loss and microaneurysm formation in PDGF-B-deficient mice.', *Science (New York, N.Y.)*. United States, 277(5323), pp. 242–245.

Lindsey, S. E., Butcher, J. T. and Yalcin, H. C. (2014) 'Mechanical regulation of cardiac development', *Frontiers in Physiology*, 5 AUG(August), pp. 1–15. doi: 10.3389/fphys.2014.00318.

Liu, J., Sun, N., Bruce, M. A., Wu, J. C. and Butte, M. J. (2012) 'Atomic force mechanobiology of pluripotent stem cell-derived cardiomyocytes.', *PloS one*. United States, 7(5), p. e37559. doi: 10.1371/journal.pone.0037559.

Liu, W., Yasui, K., Opthof, T., Ishiki, R., Lee, J. K., Kamiya, K., Yokota, M. and Kodama, I. (2002) 'Developmental changes of Ca2+handling in mouse ventricular cells from early embryo to adulthood', *Life Sciences*, 71(11), pp. 1279–1292. doi: 10.1016/S0024-3205(02)01826-X.

Livshts, M. A., Khomyakova, E., Evtushenko, E. G., Lazarev, V. N., Kulemin, N. A., Semina, S. E., Generozov, E. V. and Govorun, V. M. (2015) 'Isolation of exosomes by differential centrifugation: Theoretical analysis of a commonly used protocol', *Scientific Reports*, 5(May), pp. 1–13. doi: 10.1038/srep17319.

Llames, S., García-Pérez, E., Meana, Á., Larcher, F. and del Río, M. (2015) 'Feeder Layer Cell Actions and Applications.', *Tissue engineering. Part B, Reviews*, 21(4), pp. 345–353. doi: 10.1089/ten.TEB.2014.0547.

Lobb, R. J., Becker, M., Wen, S. W., Wong, C. S. F., Wiegmans, A. P., Leimgruber, A. and Möller, A. (2015) 'Optimized exosome isolation protocol for cell culture supernatant and human plasma', *Journal of Extracellular Vesicles*, 4(1), pp. 1–11. doi: 10.3402/jev.v4.27031.

Loh, Y.-H., Wu, Q., Chew, J.-L., Vega, V. B., Zhang, W., Chen, X., Bourque, G., George, J., Leong, B., Liu, J., Wong, K.-Y., Sung, K. W., Lee, C. W. H., Zhao, X.-D., Chiu, K.-P., Lipovich, L., Kuznetsov, V. A., Robson, P., Stanton, L. W., Wei, C.-L., Ruan, Y., Lim, B. and Ng, H.-H. (2006) 'The Oct4 and Nanog transcription network regulates pluripotency in mouse embryonic stem cells.', *Nature genetics*. United States, 38(4), pp. 431–440. doi: 10.1038/ng1760.

Lopaschuk, G. D., Spafford, M. A. and Marsh, D. R. (1991) 'Glycolysis is predominant source of myocardial ATP production immediately after birth.', *The American journal of physiology*. United States, 261(6 Pt 2), pp. H1698-705. doi: 10.1152/ajpheart.1991.261.6.H1698.

Lundy, S. D., Zhu, W.-Z., Regnier, M. and Laflamme, M. A. (2013) 'Structural and

Functional Maturation of Cardiomyocytes Derived from Human Pluripotent Stem Cells', *Stem Cells and Development*, 22(14), pp. 1991–2002. doi: 10.1089/scd.2012.0490.

Ma, J., Guo, L., Fiene, S. J., Anson, B. D., Thomson, J. A., Kamp, T. J., Kolaja, K. L., Swanson, B. J., January, C. T., Kl, K., Bj, S. and Ct, J. (2011) 'High purity human-induced pluripotent stem cell-derived cardiomyocytes : electrophysiological properties of action potentials and ionic currents', *American journal of physiology. Heart and circulatory physiology*. United States, 301(5), pp. 2006–2017. doi: 10.1152/ajpheart.00694.2011.

MacFadyen, J. R., Haworth, O., Roberston, D., Hardie, D., Webster, M.-T., Morris, H. R., Panico, M., Sutton-Smith, M., Dell, A., van der Geer, P., Wienke, D., Buckley, C. D. and Isacke, C. M. (2005) 'Endosialin (TEM1, CD248) is a marker of stromal fibroblasts and is not selectively expressed on tumour endothelium.', *FEBS letters*. England, 579(12), pp. 2569–2575. doi: 10.1016/j.febslet.2005.03.071.

Magyar, J., Iost, N., Kortvely, A., Banyasz, T., Virag, L., Szigligeti, P., Varro, A., Opincariu, M., Szecsi, J., Papp, J. G. and Nanasi, P. P. (2000) 'Effects of endothelin-1 on calcium and potassium currents in undiseased human ventricular myocytes.', *Pflugers Archiv : European journal of physiology*. Germany, 441(1), pp. 144–149. doi: 10.1007/s004240000400.

Maier, L. S., Zhang, T., Chen, L., DeSantiago, J., Brown, J. H. and Bers, D. M. (2003) 'Transgenic CaMKIIdeltaC overexpression uniquely alters cardiac myocyte Ca2+ handling: reduced SR Ca2+ load and activated SR Ca2+ release.', *Circulation research*. United States, United States, 92(8), pp. 904–911. doi: 10.1161/01.RES.0000069685.20258.F1.

Mallat, Z., Taleb, S., Ait-Oufella, H. and Tedgui, A. (2009) 'The role of adaptive T cell immunity in atherosclerosis.', *Journal of lipid research*. United States, 50 Suppl, pp. S364-9. doi: 10.1194/jlr.R800092-JLR200.

Margariti, A. (2014) 'Peripheral neuropathy may be a potential risk of cardiovascular disease in diabetes mellitus', *Heart*, 100(23), pp. 1823–1824. doi: 10.1136/heartjnl-2014-306258.

Marino, A., Martelli, A., Citi, V., Fu, M., Wang, R., Calderone, V. and Levi, R. (2016) 'The novel H2S donor 4-carboxy-phenyl isothiocyanate inhibits mast cell degranulation and renin release by decreasing intracellular calcium', *British Journal of Pharmacology*, 173(22), pp. 3222–3234. doi: 10.1111/bph.13583.

McAnulty, R. J. and Laurent, G. J. (1987) 'Collagen synthesis and degradation in vivo. Evidence for rapid rates of collagen turnover with extensive degradation of newly synthesized

collagen in tissues of the adult rat.', *Collagen and related research*. Germany, 7(2), pp. 93–104.

McCain, M. L. and Parker, K. K. (2011) 'Mechanotransduction: The role of mechanical stress, myocyte shape, and cytoskeletal architecture on cardiac function', *Pflugers Archiv European Journal of Physiology*, 462(1), pp. 89–104. doi: 10.1007/s00424-011-0951-4.

Medvedev, S. P., Shevchenko, A. I. and Zakian, S. M. (2010) 'Induced Pluripotent Stem Cells: Problems and Advantages when Applying them in Regenerative Medicine', *Acta naturae*. A.I. Gordeyev, 2(2), pp. 18–28. Available at: https://www.ncbi.nlm.nih.gov/pubmed/22649638.

Menon, B., Johnson, J. N., Ross, R. S., Singh, M. and Singh, K. (2007) 'Glycogen synthase kinase-3beta plays a pro-apoptotic role in beta-adrenergic receptor-stimulated apoptosis in adult rat ventricular myocytes: Role of beta1 integrins.', *Journal of molecular and cellular cardiology*. England, 42(3), pp. 653–661. doi: 10.1016/j.yjmcc.2006.12.011.

Michela, N., Tessa, P., C., S. F., Roger, P. and D., S. M. (2011) 'Cardiopoietic Factors', *Circulation Research*. American Heart Association, 108(1), pp. 129–152. doi: 10.1161/CIRCRESAHA.110.223792.

Miragoli, M., Gaudesius, G. and Rohr, S. (2006) 'Electrotonic modulation of cardiac impulse conduction by myofibroblasts.', *Circulation research*. United States, 98(6), pp. 801–810. doi: 10.1161/01.RES.0000214537.44195.a3.

Mittal, A., Pulina, M., Hou, S. Y. and Astrof, S. (2013) 'Fibronectin and integrin alpha 5 play requisite roles in cardiac morphogenesis', *Developmental Biology*, 381(1), pp. 73–82. doi: 10.1016/j.ydbio.2013.06.010.

Mohan, R. R., Mohan, R. R. and Wilson, S. E. (2001) 'Discoidin domain receptor (DDR) 1 and 2: collagen-activated tyrosine kinase receptors in the cornea.', *Experimental eye research*. England, 72(1), pp. 87–92. doi: 10.1006/exer.2000.0932.

Mol, E. A., Goumans, M., Doevendans, P. A., Sluijter, J. P. G. and Vader, P. (2017) 'Higher functionality of extracellular vesicles isolated using size-exclusion chromatography compared to ultracentrifugation', *Nanomedicine: Nanotechnology, Biology, and Medicine*. Elsevier Inc., 13(6), pp. 2061–2065. doi: 10.1016/j.nano.2017.03.011.

Momen-Heravi, F., Balaj, L., Alian, S., Trachtenberg, A. J., Hochberg, F. H., Skog, J. and Kuo, W. P. (2012) 'Impact of biofluid viscosity on size and sedimentation efficiency of the isolated microvesicles.', *Frontiers in physiology*. Switzerland, 3, p. 162. doi:

10.3389/fphys.2012.00162.

Monguió-Tortajada, M., Gálvez-Montón, C., Bayes-Genis, A., Roura, S. and Borràs, F. E. (2019) 'Extracellular vesicle isolation methods: rising impact of size-exclusion chromatography', *Cellular and Molecular Life Sciences*. Springer International Publishing, 76(12), pp. 2369–2382. doi: 10.1007/s00018-019-03071-y.

Montecalvo, A., Larregina, A. T., Shufesky, W. J., Stolz, D. B., Sullivan, M. L. G., Karlsson, J. M., Baty, C. J., Gibson, G. A., Erdos, G., Wang, Z., Milosevic, J., Tkacheva, O. A., Divito, S. J., Jordan, R., Lyons-Weiler, J., Watkins, S. C. and Morelli, A. E. (2012) 'Mechanism of transfer of functional microRNAs between mouse dendritic cells via exosomes', *Blood*. 2011/10/26. American Society of Hematology, 119(3), pp. 756–766. doi: 10.1182/blood-2011-02-338004.

Moore-Morris, T., Cattaneo, P., Guimarães-Camboa, N., Bogomolovas, J., Cedenilla, M., Banerjee, I., Ricote, M., Kisseleva, T., Zhang, L., Gu, Y., Dalton, N. D., Peterson, K. L., Chen, J., Pucéat, M. and Evans, S. M. (2018) 'Infarct fibroblasts do not derive from bone marrow lineages', *Circulation Research*, 122(4), pp. 583–590. doi: 10.1161/CIRCRESAHA.117.311490.

Moore-Morris, T., Guimaraes-Camboa, N., Banerjee, I., Zambon, A. C., Kisseleva, T., Velayoudon, A., Stallcup, W. B., Gu, Y., Dalton, N. D., Cedenilla, M., Gomez-Amaro, R., Zhou, B., Brenner, D. A., Peterson, K. L., Chen, J. and Evans, S. M. (2014) 'Resident fibroblast lineages mediate pressure overload-induced cardiac fibrosis.', *The Journal of clinical investigation*. United States, 124(7), pp. 2921–2934. doi: 10.1172/JCI74783.

Moretti, A., Bellin, M., Welling, A., Jung, C. B., Lam, J. T., Bott-Flügel, L., Dorn, T., Goedel, A., Höhnke, C., Hofmann, F., Seyfarth, M., Sinnecker, D., Schömig, A. and Laugwitz, K.-L. (2010) 'Patient-Specific Induced Pluripotent Stem-Cell Models for Long-QT Syndrome', *New England Journal of Medicine*, 363(15), pp. 1397–1409. doi: 10.1056/NEJMoa0908679.

Mork, C., van Deurs, B. and Petersen, O. W. (1990) 'Regulation of vimentin expression in cultured human mammary epithelial cells.', *Differentiation; research in biological diversity*. England, 43(2), pp. 146–156.

Mouton, A. J., Ma, Y., Rivera Gonzalez, O. J., Daseke, M. J., Flynn, E. R., Freeman, T. C., Garrett, M. R., DeLeon-Pennell, K. Y. and Lindsey, M. L. (2019) 'Fibroblast polarization over the myocardial infarction time continuum shifts roles from inflammation to angiogenesis', *Basic Research in Cardiology*. Springer Berlin Heidelberg, 114(2), pp. 1–16. doi: 10.1007/s00395-019-0715-4.

Mulcahy, L. A., Pink, R. C. and Carter, D. R. F. (2014) 'Routes and mechanisms of

extracellular vesicle uptake', *Journal of Extracellular Vesicles*, 3(1), pp. 1–14. doi: 10.3402/jev.v3.24641.

Mummery, C. L., Zhang, J., Ng, E. S., Elliott, D. A., Elefanty, A. G. and Kamp, T. J. (2012) 'Differentiation of human embryonic stem cells and induced pluripotent stem cells to cardiomyocytes: a methods overview.', *Circulation research*. United States, 111(3), pp. 344–358. doi: 10.1161/CIRCRESAHA.110.227512.

Munoz-Chapuli, R., Perez-Pomares, J. M., Macias, D., Garcia-Garrido, L., Carmona, R. and Gonzalez-Iriarte, M. (2001) 'The epicardium as a source of mesenchyme for the developing heart.', *Italian journal of anatomy and embryology = Archivio italiano di anatomia ed embriologia*. Italy, 106(2 Suppl 1), pp. 187–196.

Muralidharan-Chari, V., Clancy, J. W., Sedgwick, A. and D'Souza-Schorey, C. (2010) 'Microvesicles: Mediators of extracellular communication during cancer progression', *Journal of Cell Science*, 123(10), pp. 1603–1611. doi: 10.1242/jcs.064386.

Mussini, E., Hutton, J. J. J. and Udenfriend, S. (1967) 'Collagen proline hydroxylase in wound healing, granuloma formation, scurvy, and growth.', *Science (New York, N.Y.)*. United States, 157(3791), pp. 927–929.

Musunuru, K., Sheikh, F., Gupta, R. M., Houser, S. R., Maher, K. O., Milan, D. J., Terzic, A. and Wu, J. C. (2018) *Induced Pluripotent Stem Cells for Cardiovascular Disease Modeling and Precision Medicine: A Scientific Statement From the American Heart Association*, *Circ Genom Precis Med*. doi: 10.1161/HCG.0000000000000043.

Myasoedova, V. A., Chistiakov, D. A., Grechko, A. V and Orekhov, A. N. (2018) 'Matrix metalloproteinases in pro-atherosclerotic arterial remodeling.', *Journal of molecular and cellular cardiology*. England, 123, pp. 159–167. doi: 10.1016/j.yjmcc.2018.08.026.

Nakaya, M., Watari, K., Tajima, M., Nakaya, T., Matsuda, S., Ohara, H., Nishihara, H., Yamaguchi, H., Hashimoto, A., Nishida, M., Nagasaka, A., Horii, Y., Ono, H., Iribe, G., Inoue, R., Tsuda, M., Inoue, K., Tanaka, A., Kuroda, M., Nagata, S. and Kurose, H. (2017) 'Cardiac myofibroblast engulfment of dead cells facilitates recovery after myocardial infarction', *Journal of Clinical Investigation*, 127(1), pp. 383–401. doi: 10.1172/JCI83822.

Nazarenko, I., Rana, S., Baumann, A., McAlear, J., Hellwig, A., Trendelenburg, M., Lochnit, G., Preissner, K. T. and Zöller, M. (2010) 'Cell surface tetraspanin Tspan8 contributes to molecular pathways of exosome-induced endothelial cell activation', *Cancer Research*, 70(4), pp. 1668–1678. doi: 10.1158/0008-5472.CAN-09-2470.

Nerbonne, J. M. and Kass, R. S. (2005) 'Molecular physiology of cardiac repolarization.', *Physiological reviews*. United States, 85(4), pp. 1205–1253. doi: 10.1152/physrev.00002.2005.

Nguyen, N., Nguyen, W., Nguyenton, B., Ratchada, P., Page, G., Miller, P. E., Ghetti, A. and Abi-Gerges, N. (2017) 'Adult human primary cardiomyocyte-based model for the simultaneous prediction of drug-induced inotropic and pro-arrhythmia risk', *Frontiers in Physiology*, 8(DEC), pp. 1–16. doi: 10.3389/fphys.2017.01073.

Nian, M., Lee, P., Khaper, N. and Liu, P. (2004) 'Inflammatory cytokines and postmyocardial infarction remodeling.', *Circulation research*. United States, 94(12), pp. 1543–1553. doi: 10.1161/01.RES.0000130526.20854.fa.

Nordin, J. Z., D, M., Lee, Y., Vader, P., Mäger, I., Johansson, H. J., Heusermann, W., Wiklander, O. P. B., D, M., Hällbrink, M., Seow, Y., Bultema, J. J., Gilthorpe, J., Davies, T., Fairchild, P. J., Gabrielsson, S., Meisner-kober, N. C., Lehtiö, J., Smith, C. I. E., Wood, M. J. A. and Andaloussi, S. E. L. (2015) 'Ultrafiltration with size-exclusion liquid chromatography for high yield isolation of extracellular vesicles preserving intact biophysical and functional properties', *Nanomedicine: Nanotechnology, Biology, and Medicine*. The Authors, 11(4), pp. 879–883. doi: 10.1016/j.nano.2015.01.003.

Normand, C., Kaye, D. M., Povsic, T. J. and Dickstein, K. (2019) 'Beyond pharmacological treatment: an insight into therapies that target specific aspects of heart failure pathophysiology.', *Lancet (London, England)*. England, 393(10175), pp. 1045–1055. doi: 10.1016/S0140-6736(18)32216-5.

Norris, R. A., Borg, T. K., Butcher, J. T., Baudino, T. A., Banerjee, I. and Markwald, R. R. (2008) 'Neonatal and adult cardiovascular pathophysiological remodeling and repair: developmental role of periostin.', *Annals of the New York Academy of Sciences*. United States, 1123, pp. 30–40. doi: 10.1196/annals.1420.005.

Novak, A., Barad, L., Zeevi-Levin, N., Shick, R., Shtrichman, R., Lorber, A., Itskovitz-Eldor, J. and Binah, O. (2012) 'Cardiomyocytes generated from CPVT D307H patients are arrhythmogenic in response to β-adrenergic stimulation', *Journal of Cellular and Molecular Medicine*, 16(3), pp. 468–482. doi: 10.1111/j.1582-4934.2011.01476.x.

O'Brien, J. R. (1969) 'Cell membrane damage, platelet stickiness and some effects of aspirin.', *British journal of haematology*. England, 17(6), pp. 610–611.

Oh, Y., Cho, G.-S., Li, Z., Hong, I., Zhu, R., Kim, M.-J., Kim, Y. J., Tampakakis, E., Tung, L.,

Huganir, R., Dong, X., Kwon, C. and Lee, G. (2016) 'Functional Coupling with Cardiac Muscle Promotes Maturation of hPSC-Derived Sympathetic Neurons', *Cell Stem Cell*, 19(1), pp. 95–106. doi: 10.1016/j.stem.2016.05.002.

Okada, H., Lai, N. C., Kawaraguchi, Y., Liao, P., Copps, J., Sugano, Y., Okada-maeda, S., Banerjee, I., Schilling, J. M., Gingras, A. R., Asfaw, E. K., Suarez, J., Kang, S., Perkins, G. A., Au, C. G., Israeli-rosenberg, S., Manso, A. M., Liu, Z., Milner, D. J., Kaufman, S. J., Patel, H. H., Roth, D. M., Hammond, H. K., Taylor, S. S., Dillmann, W. H., Goldhaber, J. I. and Ross, R. S. (2013) 'Integrins protect cardiomyocytes from ischemia / reperfusion injury', 123(10). doi: 10.1172/JCI64216.4294.

Okita, K., Ichisaka, T. and Yamanaka, S. (2007) 'Generation of germline-competent induced pluripotent stem cells.', *Nature*, 448(7151), pp. 313–317. doi: 10.1038/nature05934.

Olaso, E., Ikeda, K., Eng, F. J., Xu, L., Wang, L. H., Lin, H. C. and Friedman, S. L. (2001) 'DDR2 receptor promotes MMP-2-mediated proliferation and invasion by hepatic stellate cells.', *The Journal of clinical investigation*. United States, 108(9), pp. 1369–1378. doi: 10.1172/JCI12373.

Olivetti, G., Anversa, P. and Loud, A. V (1980) 'Morphometric study of early postnatal development in the left and right ventricular myocardium of the rat. II. Tissue composition, capillary growth, and sarcoplasmic alterations.', *Circulation research*. United States, 46(4), pp. 503–512.

Olivetti, G., Cigola, E., Maestri, R., Corradi, D., Lagrasta, C., Gambert, S. R. and Anversa, P. (1996) 'Aging, cardiac hypertrophy and ischemic cardiomyopathy do not affect the proportion of mononucleated and multinucleated myocytes in the human heart', *Journal of Molecular and Cellular Cardiology*, 28(7), pp. 1463–1477. doi: 10.1006/jmcc.1996.0137.

Olivey, H. E., Mundell, N. A., Austin, A. F. and Barnett, J. V (2006) 'Transforming growth factor-beta stimulates epithelial-mesenchymal transformation in the proepicardium.', *Developmental dynamics : an official publication of the American Association of Anatomists*. United States, 235(1), pp. 50–59. doi: 10.1002/dvdy.20593.

Olson, H., Betton, G., Robinson, D., Thomas, K., Monro, A., Kolaja, G., Lilly, P., Sanders, J., Sipes, G., Bracken, W., Dorato, M., Van Deun, K., Smith, P., Berger, B. and Heller, A. (2000) 'Concordance of the toxicity of pharmaceuticals in humans and in animals', *Regulatory Toxicology and Pharmacology*, 32(1), pp. 56–67. doi: 10.1006/rtph.2000.1399.

Orchard, C. H., Pasek, M. and Brette, F. (2009) 'The role of mammalian cardiac t-

tubules in excitation-contraction coupling: experimental and computational approaches.', *Experimental physiology*. England, 94(5), pp. 509–519. doi: 10.1113/expphysiol.2008.043984.

Otsuji, T. G., Minami, I., Kurose, Y., Yamauchi, K., Tada, M. and Nakatsuji, N. (2010) 'Progressive maturation in contracting cardiomyocytes derived from human embryonic stem cells: Qualitative effects on electrophysiological responses to drugs.', *Stem cell research*. England, 4(3), pp. 201–213. doi: 10.1016/j.scr.2010.01.002.

Palmer, B. M., Lynch, J. M., Snyder, S. M. and Moore, R. L. (1999) 'Effects of chronic run training on Na+-dependent Ca2+ efflux from rat left ventricular myocytes.', *Journal of applied physiology (Bethesda, Md. : 1985)*. United States, 86(2), pp. 584–591. doi: 10.1152/jappl.1999.86.2.584.

Paolillo, M. and Schinelli, S. (2017) 'Integrins and exosomes, a dangerous liaison in cancer progression', *Cancers*, 9(8). doi: 10.3390/cancers9080095.

Parameswaran, S., Kumar, S., Verma, R. S. and Sharma, R. K. (2013) 'Cardiomyocyte culture — an update on the in vitro cardiovascular model and future challenges', *Canadian Journal of Physiology and Pharmacology*, 91(12), pp. 985–998. doi: 10.1139/cjpp-2013-0161.

Park, M. and Yoon, Y. S. (2018) 'Cardiac regeneration with human pluripotent stem cell-derived cardiomyocytes', *Korean Circulation Journal*, 48(11), pp. 974–988. doi: 10.4070/kcj.2018.0312.

Park, S. J., Kim, J. M., Kim, J., Hur, J., Park, S., Kim, K., Shin, H. J. and Chwae, Y. J. (2018) 'Molecular mechanisms of biogenesis of apoptotic exosome-like vesicles and their roles as damage-associated molecular patterns', *Proceedings of the National Academy of Sciences of the United States of America*, 115(50), pp. E11721–E11730. doi: 10.1073/pnas.1811432115.

Pathak, M., Sarkar, S., Vellaichamy, E. and Sen, S. (2001) 'Role of Myocytes in Myocardial Collagen Production', pp. 833–841.

Paulson, K. E., Zhu, S.-N., Chen, M., Nurmohamed, S., Jongstra-Bilen, J. and Cybulsky, M. I. (2010) 'Resident intimal dendritic cells accumulate lipid and contribute to the initiation of atherosclerosis.', *Circulation research*. United States, 106(2), pp. 383–390. doi: 10.1161/CIRCRESAHA.109.210781.

Peachey, L. D. and Huxley, A. F. (1962) 'STRUCTURAL IDENTIFICATION OF TWITCH AND SLOW STRIATED MUSCLE FIBERS OF THE FROG', *The Journal of Cell Biology*, 13(1), p. 177 LP-180. doi: 10.1083/jcb.13.1.177.

Peng, Y., Gregorich, Z. R., Valeja, S. G., Zhang, H., Cai, W., Chen, Y. C., Guner, H., Chen,

A. J., Schwahn, D. J., Hacker, T. A., Liu, X. and Ge, Y. (2014) 'Top-down proteomics reveals concerted reductions in myofilament and Z-disc protein phosphorylation after acute myocardial infarction', *Molecular and Cellular Proteomics*, 13(10), pp. 2752–2764. doi: 10.1074/mcp.M114.040675.

Perbellini, F., Watson, S. A., Bardi, I. and Terracciano, C. M. (2018) 'Heterocellularity and Cellular Cross-Talk in the Cardiovascular System', *Frontiers in Cardiovascular Medicine*, 5(November), pp. 1–11. doi: 10.3389/fcvm.2018.00143.

Perrone, C. A., Tritschler, D., Taulman, P., Bower, R., Yoder, B. K. and Porter, M. E. (2003) 'A novel dynein light intermediate chain colocalizes with the retrograde motor for intraflagellar transport at sites of axoneme assembly in chlamydomonas and Mammalian cells.', *Molecular biology of the cell*. United States, 14(5), pp. 2041–2056. doi: 10.1091/mbc.e02-10-0682.

Perry, M. D., Ng, C.-A., Mann, S. A., Sadrieh, A., Imtiaz, M., Hill, A. P. and Vandenberg, J. I. (2015) 'Getting to the heart of hERG K(+) channel gating.', *The Journal of physiology*. England, 593(12), pp. 2575–2585. doi: 10.1113/JP270095.

Petroff, M. G., Kim, S. H., Pepe, S., Dessy, C., Marban, E., Balligand, J. L. and Sollott, S. J. (2001) 'Endogenous nitric oxide mechanisms mediate the stretch dependence of Ca2+ release in cardiomyocytes.', *Nature cell biology*. England, 3(10), pp. 867–873. doi: 10.1038/ncb1001-867.

Phuyal, S., Hessvik, N. P., Skotland, T., Sandvig, K. and Llorente, A. (2014) 'Regulation of exosome release by glycosphingolipids and flotillins', *FEBS Journal*, 281(9), pp. 2214–2227. doi: 10.1111/febs.12775.

Piacentino, V. 3rd, Weber, C. R., Chen, X., Weisser-Thomas, J., Margulies, K. B., Bers, D. M. and Houser, S. R. (2003) 'Cellular basis of abnormal calcium transients of failing human ventricular myocytes', *Circulation Research*. United States, 92(6), pp. 651–658. doi: 10.1161/01.RES.0000062469.83985.9B.

Pinsky, D. J., Patton, S., Mesaros, S., Brovkovych, V., Kubaszewski, E., Grunfeld, S. and Malinski, T. (1997) 'Mechanical transduction of nitric oxide synthesis in the beating heart.', *Circulation research*. United States, 81(3), pp. 372–379.

Pinto, A. R., Ilinykh, A., Ivey, M. J., Kuwabara, J. T., D'Antoni, M. L., Debuque, R., Chandran, A., Wang, L., Arora, K., Rosenthal, N. A. and Tallquist, M. D. (2016) 'Revisiting Cardiac Cellular Composition.', *Circulation research*. United States, 118(3), pp. 400–409. doi:

10.1161/CIRCRESAHA.115.307778.

Pinz, I., Zhu, M., Mende, U. and Ingwall, J. S. (2011) 'An Improved Isolation Procedure for Adult Mouse Cardiomyocytes', *Cell Biochemistry and Biophysics*, 61(1), pp. 93–101. doi: 10.1007/s12013-011-9165-9.

Pioner, J. M., Racca, A. W., Klaiman, J. M., Yang, K.-C., Guan, X., Pabon, L., Muskheli, V., Zaunbrecher, R., Macadangdang, J., Jeong, M. Y., Mack, D. L., Childers, M. K., Kim, D.-H., Tesi, C., Poggesi, C., Murry, C. E. and Regnier, M. (2016) 'Isolation and Mechanical Measurements of Myofibrils from Human Induced Pluripotent Stem Cell-Derived Cardiomyocytes.', *Stem cell reports*. United States, 6(6), pp. 885–896. doi: 10.1016/j.stemcr.2016.04.006.

Pirkmajer, S. and Chibalin, A. V. (2011) ' Serum starvation: caveat emptor ', *American Journal of Physiology-Cell Physiology*, 301(2), pp. C272–C279. doi: 10.1152/ajpcell.00091.2011.

Poindexter, B. J., Smith, J. R., Buja, L. M. and Bick, R. J. (2001) 'Calcium signaling mechanisms in dedifferentiated cardiac myocytes: Comparison with neonatal and adult cardiomyocytes', *Cell Calcium*. Netherlands, 30(6), pp. 373–382. doi: 10.1054/ceca.2001.0249.

Porter, K. E. and Turner, N. A. (2009) 'Cardiac fibroblasts: At the heart of myocardial remodeling', *Pharmacology and Therapeutics*, 123(2), pp. 255–278. doi: 10.1016/j.pharmthera.2009.05.002.

Pott, C., Eckardt, L. and Goldhaber, J. I. (2011) 'Triple threat: the Na+/Ca2+ exchanger in the pathophysiology of cardiac arrhythmia, ischemia and heart failure.', *Current drug targets*. United Arab Emirates, 12(5), pp. 737–747.

Prendergast, B. D., Sagach, V. F. and Shah, A. M. (1997) 'Basal release of nitric oxide augments the Frank-Starling response in the isolated heart.', *Circulation*. United States, 96(4), pp. 1320–1329. doi: 10.1161/01.cir.96.4.1320.

Protasi, F., Sun, X. H. and Franzini-Armstrong, C. (1996) 'Formation and maturation of the calcium release apparatus in developing and adult avian myocardium', *Developmental Biology*, 173(1), pp. 265–278. doi: 10.1006/dbio.1996.0022.

Pulina, M. V, Hou, S.-Y., Mittal, A., Julich, D., Whittaker, C. A., Holley, S. A., Hynes, R. O. and Astrof, S. (2011) 'Essential roles of fibronectin in the development of the left-right embryonic body plan.', *Developmental biology*. United States, 354(2), pp. 208–220. doi:

10.1016/j.ydbio.2011.03.026.

Purushothaman, A., Bandari, S. K., Liu, J., Mobley, J. A., Brown, E. E. and Sanderson, R. D. (2016) 'Fibronectin on the Surface of Myeloma Cell-derived Exosomes Mediates Exosome-Cell Interactions.', *The Journal of biological chemistry*. United States, 291(4), pp. 1652–1663. doi: 10.1074/jbc.M115.686295.

Van Putten, R. M. E. M., Mengarelli, I., Guan, K., Zegers, J. G., Van Ginneken, A. C. G., Verkerk, A. O. and Wilders, R. (2015) 'Ion channelopathies in human induced pluripotent stem cell derived cardiomyocytes: A dynamic clamp study with virtual IK1', *Frontiers in Physiology*, 6(FEB), pp. 1–16. doi: 10.3389/fphys.2015.00007.

Pyo, R. T., Sui, J., Dhume, A., Palomeque, J., Blaxall, B. C., Diaz, G., Tunstead, J., Logothetis, D. E., Hajjar, R. J. and Schecter, A. D. (2006) 'CXCR4 modulates contractility in adult cardiac myocytes', *Journal of molecular and cellular cardiology*. 2006/09/28, 41(5), pp. 834–844. doi: 10.1016/j.yjmcc.2006.08.008.

Rajendran, P., Rengarajan, T., Thangavel, J., Nishigaki, Y., Sakthisekaran, D., Sethi, G. and Nishigaki, I. (2013) 'The vascular endothelium and human diseases', *International Journal of Biological Sciences*, 9(10), pp. 1057–1069. doi: 10.7150/ijbs.7502.

Ramay, H. R., Liu, O. Z. and Sobie, E. A. (2011) 'Recovery of cardiac calcium release is controlled by sarcoplasmic reticulum refilling and ryanodine receptor sensitivity', *Cardiovascular Research*, 91(4), pp. 598–605. doi: 10.1093/cvr/cvr143.

Ramirez-Montagut, T., Blachere, N. E., Sviderskaya, E. V, Bennett, D. C., Rettig, W. J., Garin-Chesa, P. and Houghton, A. N. (2004) 'FAPalpha, a surface peptidase expressed during wound healing, is a tumor suppressor.', *Oncogene*. England, 23(32), pp. 5435–5446. doi: 10.1038/sj.onc.1207730.

Rana, M. S., Christoffels, V. M. and Moorman, A. F. M. (2013) 'A molecular and genetic outline of cardiac morphogenesis.', *Acta physiologica (Oxford, England)*. England, 207(4), pp. 588–615. doi: 10.1111/apha.12061.

Rao, C., Prodromakis, T., Chaudhry, U., Camelliti, P., Yacoub, M. H., Darzi, A., Ali, N. N., Athanasiou, T. and Terracciano, C. M. (2012) 'Structured Culture Scaffolds Improve the Calcium Handling Properties of Cardiomyocytes Differentiated from Induced Pluripotent Stem Cells', *Biophysj*. Biophysical Society, 102(3), p. 103a. doi: 10.1016/j.bpj.2011.11.579.

Rao, C., Prodromakis, T., Kolker, L., Chaudhry, U. A. R., Trantidou, T., Sridhar, A., Weekes, C., Camelliti, P., Harding, S. E., Darzi, A., Yacoub, M. H., Athanasiou, T. and

Terracciano, C. M. (2013) 'The effect of microgrooved culture substrates on calcium cycling of cardiac myocytes derived from human induced pluripotent stem cells', *Biomaterials*. Elsevier Ltd, 34(10), pp. 2399–2411. doi: 10.1016/j.biomaterials.2012.11.055.

Raposo, G. and Stoorvogel, W. (2013) 'Extracellular vesicles: Exosomes, microvesicles, and friends', *Journal of Cell Biology*, 200(4), pp. 373–383. doi: 10.1083/jcb.201211138.

Rauch, J., Volinsky, N., Romano, D. and Kolch, W. (2011) 'The secret life of kinases: Functions beyond catalysis', *Cell Communication and Signaling*. BioMed Central Ltd, 9(1), p. 23. doi: 10.1186/1478-811X-9-23.

Rehsia, N. S. and Dhalla, N. S. (2010) 'Potential of endothelin-1 and vasopressin antagonists for the treatment of congestive heart failure.', *Heart failure reviews*. United States, 15(1), pp. 85–101. doi: 10.1007/s10741-009-9152-z.

Rettig, W. J., Garin-Chesa, P., Healey, J. H., Su, S. L., Ozer, H. L., Schwab, M., Albino, A. P. and Old, L. J. (1993) 'Regulation and heteromeric structure of the fibroblast activation protein in normal and transformed cells of mesenchymal and neuroectodermal origin.', *Cancer research*. United States, 53(14), pp. 3327–3335.

Rocchetti, M., Sala, L., Dreizehnter, L., Crotti, L., Sinnecker, D., Mura, M., Pane, L. S., Altomare, C., Torre, E., Mostacciuolo, G., Severi, S., Porta, A., De Ferrari, G. M., George, A. L., Schwartz, P. J., Gnecchi, M., Moretti, A. and Zaza, A. (2017) 'Elucidating arrhythmogenic mechanisms of long-QT syndrome CALM1-F142L mutation in patient-specific induced pluripotent stem cell-derived cardiomyocytes', *Cardiovascular Research*, 113(5), pp. 531–541. doi: 10.1093/cvr/cvx006.

Rohr, S. (2004) 'Role of gap junctions in the propagation of the cardiac action potential.', *Cardiovascular research*. England, 62(2), pp. 309–322. doi: 10.1016/j.cardiores.2003.11.035.

Ronaldson, K., Ma, S. P., Yeager, K., Chen, T., Song, L., Sirabella, D., Ronaldson-Bouchard, K., Ma, S. P., Yeager, K., Chen, T., Song, L., Sirabella, D., Morikawa, K., Teles, D., Yazawa, M. and Vunjak-Novakovic, G. (2018) 'Advanced maturation of human cardiac tissue grown from pluripotent stem cells', *Nature*. Springer US. doi: 10.1038/s41586-018-0016-3.

Ross, R. S. and Borg, T. K. (2001) 'Integrins and the myocardium', *Circulation Research*, 88(11), pp. 1112–1119. doi: 10.1161/hh1101.091862.

Rueden, C. T., Schindelin, J., Hiner, M. C., DeZonia, B. E., Walter, A. E., Arena, E. T. and Eliceiri, K. W. (2017) 'ImageJ2: ImageJ for the next generation of scientific image data.', *BMC*

bioinformatics. England, 18(1), p. 529. doi: 10.1186/s12859-017-1934-z.

Ruivo, C. F., Adem, B., Silva, M. and Melo, S. A. (2017) 'The biology of cancer exosomes: Insights and new perspectives', *Cancer Research*, 77(23), pp. 6480–6488. doi: 10.1158/0008-5472.CAN-17-0994.

Ruoslahti, E. and Pierschbacher, M. D. (1987) 'New perspectives in cell adhesion: RGD and integrins.', *Science (New York, N.Y.)*. United States, 238(4826), pp. 491–7. doi: 10.1126/science.2821619.

Ryan, A. J., Brougham, C. M., Garciarena, C. D., Kerrigan, S. W. and O'Brien, F. J. (2016) 'Towards 3D in vitro models for the study of cardiovascular tissues and disease', *Drug Discovery Today*. Elsevier Ltd, 21(9), pp. 1437–1445. doi: 10.1016/j.drudis.2016.04.014.

Saito, Y., Nakamura, K., Yoshida, M., Sugiyama, H., Ohe, T., Kurokawa, J., Furukawa, T., Takano, M., Nagase, S., Morita, H., Kusano, K. F. and Ito, H. (2015) 'Enhancement of Spontaneous Activity by HCN4 Overexpression in Mouse Embryonic Stem Cell-Derived Cardiomyocytes - A Possible Biological Pacemaker.', *PloS one*. United States, 10(9), p. e0138193. doi: 10.1371/journal.pone.0138193.

Salih, M., Zietse, R. and Hoorn, E. J. (2014) 'Urinary extracellular vesicles and the kidney: biomarkers and beyond', *American Journal of Physiology-Renal Physiology*, 306(11), pp. F1251–F1259. doi: 10.1152/ajprenal.00128.2014.

Sanguinetti, M. C. and Tristani-Firouzi, M. (2006) 'hERG potassium channels and cardiac arrhythmia.', *Nature*. England, 440(7083), pp. 463–469. doi: 10.1038/nature04710.

Sarkar, S., Vellaichamy, E., Young, D. and Sen, S. (2019) 'Influence of cytokines and growth factors in ANG II-mediated collagen upregulation by fibroblasts in rats : role of myocytes', 44195(Nb 50), pp. 107–117.

Sartiani, L., Bettiol, E., Stillitano, F., Mugelli, A., Cerbai, E. and Jaconi, M. E. (2007) 'Developmental changes in cardiomyocytes differentiated from human embryonic stem cells: a molecular and electrophysiological approach.', *Stem cells (Dayton, Ohio)*. United States, 25(5), pp. 1136–1144. doi: 10.1634/stemcells.2006-0466.

Sauk, J. J., Nikitakis, N. and Siavash, H. (2005) 'Hsp47 a novel collagen binding serpin chaperone, autoantigen and therapeutic target.', *Frontiers in bioscience : a journal and virtual library*. United States, 10, pp. 107–118.

Savarese, G. and Lund, L. H. (2017) 'Global Public Health Burden of Heart Failure', *Cardiac failure review*. Radcliffe Cardiology, 3(1), pp. 7–11. doi: 10.15420/cfr.2016:25:2.

Schaper, J., Meiser, E. and Stammler, G. (1985) 'Ultrastructural morphometric analysis of myocardium from dogs, rats, hamsters, mice, and from human hearts.', *Circulation research*. United States, 56(3), pp. 377–391.

Schick, R., Mekies, L., Shemer, Y., Hallas, T., Ben-Ari, M., Gherghiceanu, M., Simona Pane, L., My, I., Freimark, D., Arad, M., Moretti, A. and Binah, O. (2017) 'P3496Functional abnormalities in induced pluripotent stem cell-derived cardiomyocytes generated from titin-mutated dilated cardiomyopathy patients', *European Heart Journal*, 38(suppl_1), pp. 1–25. doi: 10.1093/eurheartj/ehx504.p3496.

Schneider, C. A., Rasband, W. S. and Eliceiri, K. W. (2012) 'NIH Image to ImageJ: 25 years of image analysis.', *Nature methods*. United States, 9(7), pp. 671–675.

Shai, S.-Y., Harpf, A. E., Babbitt, C. J., Jordan, M. C., Fishbein, M. C., Chen, J., Omura, M., Leil, T. A., Becker, K. D., Jiang, M., Smith, D. J., Cherry, S. R., Loftus, J. C. and Ross, R. S. (2002) 'Cardiac myocyte-specific excision of the beta1 integrin gene results in myocardial fibrosis and cardiac failure.', *Circulation research*. United States, 90(4), pp. 458–464.

Shanks, N., Greek, R. and Greek, J. (2009) 'Are animal models predictive for humans?', *Philosophy, Ethics, and Humanities in Medicine*, 4(1), pp. 1–20. doi: 10.1186/1747-5341-4-2.

Sharp, W. W., Simpson, D. G., Borg, T. K., Samarel, A. M. and Terracio, L. (1997) 'Mechanical forces regulate focal adhesion and costamere assembly in cardiac myocytes.', *The American journal of physiology*. United States, 273(2 Pt 2), pp. H546-56. doi: 10.1152/ajpheart.1997.273.2.H546.

Shelke, G. V., La, C., Gho, Y. S. and Lo, J. (2014) 'Importance of exosome depletion protocols to eliminate functional and RNA-containing extracellular vesicles from fetal bovine serum', 1, pp. 1–8.

Shelton, M., Kocharyan, A., Liu, J., Skerjanc, I. S. and Stanford, W. L. (2016) 'Robust generation and expansion of skeletal muscle progenitors and myocytes from human pluripotent stem cells', *Methods*. Elsevier Inc., 101, pp. 73–84. doi: 10.1016/j.ymeth.2015.09.019.

Shioshita, K., Miyazaki, M., Ozono, Y., Abe, K., Taura, K., Harada, T., Koji, T., Taguchi, T. and Kohno, S. (2000) 'Expression of heat shock proteins 47 and 70 in the peritoneum of patients on continuous ambulatory peritoneal dialysis.', *Kidney international*. United States, 57(2), pp. 619–631. doi: 10.1046/j.1523-1755.2000.00883.x.

Shirazi, L. F., Bissett, J., Romeo, F. and Mehta, J. L. (2017) 'Role of Inflammation in

Heart Failure', *Current Atherosclerosis Reports*. Current Atherosclerosis Reports, 19(6). doi: 10.1007/s11883-017-0660-3.

Singh, V. K., Kumar, N., Kalsan, M., Saini, A. and Chandra, R. (2015) 'Mechanism of Induction: Induced Pluripotent Stem Cells (iPSCs).', *Journal of stem cells*. United States, 10(1), pp. 43–62.

Slotkin, T. A., Lau, C. and Seidler, F. J. (1994) 'Beta-adrenergic receptor overexpression in the fetal rat: distribution, receptor subtypes, and coupling to adenylate cyclase activity via G-proteins.', *Toxicology and applied pharmacology*. United States, 129(2), pp. 223–234. doi: 10.1006/taap.1994.1247.

Smith, A. G. (2001) 'Embryo-derived stem cells: of mice and men.', *Annual review of cell and developmental biology*. United States, 17, pp. 435–462. doi: 10.1146/annurev.cellbio.17.1.435.

Smith, T. J. (2004) 'Novel aspects of orbital fibroblast pathology.', *Journal of endocrinological investigation*. Italy, 27(3), pp. 246–253. doi: 10.1007/BF03345273.

Smithies, O. (1993) 'Animal models of human genetic diseases', *Trends in Genetics*, 9(4), pp. 112–116. doi: 10.1016/0168-9525(93)90204-U.

Snider, P., Standley, K. N., Wang, J., Azhar, M., Doetschman, T. and Conway, S. J. (2009) 'Origin of Cardiac Fibroblasts and the Role of Periostin', *Circulation Research*, 105(10), pp. 934–947. doi: 10.1161/CIRCRESAHA.109.201400.

Spach, M. S. and Boineau, J. P. (1997) 'Microfibrosis produces electrical load variations due to loss of side-to-side cell connections: a major mechanism of structural heart disease arrhythmias.', *Pacing and clinical electrophysiology : PACE*. United States, 20(2 Pt 2), pp. 397–413.

Spater, D., Hansson, E. M., Zangi, L. and Chien, K. R. (2014) 'How to make a cardiomyocyte', *Development*, 141(23), pp. 4418–4431. doi: 10.1242/dev.091538.

Stephens, L. E., Sutherland, A. E., Klimanskaya, I. V, Andrieux, A., Meneses, J., Pedersen, R. A. and Damsky, C. H. (1995) 'Deletion of beta 1 integrins in mice results in inner cell mass failure and peri-implantation lethality.', *Genes & development*. United States, 9(15), pp. 1883–1895. doi: 10.1101/gad.9.15.1883.

Stevens, J. L. and Baker, T. K. (2009) 'The future of drug safety testing: expanding the view and narrowing the focus.', *Drug discovery today*. England, 14(3–4), pp. 162–167. doi: 10.1016/j.drudis.2008.11.009.

Stine, M. J., Wang, C. J., Moriarty, W. F., Ryu, B., Westra, W. H., Levchenko, A. and Alani, R. M. (2012) 'NIH Public Access', 71(7), pp. 2433–2444. doi: 10.1158/0008-5472.CAN-10-1875.Integration.

Strutz, F., Okada, H., Lo, C. W., Danoff, T., Carone, R. L., Tomaszewski, J. E. and Neilson, E. G. (1995) 'Identification and characterization of a fibroblast marker: FSP1', *Journal of Cell Biology*. United States, 130(2), pp. 393–405. doi: 10.1083/jcb.130.2.393.

Subra, C., Laulagnier, K., Perret, B. and Record, M. (2007) 'Exosome lipidomics unravels lipid sorting at the level of multivesicular bodies', *Biochimie*, 89(2), pp. 205–212. doi: 10.1016/j.biochi.2006.10.014.

Sugimoto, H., Mundel, T. M., Kieran, M. W. and Kalluri, R. (2006) 'Identification of fibroblast heterogeneity in the tumor microenvironment.', *Cancer biology & therapy*. United States, 5(12), pp. 1640–1646. doi: 10.4161/cbt.5.12.3354.

Sung, B. H., Ketova, T., Hoshino, D., Zijlstra, A. and Weaver, A. M. (2015) 'Directional cell movement through tissues is controlled by exosome secretion', *Nature Communications*. Nature Publishing Group, 6(May), pp. 1–14. doi: 10.1038/ncomms8164.

Suryakumar, G., Kasiganesan, H., Balasubramanian, S. and Kuppuswamy, D. (2010) 'Lack of beta3 integrin signaling contributes to calpain-mediated myocardial cell loss in pressure-overloaded myocardium.', *Journal of cardiovascular pharmacology*. United States, 55(6), pp. 567–573. doi: 10.1097/FJC.0b013e3181d9f5d4.

Takahashi, K., Tanabe, K., Ohnuki, M., Narita, M., Ichisaka, T., Tomoda, K. and Yamanaka, S. (2007) '/SUPP/ Induction of pluripotent stem cells from adult human fibroblasts by defined factors.', *Cell*, 131(5), pp. 861–72. doi: 10.1016/j.cell.2007.11.019.

Takahashi, K. and Yamanaka, S. (2006) 'Induction of pluripotent stem cells from mouse embryonic and adult fibroblast cultures by defined factors.', *Cell*. United States, 126(4), pp. 663–676. doi: 10.1016/j.cell.2006.07.024.

Taranger, C. K., Noer, A., Sorensen, A. L., Hakelien, A.-M., Boquest, A. C. and Collas, P. (2005) 'Induction of dedifferentiation, genomewide transcriptional programming, and epigenetic reprogramming by extracts of carcinoma and embryonic stem cells.', *Molecular biology of the cell*. United States, 16(12), pp. 5719–5735. doi: 10.1091/mbc.e05-06-0572.

Taylor, D. D. and Shah, S. (2015) 'Methods of isolating extracellular vesicles impact down-stream analyses of their cargoes', *Methods*. Elsevier Inc., 87, pp. 3–10. doi: 10.1016/j.ymeth.2015.02.019.

Taylor, D. O., Edwards, L. B., Boucek, M. M., Trulock, E. P., Aurora, P., Christie, J., Dobbels, F., Rahmel, A. O., Keck, B. M. and Hertz, M. I. (2007) 'Registry of the International Society for Heart and Lung Transplantation: twenty-fourth official adult heart transplant report--2007.', *The Journal of heart and lung transplantation : the official publication of the International Society for Heart Transplantation*. United States, 26(8), pp. 769–781. doi: 10.1016/j.healun.2007.06.004.

Tejada, T., Tan, L., Torres, R. A., Calvert, J. W., Lambert, J. P., Zaidi, M., Husain, M., Berce, M. D., Naib, H., Pejler, G., Abrink, M., Graham, R. M., Lefer, D. J., Naqvi, N. and Husain, A. (2016) 'IGF-1 degradation by mouse mast cell protease 4 promotes cell death and adverse cardiac remodeling days after a myocardial infarction', *Proceedings of the National Academy of Sciences*, 113(25), pp. 6949–6954. doi: 10.1073/pnas.1603127113.

Terracciano, C. M. N., Hardy, J., Birks, E. J., Khaghani, A., Banner, N. R. and Yacoub, M. H. (2004) 'Clinical recovery from end-stage heart failure using left-ventricular assist device and pharmacological therapy correlates with increased sarcoplasmic reticulum calcium content but not with regression of cellular hypertrophy.', *Circulation*. United States, 109(19), pp. 2263–2265. doi: 10.1161/01.CIR.0000129233.51320.92.

Terracciano, C. M., Naqvi, R. U. and MacLeod, K. T. (1995) 'Effects of rest interval on the release of calcium from the sarcoplasmic reticulum in isolated guinea pig ventricular myocytes.', *Circulation research*. United States, 77(2), pp. 354–360.

Thedieck, C., Kalbacher, H., Kuczyk, M., Muller, G. A., Muller, C. A. and Klein, G. (2007) 'Cadherin-9 is a novel cell surface marker for the heterogeneous pool of renal fibroblasts.', *PloS one*. United States, 2(7), p. e657. doi: 10.1371/journal.pone.0000657.

Thery, C., Amigorena, S., Raposo, G. and Clayton, A. (2006) 'Isolation and characterization of exosomes from cell culture supernatants and biological fluids.', *Current protocols in cell biology*. United States, Chapter 3, p. Unit 3.22. doi: 10.1002/0471143030.cb0322s30.

Thomson, J. A., Itskovitz-Eldor, J., Shapiro, S. S., Waknitz, M. A., Swiergiel, J. J., Marshall, V. S. and Jones, J. M. (1998) 'Embryonic stem cell lines derived from human blastocysts', *Science*, 282(5391), pp. 1145–1147. doi: 10.1126/science.282.5391.1145.

Tian, Y. and Morrisey, E. E. (2012) 'Importance of myocyte-nonmyocyte interactions in cardiac development and disease', *Circulation Research*, 110(7), pp. 1023–1034. doi: 10.1161/CIRCRESAHA.111.243899.

Tohyama, S., Hattori, F., Sano, M., Hishiki, T., Nagahata, Y., Matsuura, T., Hashimoto, H., Suzuki, T., Yamashita, H., Satoh, Y., Egashira, T., Seki, T., Muraoka, N., Yamakawa, H., Ohgino, Y., Tanaka, T., Yoichi, M., Yuasa, S., Murata, M., Suematsu, M. and Fukuda, K. (2013) 'Distinct metabolic flow enables large-scale purification of mouse and human pluripotent stem cell-derived cardiomyocytes.', *Cell stem cell*. United States, 12(1), pp. 127–137. doi: 10.1016/j.stem.2012.09.013.

Trajkovic, K., Hsu, C., Chiantia, S., Rajendran, L., Wenzel, D., Wieland, F., Schwille, P., Brügger, B. and Simons, M. (2008) 'Supporting online material for: Ceramide Triggers Budding of Exosome Vesicles into Multivesicular Endosomes', *Science*, 319(1244), pp. 1–15. doi: 10.1126/science.1153124.

Trams, E. G., Lauter, C. J., Salem, N. J. and Heine, U. (1981) 'Exfoliation of membrane ecto-enzymes in the form of micro-vesicles.', *Biochimica et biophysica acta*. Netherlands, 645(1), pp. 63–70. doi: 10.1016/0005-2736(81)90512-5.

Tse, H.-F., Ho, J. C. Y., Choi, S.-W., Lee, Y.-K., Butler, A. W., Ng, K.-M., Siu, C.-W., Simpson, M. A., Lai, W.-H., Chan, Y.-C., Au, K.-W., Zhang, J., Lay, K. W. J., Esteban, M. A., Nicholls, J. M., Colman, A. and Sham, P. C. (2013) 'Patient-specific Induced Pluripotent Stem Cells Derived Cardiomycoytes Recapitulates the Pathogenic Phenotypes of Dilated Cardiomyopathy due to a Novel DES Mutation Identified by Whole Exome Sequencing.', *Human Molecular Genetics*, (852), pp. 1–28. Available at: http://eutils.ncbi.nlm.nih.gov/entrez/eutils/elink.fcgi?dbfrom=pubmed&id=23300193&retmode=ref&cmd=prlinks\npapers2://publication/doi/10.1093/hmg/dds556.

Tsuruda, T., Costello-Boerrigter, L. C. and Burnett, J. C. J. (2004) 'Matrix metalloproteinases: pathways of induction by bioactive molecules.', *Heart failure reviews*. United States, 9(1), pp. 53–61. doi: 10.1023/B:HREV.0000011394.34355.bb.

Tsutamoto, T., Wada, A., Maeda, K., Mabuchi, N., Hayashi, M., Tsutsui, T., Ohnishi, M., Sawaki, M., Fujii, M., Matsumoto, T., Horie, H., Sugimoto, Y. and Kinoshita, M. (2000) 'Transcardiac extraction of circulating endothelin-1 across the failing heart.', *The American journal of cardiology*. United States, 86(5), pp. 524–528.

Ueno, S., Weidinger, G., Osugi, T., Kohn, A. D., Golob, J. L., Pabon, L., Reinecke, H., Moon, R. T. and Murry, C. E. (2007) 'Biphasic role for Wnt/beta-catenin signaling in cardiac specification in zebrafish and embryonic stem cells.', *Proceedings of the National Academy of Sciences of the United States of America*. United States, 104(23), pp. 9685–9690. doi:

10.1073/pnas.0702859104.

Umesh, A., Thompson, M. A., Chini, E. N., Yip, K. P. and Sham, J. S. K. (2006) 'Integrin ligands mobilize Ca2+ from ryanodine receptor-gated stores and lysosome-related acidic organelles in pulmonary arterial smooth muscle cells', *Journal of Biological Chemistry*, 281(45), pp. 34312–34323. doi: 10.1074/jbc.M606765200.

Vandenberg, J. I., Perry, M. D., Perrin, M. J., Mann, S. A., Ke, Y. and Hill, A. P. (2012) 'hERG K(+) channels: structure, function, and clinical significance.', *Physiological reviews*. United States, 92(3), pp. 1393–1478. doi: 10.1152/physrev.00036.2011.

Varro, A., Negretti, N., Hester, S. B. and Eisner, D. A. (1993) 'An estimate of the calcium content of the sarcoplasmic reticulum in rat ventricular myocytes.', *Pflugers Archiv : European journal of physiology*. Germany, Germany, 423(1–2), pp. 158–160.

Veerman, C. C., Mengarelli, I., Guan, K., Stauske, M., Barc, J., Tan, H. L., Wilde, A. A. M., Verkerk, A. O. and Bezzina, C. R. (2016) 'HiPSC-derived cardiomyocytes from Brugada Syndrome patients without identified mutations do not exhibit clear cellular electrophysiological abnormalities', *Scientific Reports*. Nature Publishing Group, 6(August), pp. 1–10. doi: 10.1038/srep30967.

Venetucci, L. A., Trafford, A. W. and Eisner, D. A. (2006) 'Increasing Ryanodine Receptor Open Probability Alone Does Not Produce Arrhythmogenic Calcium Waves', *Circulation Research*, 100(1), pp. 105–111. doi: 10.1161/01.res.0000252828.17939.00.

Verkerk, A. O. and Wilders, R. (2015) 'Pacemaker activity of the human sinoatrial node: an update on the effects of mutations in HCN4 on the hyperpolarization-activated current.', *International journal of molecular sciences*. Switzerland, 16(2), pp. 3071–3094. doi: 10.3390/ijms16023071.

Vickers, K. C., Palmisano, B. T., Shoucri, B. M., Shamburek, R. D. and Remaley, A. T. (2011) 'HHS Public Access', 13(4), pp. 423–433. doi: 10.1038/ncb2210.MicroRNAs.

Vidarsson, H., Hyllner, J. and Sartipy, P. (2010) 'Differentiation of human embryonic stem cells to cardiomyocytes for in vitro and in vivo applications.', *Stem cell reviews and reports*. United States, 6(1), pp. 108–120. doi: 10.1007/s12015-010-9113-x.

Vlassov, A. V, Magdaleno, S., Setterquist, R. and Conrad, R. (2012) 'Exosomes: current knowledge of their composition, biological functions, and diagnostic and therapeutic potentials.', *Biochimica et biophysica acta*. Netherlands, 1820(7), pp. 940–948. doi: 10.1016/j.bbagen.2012.03.017.

Vogel, W. F., Abdulhussein, R. and Ford, C. E. (2006) 'Sensing extracellular matrix: an update on discoidin domain receptor function.', *Cellular signalling*. England, 18(8), pp. 1108–1116. doi: 10.1016/j.cellsig.2006.02.012.

Vornanen, M., Shepherd, N. and Isenberg, G. (2017) 'Tension-voltage relations of single myocytes reflect Ca release triggered by Na/Ca exchange at 35 degrees C but not 23 degrees C', *American Journal of Physiology-Cell Physiology*, 267(2), pp. C623–C632. doi: 10.1152/ajpcell.1994.267.2.c623.

Vozenin, M. C., Lefaix, J. L., Ridi, R., Biard, D. S., Daburon, F. and Martin, M. (1998) 'The myofibroblast markers alpha-SM actin and beta-actin are differentially expressed in 2 and 3-D culture models of fibrotic and normal skin.', *Cytotechnology*. United States, 26(1), pp. 29–38. doi: 10.1023/A:1007992824966.

Wagner, J., Riwanto, M., Besler, C., Knau, A., Fichtlscherer, S., Roxe, T., Zeiher, A. M., Landmesser, U. and Dimmeler, S. (2013) 'Characterization of levels and cellular transfer of circulating lipoprotein-bound microRNAs.', *Arteriosclerosis, thrombosis, and vascular biology*. United States, 33(6), pp. 1392–1400. doi: 10.1161/ATVBAHA.112.300741.

Wang, B., Kit-Anan, W. and Terracciano, C. (2018) 'Many Cells Make Life Work—Multicellularity in Stem Cell-Based Cardiac Disease Modelling', *International Journal of Molecular Sciences*, 19(11), p. 3361. doi: 10.3390/ijms19113361.

Wang, C., Ho, P. C. and Lim, L. Y. (2010) 'Wheat germ agglutinin-conjugated markers', *International Journal of Pharmaceutics*, 400(1–2), pp. 201–210. doi: 10.1016/j.ijpharm.2010.08.023.

Wang, G., McCain, M. L., Yang, L., He, A., Pasqualini, F. S., Agarwal, A., Yuan, H., Jiang, D., Zhang, D., Zangi, L., Geva, J., Roberts, A. E., Ma, Q., Ding, J., Chen, J., Wang, D.-Z. Z., Li, K., Wang, J., Wanders, R. J. A. A., Kulik, W., Vaz, F. M., Laflamme, M. A., Murry, C. E., Chien, K. R., Kelley, R. I., Church, G. M., Parker, K. K. and Pu, W. T. (2014) 'Modeling the mitochondrial cardiomyopathy of Barth syndrome with induced pluripotent stem cell and heart-on-chip technologies', *Nature Medicine*, 20(6), pp. 616–623. doi: 10.1038/nm.3545.

Wang, N., Tytell, J. D. and Ingber, D. E. (2009) 'Mechanotransduction at a distance: mechanically coupling the extracellular matrix with the nucleus.', *Nature Reviews Molecular Cell Biology*. England, 10(1), pp. 75–82. doi: 10.1038/nrm2594.

Wang, R. N., Green, J., Wang, Z., Deng, Y., Qiao, M., Peabody, M., Zhang, Q., Ye, J., Yan, Z., Denduluri, S., Idowu, O., Li, M., Shen, C., Hu, A., Haydon, R. C., Kang, R., Mok, J., Lee, M. J.,

Luu, H. L. and Shi, L. L. (2014) 'Bone Morphogenetic Protein (BMP) signaling in development and human diseases', *Genes & diseases*. Chongqing Medical University, 1(1), pp. 87–105. doi: 10.1016/j.gendis.2014.07.005.

Wang, W. E., Li, L., Xia, X., Fu, W., Liao, Q., Lan, C., Yang, D., Chen, H., Yue, R., Zeng, C., Zhou, L., Zhou, B., Duan, D. D., Chen, X., Houser, S. R. and Zeng, C. (2017) 'Dedifferentiation, proliferation, and redifferentiation of adult mammalian cardiomyocytes after ischemic injury', *Circulation*, 136(9), pp. 834–848. doi: 10.1161/CIRCULATIONAHA.116.024307.

Wang, X., Huang, W., Liu, G., Cai, W., Millard, R. W., Wang, Y., Chang, J., Peng, T. and Fan, G.-C. (2014) 'Cardiomyocytes mediate anti-angiogenesis in type 2 diabetic rats through the exosomal transfer of miR-320 into endothelial cellsWang, X., Huang, W., Liu, G., Cai, W., Millard, R. W., Wang, Y., Chang, J., Peng, T. and Fan, G.-C. (2014) 'Cardiomyocytes medi', *Journal of molecular and cellular cardiology*. 2014/05/10, 74, pp. 139–150. doi: 10.1016/j.yjmcc.2014.05.001.

Wartiovaara, J., Linder, E., Ruoslahti, E. and Vaheri, A. (1974) 'Distribution of fibroblast surface antigen: association with fibrillar structures of normal cells and loss upon viral transformation.', *The Journal of experimental medicine*. United States, 140(6), pp. 1522–1533. doi: 10.1084/jem.140.6.1522.

Webber, J. and Clayton, A. (2013) 'How pure are your vesicles?', *Journal of Extracellular Vesicles*, 2(1), pp. 1–6. doi: 10.3402/jev.v2i0.19861.

Weber, K. T. (1989) 'Cardiac interstitium in health and disease: the fibrillar collagen network.', *Journal of the American College of Cardiology*. United States, 13(7), pp. 1637–1652.

Van Der Wees, C. G. C., Bax, W. H., Van Der Valk, E. J. M. and Van Der Laarse, A. (2006) 'Integrin stimulation induces calcium signalling in rat cardiomyocytes by a NO-dependent mechanism', *Pflugers Archiv European Journal of Physiology*, 451(4), pp. 588–595. doi: 10.1007/s00424-005-1402-x.

Wen, J.-Y., Wei, C.-Y., Shah, K., Wong, J., Wang, C. and Chen, H.-S. V. (2015) 'Maturation-Based Model of Arrhythmogenic Right Ventricular Dysplasia Using Patient-Specific Induced Pluripotent Stem Cells', *Circulation Journal*, 79(7), pp. 1402–1408. doi: 10.1253/circj.CJ-15-0363.

Wetzel, A., Wetzig, T., Haustein, U. F., Sticherling, M., Anderegg, U., Simon, J. C. and Saalbach, A. (2006) 'Increased neutrophil adherence in psoriasis: role of the human endothelial cell receptor Thy-1 (CD90).', *The Journal of investigative dermatology*. United

States, 126(2), pp. 441–452. doi: 10.1038/sj.jid.5700072.

Wheelwright, M., Win, Z., Mikkila, J. L., Amen, K. Y., Alford, P. W. and Metzger, J. M. (2018) 'Investigation of human iPSC-derived cardiac myocyte functional maturation by single cell traction force microscopy.', *PloS one*. United States, 13(4), p. e0194909. doi: 10.1371/journal.pone.0194909.

White, C. I., Jansen, M. A., McGregor, K., Mylonas, K. J., Richardson, R. V., Thomson, A., Moran, C. M., Seckl, J. R., Walker, B. R., Chapman, K. E. and Gray, G. A. (2016) 'Cardiomyocyte and vascular smooth muscle-independent 11β-hydroxysteroid dehydrogenase 1 amplifies infarct expansion, hypertrophy, and the development of heart failure after myocardial infarction in male mice', *Endocrinology*, 157(1), pp. 346–357. doi: 10.1210/en.2015-1630.

Whitelaw, C. B. A., Sheets, T. P., Lillico, S. G. and Telugu, B. P. (2016) 'Engineering large animal models of human disease', *Journal of Pathology*, 238(2), pp. 247–256. doi: 10.1002/path.4648.

van Wijk, B., Moorman, A. F. M. and van den Hoff, M. J. B. (2007) 'Role of bone morphogenetic proteins in cardiac differentiation', *Cardiovascular Research*, 74(2), pp. 244–255. doi: 10.1016/j.cardiores.2006.11.022.

Willms, E., Johansson, H. J., Mäger, I., Lee, Y., Blomberg, K. E. M., Sadik, M., Alaarg, A., Smith, C. I. E., Lehtiö, J., El Andaloussi, S., Wood, M. J. A. and Vader, P. (2016) 'Cells release subpopulations of exosomes with distinct molecular and biological properties', *Scientific Reports*. Nature Publishing Group, 6(February), pp. 1–12. doi: 10.1038/srep22519.

Wright, C. S. (1984) 'Structural comparison of the two distinct sugar binding sites in wheat germ agglutinin isolectin II.', *Journal of molecular biology*. England, England, 178(1), pp. 91–104.

Wu, C.-K., Lee, J.-K., Chiang, F.-T., Yang, C.-H., Huang, S.-W., Hwang, J.-J., Lin, J.-L., Tseng, C.-D., Chen, J.-J. and Tsai, C.-T. (2011) 'Plasma levels of tumor necrosis factor-alpha and interleukin-6 are associated with diastolic heart failure through downregulation of sarcoplasmic reticulum Ca2+ ATPase.', *Critical care medicine*. United States, 39(5), pp. 984–992. doi: 10.1097/CCM.0b013e31820a91b9.

Xi, J., Khalil, M., Shishechian, N., Hannes, T., Pfannkuche, K., Liang, H., Fatima, A., Haustein, M., Suhr, F., Bloch, W., Reppel, M., Saric, T., Wernig, M., Janisch, R., Brockmeier, K., Hescheler, J. and Pillekamp, F. (2010) 'Comparison of contractile behavior of native murine

ventricular tissue and cardiomyocytes derived from embryonic or induced pluripotent stem cells.', *FASEB journal : official publication of the Federation of American Societies for Experimental Biology*. United States, 24(8), pp. 2739–2751. doi: 10.1096/fj.09-145177.

Xiang, Y., Rybin, V. O., Steinberg, S. F. and Kobilka, B. (2002) 'Caveolar localization dictates physiologic signaling of β2-adrenoceptors in neonatal cardiac myocytes', *Journal of Biological Chemistry*, 277(37), pp. 34280–34286. doi: 10.1074/jbc.M201644200.

Yabluchanskiy, A., Ma, Y., Deleon-Pennell, K. Y., Altara, R., Halade, G. V., Voorhees, A. P., Nguyen, N. T., Jin, Y. F., Winniford, M. D., Hall, M. E., Han, H. C. and Lindsey, M. L. (2016) 'Myocardial infarction superimposed on aging: MMP-9 deletion promotes M2 macrophage polarization', *Journals of Gerontology - Series A Biological Sciences and Medical Sciences*, 71(4), pp. 475–483. doi: 10.1093/gerona/glv034.

Yamasaki-Mann, M., Demuro, A. and Parker, I. (2010) 'Modulation of endoplasmic reticulum Ca2+ store filling by cyclic ADP-ribose promotes inositol trisphosphate (IP3)-evoked Ca 2+ signals', *Journal of Biological Chemistry*, 285(32), pp. 25053–25061. doi: 10.1074/jbc.M109.095257.

Yáñez-Mó, M., Siljander, P. R.-M., Andreu, Z., Zavec, A. B., Borràs, F. E., Buzas, E. I., Buzas, K., Casal, E., Cappello, F., Carvalho, J., Colás, E., Cordeiro-da Silva, A., Fais, S., Falcon-Perez, J. M., Ghobrial, I. M., Giebel, B., Gimona, M., Graner, M., Gursel, I., Gursel, M., Heegaard, N. H. H., Hendrix, A., Kierulf, P., Kokubun, K., Kosanovic, M., Kralj-Iglic, V., Krämer-Albers, E.-M., Laitinen, S., Lässer, C., Lener, T., Ligeti, E., Linē, A., Lipps, G., Llorente, A., Lötvall, J., Manček-Keber, M., Marcilla, A., Mittelbrunn, M., Nazarenko, I., Nolte-'t Hoen, E. N. M., Nyman, T. A., O'Driscoll, L., Olivan, M., Oliveira, C., Pállinger, É., Del Portillo, H. A., Reventós, J., Rigau, M., Rohde, E., Sammar, M., Sánchez-Madrid, F., Santarém, N., Schallmoser, K., Ostenfeld, M. S., Stoorvogel, W., Stukelj, R., Van der Grein, S. G., Vasconcelos, M. H., Wauben, M. H. M. and De Wever, O. (2015) 'Biological properties of extracellular vesicles and their physiological functions.', *Journal of extracellular vesicles*, 4(May), p. 27066. doi: 10.3402/jev.v4.27066.

Yang, X., Pabon, L. and Murry, C. E. (2014) 'Engineering Adolescence: Maturation of Human Pluripotent Stem Cell-Derived Cardiomyocytes', *Circulation Research*, 114(3), pp. 511–523. doi: 10.1161/CIRCRESAHA.114.300558.

Yazawa, M., Hsueh, B., Jia, X., Pasca, A. M., Bernstein, J. A., Hallmayer, J. and Dolmetsch, R. E. (2011) 'Using induced pluripotent stem cells to investigate cardiac

phenotypes in Timothy syndrome', *Nature*. Nature Publishing Group, 471(7337), pp. 230–236. doi: 10.1038/nature09855.

Yokoo, N., Baba, S., Kaichi, S., Niwa, A., Mima, T., Doi, H., Yamanaka, S., Nakahata, T. and Heike, T. (2009) 'The effects of cardioactive drugs on cardiomyocytes derived from human induced pluripotent stem cells.', *Biochemical and biophysical research communications*. United States: Elsevier Inc., 387(3), pp. 482–8. doi: 10.1016/j.bbrc.2009.07.052.

Yu, C. -h. C., Law, J. B. K., Suryana, M., Low, H. Y. and Sheetz, M. P. (2011) 'Early integrin binding to Arg-Gly-Asp peptide activates actin polymerization and contractile movement that stimulates outward translocation', *Proceedings of the National Academy of Sciences*. National Academy of Sciences, 108(51), p. 20585 LP-20590. doi: 10.1073/pnas.1109485108.

Yu, J., Vodyanik, M. A., Smuga-Otto, K., Antosiewicz-Bourget, J., Frane, J. L., Tian, S., Nie, J., Jonsdottir, G. A., Ruotti, V., Stewart, R., Slukvin, I. I. and Thomson, J. A. (2007) 'Induced pluripotent stem cell lines derived from human somatic cells.', *Science (New York, N.Y.)*. United States, 318(5858), pp. 1917–1920. doi: 10.1126/science.1151526.

Yu, Z., IJzerman, A. P. and Heitman, L. H. (2015) 'K<inf>v</inf>11.1 (hERG)-induced cardiotoxicity: A molecular insight from a binding kinetics study of prototypical K<inf>v</inf>11.1 (hERG) inhibitors', *British Journal of Pharmacology*, 172(3), pp. 940–955. doi: 10.1111/bph.12967.

Zeisberg, E. M., Tarnavski, O., Zeisberg, M., Dorfman, A. L., McMullen, J. R., Gustafsson, E., Chandraker, A., Yuan, X., Pu, W. T., Roberts, A. B., Neilson, E. G., Sayegh, M. H., Izumo, S. and Kalluri, R. (2007) 'Endothelial-to-mesenchymal transition contributes to cardiac fibrosis.', *Nature medicine*. United States, 13(8), pp. 952–961. doi: 10.1038/nm1613.

Zeng, Q., Guo, Y., Liu, L., Zhang, X., Li, R., Zhang, C., Hao, Q., Shi, C., Wu, J. and Guan, J. (2013) 'Cardiac fibroblast-derived extracellular matrix produced in vitro stimulates growth and metabolism of cultured ventricular cells.', *International heart journal*. Japan, 54(1), pp. 40–44.

Zhang, J. (2015) 'Engineered Tissue Patch for Cardiac Cell Therapy', *Current Treatment Options in Cardiovascular Medicine*, 17(8). doi: 10.1007/s11936-015-0399-5.

Zhang, J., Lian, Q., Zhu, G., Zhou, F., Sui, L., Tan, C., Mutalif, R. A., Navasankari, R., Zhang, Y., Tse, H. F., Stewart, C. L. and Colman, A. (2011) 'A human iPSC model of hutchinson gilford progeria reveals vascular smooth muscle and mesenchymal stem cell defects', *Cell*

Stem Cell. Elsevier Inc., 8(1), pp. 31–45. doi: 10.1016/j.stem.2010.12.002.

Zhang, J. Q., Elzey, B., Williams, G., Lu, S., Law, D. J. and Horowits, R. (2001) 'Ultrastructural and biochemical localization of N-RAP at the interface between myofibrils and intercalated disks in the mouse heart.', *Biochemistry*. United States, 40(49), pp. 14898–14906.

Zhang, J., Wilson, G. F., Soerens, A. G., Koonce, C. H., Yu, J., Palecek, S. P., Thomson, J. A. and Kamp, T. J. (2009) 'Functional cardiomyocytes derived from human induced pluripotent stem cells.', *Circulation research*. United States, 104(4), pp. e30-41. doi: 10.1161/CIRCRESAHA.108.192237.

Zhang, X.-H., Haviland, S., Wei, H., Saric, T., Fatima, A., Hescheler, J., Cleemann, L. and Morad, M. (2013) 'Ca2+ signaling in human induced pluripotent stem cell-derived cardiomyocytes (iPS-CM) from normal and catecholaminergic polymorphic ventricular tachycardia (CPVT)-afflicted subjects.', *Cell calcium*. Netherlands, 54(2), pp. 57–70. doi: 10.1016/j.ceca.2013.04.004.

Zhang, X. H. and Morad, M. (2016) 'Calcium signaling in human stem cell-derived cardiomyocytes: Evidence from normal subjects and CPVT afflicted patients', *Cell Calcium*. Elsevier Ltd, 59(2–3), pp. 98–107. doi: 10.1016/j.ceca.2015.12.002.

Zhang, Y., Li, T. S., Lee, S. T., Wawrowsky, K. A., Cheng, K., Galang, G., Malliaras, K., Abraham, M. R., Wang, C. and Marbán, E. (2010) 'Dedifferentiation and proliferation of mammalian cardiomyocytes', *PLoS ONE*, 5(9), pp. 1–13. doi: 10.1371/journal.pone.0012559.

Zhou, B., von Gise, A., Ma, Q., Hu, Y. W. and Pu, W. T. (2010) 'Genetic fate mapping demonstrates contribution of epicardium-derived cells to the annulus fibrosis of the mammalian heart.', *Developmental biology*. United States, 338(2), pp. 251–261. doi: 10.1016/j.ydbio.2009.12.007.

Zhou, P. and Pu, W. T. (2016) 'Recounting Cardiac Cellular Composition', *Circulation Research*, 118(3), pp. 368–370. doi: 10.1161/CIRCRESAHA.116.308139.

Zhou, Z., Gong, Q., Ye, B., Fan, Z., Makielski, J. C., Robertson, G. A. and January, C. T. (1998) 'Properties of HERG channels stably expressed in HEK 293 cells studied at physiological temperature', *Biophysical Journal*, 74(1), pp. 230–241. doi: 10.1016/S0006-3495(98)77782-3.

Zwi-Dantsis, L., Wang, B., Marijon, C., Zonetti, S., Ferrini, A., Massi, L., Stuckey, D. J., Terracciano, C. M. and Stevens, M. M. (2019) 'Remote Magnetic Nanoparticle Manipulation Enables the Dynamic Patterning of Cardiac Tissues', *Advanced Materials*, 1904598, pp. 1–6. doi: 10.1002/adma.201904598.

Zwi, L., Caspi, O., Arbel, G., Huber, I., Gepstein, A., Park, I. H. and Gepstein, L. (2009) 'Cardiomyocyte differentiation of human induced pluripotent stem cells', *Circulation*, 120(15), pp. 1513–1523. doi: 10.1161/CIRCULATIONAHA.109.868885.

8 Copyright permission

Table or figure	Reference	Information	Copyright holder	Details
Table 1.1	Wang, Kit-Anan and Terracciano, 2018	The role of non-myocyte cell types in health and in disease.	MDPI	Licensed under an open access Creative Commons CC BY 4.0 license
Table 1.2	Wang, Kit-Anan and Terracciano, 2018	Fibroblast markers and co-expression in non-fibroblasts	MDPI	Licensed under an open access Creative Commons CC BY 4.0 license
Table 1.3	Wang, Kit-Anan and Terracciano, 2018	Differences between hiPSC-CMs and contractile cardiomyocytes	MDPI	Licensed under an open access Creative Commons CC BY 4.0 license
Table 1.4	Wang, Kit-Anan and Terracciano, 2018	Summary of the available hiPSC-derived cells used in-disease modelling	MDPI	Licensed under an open access Creative Commons CC BY 4.0 license
Figure 1.1	Lindsey, Butcher and Yalcin, 2014	Schematic overview of heart development	Frontiers Media SA	Licensed under an open access Creative Commons CC BY 4.0 license
Figure 1.2	Peng et al., 2014	Contractile apparatus of the myocardium	The American Society for Biochemistry and Molecular Biology, Inc.	Licensed under an open access Creative Commons CC BY 4.0 license
Figure 1.3	Colombo, Raposo and Théry, 2014	Extracellular vesicle composition	Annual Reviews.	Permission granted by written confirmation on January 7th 2020.
Figure 1.4	Raposo and Stoorvogel, 2013	Release of microvesicles and exosomes	Journal of Cell Biology	Permission granted by written confirmation

				on July 3rd 2019.
Figure 1.5	Chin, Hool and Choi, 2019	Integrin positioning and signalling in cardiomyocytes	Frontiers in Bioengineering and Biotechnology	Licensed under an open access Creative Commons CC BY 4.0 license
Figure 1.6	Van Putten et al., 2015	Comparing the morphology and electrophysiology of human induced pluripotent stem cell derived cardiomyocytes (hiPSC-CMs) and native human ventricular myocytes.	Frontiers in Physiology	Licensed under an open access Creative Commons CC BY 4.0 license
Figure 1.7	Bers, 2002	Ca^{2+} cycling in adult ventricular myocytes	Springer Nature	Permission granted by written confirmation on July 3rd 2019.
Figure 1.8	Karakikes et al., 2015	Comparison of action potentials (APs) of ventricular-like human induced pluripotent stem cell-derived (hiPSC)-cardiomyocytes and adult ventricular cardiomyocytes	Circulation Research	Permission granted by written confirmation on July 3rd 2019.
Figure 1.9	Kane et al., 2015	Ultrastructural differences between adult cardiomyocytes and hiPSC-CMs in excitation-contraction coupling domains	Frontiers in Cell and Developmental Biology	Licensed under an open access Creative Commons CC BY 4.0 license
Figure 2.3	Curtis et al., 2017	Cell patterning approach	Oxford University Press	Permission granted by written confirmation on January 7th 2020.

Copyright Clearance Center Marketplace™

Annual Reviews, Inc. - License Terms and Conditions

Order Date	07-Jan-2020
Order license ID	1012280-1
ISSN	1530-8995
Type of Use	Republish in a thesis/dissertation
Publisher	ANNUAL REVIEWS
Portion	Chart/graph/table/figure

LICENSED CONTENT

Publication Title	Annual review of cell and developmental biology	**Country**	United States of America
Author/Editor	ANNUAL REVIEWS, INC.	**Rightsholder**	Annual Reviews, Inc.
Date	01/01/1995	**Publication Type**	e-Journal
Language	English	**URL**	http://arjournals.annualreviews.org/loi/cellbio

REQUEST DETAILS

Portion Type	Chart/graph/table/figure	**Distribution**	Worldwide
Number of charts / graphs / tables / figures requested	1	**Translation**	Original language of publication
Format (select all that apply)	Electronic	**Copies for the disabled?**	No
Who will republish the content?	Academic institution	**Minor editing privileges?**	No
Duration of Use	Life of current and all future editions	**Incidental promotional use?**	No
Lifetime Unit Quantity	Up to 499	**Currency**	EUR
Rights Requested	Main product		

NEW WORK DETAILS

Title	Thesis - Regulation of human cardiomyocyte excitation-contraction coupling by human cardiac fibroblasts	**Institution name**	National Heart and Lung Institute, Imperial College London
Instructor name	Brian Wang	**Expected presentation date**	2020-01-07

ADDITIONAL DETAILS

Order reference number	N/A	**The requesting person / organization to appear on the license**	Brian Wang

REUSE CONTENT DETAILS

Title, description or numeric reference of the portion(s)	Figure 2. Overall composition of extracellular vesicles (EVs).
Editor of portion(s)	N/A
Volume of serial or monograph	30
Page or page range of portion	266
Title of the article/chapter the portion is from	Biogenesis, Secretion, and Intercellular Interactions of Exosomes and Other Extracellular Vesicles
Author of portion(s)	ANNUAL REVIEWS, INC.
Issue, if republishing an article from a serial	1
Publication date of portion	1995-01-01

Rockefeller University Press LICENSE
TERMS AND CONDITIONS

Jul 03, 2019

This is a License Agreement between Mr. Brian Wang ("You") and Rockefeller University Press ("Rockefeller University Press") provided by Copyright Clearance Center ("CCC"). The license consists of your order details, the terms and conditions provided by Rockefeller University Press, and the payment terms and conditions.

All payments must be made in full to CCC. For payment instructions, please see information listed at the bottom of this form.

License Number	4621460472152
License date	Jul 03, 2019
Licensed content publisher	Rockefeller University Press
Licensed content title	The journal of cell biology
Licensed content date	Dec 31, 1969
Type of Use	Thesis/Dissertation
Requestor type	Academic institution
Format	Print, Electronic
Portion	image/photo
Number of images/photos requested	1
The requesting person/organization is:	Brian Wang
Title or numeric reference of the portion(s)	Figure 2. Release of MVs and exosomes
Title of the article or chapter the portion is from	Extracellular vesicles: Exosomes, microvesicles, and friends
Editor of portion(s)	N/A
Author of portion(s)	Raposo, Graça; Stoorvogel, Willem
Volume of serial or monograph.	N/A
Issue, if republishing an article from a serial	4
Page range of the portion	373-383
Publication date of portion	18 February, 2013

Rights for	Main product
Duration of use	Life of current edition
Creation of copies for the disabled	no
With minor editing privileges	no
For distribution to	Worldwide
In the following language(s)	Original language of publication
With incidental promotional use	no
The lifetime unit quantity of new product	Up to 499
Title	Thesis - Cardiac fibroblast regulation of human cardiomyocyte excitation-contraction coupling in health and disease
Institution name	Imperial College London
Expected presentation date	Jul 2019
Total (may include CCC user fee)	0.00 USD

SPRINGER NATURE LICENSE TERMS AND CONDITIONS

Jul 03, 2019

This Agreement between Mr. Brian Wang ("You") and Springer Nature ("Springer Nature") consists of your license details and the terms and conditions provided by Springer Nature and Copyright Clearance Center.

License Number	4621441234161
License date	Jul 03, 2019
Licensed Content Publisher	Springer Nature
Licensed Content Publication	Nature
Licensed Content Title	Cardiac excitation–contraction coupling
Licensed Content Author	Donald M. Bers
Licensed Content Date	Jan 10, 2002
Type of Use	Thesis/Dissertation
Requestor type	academic/university or research institute
Format	print and electronic
Portion	figures/tables/illustrations
Number of figures/tables/illustrations	1
High-res required	no
Will you be translating?	no
Circulation/distribution	<501
Author of this Springer Nature content	no
Title	Thesis - Cardiac fibroblast regulation of human cardiomyocyte excitation-contraction coupling in health and disease
Institution name	Imperial College London
Expected presentation date	Jul 2019
Portions	Figure 1

WOLTERS KLUWER HEALTH, INC. LICENSE TERMS AND CONDITIONS

Jul 03, 2019

This Agreement between Mr. Brian Wang ("You") and Wolters Kluwer Health, Inc. ("Wolters Kluwer Health, Inc.") consists of your license details and the terms and conditions provided by Wolters Kluwer Health, Inc. and Copyright Clearance Center.

License Number	4621450542322
License date	Jul 03, 2019
Licensed Content Publisher	Wolters Kluwer Health, Inc.
Licensed Content Publication	Circulation Research
Licensed Content Title	Human Induced Pluripotent Stem Cell–Derived Cardiomyocytes
Licensed Content Author	Ioannis Karakikes, Mohamed Ameen, Vittavat Termglinchan, et al
Licensed Content Date	Jun 19, 2015
Licensed Content Volume	117
Licensed Content Issue	1
Type of Use	Dissertation/Thesis
Requestor type	Individual
STM publisher name	
Portion	Figures/table/illustration
Number of figures/tables/illustrations	1
Figures/tables/illustrations used	Figure 3
Author of this Wolters Kluwer article	No
Title of your thesis / dissertation	Thesis - Cardiac fibroblast regulation of human cardiomyocyte excitation-contraction coupling in health and disease
Expected completion date	Jul 2019
Estimated size(pages)	1
Requestor Location	Mr. Brian Wang

OXFORD UNIVERSITY PRESS LICENSE
TERMS AND CONDITIONS

Jan 09, 2020

This Agreement between Mr. Brian Wang ("You") and Oxford University Press ("Oxford University Press") consists of your license details and the terms and conditions provided by Oxford University Press and Copyright Clearance Center.

License Number	4744790220113
License date	Jan 09, 2020
Licensed content publisher	Oxford University Press
Licensed content publication	Integrative Biology
Licensed content title	Patterning of sharp cellular interfaces with a reconfigurable elastic substrate
Licensed content author	Curtis, Allison; Li, David J.
Licensed content date	Jan 23, 2017
Type of Use	Thesis/Dissertation
Institution name	
Title of your work	Thesis - Cardiac fibroblast regulation of human cardiomyocyte excitation-contraction coupling in health and disease